

**Influence of land cover degradation on the water balance of the Northern
Drakensberg high altitude mesic grasslands, South Africa**

by

BYRON ANDREW GRAY

**Submitted in fulfilment of the academic requirements of
Doctor of Philosophy**

in Hydrology

School of Agriculture, Earth and Environmental Sciences

College of Agriculture, Engineering and Science

University of KwaZulu-Natal

Pietermaritzburg

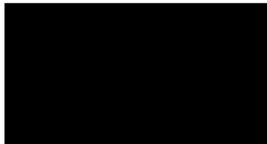
South Africa

January 2022

PREFACE

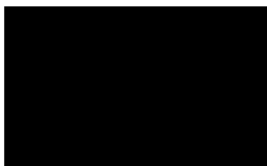
The research contained in this thesis was completed by the candidate while in the Discipline of Hydrology, School of Agriculture, Earth and Environmental Sciences, University of KwaZulu-Natal, Pietermaritzburg Campus, South Africa. The research was financially supported by the National Research Foundation (NRF).

The contents of this work have not been submitted in any form to another university and, except where the work of others is acknowledged in the text, the results reported are due to investigations by the candidate.



Signed: Dr M.L. Toucher

Date: January 2022



Signed: Professor A.D. Clulow

Date: January 2022



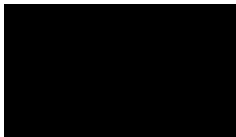
Signed: Professor M.J. Savage

Date: January 2022

DECLARATION 1: PLAGIARISM

I, *Byron Andrew Gray*, declare that

- (i) The research reported in this thesis, except where otherwise indicated, is my original work;
- (ii) This thesis has not been submitted for any degree or examination at any other university;
- (iii) This thesis does not contain other persons' data, pictures, graphs or other information, unless specifically acknowledged as being sourced from other persons; and
- (iv) This thesis does not contain other persons' writing, unless specifically acknowledged as being sourced from other researchers. Where other written sources have been quoted, then:
 - a) their words have been re-written, but the general information attributed to them has been referenced;
 - b) where their exact words have been used, their writing has been placed inside quotation marks, and referenced.
- (v) Where I have reproduced a publication of which I am an author, co-author or editor, I have indicated in detail which part of the publication was written by myself alone and have fully referenced such publications.
- (vi) This thesis does not contain text, graphics or tables copied and pasted from the Internet, unless specifically acknowledged, and the source being detailed in the thesis and in the References sections.



Signed: Byron Andrew Gray

Date: January 2022

DECLARATION 2: PUBLICATIONS

DETAILS OF CONTRIBUTION TO PUBLICATIONS that form part of and/or include research presented in this thesis (including publications submitted and published, giving details of the contributions of each author to the research and writing of each publication):

Publication 1 – Chapter 2 of this thesis

Gray, B.A., Toucher, M.L., Savage, M.J., Clulow, A.D., 2021. The potential of surface renewal for determining sensible heat flux for indigenous vegetation for a first-order montane catchment. *Hydrological Sciences Journal*, DOI: 10.1080/02626667.2021.1910268

Pre-site setup and programming of equipment was conducted by BA Gray with assistance from AD Clulow and MJ Savage and ML Toucher. The setup and installation of the system for the summer and winter calibration campaigns was conducted by BA Gray and assisted by South African Environmental Observation Network (SAEON) technicians. BA Gray was responsible for the maintenance and data collection. Data processing, analysis and interpretation was conducted by BA Gray with assistance from AD Clulow, MJ Savage and ML Toucher. The manuscript was written in its entirety along with all figures and tables were created by BA Gray unless otherwise referenced. Final editing and comment were provided by co-authors.

Publication 2 – Chapter 3 of this thesis

Gray, B.A., Toucher, M.L., Savage, M.J., Clulow, A.D., 2021. Seasonal evapotranspiration over an invader vegetation (*Pteridium aquilinum*) in a degraded montane grassland using surface renewal. *Submitted to Journal of Hydrology: Regional Studies*.

Pre-site setup and programming of equipment was conducted by BA Gray with assistance from AD Clulow and MJ Savage. Setup and installation of system at Cathedral Peak was conducted by BA Gray with assistance from SAEON technicians. Maintenance and data collection was conducted by BA Gray. Data processing, analysis and interpretation was conducted by BA Gray with assistance from AD Clulow, MJ Savage and ML Toucher. The manuscript was written in its entirety along with all figures and tables by BA Gray unless otherwise referenced. Final editing and comment were provided by co-authors.

Publication 3 – Chapter 4 of this thesis

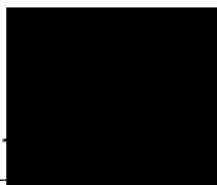
Gray, B.A., Toucher, M.L., Clulow, A.D., Savage, M.J., 2021. Impact of land cover change on the water balance of a first-order Afromontane grassland catchment in a strategic water source area. *Submitted to the Journal of Hydrology*.

Pre-site setup and programming of surface renewal equipment was conducted by BA Gray with assistance from AD Clulow and MJ Savage. Data collection and equipment maintenance was the responsibility of BA Gray. Analysis was conducted by BA Gray with assistance from ML Toucher. The report was written in its entirety along with all figures and tables by BA Gray unless otherwise referenced. Final edits and comments were provided by the co-authors.

Publication 4 – Chapter 5 of this thesis

Gray, B.A., Toucher, M.L., Clulow, A.D., Savage, M.J., 2021. The hydrological impacts of land degradation within a strategic water source area of South Africa. *Intention to submit to Water SA*.

The data collection, setup and confirmation of the ACRU agrohydrological model was conducted by BA Gray and ML Toucher. The analysis of the results was conducted by BA Gray with assistance from ML Toucher. The paper was written in its entirety along with all figures and tables by BA Gray unless otherwise referenced. Final edits, comments and advice were provided by ML Toucher. Final edits and comments were provided by the co-authors.

A solid black rectangular box used to redact the signature of the author.

Signed: Byron Andrew Gray

Date: January 2022

SUMMARY

Mountainous regions provide vital ecosystem services, such as water provisions to low land areas. However, these regions are also considered sensitive to the effects of environmental change, due to their high levels of endemism and biodiversity. Thus, environmental change within these regions could have significant consequences beyond the extent of the region itself. An important implication of environmental change is the impact a change in land cover could have on the water balance of a catchment, especially within the headwater catchments.

The Drakensberg mountains in South Africa, is such a mountain region, which is vital for its provision of ecosystem services and generation of water resources. This mountainous region is under threat from anthropogenic environmental change. The Drakensberg mountain range has been identified within South Africa as a strategic water source area (SWSA) and within the Northern-Drakensberg SWSA exists the Maloti-Drakensberg Park, which is a protected area managed by Ezemvelo KZN Wildlife and a World Heritage site. The Northern-Drakensberg mountain range natural grasslands are under threat from two forms of land cover change degradation, that of woody encroachment and following disturbance, invasion of bracken fern. Woody encroachment occurs within the natural grasslands following the removal of fire, which is of concern within the protected areas, where fire is a current management tool to maintain the natural grassland cover. Outside the protected area, disturbances due to human activities such as overgrazing and poor land management have led to a substantial level of degradation occurring, providing ideal conditions for the invasion of bracken fern.

To safeguard and maintain the assurance of supply from an important SWSA of South Africa, there is the need for improved understanding on the impacts of land cover change and degradation within the Northern-Drakensberg mountain range on the water balance of the region. Thus, the overall aim of this thesis is to understand the influence of land cover change related degradation on the water balance of the Northern-Drakensberg high-altitude mesic grasslands and what this in turn means for the water supply generated from this SWSA of South Africa. To achieve the main aim, the research was scaled from a point measurement to a basin scale where management decisions are made.

To improve our understanding of the impact of degradation related land cover change on the water balance an observational approach is required. Located within the Maloti-Drakensberg Park is the long-term Cathedral Peak research catchments which provided the platform for the observation component of this research. Of interest in the Cathedral Peak research catchments

were three hydrologically individual catchments. Catchment III which consists of a degraded bracken fern land cover following the historical research experiments within the catchment on the impacts of commercial *Pinus patula* plantation on streamflow. Despite rehabilitation efforts following the removal of the plantation, the catchment transitioned to a degraded state and is currently near-completely invaded with bracken fern. Catchment VI which is under natural grassland condition, is managed with a bi-annual spring burn as proven best practice within the Drakensberg region. This catchment formed the baseline catchment for this research. Catchment IX is a woody encroached land cover following the protection of fire since the 1950s as part of research into the implications of removing fire from the natural grasslands. These three catchments provided the ideal platform from which the change in water balance components under each land cover could be monitored and investigated.

The process of evapotranspiration (ET), which forms the connection between the energy and water balances, is well understood to be one of the most affected components of the water balance following a change of land cover. Therefore, ET was the focus of the initial point observation research. Due to the cost and stringency of the prominent method for ET measurement of eddy covariance (EC), an alternative more financially feasible method of surface renewal (SR) was tested over both *Leucosidea sericea* (woody) and *Pteridium aquilinum* (bracken) vegetation in comparison to EC. It was determined that the SR method, and in particular the SR dissipation theory (SRDT) method, which is independent of EC, was the best alternative and cheapest method to EC. The SR method is now used within the Cathedral Peak research catchments for long-term estimations of ET over both vegetation canopies. During this research, calibration factors (α) for the surface renewal 1 (SR1) method were determined for both the *Leucosidea sericea* (woody) and *Pteridium aquilinum* (bracken) vegetation types for winter and summer.

Having confirmed the SRDT ability as an alternative to EC, the seasonal ET of *Leucosidea sericea* (woody) and *Pteridium aquilinum* (bracken) was determined. Providing first insight into the seasonality of ET over these vegetation types. Both vegetations followed a similar seasonal ET cycle to the natural grasslands, with the largest difference occurring in winter when the grasslands become dormant. It was also found that the energy balance was altered under the degraded land covers, with both forms increasing available energy and latent heat flux.

Following the understanding of the seasonal change in ET through point measurements, the research focus was scaled up to the research catchment. A comparison of catchment VI and IX was conducted to identify changes in the headwater catchment water balance between the

natural grassland and woody encroachment land covers. Long-term data sets of precipitation and streamflow from the Cathedral Peak research catchments, in combination with the seasonal ET observations showed that over time, as woody encroachment increased, the catchment rainfall:runoff response ratio decreased, as did streamflow under woody encroachment compared to natural grassland.

Having gained an understanding of the impacts on a water balance of a headwater catchment, hydrological modelling in combination with scenario analysis was used to understand the impacts on water supply from the upper-uThukela catchment were both land cover degradation threats left unmanaged. Land cover parameters were unavailable for *Leucosidea sericea* (woody) and *Pteridium aquilinum* (bracken), and therefore were derived from understanding gained during observation. The ACRU agrohydrological model was utilised and confirmed to simulate current land cover conditions within the upper-uThukela satisfactorily at both the headwater and catchment levels. It was identified that both forms of land cover change resulted in a reduction in streamflow. This was largest for woody encroachment. The most affected flows were the low flows and winter dry period flows. Headwater catchments were also identified as the most impacted by land cover change.

The key conclusions of the research were:

- that the surface renewal methodology is a viable alternative for obtaining estimates of evapotranspiration over indigenous vegetation types;
- that the energy balance and ET of woody vegetation in comparison to the natural grassland was significantly altered;
- the importance of fire, as not only a management tool for the maintenance of the natural grasslands, but also to ensure the sustainability of the vital water resources and ensuring water security;
- that there is an evident lag between the onset of degradation in the form of woody encroachment and the resultant impacts on streamflow;

- the disproportionately large impact degradation related land cover change within these headwater catchments has on the downstream water balance relative to low land catchments.

Following the analysis and with the understanding gained, it is recommended that the natural grasslands continue to be managed using fire, and continued protection of the natural grasslands needs to be maintained. Observation within these headwaters is key to improving the understanding of change and to drive decision making, allowing for the optimal management of the important SWSA.

ACKNOWLEDGEMENTS

I would firstly like to thank Dr Michele Toucher for her continuous assistance, encouragement, advice, and for providing that much needed motivation and patience when things got tough. You have been invaluable in completing this thesis and I am very grateful to have had you as a mentor over the years.

Thank you to both Alistair Clulow and Prof Michael Savage for their supervision, guidance, advice and encouragement throughout this process. Thank you both for being so willing to share your vast knowledge, wisdom and technical expertise.

Thanks to Ms Sue van Rensburg and the staff and students of the South African Environmental Observation Network (SAEON): Grasslands-Forest-Wetlands Node for hosting me and providing logistical and social support throughout this process. I would also like to thank the Cathedral Peak team and in particular Mr Kent Lawrence and Mr Siphiwe Mfeka for their support and assistance within the installation of the equipment and during monthly fields trips.

The National Research Foundation (NRF) for the funding received over the period of the project.

The Centre for Water Resources Research (CWRR) for the use of their facilities, equipment and all the assistance received from the staff.

Ezemvelo KZN Wildlife for allowing and supporting this research within the Maloti-Drakensberg Park, and the accommodation at site

To my family, especially my parents for encouraging me to take this on and supporting me throughout the journey! Thank you both for your optimism, confidence in me and belief that this could be achieved!

A big thank you to my fiancé Sarah, for enduring this with me from the beginning, for the constant encouragement, support, patience and sacrifices you have had to make, especially over weekends and the late nights. Thank you for always being there for me and allowing me to achieve this!

TABLE OF CONTENTS

PREFACE	ii
DECLARATION 1: PLAGIARISM	iii
DECLARATION 2: PUBLICATIONS	iv
SUMMARY	vi
ACKNOWLEDGEMENTS	x
TABLE OF CONTENTS	xii
LIST OF TABLES	xvi
LIST OF FIGURES	xvii
1.INTRODUCTION.....	1
1.1 Background	1
1.2 Rationale for the study	4
1.3 Research objectives	7
1.4 Research approach.....	8
1.5 References	10
2.THE POTENTIAL OF SURFACE RENEWAL FOR DETERMINING SENSIBLE HEAT FLUX FOR INDIGENOUS VEGETATION FOR A FIRST-ORDER MONTANE CATCHMENT	18
Abstract	18
2.1 Introduction	18
2.2 Materials and Methods	22
2.2.1 Research site, vegetation and campaigns	22
2.2.2 Equipment	24
2.2.3 SR theory.....	25
2.2.4 EC Theory	28
2.2.5 Data analysis and processing.....	29
2.3 Results	30
2.3.1 SR1 calibration and validation	30
2.3.2 Comparison of SR1, SRDT and SR2 with the benchmark EC	32
2.3.3 Data availability and performance of EC, SSR1, SRDT and SR2.....	35
2.4 Discussion	38
2.5 Conclusion.....	42
2.6 Acknowledgements	43
2.7 References	43

3. SEASONAL EVAPOTRANSPIRATION OVER AN INVADER VEGETATION (<i>PTERIDIUM AQUILINUM</i>) IN A DEGRADED MONTANE GRASSLAND USING SURFACE RENEWAL	49
Abstract	49
3.1 Introduction	49
3.2 Materials and methods	53
3.2.1 Research site.....	53
3.2.2 Observation equipment	55
3.2.3 Estimation of energy fluxes.....	56
3.2.4 Calculation of ET_o and k_c	57
3.2.5 Data analysis	58
3.2.6 Patching missing data.....	60
3.3 Results	61
3.3.1 Determination of α for calibration of the SR1 method	61
3.3.2 Comparison between EC, SR1 and SRDT methods	61
3.3.3 Assessment of seasonality of ET based on H_{SRDT}	62
3.4 Discussion	68
3.5 Conclusions	72
3.6 Acknowledgements	72
3.7 References	72
4. IMPACT OF LAND COVER CHANGE ON THE WATER BALANCE OF A FIRST- ORDER AFROMONTANE GRASSLAND CATCHMENT IN A STRATEGIC WATER SOURCE AREA	80
Abstract	80
4.1 Introduction	80
4.2 Material and Methods.....	85
4.2.1 Research site.....	85
4.2.2 Catchment VI: Near-natural grassland.....	87
4.2.3 Catchment IX: Woody encroached grassland	87
4.2.4 Soils.....	88
4.2.5 Equipment and processing	89
4.3 Theory/Calculation.....	91
4.3.1 Water balance method.....	91
4.3.2 Data quality control and patching	92
4.4 Results	93

4.4.1 Long-term change in precipitation, streamflow, catchment response and vegetation	93
4.4.2 Recent energy balance.....	95
4.4.3 Evapotranspiration	96
4.4.4 Soil water content.....	97
4.4.5 Water balance	100
4.5 Discussion	100
4.6 Conclusions	104
4.7 Acknowledgements	104
4.8 Funding.....	105
4.9 References	105
4.10 Appendix	111
5.THE HYDROLOGICAL IMPACTS OF LAND DEGRADATION WITHIN A STRATEGIC WATER SOURCE AREA OF SOUTH AFRICA	113
Abstract	113
5.1 Introduction	113
5.2. Materials and Methods	116
5.2.1 ACRU hydrological model	116
5.2.2 Catchment description.....	118
5.2.3 Model configuration and input data sources	121
5.2.4 Confirmation of ACRU model results	123
5.2.5 Land cover scenarios.....	124
5.3. Results	126
5.3.1 Confirmation studies	126
5.3.2 Bracken invasion scenario results	127
5.3.3 Woody encroachment scenario results	131
5.4. Discussion	134
5.5 Conclusions	137
5.6 References	137
5.7 Appendix	143
6.SYNTHESIS: KEY CONCLUSIONS AND RECOMMENDATIONS.....	145
6.1 Key conclusions from the study	145
6.2 Revisiting the aims and objectives	149
6.3 Contributions to new knowledge.....	149
6.4 Management and future research recommendations	151

6.4.1 Importance of observation and monitoring to optimise management.....	151
6.4.2 Nexus approach for process understanding and management	152
6.4.3 Consideration of uncertainty	152
6.4.4 Climate change lens	154
6.5 References	154

LIST OF TABLES

Table 2.1: A summary of the α values calculated for the correction of the sensible heat flux (H) estimated by SR1 approach from the summer and winter campaigns for the 0.4- and 0.8-s lags under unstable conditions.....	31
Table 2.2: Average energy balance closure for the EC method for unstable conditions over the duration of the summer campaign.	36
Table 2.3: Average energy balance closure for the EC method for unstable conditions over the duration of the winter campaign.....	37
Table 2.4: The data available across the four methods for the 162 possible 30-min measurement periods, when unstable conditions occurred during the summer campaign.....	38
Table 2.5: The data available across the four methods for the 143 possible 30-min measurement periods, when unstable conditions occurred during the winter campaign.	38
Table 3.1: The α determined for summer (12/12/2019 – 17/12/2019) and winter (27/07/2020 – 03/08/2020) and for 0.4- and 0.8-s lags and the average of the two lags for unstable conditions.	61
Table 4.1: The water balance of catchment VI (near-natural grassland) and catchment IX (woody encroached grassland) over the two respective hydrological years.	100
Table 5.1: The monthly parameters used for the ACRU model in simulation of 100 % bracken invasion and Woody encroachment.	125
Table 5.2: Statistics of performance from the ACRU model between observed and simulated streamflows for subcatchment CPIV and the upper-uThukela catchment (outlet)	127
Table 5.3: The significant counts (SC) determined for Group 2 parameters using the Indicator of Hydrologic Alteration (IHA) software for comparison of the simulated baseline streamflow and 100 % bracken invasion land cover change streamflow at three separate locations within the focus catchment.	131
Table 5.4: The significant counts (SC) determined for the Group 2 hydrological parameters using the Indicator of Hydrologic Alteration (IHA) software for comparison of the simulated baseline streamflow and 100 % woody encroachment land cover change streamflow at three separate locations within the focus catchment.	134

LIST OF FIGURES

Figure 1.1: The pyramid structure of the research project which allowed for the achievement of the overall aim and objectives.	9
Figure 2.1: The location of the Cathedral Peak research catchment and, within them, the location of catchment IX. In the centre of the catchment, the location of the eddy covariance (EC) and surface renewal (SR) systems, meteorological station and raingauge.	23
Figure 2.2: The calibration period between surface renewal 1 (SR1) and eddy covariance (EC) using the estimation and measurement of 30-min sensible heat flux (H) by the respective systems for unstable conditions during the summer campaign for the (a) 0.4- and (b) 0.8-s lag and winter campaign for the (c) 0.4- and (d) 0.8-s lag.	30
Figure 2.3: The linear regressions for unstable conditions showing the relationship between the corrected 30-min sensible heat flux (H) from surface renewal 1 (SR1) method against the H measured by the eddy covariance (EC) method for the two-day validation periods during the (a) summer and (b) winter campaigns.	31
Figure 2.4: The relationship between the three surface renewal (SR) approaches and the eddy covariance (EC) method, using linear regressions between (a) sensible heat flux from surface renewal 1 (H_{SR1}), (b) sensible heat flux from surface renewal 2 (H_{SR2}), (c) sensible heat flux from surface renewal dissipation theory (H_{SRDT}) and sensible heat flux from eddy covariance (H_{EC}) for unstable conditions during the summer campaign....	32
Figure 2.5: The relationship between the three surface renewal (SR) approaches and the eddy covariance (EC) method, using linear regressions between 30-min (a) sensible heat-flux from surface renewal 1 (H_{SR1}), (b) sensible heat flux from surface renewal 2 (H_{SR2}), and (c) sensible heat flux from surface renewal dissipation theory (H_{SRDT}) and the sensible heat flux from eddy covariance (H_{EC}) for unstable conditions during the winter campaign.	33
Figure 2.6: A comparison of the energy balance components (a) net radiation (R_n) and soil heat flux (G) and (b) sensible heat flux (H) measured by eddy covariance (EC), surface renewal 1 (SR1), surface renewal 2 (SR2) and surface renewal dissipation theory (SRDT) methods for unstable conditions over a day (26/01/2020) during the summer campaign.	34

Figure 2.7: A comparison of the energy balance components (a) net radiation (R_n) and soil heat flux (G) and (b) sensible heat flux (H) estimated by eddy covariance (EC), surface renewal 1 (SR1), surface renewal 2 (SR2) and surface renewal dissipation theory (SRDT) methods for unstable conditions over a day (15/7/2020) during the winter campaign.	35
Figure 3.1: The location of the Cathedral Peak research catchment III, the focus site for this research. The locations of the raingauge, surface renewal system and the Mikes Pass meteorological station are visible within the Cathedral Peak research catchments, South Africa.....	55
Figure 3.2: The bracken canopy change at the monitoring site in CIII with SR and EC systems visible, the day before the summer campaign (11/12/2019; top left), autumn (23/03/2020; top right), day before winter campaign (17/07/2020; bottom left), and spring (05/10/2020; bottom right). All photos are post-fire.....	57
Figure 3.3: The comparison between half-hourly H_{SR1} and H_{SRDT} , with half-hourly H_{EC} for the summer (a, b) and winter campaigns (c, d).	62
Figure 3.4: The average daily energy balance per month using SRDT, as a percentage of R_n (when $R_n > 0$). The average daily R_n for each month is indicated by the solid line. (The * indicates months where patched data were used due to equipment loss and malfunction).	63
Figure 3.5: The monthly total ET_{SRDT} over the bracken canopy on the bottom axis, with monthly total rainfall on the top axis. (The * indicates the period where patched data are used due to the fire damage and equipment malfunction).....	64
Figure 3.6: The 30-day moving average of daily ET_{SRDT} and the monthly k_c . The seasons are indicated by the background shading. The period where patched data were used is shown as a dotted trendline.....	66
Figure 3.7: A comparison of the daily ET_{SRDT} in consecutive years from 1 st December to 18 th July for the pre-fire period and the post-fire period over the bracken canopy. The 30-day moving average daily ET_{SRDT} is indicated by the solid line, accumulated daily ET_{SRDT} dashed line (---), accumulated daily rainfall indicated by the dotted lines (•••) (above), and the accumulated R_n (below) for each respective period.	67

Figure 4.1: The location of the natural grassland and woody encroached grassland catchments within the Cathedral Peak research catchments with the observation equipment locations detailed. The images of CVI and CIX were captured on 28 May 2020 (Source: Esri).	86
Figure 4.2: The extent of the 2019 fire across the lower part of catchment IX. The woody encroached areas remained untouched, while the grassland areas were burnt. (Photo taken from the top of surface renewal tower on 4 July 2019).	88
Figure 4.3: A representation of the annual precipitation and streamflow of the (a) natural (CVI) and (b) woody encroached (CIX) grassland catchments for the historical (1961 – 1986) and current (2016 – 2019) observation periods, as well as a comparison of the runoff responses of the respective catchments over time (c).	95
Figure 4.4: The partitioning of R_n between the remaining three energy balance components (G , H and LE) for the respective land covers of the (a) natural grassland in Catchment VI, and (b) woody encroachment in catchment IX. (The * denotes months where patching was used).	96
Figure 4.5: A comparison between the accumulated ET and 30-day moving average daily ET of the natural (black) and woody encroached (grey) grassland, over two hydrological years (2018/2019; 2019/2020).	97
Figure 4.6: The average, upper and lower volumetric soil water content within 1 m of the soil profile across both catchment (a) VI and (b) IX based on the point measurement across the six Diviner tubes per catchment from March 2019 to October 2020.	98
Figure 4.7: The average volumetric soil water content within the first metre of soil at a depth of (a) 0.1 m, (b) 0.3 m, (c) 0.6 m, and (d) 0.9 m across both catchment VI and IX.	99
Figure 5.1: Flow diagram of the representation of the water budget in the ACRU model (Schulze, 1995).	117
Figure 5.2: The location and layout of the upper-uThukela catchment area with climate stations and streamflow gauging weirs indicated, as well as an illustration of the 39 subcatchments delineated.	119
Figure 5.3: The layout of the respective land covers which were used to form the HRU's within the subcatchments.	120

Figure 5.4: The cascading routing structure of Hydrologic Response Units (HRU) for each subcatchment in the ACRU agrohydrological model.	121
Figure 5.5: The relative change per subcatchment for the mean annual, mean of the three driest months (June, July, August) and mean of the three wettest months (December, January, February) streamflows following 100 % bracken invasion.	128
Figure 5.6: The relative change in streamflow following 100 % bracken invasion of each subcatchment for the 1:10 dry and 1:10 year wet periods, annual, winter months (June, July, August), and summer months (December, January, February).	130
Figure 5.7: The relative change per subcatchment for the mean annual, mean of the three driest months (June, July, August) and mean of the three wettest months (December, January, February) streamflows following 100 % woody encroachment.	132
Figure 5.8: The relative change in streamflow following 100 % woody encroachment of each subcatchment for the 1:10 dry and 1:10 year wet periods, annual, winter months (June, July, August), and summer months (December, January, February).	133

1. INTRODUCTION

1.1 Background

The International Association of Hydrological Sciences (IAHS) scientific decade 2013-2022 titled “Panta Rhei” (Montanari et al., 2013) is focussed on the need for hydrological sciences to move beyond the dependence on the assumption of stationarity and to improve the sciences ability and understanding of the system behaviour under change, to allow for improved predictions under change (Ehret et al., 2014). In 2021, the World Meteorological Organisation (WMO) announced a new Vision and Strategy for Hydrology (World Meteorological Organisation, 2021). This initiative, in response to the challenges faced by society due to global change, outlines eight goals to be in place by 2030 whose key action plans revolve around the need for high quality data, improving our hydrological understanding, and using this knowledge to guide planning and decision making moving forward (World Meteorological Organisation, 2021). Further to these two initiatives, the United Nations have also identified land degradation as one of the highest priorities on their global agenda (Turpie et al., 2021). A target of sustainability development goal (SDG) 15 is to reverse and halt land degradation of all forms (Turpie et al., 2021). The IPCC special report on Climate Change and Land Degradation defines land degradation as “a negative trend in land condition, caused by direct or indirect human-induced processes including anthropogenic climate change, expressed as long-term reduction or loss of at least one of the following: biological productivity, ecological integrity, or value to humans” (Olsson et al., 2019: 347) An area highly susceptible to the effects of environmental change and degradation are mountainous areas (Benston, 2003; Huber et al., 2005; Benston and Stoffel, 2014; Moran-Tejeda et al., 2014; Haro-Monteagudo et al., 2020). Mountainous regions are “sentinels for environmental change” (Benston and Stoffel, 2014) due to their steep topographical extent which has resulted in high levels of endemism and biodiversity in these regions (Benston, 2003). Mountains provide vital ecosystem services (Benston and Stoffel, 2014), for example, lowland areas often have a dependence on mountain regions for water resources (Nazemi et al., 2017). Environmental change in mountainous areas could modify vegetation distribution and characteristics (Beniston, 2003), and alter the water balance (Delago et al., 2010; Nazemi et al., 2017). Changes and degradation of the mountain systems reduces their ability to provide ecosystems services, and resource delivery to not only the upland systems, but also lowland populations (Benston and Stoffel, 2014; Kelleher et al., 2015), extending the consequences of environmental change beyond the local area. It is therefore important to understand how environmental degradation within mountainous areas impacts on

the water balance, altering water supply, to inform catchment and water resource management (Yang et al., 2015).

Climate change and land cover/use change have been identified as the most significant influences on water supply from a catchment or region (Yang et al., 2015). The exact extent of climate change is associated with a large amount of uncertainty, while the impacts of land cover change are less uncertain (Olsson et al., 2019). Land cover change, and in turn land degradation, is also manageable at a local to regional scale, while climate change is influenced and dependent on a global effort (Olsson et al., 2019). Climate change can also drive land degradation through changes to temperatures and rainfall patterns (i.e., intensity, timing and distribution) altering coverage levels and vegetation types (Olsson et al., 2019). While land degradation can feed back into the climate system and accelerate climate change, through means such as changes in land coverage and surface albedo (Olsson et al., 2019). Through management of land cover change, the impacts of climate change can be reduced, and the importance of local knowledge and site-specific solutions are key to the success, contributing to a form of climate change mitigation (Olsson et al., 2019).

Through altering how precipitation is partitioned, land cover change influences all components of the water balance (Yin et al., 2017) and ultimately water supply, with the greatest changes impacting on total evaporation (ET) (Li et al., 2017). This is significant considering that ET is the link between the energy and water balances (Burba and Verma, 2005; Castellvi, 2011; Fischer et al., 2016; Chemura et al., 2020). A change in land cover also alters the energy balance through altering the surface albedo, surface roughness, soil temperature, and available energy flux (Zou et al., 2014; Fischer et al., 2016; Acharya et al., 2017). These in turn alter the partitioning of the energy balance components, and the ratio between sensible and latent heat fluxes (Archer et al., 2017), and thus ET. The extent to which water supply is altered by land cover change is determined by the spatial extent, degree of change and the location within the catchment (Warburton et al., 2012). Identifying land cover change and understanding its influence at a local scale is simple. However, understanding land cover influence at the catchment, or basin scale is more difficult when considering the several other land covers which are also occurring and how their combined influence develops along the basin profile (Warburton et al., 2012; Gleeson et al., 2020). Temporally, the time between when land cover change begins, and when it influences hydrological processes is not immediate, and can vary depending on circumstances (Schulze, 2003).

The common methods for the assessment of environmental change impacts on catchment hydrology are paired catchment experiments, statistical analysis, or hydrological models (Yang et al., 2017), and the emerging concept of ‘comparative hydrology’ (Wagener et al., 2007; Kelleher et al., 2015). Paired catchments analysis is where the streamflow regimes of two or more catchments that are similar in physical characteristics are compared to determine the influence of an anthropogenic disturbance on the flow regime, such as a land cover change (Yang et al., 2017). Hydrological modelling is the most extensively used method. However, regardless of purpose, hydrological models have been developed using the same method of data acquisition, development and translation of conceptual framework into a mathematical model and then calibration and model validation using acquired historical dataset(s) (Bloschel and Sivapalan, 1995). This method of model development and testing is sufficient and justifiable if the hydrological cycle were consistent, linear and with slow natural change (Bloschel and Sivapalan, 1995; Wagener et al., 2010; Ehret et al., 2014). The current dilemma is that environmental change is altering the hydrological cycle at an unprecedented rate, and therefore removing our ability to predict future change, with any certainty, based on past observation (Sivapalan, 2003). Thus, there is a need to develop models which are governed by physical laws and provide a true representation of the hydrological processes (Sivapalan, 2003; Kirchner, 2006). To achieve that, an integrated approach between field observation and modelling is required (Burt and McDonnell, 2015; Beven et al., 2020). The challenge is to convert the conceptual understanding gained through observation to represent hydrological processes at a range of scales (Brookes and Vivoni, 2008), while being mindful of the spatial and temporal heterogeneity which exists in hydrological processes (Kirchner, 2006; van Beuskom et al., 2014; Gu et al., 2018; Beven et al., 2020; Gleeson et al., 2020). Models are only as good as our understanding of the hydrological system, and there are aspects that are not fully understood, and large uncertainties in the estimates of the water balance components (Burt and McDonnell, 2015; Beven et al., 2020).

Despite the need for observation of change and process understanding, field-based studies and monitoring networks are declining globally (Sivapalan, 2003; Burt and McDonnell, 2015; Tetzlaff et al., 2017; Gu et al., 2018), with cost being a primary driver of the declines in Africa and other developing countries. Across Africa there is a lack of good quality long-term hydrological datasets (Hughes et al., 2015). Therefore, African research on hydrological processes and the development of local hydrological understanding have been hampered. Thus, it is important to test, develop and demonstrate the adequacy of cheaper and simpler methodologies and techniques.

1.2 Rationale for the study

The Drakensberg mountain range is an important strategic water source area of South Africa, that is under threat from anthropogenic environmental change. The mean annual rainfall (MAP) in South Africa is only 490 mm and the country is considered arid (Le Maitre et al., 2020). Due to the uneven distribution of rainfall across the country, between South Africa and neighbouring countries Eswatini and Lesotho, only 8 % of the land area is responsible for generating 50 % of the water supply (Nel et al., 2017). The Drakensberg mountain range is located in the summer rainfall region of South Africa. This region experiences wet hot summers and cool dry winters (Toucher et al., 2016). Within the vicinity of the upper-uThukela catchment, the MAP is approximately 1 205 mm, which is far greater than the countries MAP. The main driving mechanism forming summer rainfall is orographic, with rainfall events dominated by thunderstorms (Nanni, 1956; Bosch, 1979). Summer rainfall occurs mainly during the months between October and March. The mean annual temperature on the escarpment is 14 °C, rising to 17 °C in the lowland areas.

Climate change within the region, as with other areas of the world, is a significant issue. The mountainous areas of the summer rainfall region such as the Drakensberg are expected to see an increase in MAP with higher rainfall in summer and autumn (Midgley et al., 2005; Hewitson and Crane, 2009; Lumsden et al., 2009; Schulze, 2011, Engelbrecht, 2019), and an associated increase in streamflows. This is however, expected to result in a more variable rainfall inter annually (Midgley et al., 2005; Hewitson and Crane, 2009; Lumsden et al., 2009; Schulze, 2011, Engelbrecht, 2019). There will also be an increase in rainfall intensity (Midgley et al., 2005; Hewitson and Crane, 2009; Lumsden et al., 2009; Schulze, 2011, Engelbrecht, 2019). Air temperatures are expected to increase across the country with higher increases predicted for the interior, in comparison to the coastal areas (Midgley et al., 2005; Hewitson and Crane, 2009; Lumsden et al., 2009; Schulze, 2011; Engelbrach et al., 2019). This comes with a greater interannual variability across the region, with the air temperatures within the mountainous areas remaining constant inter annually (Midgley et al., 2005; Hewitson and Crane, 2009; Lumsden et al., 2009; Schulze, 2011, Engelbrecht, 2019).

Although climate change is a larger scale issue, land cover change is an issue which needs to be investigated at a more local scale. Due to the high-water demand in the country, there is a current focus on protecting the strategic water source areas from land cover changes which could alter the already limited and pressured water supply (Le Maitre et al., 2020). The vegetation of the Drakensberg mountain range is fire-adapted mesic high-altitude grasslands.

These grasslands are critical for the maintenance of the ecosystem services, such as water resources, generated from the landscape (Brown and Bezuidenhout, 2020). However, these natural grasslands are susceptible to environmental degradation, two forms of which are woody encroachment (Bond and Parr, 2010) and following disturbance, the invasion of bracken fern, which is considered as one of the dominant global weeds in degraded lands (Gallegos et al., 2015). Both forms of degradation occur through different mechanisms, and within different areas of the region.

Within the protected area of the Drakensberg mountain range, which is known as the Maloti Drakensberg Park, a significant threat is that of woody encroachment. Fire is a common management tool within the Maloti Drakensberg Park (Gordijn et al., 2018), as the grasslands are fire adapted and research has shown that the removal of fire from the landscape leads to woody encroachment (De Villiers and O'Connor, 2011). Woody encroachment can be considered a global positive for carbon sequestration and provides prospects to attain carbon credits (Archer, 2010), but at the local level, is potentially considered a water provision problem. It is important to understand that the potential global benefit of woody encroachment as a carbon sink may be outweighed by the loss of habitat, biodiversity and ecosystem services at local levels across the world, and this should guide the development of management strategies and policy (Archer, 2010).

Outside of the protected areas, disturbances often associated with human activities, such as overgrazing and poor land management (Hoffman and Todd, 2000; Yalaw et al., 2019), have led to the degradation of the natural grasslands. This creates ideal conditions for the invasion of bracken, which is a dominant vegetation that consumes the landscape (McGlone et al., 2005; Grab and Knight, 2018). Disturbances such as these are more prevalent outside of the protected areas but are also found within the protected areas around settlements and man-made structures, as well as following the occurrence of a wildfire. A commonality between both forms of degradation is that they introduce vegetation change, and alter the water balance (Acharya et al., 2017; Gwate et al., 2018). Thus, there is a strong need to understand how and what changes occur to the water balance, to advise on the management of the land, as well as the management of the water resources. This understanding would allow for informed decision making regarding the management of this strategic water source area of South Africa.

The Cathedral Peak research catchments, which are located within the Maloti Drakensberg Park, were established in 1948 to investigate the influence of land management on streamflow (Nanni, 1956). The research catchments consist of a network of ten hydrologically separate

catchments which were each subjected to a different land management treatment. The catchments were monitored until 1995 and contributed to the understanding of land cover influences on South African hydrology. In 2012, monitoring in the catchment resumed with focus of continued observation, being catchments III, VI and IX. Catchment VI is considered the baseline catchment and has been maintained in a near natural condition with a dominant *Themeda triandra* cover, with no land cover changes within recent history. The catchment is maintained through a biannual spring burn, which is the accepted management method for the uKhalahamba Drakensberg grasslands (Toucher et al., 2016). Catchment III was planted with *Pinus patula* in 1959 until 1981 when a fire burnt out the catchment. Despite rehabilitation attempts using *Eragrostis curvula*, the catchment deteriorated into a degraded state, with erosion on the steeper slopes visible. As a result of the degraded state, bracken has invaded and is now the dominant landcover. Catchment IX was used to test whether the removal of fire from the natural grasslands would lead to woody encroachment and was protected from fire since 1952 (De Villiers and O'Connor, 2011). Whilst being fire protected, runaway fires have burnt the catchment on several occasions (De Villiers and O'Connor, 2011). Despite this, woody encroachment occurred, and the current catchment landcover is dominated by woody vegetation. These three catchments provide the ideal platform within the strategic water source area, to study and observe the differences in the water balance components for three varying land covers under one climate.

In many, but not all regions of the world, evapotranspiration (ET) is the dominant output component of the water balance (Beven et al., 2020). ET is also the component which links the energy and water balances (Burba and Verma, 2005; Castellvi, 2011; Fischer et al., 2016; Chemura et al., 2020) and is most affected by land cover change (Zhang and Schilling, 2006; Chemura et al., 2020). The current benchmark method for the estimation of ET is that of the eddy covariance (EC) method (Zapata and Martinez-Cob, 2002; Rosa and Tanny, 2015; Kelly and Higgins, 2018; Poznikova et al., 2018; Moran et al., 2020). The EC methodology is complicated, restricted, and requires the use of expensive sensors and equipment (Castellvi et al., 2002; Snyder et al., 2008; Castellvi and Snyder, 2009a; Poblete-Eceverria et al., 2014; Hayman et al., 2019). An alternative to the benchmark EC method, is that of the surface renewal (SR) method (Hu et al., 2018). The SR method has received added attention due to the method's simpler methodology, reduced sensor requirement, greater reliability and reduced cost (Paw U et al., 1995; Suvocarev et al., 2019).

The original surface renewal method (SR1; Paw U et al., 1995; Snyder et al., 1996) requires calibration using the EC method, a restriction of the method, that has led to the exploration and development of the surface renewal 2 method (SR2; Castellvi et al., 2002; Castellvi, 2004) and surface renewal dissipation theory method (SRDT; Castellvi and Snyder, 2009b). The requirement for calibration using the EC method, is to account for the misrepresentation of the temperature change of the air parcel observed by the fine-wire thermocouple in the SR method (Spano et al., 2000; Mengistu and Savage, 2010). The SR2 and SRDT methods remove the requirement for the calibration against EC, with the SR2 method requiring only one additional sensor for the measurement of horizontal windspeed above the canopy surface (Castellvi et al., 2002; Castellvi, 2004), and the SRDT method requiring no additional sensors to the SR1 method (Castellvi and Snyder, 2009b), making them both suggestively cheaper methods. Considering the requirement for ET data to assist in understanding the impacts of land cover change on an important water balance component, within a budget-restricted monitoring network, the SR methods, especially the two independent of EC, provide a valuable and highly feasible alternative, which are also suitable for the steep and variable terrain of mountainous head water regions.

1.3 Research objectives

To safeguard and maintain the assurance of water supply from an important strategic water source area of South Africa, there is the need for an improved understanding on the impacts of land cover change and degradation within the Drakensberg mountain range on the water balance of the region. Thus, the overall aim of this thesis is to understand the influence of land cover change related degradation on the water balance of the Northern-Drakensberg high-altitude mesic grasslands and what this in turn means for the water supply generated from this strategic water source area of South Africa.

To achieve the overall aim, the following objectives are pursued:

- Identify an alternative method, for the estimation of evapotranspiration, which is robust enough for use within a remote mountainous area and financially feasible for a budget restricted monitoring network (Chapter 2).
- Understand the seasonal evapotranspiration of woody encroachment which invades following the removal of fire from a natural grassland (Chapters 2 and 4).

- Understand the seasonal evapotranspiration of the bracken canopy which invades following degradation of a natural grassland (Chapter 3).
- Understand the change in the overall water balance following a transition from a natural grassland vegetation type to an alternate vegetation state following anthropogenic influence, using the paired catchment approach and monitoring of the water balance components (Chapter 4).
- To use hydrological modelling with parameters determined from observation, in combination with scenario analysis, to understand the potential changes in the water supply from the upper-uThukela catchment following different levels of land cover change (Chapter 5).

1.4 Research approach

The thesis consists of six chapters, of which four (Chapters 2 – 5) present the findings of the research in individual research papers prepared for publication in refereed journals. The structure of the research papers is outlined in Figure 1.1 in the form of a pyramid representing the zooming out from a methodological focus on a point measurement methodology (Chapter 2), to understanding change within a hydrological component, using the point measurement (Chapter 3), and then understanding the changes in the water balance at a catchment scale (Chapter 4) and applying this understanding through hydrological modelling at the basin scale where decision making is conducted (Chapter 5). The pyramid diagram (Figure 1.1) represents the stepwise approach of objectives which was used to achieve the overall aim of this research, to understand the large-scale effects of land cover change related degradation on the water supply generated by the Northern-Drakensberg high-altitude mesic grasslands. Each research paper consists of a literature review related to the aim and methodology of that paper, and references in the format of the journal of the submitted paper.

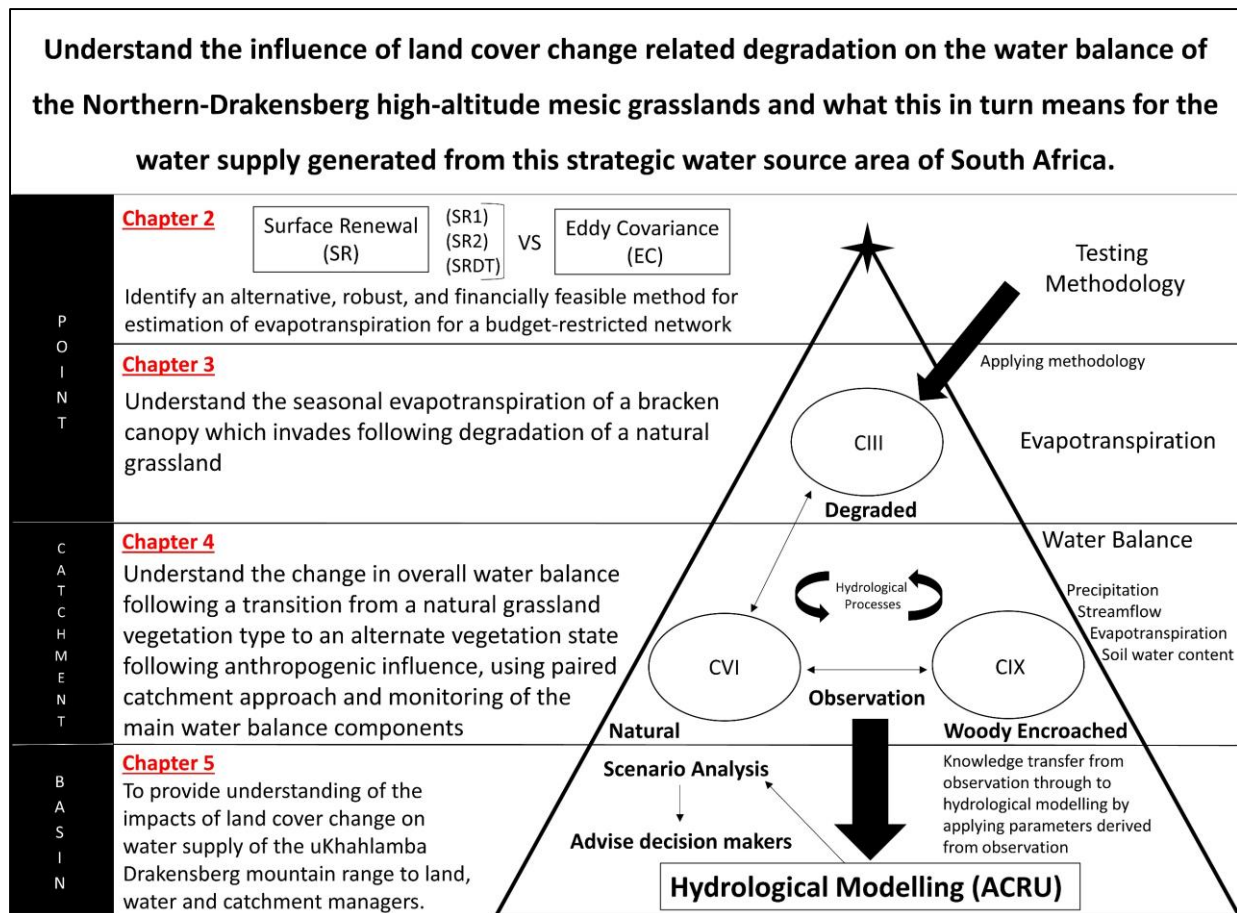


Figure 1.1: The pyramid structure of the research project which allowed for the achievement of the overall aim and objectives.

1.5 References

- Acharya, B.S., Hao, Y., Ochsner, T.E., Zou, C.B., 2017. Woody plant encroachment alters soil hydrological properties and reduces downward flux of water in tallgrass prairie. *Plant Soil*. 414, 379 – 391.
- Archer, S.R., 2010. Rangeland Conservation and Shrub Encroachment: New Perspectives on an Old Problem. *Wild Rangelands: Conserving Wildlife While Maintaining Livestock in Semi-Arid Ecosystems*. 1, 53-97.
- Archer, S.R., Andersen, E.M., Predick, K.I., Schwinning, S., Steidl, R.J., Woods, S.R., 2017. Woody Plant Encroachment: Causes and Consequences. In: Briske, D.D. (Eds), *Rangeland Systems: Processes, Management and Challenges*. Springer., Gewerbestrasse, Switzerland, pp. 25 – 84.
- Beniston, M., 2003. Climate change in mountain regions: a review of possible impacts. *Climate Change*. 59, 5-31.
- Beniston, M., Stoffel, M., 2014. Assessing the impacts of climatic change on mountain water resources. *Science of the Total Environment*. 493, 1129-1137.
- Beven, K., Asadullah, A., Bates, P., Blyth, E., Chappell, N., Child, S., Cloke, H., Dadson, S., Everard, N., Fowler, H.J., Freer, J., Hannah, D.M., Heppell, K., Holden, J., Lamb, R., Lewis, H., Morgan, G., Parry, L., Wagener, T., 2020. Developing observational methods to drive future hydrological science: Can we make a start as a community? *Hydrological Processes*. 34, 868-873.
- Bloschel, G., Sivapalan, M., 1995. Scale issues in Hydrological Modelling: A Review. *Hydrological Processes*. 9, 251-290.
- Bond, W.J., Parr, C.L., 2010. Beyond the forest edge: Ecology, diversity and conservation of the grassy biomes. *Biological Conservation*. 143, 2395 – 2404.
- Bosch, J., 1979. Treatment Effects on Annual and Dry Period Streamflow at Cathedral Peak. *South African Forestry Journal*, 108, 29-38.
- Brookes, P.D., Vivoni, E.R., 2008. Mountain ecohydrology: quantifying the role of vegetation in the water balance of montane catchments. *Ecohydrology*. 1, 187-192.
- Brown, L.R., Bezuidenhout, H., 2020. Grassland Vegetation of Southern Africa. *Encyclopedia of the World's Biomes*. 3, 814-826.
- Burba, G.G., Verma, S.B., 2005. Seasonal and interannual variability in evapotranspiration of native tallgrass prairie and cultivated wheat ecosystems. *Agricultural and Forest Meteorology*. 135, 190-201.
- Burt, T.P., McDonnell, J.J., 2015. Whither field hydrology? The need for discovery science and outrageous hydrological hypotheses. *Water Resource Research*. 51, 5919-5928.
- Castellví, F., 2004. Combining surface renewal analysis and similarity theory: A new approach for estimating sensible heat flux. *Water Resources Research*. 40(5), W05201.

- Castellví, F., 2011. Is it worthy to apply different methods to determine latent heat fluxes? – A study case over a peach orchard. *Evapotranspiration-From Measurements to Agricultural and Environmental Applications*. 43-58.
- Castellví, F., Perez, P.J., Ibañez, M., 2002. A method based on high frequency temperature measurements to estimate sensible heat flux avoiding the height dependence. *Water Resources Research*. 38(6), WR000486-20.
- Castellví, F., Snyder, R.L., 2009a. On the performance of surface renewal analysis to estimate sensible heatflux over two growing rice fields under the influence of regional advection. *Journal of Hydrology*. 375, 546-553.
- Castellví, F., Snyder, R.L., 2009b. Combining the dissipation method and surface renewal analysis to estimate scalar fluxes from the time traces over rangeland grass near Ione (California). *Hydrological Processes*. 23, 842-857.
- Chemura, A., Rwasoka, D., Mutanga, O., Dube, T., Mushore, T., 2020. The impact of land-use/land cover changes on water balance of the heterogenous Buzi sub-catchment, Zimbabwe. *Remote Sensing Applications: Society and Environment*. 18, 100292.
- Dallas, H.F., Rivers-More, N., 2014. Ecological consequences of global climate change for freshwater ecosystems in South Africa. *South Africa Journal of Science*. 110(5/6), 1-11.
- Delago, J., Llorens, P., Nord, G., Calder, I.R., Gallart, F., 2010. Modelling the hydrological response of a Mediterranean medium-sized headwater basin subject to land cover change: The Cardener River Basin (NE Spain). *Journal of Hydrology*. 383, 125-134.
- De Villiers, A.D., O'Connor, T., 2011. Effect of a single fire on woody vegetation in Catchment IX, Cathedral Peak, KwaZulu-Natal Drakensberg, following extended partial exclusion of fire. *African Journal of Range and Forage Science*. 28(3), 111-120.
- Ehret, U., Gupta, H.V., Sivapalan, M., Weijs, S.V., Schymanski, S.J., Blöschl, G., Gelfan, A.N., Harman, C., Kleidon, A., Bogaard, T.A., Wang, D., Wagener, T., Scherer, U., Zehe, E., Bierkens, M.F.P., Di Baldassarre, G., Parajka, J., van Beek, L.P.H., van Griensven, A., Westhoff, M.C., Winsemius, H.C., 2014. Advancing catchment hydrology to deal with predictions under change. *Hydrology and Earth System Science*. 18, 649-671.
- Engelbrecht, F., 2019. Green Book – Detailed Projections of Future Climate Change over South Africa. Technical report, Pretoria: CSIR.
- Fischer, J.B., Melton, F., Middleton, E., Hain, C., Anderson, M., Allen, R., McCabe, M.F., Hoo, S., Baldocchi, D., Townsend, P.A., Kilic, A., Tu, K., Miralles, D.D., Perret, J., Lagouarde, J.P., Waliser, D., Purdy, A.J., French, A., Schimel, D., Famiglietti, J.S., Stephens, G., Wood, E.F., 2016. The future of evapotranspiration: Global requirements for ecosystem functioning, carbon and climate feedbacks, agricultural management, and water resources. *Water Resources Research*. 53, 2618-2626.
- Gallegos, S.C., Hensen, I., Saavedra, F., Schleuning, M., 2015. Bracken fern facilitates tree seedling recruitment in tropical fire-degraded habitats. *Forest Ecology and Management*. 337, 135-143.

- Gleeson, T., Wang-Erlandsson, L., Porkka, M., Zipper, S.C., Jaramillo, F., Gerten, D., Fetzer, I., Cornell, S.E., Piemontese, L., Gordon, L.J., Rockstrom, J., Oi, T., Sivapalan, M., Wada, Y., Brauman, K.A., Florke, M., Bierkens, M.F.P., Lehner, B., Keys, P., Kummu, M., Wagener, T., Dadson, S., Troy, T.J., Steffen, W., Falkenmark, M., Famiglietti, J.S., 2020. Illuminating water cycle modifications and Earth system resilience in the Anthropocene. *Water Resources Research*. 56, e2019WR024957.
- Gordijn, P.J., Everson, T.M., O'Connor, T.G., 2018. Resistance of Drakensberg grasslands to compositional change depends on the influence of fire-return interval and grassland structure on richness and spatial turnover. *Perspectives in Plant Ecology, Evolution and Systematics*. 34, 26-36.
- Grab, S.W., Knight, J., 2018. Southern African montane environments. *Southern African Landscapes and Environmental Change*. Routledge, United Kingdom.
- Gu, W., Liu, J., Lin, H., Lin, J., Liu, H., Liao, A., Wang, N., Wang, W., Ma, T., Yang, N., Li, X., Zhuo, P., Cai, Z., 2018. Why Hydrological Maze: The Hydropedological Trigger? Review of Experiments at Chuzhou Hydrology Laboratory. *Vadose Zone Journal*. 17, 170174.
- Gwate, O., Mantel, S.K., Gibson, L.A., Munch, Z., Palmer, A.R., 2018. Exploring dynamic of evapotranspiration in selected land cover classes in a sub-humid grassland: A case study in quaternary catchment S50E, South Africa. *Journal of Arid Environments*. 157, 66-76.
- Haro-Montegudo, D., Palazon, L., Begueria, S., 2020. Long-term sustainability of large water resource systems under climate change: A cascade modeling approach. *Journal of Hydrology*. 582, 124546.
- Haymann, N., Lukyanov, V., Tanny, J., 2019. Effects of variable fetch and footprint on surface renewal measurements of sensible and latent heat fluxes in cotton. *Agricultural and Forest Meteorology*. 268, 63-73.
- Hewitson, B., Crane, R.G., 2006. Consensus between GCM climate change projections with empirical downscaling: Precipitation downscaling over South Africa. *International Journal of Climatology*. 26, 1315-1337.
- Hoffman, M.T., Todd, S., 2000. A National Review of Land Degradation in South Africa: The Influence of Biophysical and Socio-economic Factors. *Journal of Southern African Studies*. 26(4), 743-758.
- Hu, Y., Buttar, N.A., Tanny, J., Snyder, R.L., Savage, M.J., Lakhari, I.A., 2018. Surface renewal application for estimating evapotranspiration: A review. *Advances in Meteorology*. 2018, 1-11.
- Huber, U.M., Bugmann, K.M., Reasoner, M.A., 2005. *Global change and mountain regions: an overview of current knowledge*, Springer, Dordrecht, Netherlands.
- Hughes, D.A., Jewitt, G., Mahe, G., Mazvimavi, D., Stisen, S., 2015. A review of aspects of hydrological sciences research in Africa over the past decade. *Hydrological Sciences Journal*. 60(11), 1865-1879.

- Kelleher, C., Wagener, T., McGlynn, B., 2015. Model-based analysis of the influence of catchment properties on hydrologic partitioning across five mountain headwater subcatchments. *Water Resources Research*. 51, 4109-4136.
- Kelley, J., Higgins, C., 2018. Computational efficiency for the surface renewal method. *Atmospheric Measurement Techniques*. 11, 2151-2158.
- Kirchner, J.W., 2006. Getting the right answers for the right reasons: Linking measurements, analyses, and models to advance the science of hydrology. *Water Resources Research*. 42, W03S04.
- Le Maitre, D.C., Blignaut, J.N., Clulow, A., Dzikiti, S., Everson, C.S., Gorgens, A.H.M., Gush, M.B., 2020. Impacts of Plant Invasions on Terrestrial Water Flows in South Africa. In *Biological Invasions in South Africa*. Springer, Cham.
- Li, G., Zhang, F., Jing, Y., Liu, Y., Sun, G., 2017. Response of evapotranspiration to changes in land use and land cover and climate in China during 2001-2013. *Science of the Total Environment*. 596-597, 256-265.
- Lumsden, T.G., Schulze, R.E., Hewitson, B.C., 2009. Evaluation of potential changes in hydrologically relevant statistics of rainfall in southern Africa under conditions of climate change. *Water SA*. 35, 649-656.
- McGlone, M.S., Wilmshurst, J.M., Leach, H.M., 2005. An ecological and historical review of bracken (*Pteridium esculentum*) in New Zealand, and its cultural significance. *New Zealand Journal of Ecology*. 29(2), 165-184.
- Mengistu, M.G., Savage, M.J., 2010. Surface renewal method for estimating sensible heat flux. *Water SA*. 36(1), 9-18.
- Midgley, G.F., Chapman, R.A., Hewitson, B., Johnston, P., De Wit, M., Ziervogel, G., Mukheibir, P., Van Niekerk, L., Tadross, M., van Wilgen, B., 2005. A status quo, vulnerability and adaptation assessment of the physical and socio-economic effects of climate change in the Western Cape. Report to the Western Cape Government, Cape Town, South Africa.
- Montanari, A., Young, G., Savenije, H.H.G., Hughes, D., Wagener, T., Ren, L.L., Koutsoyiannis, D., Cudennec, C., Toth, E., Grimaldi, S., Blöschl, G., Sivapalan, M., Beven, K., Gupta, H., Hipsey, M., Schaeffli, B., Arheimer, B., Boegh, E., Schymanski, S.J., Di Baldassarre, G., Yu, B., Hubert, P., Huang, Y., Schumann, A., Post, D.A., Srinivasan, V., Harman, C., Thompson, S., Rogger, M., Viglione, A., McMillan, H., Characklis, G., Pang, Z., and Belyaev, V., 2013. "Panta Rhei-Everything Flows": Change in hydrology and society-The IAHS Scientific Decade 2013-2022. *Hydrological Sciences Journal*. 58(6), 1256-1275.
- Morán, A., Ferreyra, R., Sellés, G., Salgado, E., Cáceres-Mella, A., Poblete-Echeverría, C., 2020. Calibration of the Surface Renewal Method (SR) under Different Meteorological Conditions in an Avocado Orchard. *Agronomy*. 10, 730.
- Moran-Tejeda, E., Zabalza, J., Rahman, K., Gago-Silva, A., Lopez-Moreno, J.I., Vincente-Serrano, S., Lehmann, A., Tague, C.L., Beniston, M., 2014. Hydrological impacts of climate

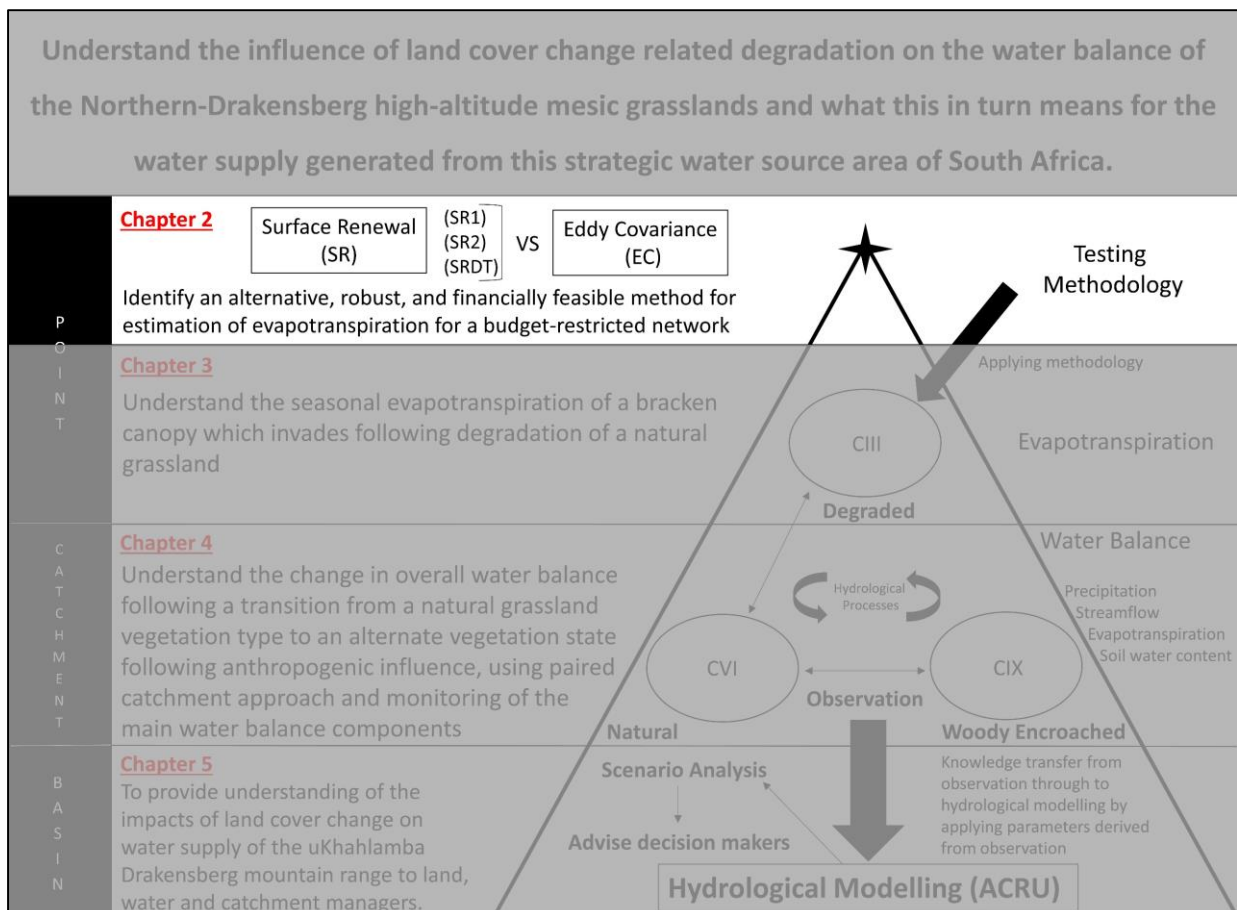
- and land-use changes in a mountain watershed: uncertainty estimation based on model comparison. *Ecohydrology*. 8(8), 1396-1416.
- Nanni, U.W., 1956. Forest Hydrological Research at the Cathedral Peak Research Station. *Journal of the South African Forestry Association*. 27(1), 2-35.
- Nazemi, A., Wheather, H.S., Chun, K.P., Bonsal, B., Mekonnen, M., 2017. Forms and drivers of annual streamflow variability in the headwaters of Canadian Prairies during the 20th century. *Hydrological Processes*. 31, 221-239.
- Nel, J.L., Le Maitre, D.C., Roux, D.J., Colvin, C., Smith, J.S., Smith-Adao, L.B., Maherry, A., Sitas, N., 2017. Strategic water source areas for urban water security: Making the connection between protecting ecosystems and benefiting from their services. *Ecosystem Services*. 28, 251-259.
- Olsson, L., Barbosa, H., Delusca, K., Flores-Renteria, D., Hermans, K., Jobbagy, E., Kurz, W., Li, D., Sonwa, D.J., Stringer, L., 2019. Land Degradation. In: *Climate Change and Land: An IPCC special report on climate change, desertification, land degradation, sustainable land management, food security, and greenhouse gas fluxes in terrestrial ecosystems*. [Shukla, P.R., Skea, J., Calvo Buendia, E., Masson-Delmotte, V., Portner, H.O., Roberts, D.C., Zhai, P., Slade, R., Connors, S., van Diemen, R., Ferrat, M., Haughey, E., Luz, S., Neogi, S., Pathak, M., Petzold, J., Portugal Pereira, J., Vyas, P., Huntley, E., Kissick, K., Belkacemi, M., Malley, J., (eds)] In press.
- Paw U, K.T., Qiu, J., Su, H.B., Watanabe, T., Brunet, Y., 1995. Surface renewal analysis: a new method to obtain scalar fluxes. *Agricultural and Forest Meteorology*. 74, 119-137.
- Poblete-Echeverría, C., Sepúlveda-Reyes, D., Ortega-Farías, S., 2014. Effect of height and time lag on the estimation of sensible heat flux over drip-irrigated vineyard using the surface renewal (SR) method across distinct phenological stages. *Agricultural Water Management*. 141, 74-83.
- Pozníková, G., Fischer, M., van Kesteren, B., Orság, M., Hlavinka, P., Žalud, Z., Trnka, M., 2018. Quantifying turbulent energy fluxes and evapotranspiration in agricultural field conditions: A comparison of micrometeorological methods. *Agricultural Water Management*. 209, 249-263.
- Rosa, R., Tanny, J., 2015. Surface renewal and eddy covariance measurements of sensible and latent heat fluxes of cotton during two growing seasons. *Biosystems Engineering*. 136, 149-161.
- Schulze, R.E., 2003. *Modelling as a Tool in Integrated Water Resources Management: Conceptual Issues and Case Study Applications*. Water Research Commission, Pretoria, South Africa. 749/1/04.
- Schulze, R.E., 2011. A perspective on climate change and the South African water sector. Water Research Commission report 1843/2/11. Pretoria, South Africa.
- Sivapalan, M., 2003. Prediction in ungauged basins: a grand challenge for theoretical hydrology. *Hydrological processes*. 17, 3163-3170.

- Snyder, R.L., Spano, D., Paw U, K.T., 1996. Surface renewal analysis for sensible and latent heat flux density. *Boundary-Layer Meteorology*. 77, 249-266.
- Snyder, R.L., Spano, D., Duce, P., Paw U, K.T., Rivera, M., 2008. Surface Renewal Estimation of Pasture Evapotranspiration. *Journal of Irrigation and Drainage Engineering*. 134(6), 716-721.
- Spano, D., Snyder, R.L., Duce, P., Paw U, K.T., 2000. Estimating sensible and latent heat flux densities from grapevine canopies using surface renewal. *Agricultural and Forest Meteorology*. 104, 171-183.
- Suvočarev, K., Castellví, F., Reba, M.L., Runkle, B.R.K., 2019. Surface renewal measurements of H , λE and CO_2 fluxes over two different agricultural systems. *Agricultural and Forest Meteorology*. 279, 107763.
- Tetzlaff, D., Carey, S.K., McNamara, J.P., Laudon, H., Soulsby, C., 2017. The essential value of long-term experimental data for hydrology and water management. *Water Resources Research*. 53, 2598-2604.
- Toucher, M.L., Clulow, A., Van Rensburg, S., Morris, F., Gray, B., Majozi, S., Everson, C.E., Jewitt, G.P.W., Taylor, M.A., Mfeka, S., Lawrence, K., 2016. Establishment of a more robust observation network to improve understanding of global change in the sensitive and critical water supply area of the Drakensberg. 2236/1/16. Water Research Commission, Pretoria, South Africa.
- Turpie, J., Benn, G., Thompson, M., Barker, N., 2021. Accounting for land cover changes and degradation in the Katse and Mohale Dam catchments of the Lesotho highlands. *African Journal of Range & Forage Science*. 38(1), 53-66.
- van Beuskom, A.E., Hay, L.E., Viger, R.J., Gould, W.A., Collazo, J.A., Khalyani, A.H., 2014. The effects of changing land cover on streamflow simulation in Puerto Rico. *Journal of the American Water Resources Association*. 50(6), 1575-1593.
- Wagener, T., Sivapalan, M., Troch, P., Woods, R., 2007. Catchment Classification and Hydrologic Similarity. *Geography Compass*. 1(4). 901-931.
- Wagener, T., Sivapalan, M., Troch, P.A., McGlynn, B.L., Harman, C.J., Gupta, H.V., Kumar, P., Rao, P.S.C., Basu, N.B., Wilson, J.S., 2010. The future of hydrology: An evolving science for a changing world. *Water Resources Research*. 46, W05301.
- Warburton, M.L., Schulze, R.E., Jewitt, G.P.W., 2012. Hydrological impacts of land use change in three diverse South African catchments. *Journal of Hydrology*. 414-415, 118-135.
- World Meteorological Organization., 2021. Water: Eight Ambitions. Available at <https://public.wmo.int/en/our-mandate/water> [Accessed 25 July 2021].
- Yalew, S.G., Pilz, T., Schweitzer, C., Lierschl, S., van der Kwast, J., van Griensven, A., Mul M.L., Dickens, C., van der Zaag, P., 2018. Coupling land-use change and hydrologic models for quantification of catchment ecosystem services. *Environmental Modelling and Software*. 109, 315-328.
- Yang, Q., Tian, H., Friedrichs, M.A.M., Liu, M., Li, X., Yang, J., 2015. Hydrological responses to climate and land-use changes along the Northern American East Coast: A 110-year

- historical reconstruction. *Journal of the American Water Resources Association*. 51(1), 47-67.
- Yang, L., Feng, Q., Yin, Z., Wen, X., Si, J., Li, C., 2017. Identifying separate impacts of climate and land use/cover change on hydrological processes in upper stream of Heihe River, Northwest China. *Hydrological Processes*. 31, 1100-1112.
- Yin, J., He, F., Xiong, Y.J., Qiu, G.Y., 2017. Effects of land use/land cover and climate changes on surface runoff in a semi-humid and semi-arid transition zone in northwest China. *Hydrology and Earth System Sciences*. 21, 183-196.
- Zapata, N., Martínez-Cob, A., 2002. Evaluation of the surface renewal method to estimate wheat evapotranspiration. *Agricultural Water Management*. 55, 141-157.
- Zhang, Y.K., Schilling, K.E., 2006. Effects of land cover on water table, soil moisture, evapotranspiration, and groundwater recharge: A Field observation and analysis. *Journal of Hydrology*. 319, 328-338.
- Zou, C.B., Turton, D.J., Will, R.E., Engle, D.M., Fuhlendorf, S.D., 2014. Alteration of hydrological processes and streamflow with juniper (*Juniperus virginiana*) encroachment in a mesic grassland catchment. *Hydrological processes*. 28, 6173-6182.

Lead in to Chapter 2

To achieve the overall aim of this thesis, it is necessary to start with identifying a methodology to observe and measure the individual water balance components. A first step and a specific objective of Chapter 2 was to identify a robust and financially feasible alternative methodology to eddy covariance (EC) to estimate the evapotranspiration (ET) of the *Leucosidea sericea* (woody) and *Pteridium aquilinum* (bracken). Chapter 2 details the comparisons between the well-accepted but costly and stringent EC method and the three methodologies of the alternative, cheaper and simpler surface renewal (SR) approach. The independent surface renewal dissipation theory (SRDT) methodology was identified as the best and most financially feasible alternative to EC. The SRDT method was selected as the methodology for the estimation of the water and energy balance component ET moving forward within this thesis.



2. THE POTENTIAL OF SURFACE RENEWAL FOR DETERMINING SENSIBLE HEAT FLUX FOR INDIGENOUS VEGETATION FOR A FIRST-ORDER MONTANE CATCHMENT

Abstract

Eddy covariance (EC) systems are expensive and not financially viable in a budget-restricted hydrological monitoring network. The surface renewal (SR) method is a cheaper alternative that requires a reduced fetch, but is currently dependent on EC for calibration. The SR methods not requiring calibration (surface renewal 2 (SR2) and surface renewal dissipation theory (SRDT)) have been used, but are not widely tested over indigenous vegetation. The aim of this research was to test the SR approach as a viable alternative to EC for the estimation of sensible heat flux (H) over indigenous vegetation (*Leucosidea sericea*) in a montane catchment for unstable periods. For a summer (7 d) and winter (9 d) campaigns, the three SR methods showed a good relationship with the EC method for the estimation of H . Overall, the SRDT method was the most viable alternative to EC and produced acceptable estimates of H over an indigenous vegetation canopy in a montane catchment.

Keywords: *eddy covariance, energy balance, dissipation method, uKhahlamba-Drakensberg mountain range, budget-restricted monitoring network.*

2.1 Introduction

Environmental change is significantly affecting the strategic water source areas of South Africa (Le Maitre *et al.* 2018). Changes in land cover alter the water balance of an area, with evapotranspiration (ET) being one of the components considerably affected (Zhang and Schilling 2006, Chemura *et al.* 2020). Therefore, estimates of ET and the changes thereof under environmental change are becoming increasingly important, particularly for first-order montane catchments.

Widely used eddy covariance (EC) systems are the benchmark in ET measurement methods as they provide a direct measurement of sensible heat flux (H) and latent energy flux (LE) (Zapta and Martínez-Cob 2002, Rosa and Tanny 2015, Hu *et al.* 2018, Pozníková *et al.* 2018, Buttar *et al.* 2019). Estimates of ET using EC systems can be validated against itself through

the measurement of H and then by closing the surface energy balance if the remaining energy balance components are known (Hu *et al.* 2018, Pozníková *et al.* 2018). However, there are several challenges associated with EC systems such as the requirement for a suitably large fetch area (Liu *et al.* 2013), with cost being the greatest challenge in developing countries. Due to the cost of EC systems, it is often prohibitive to incorporate them in long-term monitoring networks in financially strained developing countries, as when systems are purchased, they are often shared between several research projects, both within and across institutions. Added risks of remote mountainous areas, such as fire and theft, limit the ability to install an expensive and highly valued piece of equipment for long periods. It is often in these developing countries where the need for ET (or all environmental) data is greatest due to issues such as water scarcity, widespread and rapid landcover change, and degradation. South Africa is an example of such a water scarce, developing country where the financial resources available for monitoring equipment are low but the need for data is great, particularly to allow for efficient management of the strategic water source areas to maximise water availability. There is a need to identify a cheaper method, with reduced fetch requirements which works in the often-undulating mountainous terrain of the strategic water source areas. In response to this challenge and the others associated with EC systems, alternative, more cost-effective methods for estimating ET , through measurement of H , are being used more widely by disciplines outside micrometeorology such as ecophysiological, ecohydrological, agricultural and forest studies (Pozníková *et al.* 2018).

Currently there are several alternative methods for the measurement and estimation of ET , e.g.: weighing lysimeter, Bowen ratio, optical scintillation (OS) and surface renewal (SR) (Liu *et al.* 2013, Hu *et al.* 2018). Use of the weighing lysimeter and OS, require expensive sensors, which are sensitive and susceptible to damage, while also requiring a uniform canopy and large fetch (Hu *et al.* 2018). Compared to the other methods listed, OS is difficult and time consuming to install and set up (Pozníková *et al.* 2018).

An alternative method for the estimation of ET is SR. This method has become more widely used (Hu *et al.* 2018), and is considered to be the leading alternative to EC for estimation of ET (Castellví and Snyder 2009b, Clulow *et al.* 2012, Suvočarev *et al.* 2014, Hu *et al.* 2018). Due to the simpler nature of the equipment required, SR is a cheaper alternative to EC (Paw U *et al.* 1995, Suvočarev *et al.* 2019) by up to 75 %. The SR method makes use of high-frequency air temperature measurements in close proximity to the top of the canopy, and is able to estimate H , by identifying ramp events within the high-frequency temperature data caused by an

exchange of fluxes (Paw U *et al.* 1995, Snyder *et al.* 1996, Spano *et al.* 2000, Hu *et al.* 2018). The SR method is able to operate with the sensors in either the roughness sublayer or the inertial sublayer (Paw U *et al.* 1995, Castellví and Snyder 2009a, Suvočarev *et al.* 2019), implying that there is no need to change the positioning of the sensor with canopy growth, provided the canopy height does not exceed sensor height (Castellví 2004). Whereas EC, is required to be within the inertial sublayer (Castellví 2011, Suvočarev *et al.* 2014). Further to this, SR has fewer requirements that need to be met in order to operate accurately. For example, the EC method requires a large fetch, homogeneous surface or canopy, sensor levelling and orientation, and relatively flat terrain topography, to be able to accurately measure *ET* (Poblete-Echeverría *et al.* 2014, Suvočarev *et al.* 2019). In contrast, SR has been shown to be less sensitive to inadequate fetch, does not require a homogeneous site and can be used over a heterogenous canopy (Snyder *et al.* 2015). Both SR and EC are sensitive to humid conditions, especially rainfall and mist (Liu *et al.* 2013, Hu *et al.* 2018). The EC method is also sensitive to insects, dirt, and low wind speed conditions (Paw U *et al.* 1995, Zapata and Martínez-Cob 2001, Hu *et al.* 2018).

The first SR approach, referred to as SR1 (Paw U *et al.* 1995, Snyder *et al.* 1996, detailed later) requires calibration with an independent measure of *H* (Castellví and Snyder 2009b) such as EC, which is an overwhelming restriction of the method. However, the more recently developed SR approaches, SR2 (Castellví *et al.* 2002, Castellví 2004, detailed later) and Surface Renewal Dissipation Theory (SRDT) method (Castellví and Snyder 2009b, detailed later) do not require calibration of *H* and are therefore independent of EC measurements. However, testing over different surface types and under varying climate conditions is still required to verify these approaches (Mengistu and Savage 2010b, Hu *et al.* 2018). The EC measurement is a necessity for the estimation of an α value required as a correction/weighting factor for the SR1 approach to correct H_{SR} for the uneven heating or cooling of the air parcel measured by the sensor (Spano *et al.* 2000, Mengistu and Savage 2010b, Hu *et al.* 2018).

In early literature, on the SR1 method during the 1990s, it was understood that α was close to 0.5 for tall and 1.0 for short canopy vegetation, when high frequency temperature measurements are taken at canopy level (Paw U *et al.* 1995, Snyder *et al.* 1996). However, later research showed this to vary based on canopy architecture, vegetation growth stage, sensor height, lag time used and thermocouple type and thickness (Spano *et al.* 2000, Zapata and Martínez-Cob 2001, Zapata and Martínez-Cob 2002, Barbagallo *et al.* 2009, Castellví and Snyder 2010, Mengistu and Savage 2010b, Shapland *et al.* 2012, Rosa *et al.* 2013, Poblete-

Echeverría *et al.* 2014, Shapland *et al.* 2014, Rosa and Tanny 2015, Haymann *et al.* 2019), but to be independent of climate. Thus α , can be transferred between sites provided there are no significant changes in canopy architecture or type (Mengistu and Savage 2010b). However, α is dependent on stability conditions, requiring calculation for both stable and unstable conditions (Castellví and Martínez-Cob 2005, Mengistu and Savage 2010b, Shapland *et al.* 2012). Under stable conditions α tends to be smaller than under unstable conditions (Shapland *et al.* 2014, Suvočarev *et al.* 2014), due to the better mixing of the air parcel under unstable conditions (Suvočarev *et al.* 2019). Some studies suggest that α decreases with an increase in sensor height (Spano *et al.* 2000, Zapata and Martínez-Cob 2001, Rosa *et al.* 2013), while some literature reports an increase with sensor height (Shapland *et al.* 2012). The α value has been determined for several agricultural crops, rangeland grasslands, teff grass, bare soil, wetlands and an open water reservoir (Spano *et al.* 2000, Zapata and Martínez-Cob 2001, Zapata and Martínez-Cob 2002, Mengistu and Savage 2010a, Clulow *et al.* 2012, Rosa *et al.* 2013, Poblete-Echeverría *et al.* 2014, Shapland *et al.* 2014, Suvočarev *et al.* 2014, Rosa and Tanny 2015, Pozníková *et al.* 2018, Haymann *et al.* 2019, Suvočarev *et al.* 2019) with values ranging from 0.07 over bare soil (Shapland *et al.* 2014), to 2.47 over a tomato crop (Rosa *et al.* 2013).

Several studies have demonstrated that following calibration and the estimation of α , the H_{SR} estimated using the SR1 approach, shows a good fit to H_{EC} across several different canopies and agricultural crops (Spano *et al.* 2000, Zapata and Martínez-Cob 2001, Barbagallo *et al.* 2009, Rosa *et al.* 2013, Poblete-Echeverría *et al.* 2014, Shapland *et al.* 2014, Linquist *et al.* 2015, Rosa and Tanny 2015, Buttar *et al.* 2019, Haymann *et al.* 2019). The difference between H_{SR1} and H_{EC} vary with sensor height and lag used (Spano *et al.* 2000, Zapata and Martínez-Cob 2001). Common agreement in literature is that the difference between H_{SR} and H_{EC} decreases with sensor height, which is related to the changes in α as mentioned above (Zapata and Martínez-Cob 2001, Castellví and Snyder 2010, Rosa *et al.* 2013). The SR2 method has also been shown to perform well against H_{EC} (Castellví and Martinz-Cob 2005, Castellví and Snyder 2009a, Castellví and Snyder 2010, Castellví 2011). However, the SR2 method was found to overestimate H_{SR} under unstable conditions (Castellví and Snyder 2009a, Castellví and Snyder 2010), and underestimate H_{SR} under stable conditions (Castellví and Snyder 2010). Other findings have shown this to not always hold true (Castellví 2011, Castellví and Snyder 2009c).

Given the above, SR has significant potential to be a strong alternative to EC for the estimation of ET . Due to the reduced cost, along with reduced fetch and lower maintenance

requirement, the SR method also provides the opportunity for replication across several sites at the same time (Castellví 2004, Suvočarev *et al.* 2019). Following the collection of data, SR data analysis processes are simpler compared to the EC method, with the EC method requiring several post-processing and quality control procedures. This makes SR more useful for personnel untrained in micrometeorology (Mbangiwa *et al.* 2019). These factors also make SR available to a much larger audience, where budget restraints have in the past, made *ET* measurements unattainable.

The aim of this research was to determine whether the surface renewal approach is a viable alternative to EC for the estimation of *H*, for use as a long-term approach for the estimation of *ET* over indigenous vegetation in a remote first-order montane location. This was achieved by calibrating the SR1 method using EC and comparing the resultant *H* values. Further to this, the performance of the EC independent SR approaches (SR2 and SRDT) in estimating *H* were evaluated.

2.2 Materials and Methods

2.2.1 Research site, vegetation and campaigns

The Cathedral Peak first-order montane research catchments (28°58'32.14" S; 29°14'8.72" E) are located on the "little berg plateau" (Nanni 1956) of the uKhahlamba-Drakensberg mountain range in KwaZulu-Natal, South Africa (Figure 2.1). The uKhahlamba-Drakensberg mountains are a strategic water source area for South Africa (Le Maitre *et al.* 2018), supplying water to both the KwaZulu-Natal and Gauteng provinces, with the latter being the key industrial area of South Africa (Heyns 2003, Gupta and van der Zaag 2008, Le Maitre *et al.* 2018). The Cathedral Peak catchments are long-term research catchments established in 1948 (Nanni 1956) to investigate the influence of land management on water. The catchments range in altitude from 1 822 to 2 454 m.a.s.l (Toucher *et al.* 2016) and experience a mean annual precipitation of 1 400 mm (Bosch 1979). Precipitation is largely driven by convective thunderstorms or orographic mechanisms, with the majority of rainfall occurring in summer (October to March) (Nanni 1956). Summers are therefore wet and humid, while winters are cold and dry (Toucher *et al.* 2016). The annual average air temperature for the research catchments is 13.8°C (Toucher *et al.* 2016). The original vegetation state of the Cathedral Peak research catchments was natural grassland of species *Themeda triandra* (Toucher *et al.* 2016), which is still the state in the undisturbed catchments.

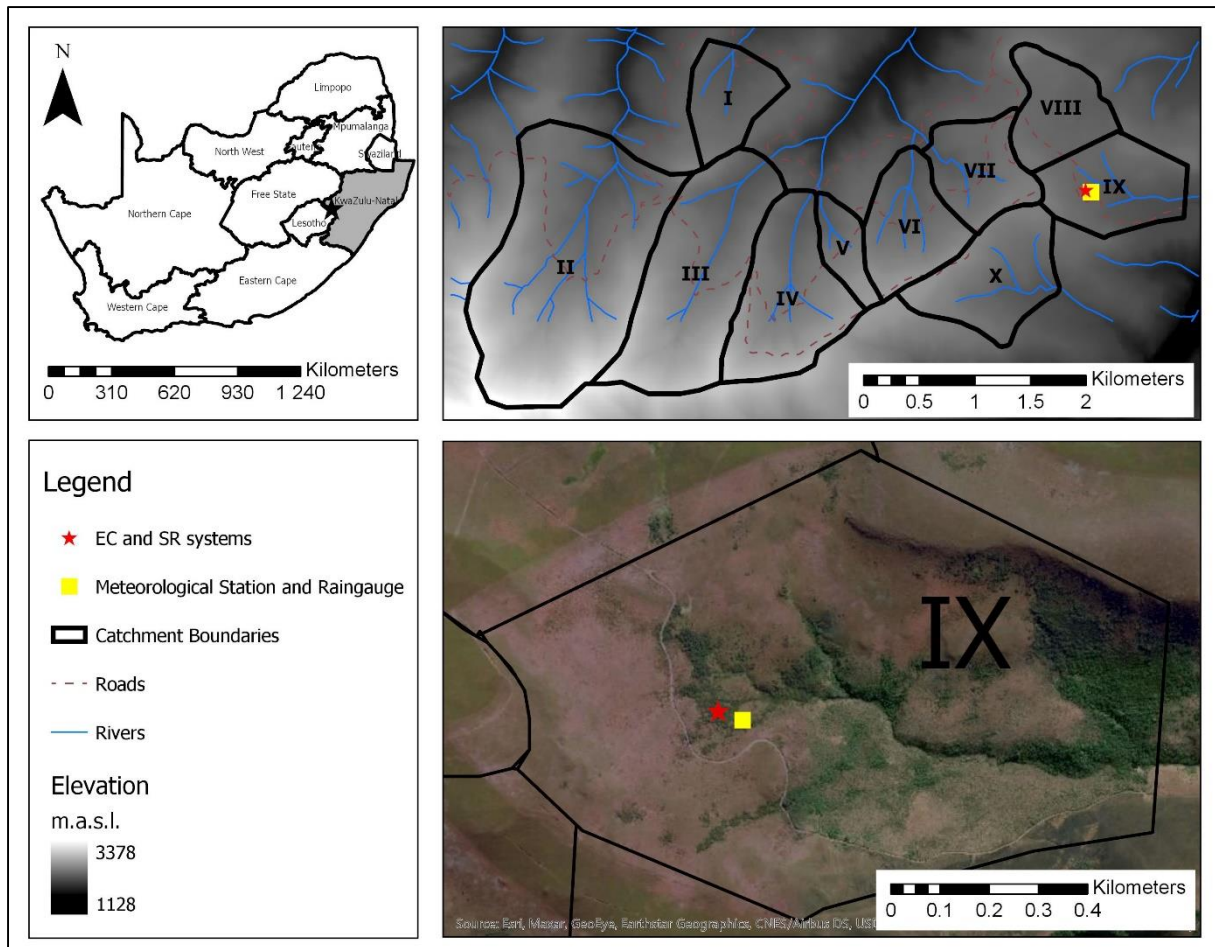


Figure 2.1: The location of the Cathedral Peak research catchment and, within them, the location of catchment IX. In the centre of the catchment, the location of the eddy covariance (EC) and surface renewal (SR) systems, meteorological station and raingauge.

A SR system (SRC9) was installed within catchment IX on the 13th of November 2018 (Figure 2.1). Historically, catchment IX was a natural grassland (De Villiers and O'Connor 2011), however the removal of fire from the grassland has moved the system towards a woody encroached landscape (De Villiers and O'Connor 2011). *Leucosidea sericea* has taken over from the natural grassland along the riparian and water course areas, and on the damper northern slopes. The canopy is heterogenous, with mixed vegetation dominated by *Leucosidea sericea*. Other vegetation types include *Buddleia salvifolia*, *Philippia evansii*, *Erica evansii* and *Pteridium aquilinum* (bracken) (De Villiers and O'Connor 2011, Toucher *et al.* 2016). The height of the *Leucosidea* averages 3.5 m. The height of the SR sensors was fixed over the measurement period as the *Leucosidea* is slow-growing. The data record for the SR system begins on 20 November 2018.

A calibration campaign was undertaken in both winter and summer where an EC system was installed alongside the SR system, and they recorded concurrently. The summer campaign was conducted from 21 to 29 January 2020 and the winter campaign from the 15 to 23 July 2020.

2.2.2 Equipment

The SRC9 system consisted of two type-E fine-wire thermocouples, placed 0.5 m and 1 m above the 3.5-m tall canopy, for high frequency (10 Hz) air temperature measurements. A four-component net radiometer (CNR4, Kipp & Zonen, Delft, The Netherlands) placed 2 m above the canopy, measured net radiation and albedo. Two 2-D sonic anemometers (ATMOS 22, Meter Environment, Pullman, USA), one placed at canopy level, and the other placed 2 m above canopy, provided a measurement of wind speed and direction and air temperature. The 2-D sonic placed at canopy height was used in the SR2 method. This equipment was installed on a 9-m lattice mast. To estimate the soil heat flux, two self-calibrating soil heat flux plates (HFP01SC-L, Hukseflux, Delft, Netherlands) were installed 0.08 m below the soil surface and 1 m apart, four soil temperature averaging probes, with two placed 0.06 m and another two placed 0.02 m below the soil surface and above each soil heat flux plate. A soil water reflectometer was installed between the soil heat flux plates at 0.025 m below the soil surface (CS616, Campbell, Logan, United States of America). The sensors were all coupled to a Campbell datalogger (CR1000).

A meteorological station (Met9) was installed 50 m from SRC9 in Catchment IX, consisting of a pyranometer (CMP3, Kipp & Zonen) positioned at 2 m to measure solar irradiance, relative humidity and air temperature sensor (CS215, Campbell) placed at 2 m within a 6-plate radiation shield, and a 2-D sonic anemometer (ATMOS 22) placed at 2 m to measure two-dimensional wind speed and air temperature. The meteorological station data were collected using a Campbell datalogger (CR300). A long-term Texas tipping-bucket raingauge (TE525, Texas Electronics, Texas United States of America) installed 1.2 m above the ground and close to the meteorological station (3-m distance) provided rainfall and intensity data.

The EC system used for the respective campaigns consisted of a Campbell datalogger (CR3000) programmed with the EasyFlux-DL program. A 3-D sonic anemometer (CSAT3A, Campbell) combined with an open-path gas analyser for H₂O and CO₂ fluxes (EC150, Campbell), which were both connected to an electronics panel (EC100, Campbell). The 3-D sonic anemometer and open-path gas analyser were installed 2 m above the canopy, alongside the SR systems on the lattice mast.

2.2.3 SR theory

The SR method uses high frequency air temperature measurements to determine H . High frequency temperature measurements are taken at up to 10 Hz (10 samples per a second), as this has been shown to produce the best results for the estimation of H (Mengistu and Savage 2010a, b, Rosa *et al.* 2013, Hu *et al.* 2018). The SR method is based on the premise that when a parcel of air comes into contact with the canopy surface, an exchange of fluxes occurs (Castellví and Snyder 2009b). In order to determine the scale of these fluxes, observations of a change in air temperature, which is a part of the exchange of fluxes, can be obtained (Paw U *et al.* 1995, Spano *et al.* 2000, Hu *et al.* 2018). The changes in air temperature are identified as ramps (Paw U *et al.* 1995, Snyder *et al.* 1996). Under unstable conditions, a parcel of air with a lower air temperature will make contact with a canopy which has a higher air temperature (Paw U *et al.* 1995, Snyder *et al.* 1996, Spano *et al.* 2000, Hu *et al.* 2018). As a result, air temperature observations by the fine-wire thermocouples positioned at canopy height will display a rapid decrease in air temperature, as the air parcel arrives, followed by a gradual warming as the exchange of fluxes occurs, one of which is sensible heat flux (Paw U *et al.* 1995, Hu *et al.* 2018). The sudden decrease in air temperature, followed by the gradual heating, forms a ramp-like appearance in the high-frequency air temperature data (Spano *et al.* 2000). This ramp is used to estimate H , which has occurred between the air parcel and the canopy (Paw U *et al.* 1995). Due to continuity, the air parcel will move back into the atmosphere and be replaced by another air parcel, creating a second ramp in the air temperature data (Paw U *et al.* 1995, Snyder *et al.* 1996, Hu *et al.* 2018). This process continues, creating several ramp events in the high frequency air temperature data. A ramp event consists of a quiescent period (s) when conditions are stationary and no change in air temperature is occurring (Paw U *et al.* 1995, Castellví 2004). This is the period when a new air parcel has arrived, and is settling, before it begins to be heated/cooled by the canopy (Paw U *et al.* 1995, Castellví 2004). The quiescent period is then followed by a ramp period (l) (when the air temperature increases for unstable conditions, or decreases in stable conditions, also referred to as inverse ramp frequency) (Savage 2017). The amplitude (a) of the ramp event and l , are determined from the second- (S_r^2), third- (S_r^3) and fifth-order (S_r^5) of the air temperature structure function (van Atta 1977, Savage 2017). The S_r^2 , S_r^3 and S_r^5 are determined in real-time, by lagging high frequency air temperature measurements, for each averaging period (Savage 2017). Time lags are determined from the scan rate and datalogger used (Savage 2017). These three factors form part of the equation to calculate sensible heat flux (H), combined with the density of air (ρ), measurement height (z), and specific heat capacity (c_p),

$$H = \rho_{air} z c_p \left(\frac{a}{s+l} \right) \quad (2.1)$$

with H determined for a chosen period of time (commonly half an hour) as the sum of H determined from each ramp event during that period (Paw U *et al.* 1995). Three SR approaches have been published for the estimation of H . Surface renewal 1 (SR1) uses high frequency air temperature measurements and the structure function theory (Paw U *et al.* 1995, Snyder *et al.* 1996). An uncorrected H value is estimated, which is then corrected for uneven heating of the air parcel below the fine-wire thermocouple by using the correction factor α (Spano *et al.* 2000, Mengistu and Savage 2010b, Hu *et al.* 2018). The α value is determined through calibration where both the SR and EC systems, measure over the same canopy for a set time period (Hu *et al.* 2018). The slope of the regression forced through 0, between uncorrected H from SR1 and the H measured by the EC, is regarded as the α value (Hu *et al.* 2018).

The surface renewal 2 (SR2) approach (Castellví *et al.* 2002, Castellví 2004) uses high frequency air temperature measurements and structure function theory like SR1, but then uses the Monin-Obukhov Similarly Theory (MOST) to estimate H . The SR2 approach requires the interval mean and standard deviation of the horizontal windspeed above the canopy surface, as well as other descriptive canopy measurements, such as canopy height (h), canopy bottom height, and canopy leaf area index.

$$H = \rho_{air} c_p K_h \frac{dT}{dz} \quad (2.2)$$

where K_h is the turbulent transfer coefficient ($\text{m}^2 \text{s}^{-1}$) or eddy diffusivity for H and T the average air temperature (K) during the measurement time, d is the zero-plane displacement height ($2/3 h$) and z the height of the fine-wire thermocouple above the surface, these are all combined with components mentioned earlier to determine H , over a chosen time interval (Mengistu and Savage 2010b, Savage 2020). The advantages of the SR2 approach are that it is independent of EC and is not significantly affected by measurement height (Mengistu and Savage 2010b).

A third and simpler SR approach (described by Castellví and Snyder 2009b), which is also independent of EC, is the SRDT method. This approach also uses high frequency air

temperature measurements and structure function theory as does SR1, but then follows the dissipation method to estimate H . The only additional requirement, is the standard deviation of air temperature (σ_T) and the determination of zero plane displacement (d) (Castellví and Snyder 2009b). An α value can then be determined half-hourly (Castellví and Snyder 2009b):

$$\alpha = \frac{1.66 a (z-d)}{\pi z \sigma_T} \quad (2.3)$$

where a ($^{\circ}\text{C}$) is the scalar ramp amplitude, τ (s) is the scalar ramp total duration,

$$H = 1.66 \frac{a}{|a|} (z - d) \frac{\rho_{air} c_p a^2}{\pi \sigma_T \tau} \quad (2.4)$$

where H can be estimated for a chosen period of time (Mengistu and Savage 2010b, Savage 2017). From the estimation of sensible heat flux, by accounting for the other energy balance components, net radiation (R_n) and soil heat flux (G), LE can be calculated, which can then be used to estimate ET from the canopy when accounting for the latent heat of vaporisation (Castellví 2004) using the surface energy balance:

$$R_n - G = H + LE \quad (2.5)$$

The G component, which is the soil heat flux at the soil surface, is calculated as the soil heat flux at the location of the soil heat flux plate (80 mm) added to the soil storage (S) above the soil heat flux plate (Campbell Scientific, 2016):

$$G = G_{80mm} + S \quad (2.6)$$

The S term is calculated by accounting for the change in soil temperature (ΔT_s) over time (t), the depth of the measured soil heat flux (d), and the heat capacity of moist soil (C_s) (Campbell Scientific, 2016),

$$S = \frac{\Delta T_s C_s d}{t} \quad (2.7)$$

where C_s is calculated by considering the density of water (ρ_b), the heat capacity of dry mineral soil (C_d), the soil water content (θ_v), the heat capacity of water (C_w), and by sampling of the bulk density (ρ_b) of the soil at the site.

2.2.4 EC Theory

The EC method makes use of the ability to accurately measure the sensible and latent heat energy, transported and mixed by turbulence in the earth's atmospheric boundary layer (Drexler *et al.* 2004). Following the principle that scalar fluxes will be transported from the canopy top to the atmospheric boundary layer through vertical air movements, a correlation between vertical wind speed and the turbulent flux of water vapour (for the estimation of latent heat flux) and air temperature (for sensible heat flux) allows for the estimation of the respective scalar fluxes (Drexler *et al.* 2004). In order to adequately estimate the sensible and latent heat fluxes, the period over which the correlation is averaged needs to be longer than the time of the eddy responsible for the carrying of the scalar fluxes within the atmospheric boundary layer (Drexler *et al.* 2004). To achieve the estimation of sensible and latent heat flux, the EC system measures three wind speed components (u , v , w) and the sonic air temperature (T_s), as well as the specific humidity (q) and scalar concentration (Pozníková *et al.* 2018). As mentioned, the EC method makes use of the covariance between the turbulent component of the vertical wind speed (w') and turbulent component of the scalar (x'):

$$F_x = \overline{\rho w' x'} = \bar{\rho} \text{cov}(w, x) \quad (2.8)$$

F_x is the flux of quantity x ($\text{kg m}^{-2} \text{s}^{-1}$) (Pozníková *et al.* 2018), the scalar flux (x) represents $c_p T$ (J kg^{-1}) when estimating sensible heat flux, where c_p is the specific heat capacity of air at constant pressure ($\text{J kg}^{-1} \text{K}^{-1}$) and T is the air temperature (Pozníková *et al.* 2018), and the scalar flux (x) represents $L_v q$ (J kg^{-1}) when estimating the latent heat flux, where L_v is the specific latent heat of vaporisation (J kg^{-1}) and q is the specific humidity (kg kg^{-1}) (Pozníková *et al.* 2018).

2.2.5 Data analysis and processing

In order to estimate H using the SR systems, 10-Hz high frequency air temperature measurements taken using fine-wire thermocouples, were collected by the CR1000 datalogger. The S_r^2 , S_r^3 , and S_r^5 values at a 30-minute time interval were downloaded and inserted into a formulated SR excel spreadsheet for the SR1 (Savage 2017), SR2 (Savage 2020) and SRDT (Savage 2014) methods. The formulated SR excel spreadsheets were used for the estimation of H for both lag times of 0.4 and 0.8 s. The H determined by both time lags were averaged as it provided the better representation and lowest standard error. Calibration of the SR1 method was conducted for each stability condition and each lag time. The H values were then corrected and averaged to calculate one H value for each half-hour period.

The EC system was run and data were processed by the EasyFlux-DL program installed on the datalogger. The EasyFlux-DL is a Campbell program for their open-path EC systems with optional energy balance sensors. The EasyFlux-DL program uses a 10-Hz measurement frequency with the EC sensors. Further to this, the EasyFlux-DL program provides “fully corrected fluxes of CO₂, latent heat (H₂O), sensible heat, ground surface flux, and momentum” (Campbell Scientific, 2020), data quality grades which are based on steady state conditions, surface layer turbulence characteristics, and wind directions (Campbell Scientific, 2020). The EasyFlux-DL program filters and removes spikes in the raw 10-Hz data, applies the double rotation method for co-ordinate rotation, applies frequency response corrections, and applies correction to determine H from the measured sonic sensible heat flux (Campbell Scientific, 2020). The 30-min data were downloaded off the logger and analysed in an excel spreadsheet. Only the 30-min H -values, 30-min sample size, and 30-min H -value quality grade was considered. A 30-min H -value estimated by the EC system was removed if the sample size for that half-hour period was less than 30 %. In addition, any 30-min H -value with a quality grade rating provided by the EasyFlux-DL program (according to Foken *et al.* 2012) of 9 was removed. The remaining 30-min H -values were used in the comparison.

To calibrate and determine α for unstable and stable conditions required for the SR1 approach in both winter and summer, two campaigns were conducted. The summer campaign took place over seven days from 22/01/2020 to 28/01/2020, and the winter campaign took place over nine days from 15/07/2020 to 23/07/2020. The summer campaign was disturbed by afternoon thunderstorms on three of the days. A total of 15 mm of rainfall fell over the duration of the summer campaign. No rainfall fell during the winter campaign.

2.3 Results

2.3.1 SR1 calibration and validation

Two campaigns were conducted over the *Leucosidea* in Catchment IX. The summer campaign provided five full days (22-26/01/2020) for calibration and another two full days (27-28/01/2020) for validation. The winter campaign provided seven full days (15-21/07/2020) for calibration and two full days for validation (22-23/07/2020). Only unstable conditions are discussed, as they are required for the occurrence of ET , and the stable conditions were statistically insignificant. Unstable conditions were defined as periods where net radiation was positive ($R_n > 0$) and the third-order air temperature structure function under both lags, is negative ($S_r^3 < 0$) as given by Savage (2014). A negative S_r^3 value corresponds to a positive SR ramp amplitude and hence, positive H for unstable conditions. Linear regressions of the uncorrected H (HUC_{SR1}) estimated by the SR system was compared to the H (H_{EC}) measured by the EC system for both the summer and winter campaigns (Figure 2.2).

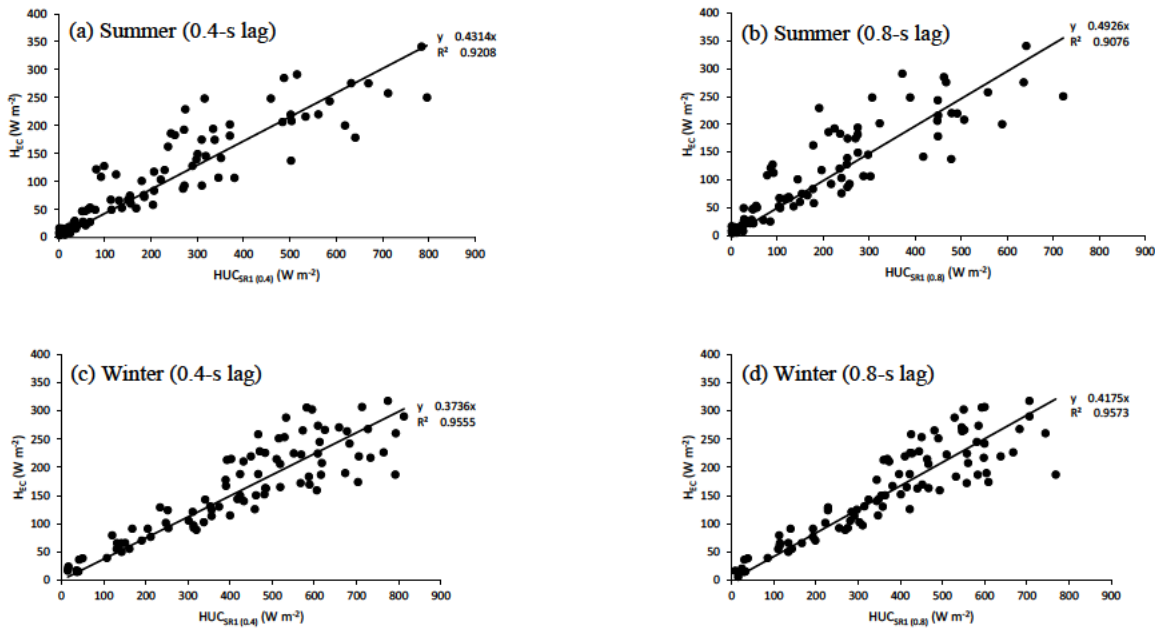


Figure 2.2: The calibration period between surface renewal 1 (SR1) and eddy covariance (EC) using the estimation and measurement of 30-min sensible heat flux (H) by the respective systems for unstable conditions during the summer campaign for the (a) 0.4- and (b) 0.8-s lag and winter campaign for the (c) 0.4- and (d) 0.8-s lag.

The α values were calculated for unstable conditions and for the respective lags over the two calibration periods (Table 2.1). The α values were smaller in winter than summer, with the larger lag producing a larger α . The α values were then applied to HUC_{SR1} half-hourly values for the 0.4- and 0.8-s lags, which were then averaged to calculate a corrected H (H_{SR1}), which was then used in the comparison with the other three methods, EC, SRDT and SR2 over the respective campaigns for unstable conditions.

Table 2.1: A summary of the α values calculated for the correction of the sensible heat flux (H) estimated by SR1 approach from the summer and winter campaigns for the 0.4- and 0.8-s lags under unstable conditions.

Condition	Unstable	
	α	
Lag (s)	0.4	0.8
Summer	0.43	0.49
Winter	0.37	0.42

Following correction of H for SR1, the α values were then applied to the two-day validation periods. The linear regressions for unstable conditions (Figure 2.3) between H_{SR1} and H_{EC} produced a good fit for both summer (slope = 0.91, intercept = 18.03 W m⁻²; R^2 = 0.86, RMSE = 30.48 W m⁻²) and winter (slope = 0.98; intercept = 19.23 W m⁻²; R^2 = 0.84; RMSE = 36.23 W m⁻²), indicating successful calibrations.

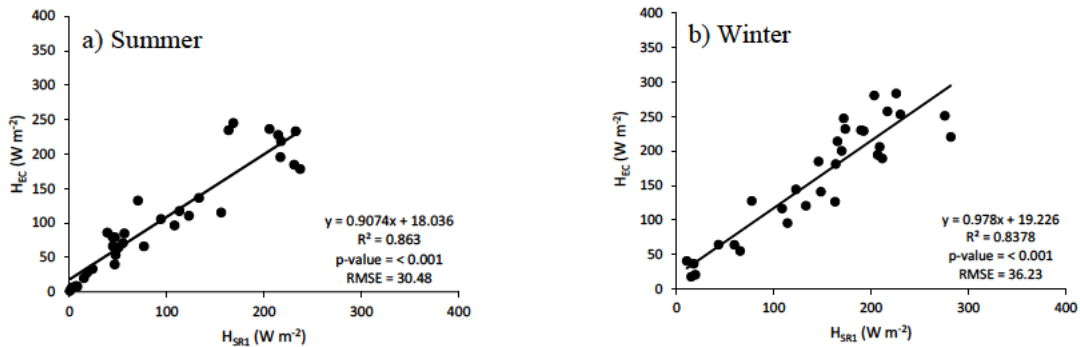


Figure 2.3: The linear regressions for unstable conditions showing the relationship between the corrected 30-min sensible heat flux (H) from surface renewal 1 (SR1) method against the H measured by the eddy covariance (EC) method for the two-day validation periods during the (a) summer and (b) winter campaigns.

2.3.2 Comparison of SR1, SRDT and SR2 with the benchmark EC

Following the calibration and validation of the estimation of H by the SR1 method, a comparison of the H estimated by all three SR approaches with the H estimated by EC for unstable conditions could be conducted. For the summer period, comparisons were made using the full seven days, and for the winter period, the full nine days, across both the calibration and validation period of SR1. Linear regressions (Figure 2.4) between the H estimated by the three SR approaches and H_{EC} , were used to understand the relationship between the different SR approaches and the EC method for estimating H .

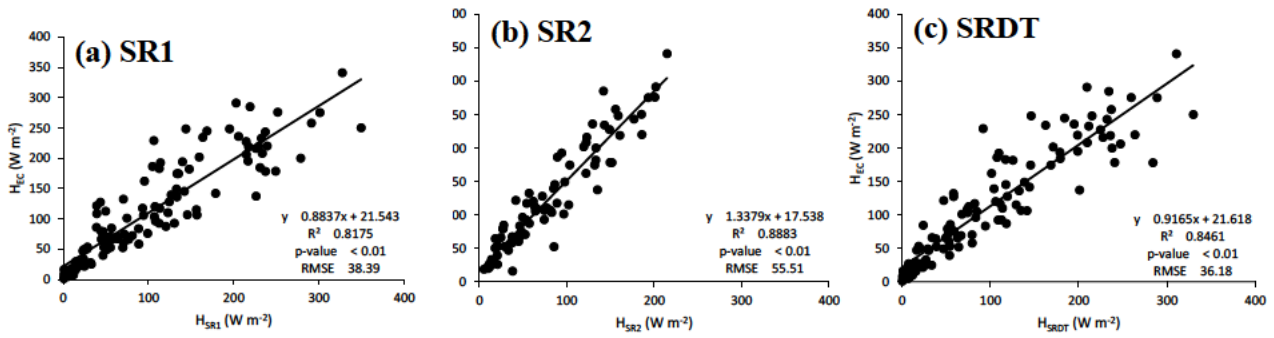


Figure 2.4: The relationship between the three surface renewal (SR) approaches and the eddy covariance (EC) method, using linear regressions between (a) sensible heat flux from surface renewal 1 (H_{SR1}), (b) sensible heat flux from surface renewal 2 (H_{SR2}), (c) sensible heat flux from surface renewal dissipation theory (H_{SRDT}) and sensible heat flux from eddy covariance (H_{EC}) for unstable conditions during the summer campaign.

The linear regression between H_{SR1} and H_{EC} showed a good relationship, indicating a successful calibration (slope = 0.88, intercept = 21.54 $W m^{-2}$; $R^2 = 0.82$, $RMSE = 38.39 W m^{-2}$). A good relationship was shown between H_{SR2} and H_{EC} (slope = 1.34, intercept = 17.54 $W m^{-2}$; $R^2 = 0.88$, $RMSE = 55.51 W m^{-2}$) with a better R^2 value than H_{SR1} , and the closest relationship was shown between H_{SRDT} and H_{EC} (slope = 0.92, intercept = 21.62 $W m^{-2}$; $R^2 = 0.85$, $RMSE = 36.18 W m^{-2}$).

As with the summer campaign, linear regressions (Figure 2.5) of the H estimated by the three SR approaches, and H_{EC} were used for the winter campaign. The linear regression between H_{SR1} and H_{EC} was expected to be closer in winter following an improved relationship shown during the winter validation period. This was found (slope = 0.92, intercept = 18.76 $W m^{-2}$; $R^2 = 0.81$, $RMSE = 36.74 W m^{-2}$), indicating a successful calibration. A good relationship was shown

between H_{SR2} and H_{EC} (slope = 1.42, intercept = 11.43 W m⁻²; $R^2 = 0.88$, RMSE = 65.59 W m⁻²) which again produced an improved R^2 compared to H_{SR1} . Although not as close a relationship was shown during the winter campaign, as was shown during the summer campaign, however, a good relationship was still found between H_{SRDT} and H_{EC} (slope = 0.85, intercept = 15.92 W m⁻²; $R^2 = 0.84$, RMSE = 37.26 W m⁻²).

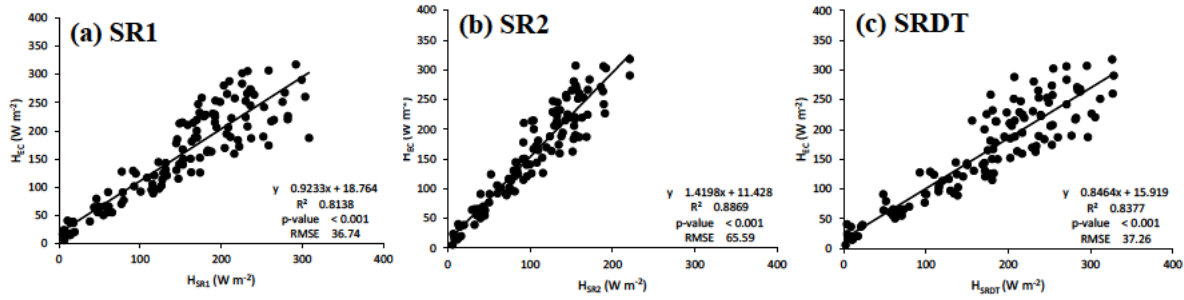


Figure 2.5: The relationship between the three surface renewal (SR) approaches and the eddy covariance (EC) method, using linear regressions between 30-min (a) sensible heat-flux from surface renewal 1 (H_{SR1}), (b) sensible heat flux from surface renewal 2 (H_{SR2}), and (c) sensible heat flux from surface renewal dissipation theory (H_{SRDT}) and the sensible heat flux from eddy covariance (H_{EC}) for unstable conditions during the winter campaign.

In order to further understand the performance and relationship between the three SR approaches and the EC method, a comparison over the duration of a day was conducted, of the estimation of H by the three SR methods and the measurement of H_{EC} , for both the summer (Figure 2.6) and winter (Figure 2.7) campaigns. Combined with the H values, the energy balance components R_n and G are presented to illustrate the relationship of the approaches to changes in energy fluxes. In order to better visualise G , it was multiplied by ten (10 x G).

Over the summer campaign, the highest R_n measured was 950 W m⁻² (on 22/01/2020 and 26/01/2020) which is much greater than the winter maximum R_n of 518 W m⁻² (on 15/07/2020), as expected. As a comparison, the lowest maximum R_n measured for a day was 273 W m⁻² (on 23/02/2020) which was lower than the lowest maximum R_n measured during the winter campaign of 401 W m⁻² (on 17/07/2020). This highlights the mixed conditions for the summer campaign.

The day chosen to show the relationship between the three SR approaches and the EC method for the summer campaign (Figure 2.6) was the 26/01/2020, as it experienced no rainfall, the highest total R_n , and the best data availability for all four methods and best energy balance closure for the EC method. Unstable conditions occurred from 08h30 to 16h00. Noticeable (Figure 2.6) is the convergence of all four H values at sunrise and sunset, as stability conditions change. Both H_{SR1} and H_{SRDT} spike and overestimate at the two peaks in R_n . The H_{SR2} is underestimated during unstable conditions throughout the day, as was found in the linear regressions.

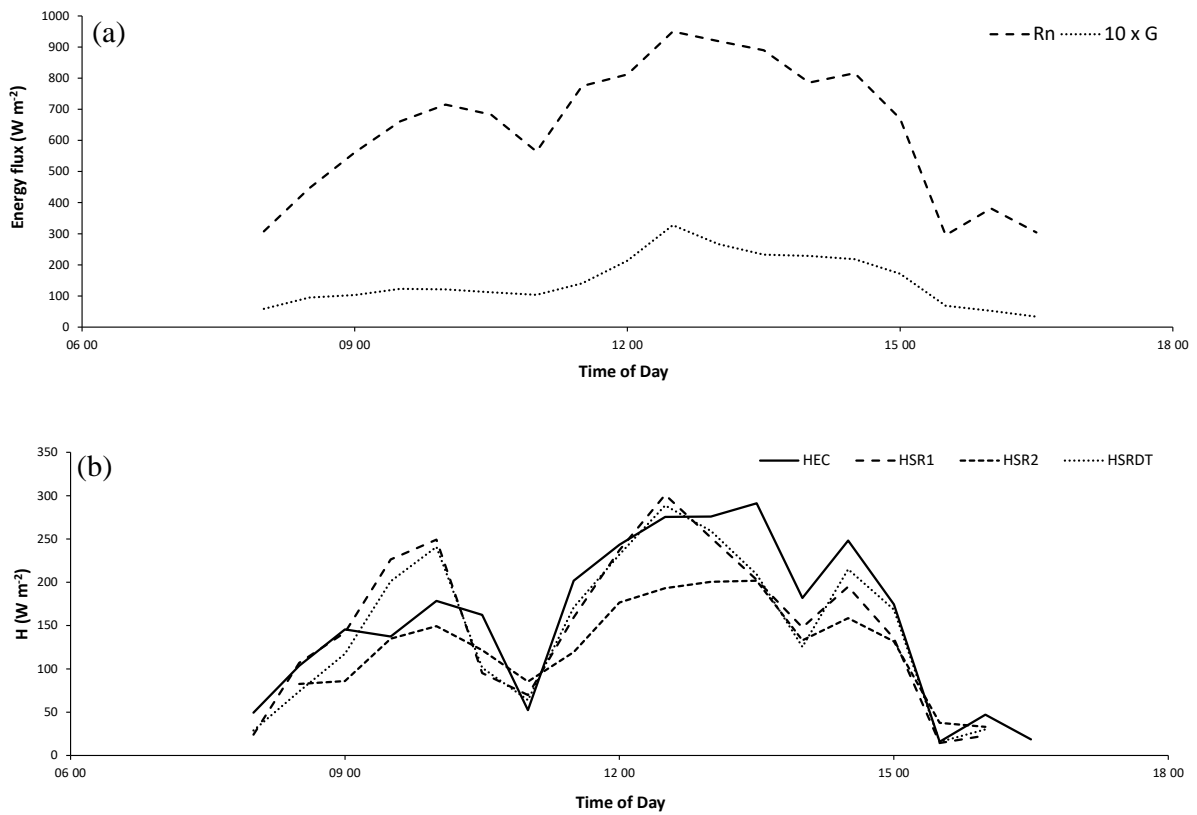


Figure 2.6: A comparison of the energy balance components (a) net radiation (R_n) and soil heat flux (G) and (b) sensible heat flux (H) measured by eddy covariance (EC), surface renewal 1 (SR1), surface renewal 2 (SR2) and surface renewal dissipation theory (SRDT) methods for unstable conditions over a day (26/01/2020) during the summer campaign.

The day chosen to show the relationship between the three SR approaches and the EC method for the winter campaign (Figure 2.7) was the 15/07/2020, as this day received the highest total R_n , the best data availability for all four methods, and an above average energy balance closure

for the EC method. Over the course of the day, R_n peaked at 518 W m^{-2} . Unstable conditions occurred between 08h30 and 16h00. The close relationship between H_{EC} and H_{SR1} and H_{SRDT} is visible over the day. The H_{SR1} and H_{SRDT} have a delayed response to an increasing R_n early in the day compared to H_{EC} . The H_{SR1} and H_{SRDT} appears sensitive to changes in R_n , with steep peaks and troughs, whereas H_{EC} follows a more stable pattern over the day, similar to R_n . The H_{SRDT} is also overestimated more than H_{SR1} . As found with the linear regressions, H_{SR2} is consistently underestimated.

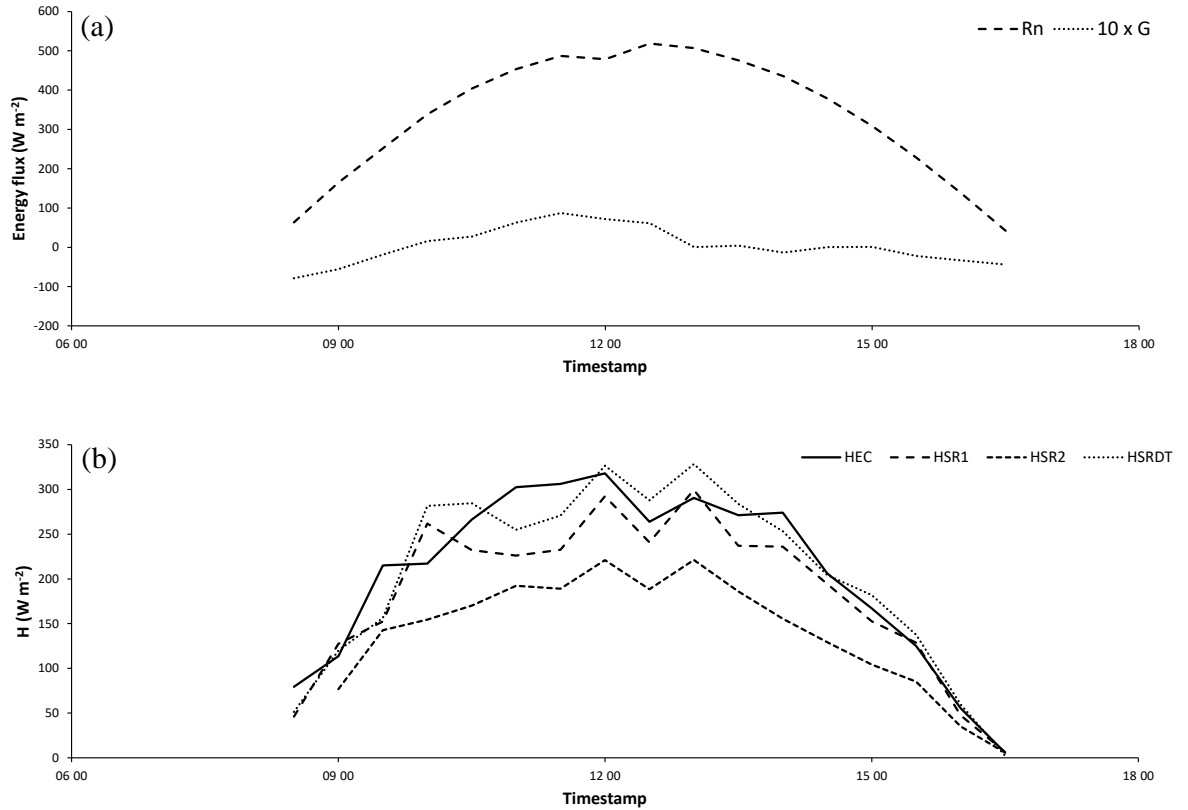


Figure 2.7: A comparison of the energy balance components (a) net radiation (R_n) and soil heat flux (G) and (b) sensible heat flux (H) estimated by eddy covariance (EC), surface renewal 1 (SR1), surface renewal 2 (SR2) and surface renewal dissipation theory (SRDT) methods for unstable conditions over a day (15/7/2020) during the winter campaign.

2.3.3 Data availability and performance of EC, SSR1, SRDT and SR2

The EC method provides direct measurements of both H and LE . In theory, based on the shortened energy balance, if the EC system were to measure H and LE accurately, and R_n and

G are accounted for accurately, complete energy balance closure would be achieved. To test the ability of EC within each campaign, energy balance closure was tested during the winter and summer campaigns. To determine the daily energy balance closure, 30-min data periods of R_n , G , H and LE were used. Data availability is an indication of the number of 30-min periods where an H measurement was obtained during unstable conditions. The reasons for no H measurement being obtained, is due to either its removal through data quality control, or no measurement was observed, due to the limitations of the method and conditions. Only periods when both an H and LE value were measured by the EC system were used. Again, only unstable conditions were considered.

The energy balance closure at a daily scale was analysed for the summer campaign (Table 2.2). Conditions over the duration of the summer campaign were variable, and this is evident in the energy balance closure of the EC system. Over the whole campaign, the energy balance closure for unstable conditions was on average 70.5 %. The day previously shown (Figure 2.6) to have the highest maximum R_n measured and no rainfall (26/01/2020), also showed the best average energy balance closure for the summer campaign at 78.5 %. The day which showed the lowest maximum R_n measured (23/01/2020) and highest rainfall, showed the 2nd lowest average energy balance closure of 60.4 % and data availability of 55.2 %. The lowest average energy balance closure of 43.5 % was measured on 27/01/2020, which was a poor condition day that experienced the 2nd highest rainfall volume, 2nd lowest total daily R_n in the summer campaign and a data availability of 78.4 %.

Table 2.2: Average energy balance closure for the EC method for unstable conditions over the duration of the summer campaign.

Day	Unstable conditions %	Data availability %	Rainfall (mm)
22/01/2020	67.7	100.0	0.00
23/01/2020	60.4	55.2	11.18
24/01/2020	72.3	85.7	1.78
25/01/2020	69.5	94.4	0.00
26/01/2020	78.5	100.0	0.00
27/01/2020	43.5	60.7	2.03
28/01/2020	64.8	72.0	0.25
Campaign	70.5	78.4	15.49

For the winter campaign (Table 2.3), the EC system measured H and LE for 86.7 % of the 30-min unstable periods during the campaign. For these 30-min periods, an average energy balance

closure of 69.7 % was achieved. Rainfall was not a factor during the winter campaign. The highest energy balance closure was 77.8 %, and occurred on a day (23/07/2020) with the third highest total R_n (9.21 MJ m⁻²). The lowest energy balance closure was 61.5 %, and occurred on the day with the lowest total R_n (7.39 MJ m⁻²), and lowest data availability (46.7 %).

Table 2.3: Average energy balance closure for the EC method for unstable conditions over the duration of the winter campaign.

Day	Unstable conditions %	Data availability %	Rainfall (mm)
15/07/2020	71.9	100.0	0.00
16/07/2020	72.2	68.8	0.00
17/07/2020	61.5	46.7	0.00
18/07/2020	66.6	100.0	0.00
19/07/2020	64.1	93.3	0.00
20/07/2020	70.3	93.8	0.00
21/07/2020	66.3	81.3	0.00
22/07/2020	67.8	100.0	0.00
23/07/2020	77.8	93.8	0.00
Campaign	69.7	86.7	0.00

As shown with the energy balance closure of the EC system, gaps in measurement of H can occur due to conditions beyond the bounds of the methodology and equipment and due to removal by data quality controls. The SR approaches are also not immune to these problems, and an assessment of the data availability in the unstable condition 30-min data periods for the estimation of H by the SR approaches and the measurement of H by EC were compared for the summer (Table 2.4) and winter (Table 2.5) campaigns.

The summer campaign was made up of 162 30-min data periods, the SR2 method performed the worst, with the lowest data availability of 62.3 %, followed by the EC method with a data availability of 78.4 %, while the SR1 and SRDT methods showed an equal data availability of 96.3 %.

The winter campaign consisted of 143 30-min periods, of which an H estimate was calculated for 99.3 % of the periods by the SR1 and SRDT approaches, while the EC method showed a data availability of 86.7 %, which was the lowest of all methods. The SR2 method was the lowest of the SR methods with a data availability of 92.3 %.

Table 2.4: The data available across the four methods for the 162 possible 30-min measurement periods, when unstable conditions occurred during the summer campaign.

	R_n (MJ m ⁻²) Total	H_{EC} Data availability %	H_{SR1} Data availability %	H_{SR2} Data availability %	H_{SRDT} Data availability %	Rainfall (mm)
22/01/2020	20.48	100.0	87.0	52.2	87.0	0.00
23/01/2020	4.29	55.2	100.0	51.7	100.0	11.18
24/01/2020	13.14	85.7	100.0	61.9	100.0	1.78
25/01/2020	10.61	94.4	94.4	61.1	94.4	0.25
26/01/2020	20.77	100.0	94.4	88.9	94.4	0.00
27/01/2020	5.51	60.7	100.0	85.7	100.0	2.03
28/01/2020	21.67	72.0	96.0	40.0	96.0	0.25
Campaign	96.48	78.4	96.3	62.3	96.3	15.49

Table 2.5: The data available across the four methods for the 143 possible 30-min measurement periods, when unstable conditions occurred during the winter campaign.

	R_n (MJ m ⁻²) Total	H_{EC} Data availability %	H_{SR1} Data availability %	H_{SR2} Data availability %	H_{SRDT} Data availability %	Rainfall (mm)
15/07/2020	10.21	100.0	100.0	94.1	100.0	0.00
16/07/2020	9.20	68.8	100.0	93.8	100.0	0.00
17/07/2020	7.39	46.7	93.3	86.7	93.3	0.00
18/07/2020	8.88	100.0	100.0	93.8	100.0	0.00
19/07/2020	9.02	93.3	100.0	100.0	100.0	0.00
20/07/2020	9.36	93.8	100.0	81.3	100.0	0.00
21/07/2020	8.60	81.3	100.0	93.8	100.0	0.00
22/07/2020	9.10	100.0	100.0	87.5	100.0	0.00
23/07/2020	9.21	93.8	100.0	100.0	100.0	0.00
Campaign	80.98	86.7	99.3	92.3	99.3	0.00

2.4 Discussion

Although EC is used to determine the α factor for the SR1 approach, it is known that EC rarely closes the energy balance over many different ecosystems (Castellví and Snyder 2009a, Stoy *et al.* 2013, Pozníková *et al.* 2018). Energy balance closure (EBC) by the EC system is better over drier surfaces, and poor over wetter surfaces such as wetlands and crops (Linguist *et al.* 2015). Over drier surfaces H dominates, and indicates that the lack of EBC is potentially related to the measurement of LE (Linguist *et al.* 2015). Precipitation also affected EBC, as EBC was found

to decrease as precipitation increased (Cui and Chui 2019) which could be related to a wetter environment or instrument disturbances. Stoy *et al.* (2013) found that across 173 FLUXNET sites, lack of EBC was systematically different, and based on canopy heterogeneity, but could not be explained by vegetation type or size. The measurement of G is an important energy balance component to measure adequately to allow optimum closure, yet not enough alone to complete closure (Stoy *et al.* 2013, Poblite-Echeverria *et al.* 2014). A range of EBCs have been documented, from low closure of 68 % over post-harvest wheat fields under wet conditions and reduced closure over rice crops (Castellví *et al.* 2006, Pozníková *et al.* 2018), to increased closures of 99 and 92 % over cotton crops and grape vineyards, respectively (Poblite-Echeverria *et al.* 2014, Rosa and Tanny 2015, Haymann *et al.* 2019). Within this study, over the summer and winter campaigns, the EC EBC shortfall was 29.5 % and 30.4 %, respectively for unstable conditions. This aligns with previous studies (Castellví *et al.* 2006, Poblite-Echeverria *et al.* 2014, Rosa and Tanny 2015, Pozníková *et al.* 2018, Haymann *et al.* 2019). Although rainfall had an effect on EBC, clear weather did not guarantee high EBC, but a higher R_n did. Thus, it is suggested that H and LE are better accounted for when surface energy balance interactions are more pronounced. The EC performance justifies it as a strong benchmark to gauge the SR approaches.

Over both the summer and winter campaigns, SR was shown through the estimation of H , to be an acceptable alternative method to EC for the estimation of ET over indigenous vegetation at this site. Following the calibration of SR1, corrected H_{SR1} showed a good relationship with H_{EC} in both summer (slope = 0.88, intercept = 21.54 W m⁻², R^2 = 0.82, RMSE = 38.39 W m⁻²) and winter (slope = 0.92, intercept = 18.76 W m⁻², R^2 = 0.81, RMSE = 36.74 W m⁻²). Literature on the ability of SR1 to estimate H over agricultural crops (cotton, fruit orchard, wheat, sorghum) and natural vegetation types (grasslands, teff grass, bare soil) is extensive (Spano *et al.* 2000, Zapata and Martínez-Cob 2001, Barbagallo *et al.* 2009, Rosa *et al.* 2013, Poblite-Echeverría *et al.* 2014, Shapland *et al.* 2014, Linquist *et al.* 2015, Rosa and Tanny 2015, Buttar *et al.* 2019, Haymann *et al.* 2019). Additionally, it has been shown to be adequate over indigenous coastal wetland vegetation in the Maputaland region of South Africa (Clulow *et al.* 2012), and now through this study, to be suitable over indigenous vegetation in the uKhahlamba-Drakensberg mountain region. The α values determined were consistent with literature (Shapland *et al.* 2014, Suvočarev *et al.* 2014) for a tall canopy. The calibration was successful as shown by the good relationship over the validation period during summer (slope = 0.91, intercept = 18.03 W m⁻², R^2 = 0.86, RMSE = 30.48 W m⁻²) and winter (slope = 0.98, intercept = 19.23 W m⁻², R^2 = 0.84, RMSE = 36.23 W m⁻²). Beyond the linear regressions, the

time series correlation over a day showed that H_{SR1} was overestimated by a small margin when R_n peaked. When R_n decreased, H_{SR1} was underestimated. This highlighted the sensitivity of SR1 to R_n fluctuations, yet the sensitivity at a sub-daily scale did not affect the accuracy of H_{SR1} estimations at the daily scale.

The independent approaches SR2 and SRDT, also showed good relationships with EC in both summer and winter. Interestingly, H_{SR2} was consistently underestimated over both campaigns (slope > 1), and can be seen in the timeseries analysis of both the summer (Figure 2.6) and winter (Figure 2.7) campaigns. The underestimation during unstable conditions does not concur with the findings of Castellví and Snyder (2009a) and Castellví and Snyder (2010), but is in agreement with the findings of Castellví and Snyder (2009c) who showed an underestimation of H_{SR2} for unstable conditions over a peach orchard. This is understandable, considering that a peach orchard canopy is closer in height and structure to the canopy of *Leucosidea sericea*, in comparison to the rice canopy and grapevines in Castellví and Snyder (2009a) and Castellví and Snyder (2010). The underestimation of H_{SR2} may be caused by the nature of a taller canopy structure. As with H_{SR1} , the slopes of the linear regression from the summer and winter campaigns, show that H_{SRDT} is close to H_{EC} for unstable conditions. There is not a large body of literature where the SRDT approach has been applied, and therefore the results could not be compared. Based on the time series analysis, the overestimation of H_{SRDT} is similar in nature to that of H_{SR1} in both the summer and winter campaigns, as it peaks during the higher periods of R_n compared to H_{EC} . As with SR1, the fluctuations between over and underestimating of H_{SRDT} at the 30-min scale, which are highly sensitive to R_n , seem to even out at the daily scale, as shown by the high correlation in the linear regression with H_{EC} . Over both campaigns the SRDT approach performed well against EC, and this is an important finding as SRDT, just like SR2, is independent of EC.

The three SR approaches have shown through the comparison with H_{EC} , that they all provide a good estimation of H for both winter and summer conditions over indigenous montane vegetation. However, in order to provide an indication of which would be better for a budget-restricted long-term monitoring network, only EC independent methods can be considered, viz. the performance of SR2 and SRDT. Based on the linear regressions, the overestimations and underestimations cancel over the course of the campaign for SRDT, but for SR2 an underestimation remains.

As discussed, to estimate H accurately is only valuable, if this estimation occurs regularly throughout a day. It is noted that SR produces 30-min periods without an H estimate, potentially

due to inadequate sampling or inability to compute the solution when required conditions are violated (Zapata and Martínez-Cob 2001, Zapata and Martínez-Cob 2002). In this study, under unstable conditions, SRDT and SR2 showed data availability of 96.3 and 62.3 % over the summer campaign and 99.3 and 92.3 % over winter campaign respectively. The lowest data availability by SRDT and SR2 were 87.0 and 40.0 % in the summer campaign, and 93.3 and 81.3 % in the winter campaign respectively. These are within range of what is expected based on previous studies (Zapata and Martínez-Cob 2001, Savage 2017). The summer campaign experienced 15.5 mm of rainfall, which has been discussed as a factor affecting SR measurements (Liu *et al.* 2013, Hu *et al.* 2018). The SRDT approach showed no considerable effects by rainfall, while the SR2 approach showed the highest data availability on the day with no rainfall. During the winter campaign when no rainfall occurred, the SR2 method had a much higher data availability compared to the summer campaign. The difference, however, cannot be attributed to rainfall or sensor fault, as both approaches use the same 30-min dataset. The inability for SR2 to compute an H value, due to the constraints of the method not being met, could be a deficiency of the SR2 approach. Additional parameters required in SR2, such as the measurement of horizontal windspeed, showed no clear pattern of influence. However, the SR2 approach showed an inability to compute H during the periods of early morning and late evening when stability conditions transition. During stability transitional periods and poor weather, SR2 performs poorly, which was possibly compounded by the mixed conditions experienced during the summer campaign.

As literature on the use of SR2 in such an environment is lacking, it is difficult to precisely conclude the cause, but rather to see this as a potential indication and suggests a future research focus. Testing this method over other indigenous vegetation types found within this region, and other sites within this landscape, could provide insight into the limitations of SR2. A longer period of observation would also provide a better indication of the conditions in which the SR2 method performs poorly. With this, the performance of the SRDT method could be site specific, and would need to be verified at other sites similar in topography and climate and across different indigenous vegetation and canopy structures.

Following the assessment of the SR approaches, based on performance under unstable conditions and data loss, the SRDT approach could be considered to be the most viable alternative to EC and SR1 and provide an adequate H value for long-term ET estimation of indigenous vegetation within and at locations similar to the strategic water resources area of the uKhahlamba-Drakensberg Mountains, South Africa. The SR system, which was installed in the

Cathedral Peak research catchments on the 13th of November 2018, continues to record to present and will continue into the future. From this research, it has been shown that the H estimates collected by the SR system, is a valuable long-term record which can be used for ET estimates with the SRDT method at this site. This provides a valuable source of data for a data scarce, water resource important area.

2.5 Conclusion

The EC method has for many years been the accepted standard in estimating ET . However, the cost is prohibitive and a cheaper alternative is needed for budget-restricted water resource monitoring networks. Due to the remoteness of mountainous regions such as Cathedral Peak, damage due to natural events such as fires, or theft, make placing an expensive EC system in these areas unfeasible. Through the comparison of the estimation of H , SR has been shown to be a viable alternative to EC, over indigenous vegetation, within a variable terrain landscape, and under an Afromontane climate. The SR1 and SRDT methods showed the closest relationships to the EC method, with the calibrated SR1 method performing better during the more consistent weather in winter, and the independent SRDT method better during the mixed-weather summer conditions relative to the EC. Consistently across both the summer and winter weather conditions, the SR2 method over-estimated H compared to the EC method, as well as being less reliable in terms of data availability compared to the other two SR methods. Thus, the SR2 method is not considered a viable independent method within the characteristics of this location. For a budget restricted long-term monitoring network, the SRDT approach, independent of EC, has been shown to be an adequate alternative for the estimation of H within this landscape, through both summer and winter weather conditions.

This finding is valuable, considering the current 2-year dataset of energy balance components (R_n , G and H) at the site. Combined with the knowledge that the SRDT method is viable, observation using SR can continue at the site, forming a valuable long-term measurement of ET over the indigenous vegetation. This will underpin an improved understanding of the relationship between land cover and the hydrological processes within a data scarce strategic water source area of South Africa.

Understanding of the SR approach has been predominately focussed on agricultural crops, with limited indigenous vegetation considered. The research here has added to the indigenous vegetation types considered. However, it provides insight into a canopy dominated by *Leucosidea sericea*, and further testing over additional indigenous vegetation types, specific to

the uKhahlamba-Drakensberg mountain range, and broader for different regions, needs to be considered and investigated.

2.6 Acknowledgements

The financial, technical and logistical assistance of the National Research Foundation's South African Environmental Observation Network (SAEON) business unit towards this research is acknowledged. Opinions expressed and conclusions arrived at are those of the author(s) and are not necessarily to be attributed to the NRF or SAEON.

2.7 References

- Barbagallo, S., Consoli, S., Russo, A., 2009. Surface energy balance over orange orchard using surface renewal analysis. *Journal of Agricultural Engineering*, 4, 39-45.
- Bosch, J., 1979. Treatment effects on annual and dry period streamflow at Cathedral Peak. *South African Forestry Journal*, 108, 29-38.
- Buttar, N.A., Hu, Y., Lakhari, I.A., Azeem, A., Zaman, M., Awais, M., 2019. Estimating sensible heat flux from *Camellia sinensis* using the surface renewal method. In *2019 ASABE Annual International Meeting* (p. 1). American Society of Agricultural and Biological Engineers, 1. Boston, Massachusetts.
- Campbell Scientific, 2016., Model HFP01SC Self-Calibrating Soil Heat Flux Plate Revision: 10/16. Available at: <https://s.campbellsci.com/documents/us/manuals/hfp01sc.pdf> [Accessed 10 October 2018].
- Campbell Scientific, 2020., EASYFLUX DL CR3000OP For CR3000 and Open-Path Eddy-Covariance System Revision: 3/18. Available at: <https://s.campbellsci.com/documents/us/manuals/easyflux-dl.pdf> [Accessed 22 May 2020].
- Castellví, F., 2004. Combining surface renewal analysis and similarity theory: A new approach for estimating sensible heat flux. *Water Resources Research*, 40(5), W05201
- Castellví, F., 2011. Is it worthy to apply different methods to determine latent heat fluxes? – A study case over a peach orchard. *Evapotranspiration-From Measurements to Agricultural and Environmental Applications*, 43-58. Rijeka, Croatia: InTech.
- Castellví, F., Martínez-Cob, A., 2005. Estimating sensible heat flux using surface renewal analysis and the flux variance method: A case study over olive trees at Sástago (NE of Spain). *Water Resources Research*, 41(9), W09422
- Castellví, F., Martínez-Cob, A., Pérez-Coveta, O., 2006. Estimating sensible and latent heat fluxes over rice using surface renewal. *Agricultural and Forest Meteorology*, 139(1-2), 164-169.
- Castellví, F., Perez, P.J., Ibañez, M., 2002. A method based on high frequency temperature measurements to estimate sensible heat flux avoiding the height dependence. *Water Resources Research*, 38(6), WR000486-20.

- Castellví, F., Snyder, R.L., 2009a. On the performance of surface renewal analysis to estimate sensible heatflux over two growing rice fields under the influence of regional advection. *Journal of Hydrology*, 375, 546-553.
- Castellví, F., Snyder, R.L., 2009b. Combining the dissipation method and surface renewal analysis to estimate scalar fluxes from the time traces over rangeland grass near Ione (California). *Hydrological Processes*, 23, 842-857.
- Castellví, F., Snyder, R.L., 2009c. Sensible heat flux estimates using surface renewal analysis: A study case over a peach orchard. *Agricultural Forest Meteorology*, 149, 1397-1402.
- Castellví, F., Snyder, R.L., 2010. A new procedure based on surface renewal analysis to estimate sensible heat flux: a case study over grapevines. *Journal of Hydrometeorology*, 11(2), 496-508.
- Chemura, A., Rwasoka, D., Mutanga, O., Dube, T., Mushore, T., 2020. The impact of land-use/land cover changes on water balance of the heterogenous Buzi sub-catchment, Zimbabwe. *Remote Sensing Applications: Society and Environment*, 18, 100292.
- Clulow, A.D., Everson, C.S., Mengistu, M.G., Jarman, C., Jewitt, G.P.W., Price, J.S., Grundling, P.L., 2012. Measurement and modelling of evaporation from a coastal wetland in Maputaland, South Africa. *Hydrology and Earth System Sciences Discussions*, 9(2), 1741-1782.
- Cui, W., Chui, T.F.M., 2019. Temporal and spatial variations of energy balance closure across FLUXNET research sites. *Agricultural and Forest Meteorology*, 271, 12-21.
- De Villiers, A.D., O'Connor, T., 2011. Effect of a single fire on woody vegetation in Catchment IX, Cathedral Peak, KwaZulu-Natal Drakensberg, following extended partial exclusion of fire. *African Journal of Range and Forage Science*, 28(3), 111-120.
- Drexler, J.Z., Snyder, R.L., Spano, D., Paw U, K.T., 2004. A review of models and micrometeorological methods used to estimate wetland evapotranspiration. *Hydrological Processes*, 18, 2071-2101.
- Foken, T., Leuning, R., Oncley, S.R., Mauder, M., Aubinet, M., 2012. Corrections and data quality control. In: Aubinet M., Vesala T., and Papale D., eds., *Eddy covariance*. Dordrecht, Springer, 85-131.
- Gupta, J., van der Zaag, P., 2008. Interbasin water transfers and integrated water resources management: Where engineering, science and politics interlock. *Physics and Chemistry of the Earth, Parts A/B/C*, 33(1-2), 28-40.
- Haymann, N., Lukyanov, V., Tanny, J., 2019. Effects of variable fetch and footprint on surface renewal measurements of sensible and latent heat fluxes in cotton. *Agricultural and Forest Meteorology*, 268, 63-73.
- Heyns, P., 2003. Water-resources management in Southern Africa. *International Waters in southern Africa*, 1, 5-37.
- Hu, Y., Buttar, N.A., Tanny, J., Snyder, R.L., Savage, M.J., Lakhari, I.A., 2018. Surface renewal application for estimating evapotranspiration: A review. *Advances in Meteorology*, 2018, 1-11.

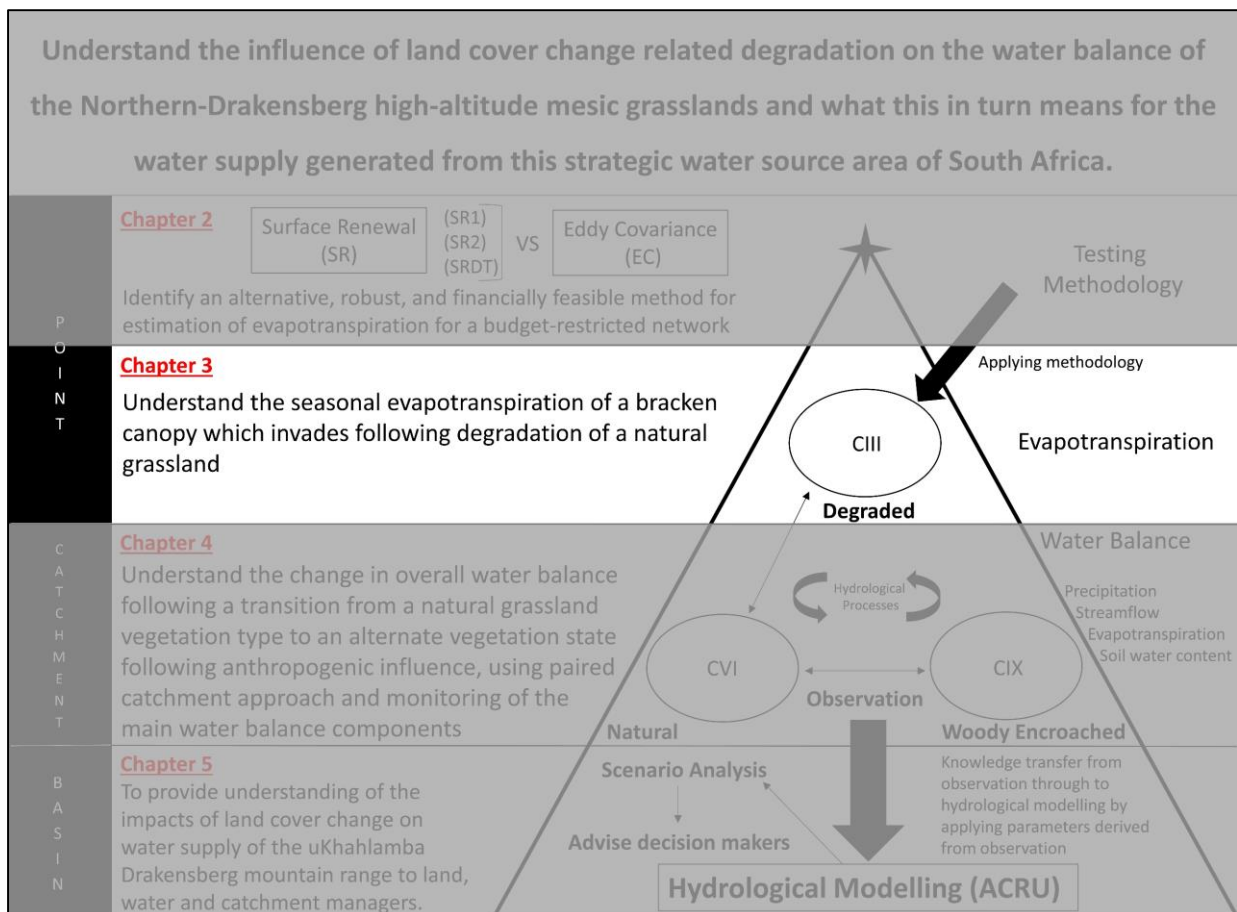
- Le Maitre, D.C., Walsdorff, A., Cape, L., Seyler, H., Audouin, M., Smith-Adao, L., Nel, J.A., Holland, M., Witthüser, K., 2018. Strategic water source areas: management framework and implementation guidelines for planners and managers. WRC Report No. TT 754/2/18, Water Research Commission, Pretoria, South Africa.
- Linquist, B., Snyder, R., Anderson, F., Espino, L., Inglese, G., Marras, S., Moratiel, R., Mutters, R., Nicolosi, P., Rejmanek, H., Russo, A., Shapland, T., Song, Z., Swelam, A., Tindula, G., Hill, J., 2015. Water balances and evapotranspiration in water- and dry-seeded rice systems. *Irrigation science*, 33, 375-385.
- Liu, S.M., Xu, Z.W., Zhu, Z.L., Jia, Z.Z., Zhu, M.J., 2013. Measurements of evapotranspiration from eddy-covariance systems and large aperture scintillometers in the Hai River Basin, China. *Journal of Hydrology*, 487, 24-38.
- Mbangiwa, N.C., Savage, M.J., Mabhaudhi, T., 2019. Modelling and measurement of water productivity and total evaporation in a dryland soybean crop. *Agricultural and Forest Meteorology*, 266-267, 65-72.
- Mengistu, M.G., Savage, M.J., 2010a. Open water evaporation estimation for a small shallow reservoir in winter using surface renewal. *Journal of Hydrology*, 380, 27-35.
- Mengistu, M.G., Savage, M.J., 2010b. Surface renewal method for estimating sensible heat flux. *Water SA*, 36(1), 9-18.
- Nanni, U.W., 1956. Forest hydrological research at the Cathedral Peak research station. *Journal of the South African Forestry Association*, 27(1), 2-35.
- Paw U, K.T., Qiu, J., Su, H.B., Watanabe, T., Brunet, Y., 1995. Surface renewal analysis: a new method to obtain scalar fluxes. *Agricultural and Forest Meteorology*, 74, 119-137.
- Poblete-Echeverría, C., Sepúlveda-Reyes, D., Ortega-Farías, S., 2014. Effect of height and time lag on the estimation of sensible heat flux over drip-irrigated vineyard using the surface renewal (SR) method across distinct phenological stages. *Agricultural Water Management*, 141, 74-83.
- Pozníková, G., Fischer, M., van Kesteren, B., Orság, M., Hlavinka, P., Žalud, Z., Trnka, M., 2018. Quantifying turbulent energy fluxes and evapotranspiration in agricultural field conditions: A comparison of micrometeorological methods. *Agricultural Water Management*, 209, 249-263.
- Rosa, R., Dicken, U., Tanny, J., 2013. Estimating evapotranspiration from processing tomato using the surface renewal technique. *Biosystems Engineering*, 114, 406-413.
- Rosa, R., Tanny, J., 2015. Surface renewal and eddy covariance measurements of sensible and latent heat fluxes of cotton during two growing seasons. *Biosystems Engineering*, 136, 149-161.
- Savage, M.J., 2014. *Web-based teaching, learning and research using real-time data from field-based agrometeorological measurement systems*. Dissertation (MSc Agric). University of KwaZulu-Natal.

- Savage, M.J., 2017. Estimation of grass reference evaporation and sensible heat flux using surface renewal and Monin-Obukhov similarity theory: A simple implementation of an iterative method. *Journal of Hydrology*, 547, 742-754.
- Savage, M.J., 2020. Flux estimation using a simple implementation of an iterative method for surface renewal methods 1 and 2. Agrometeorology Discipline, Soil-Plant-Atmosphere Research Unit, School of Agricultural, Earth and Environmental Sciences, University of KwaZulu-Natal, Pietermaritzburg, South Africa. Available at: <https://www.youtube.com/watch?v=mFOZSuqsLHI>.
- Shapland, T.M., McElrone, A.J., Snyder, R.L., Paw U, K.T., 2012. Structure function analysis of two-scale scalar ramps. Part II: ramp characteristics and surface renewal flux estimation. *Boundary-Layer Meteorology*, 145, 27-44.
- Shapland, T.M., Snyder, R.L., Paw U, K.T., McElrone, A.J., 2014. Thermocouple frequency response compensation leads to convergence of the surface renewal alpha calibration. *Agricultural and Forest Meteorology*, 189-190, 36-47.
- Snyder, R.L., Spano, D., Paw U, K.T., 1996. Surface renewal analysis for sensible and latent heat flux density. *Boundary-Layer Meteorology*, 77, 249-266.
- Snyder, R.L., Pedras, C., Montazar, A., Henry, J.M., Ackley, D., 2015. Advances in ET-based landscape irrigation management. *Agricultural Water Management*, 147, 187-197.
- Spano, D., Snyder, R.L., Duce, P., Paw U, K.T., 2000. Estimating sensible and latent heat flux densities from grapevine canopies using surface renewal. *Agricultural and Forest Meteorology*, 104, 171-183.
- Stoy, P.C., Mauder, M., Foken, T., Marcolla, B., Boegh, E., Ibrom, A., Arain, M.A., Arneth, A., Aurela, M., Bernhofer, C., Cescatti, A., Dellwik, E., Duce, P., Gianelle, D., van Gorsel, E., Kiely, G., Knohl, A., Margolis, H., McCaughey, H., Merbold, L., Montagnani, L., Papale, D., Reichstein, M., Saunders, M., Serrano-Ortiz, P., Sottocornola, M., Spano, D., Vaccari, F., Varlagin, A., 2013. A data-driven analysis of energy balance closure across FLUXNET research sites: The role of landscape scale heterogeneity. *Agricultural and Forest Meteorology*, 171-172, 137-152.
- Suvočarev, K., Shapland, T.M., Snyder, R.L., Martínez-Cob, A., 2014. Surface renewal performance to independently estimate sensible and latent heat fluxes in heterogeneous crop surfaces. *Journal of Hydrology*, 509, 83-93.
- Suvočarev, K., Castellví, F., Reba, M.L., Runkle, B.R.K., 2020. Surface renewal measurements of H , λE and CO_2 fluxes over two different agricultural systems. *Agricultural and Forest Meteorology*, 279, 107763.
- Toucher, M.L., Clulow, A., Van Rensburg, S., Morris, F., Gray, B., Majozi, S., Everson, C.E., Jewitt, G.P.W., Taylor, M.A., Mfeka, S., Lawrence, K., 2016. *Establishment of a more robust observation network to improve understanding of global change in the sensitive and critical water supply area of the Drakensberg*. 2236/1/16. Water Research Commission, Pretoria, South Africa.
- Van Atta, C.W., 1977. Effect of coherent structures on structure functions of temperature in the atmospheric boundary layer. *Archives of Mechanics*, 29(1), 161-171.

- Zapata, N., Martínez-Cob, A., 2001. Estimation of sensible and latent heat flux from natural sparse vegetation surfaces using surface renewal. *Journal of Hydrology*, 254, 215-228.
- Zapata, N., Martínez-Cob, A., 2002. Evaluation of the surface renewal method to estimate wheat evapotranspiration. *Agricultural Water Management*, 55, 141-157.
- Zhang, Y.K., Schilling, K.E., 2006. Effects of land cover on water table, soil moisture, evapotranspiration, and groundwater recharge: A field observation and analysis. *Journal of Hydrology*, 319, 328-338.

Lead in to Chapter 3

Using the SRDT methodology validated in Chapter 2, the specific objective of Chapter 3 was to apply the methodology to determine the seasonality of the evapotranspiration (ET) of the *Pteridium aquilinum* (bracken) which invades the natural mesic grasslands following disturbance and degradation. Comparing the findings of this research to previous studies conducted over the Northern Drakensberg mesic grasslands, it was identified that the bracken canopy changes the energy balance as well as increases the mean annual ET. The largest differences between the natural grassland and the bracken occur during winter. The bracken ET was also found to be sensitive to timing of summer rainfall.



3. SEASONAL EVAPOTRANSPIRATION OVER AN INVADER VEGETATION (*PTERIDIUM AQUILINUM*) IN A DEGRADED MONTANE GRASSLAND USING SURFACE RENEWAL

Abstract

Study region: Cathedral Peak Research Catchments, uKhahlamba Drakensberg mountain range, South Africa.

Study focus: The focus was to determine the seasonal pattern of evapotranspiration (*ET*) over a bracken canopy which is a product of degradation within the montane grasslands of the uKhahlamba Drakensberg mountains. Surface renewal (SR) as a viable alternative to eddy covariance for long-term estimation of *ET* within a remote high rainfall montane landscape was investigated. The SR dissipation method was used to observe *ET* over the bracken canopy for 23 months, across two years with variable seasonal rainfall timing and amounts. Added to *ET*, rainfall and all energy flux components were observed.

New hydrological insights for the region: The SR dissipation theory method was shown to be adequate for the long-term estimation of evapotranspiration over a bracken canopy within a remote high summer rainfall montane landscape. The bracken canopy was found to have a strong seasonal cycle. Autumn was identified as the period most sensitive to rainfall amount and timing, as late annual rainfall during autumn decreases bracken *ET* compared to higher summer rainfall followed by a lower autumn rainfall. Based on literature, winter was found to be the period when the largest difference in evapotranspiration occurs between the bracken and natural grassland canopies.

Keywords: *land cover change, bracken, eddy covariance, energy balance, mountainous region, long-term observation.*

3.1 Introduction

Following years of overgrazing and poor land management in areas of the Northern Drakensberg Strategic Water Source Area (SWSA), South Africa, parts of the landscape have become heavily degraded (Hoffman and Todd, 2000; Grab and Knight, 2018). The degradation manifests as reduced ground cover, changes in species composition, invasion of non-native species and erosion of high carbon-rich soils (Asmal, 1995; Bangamwabo, 2009; Everson et al.,

Submitted as: Gray, B.A., Toucher, M.L., Savage, M.J., Clulow, A.D., 2021. Seasonal evapotranspiration over an invader vegetation (*Pteridium aquilinum*) in a degraded montane grassland using surface renewal. *Journal of Hydrology: Regional Studies*.

2011; Grellier et al., 2013). A common invader associated with the degradation of the montane grasslands within the Drakensberg escarpment is that of *Pteridium aquilinum* (Grab and Knight, 2018), which is an aggressive and dominating weed (McGlone et al., 2005) commonly referred to as bracken. There is a heavy dependence on the natural resource base of this landscape at national, regional and local scales together with the livelihoods of the local population being closely linked to the natural resources and ecosystem integrity. Thus, the need for sustainable and equitable management of land, water and soil is crucial. However, the influence of degradation on the water balance of these high altitude, fire-adapted montane grassland areas is not well understood. One of the contributing reasons, is a lack of hydroclimatic data available for high altitude, fire-adapted mountainous regions, particularly in developing countries.

A key component of the hydrological cycle that is altered by the change in land cover due to degradation is evapotranspiration (ET) (Li et al., 2017). ET is also the process which links the energy and water balances (Castellví, 2011). Since ET is comprised of evaporation and transpiration (Pozníková et al., 2018; Mbangiwa et al., 2019), both are altered when a land cover change occurs. Net radiation (R_n), air temperature, humidity, wind speed and canopy conductance, influence and cause the variability of ET , while the closeness of actual ET to potential ET , is determined by precipitation and soil water (Huizhi and Jianwu, 2012). How ET is altered by land degradation in montane grasslands areas is not well understood, and the most effective method to achieve this is through in-situ observation (Williams et al., 2012).

South Africa is a developing country, where infrastructure for observation and long-term datasets are scarce. Risk of theft, and damage due to animals or fires, is high in the remote, fire-adapted montane grasslands of the Northern Drakensberg escarpment (Brown and Bezuidenhout, 2020). Combined with extreme topographical characteristics of the Drakensberg escarpment, this places added restrictions on the equipment that can be placed at a monitoring site. Therefore, the need to identify and validate a viable and adequate method for the estimation of ET within such a summer rainfall landscape is required to be able to contribute to the knowledge on seasonal ET over degraded montane grasslands.

The most common and robust method used for the measurement of ET is the eddy covariance (EC) method (Snyder et al., 2008; Castellví and Snyder, 2009a; Kelley and Higgins, 2018; Cui and Chui, 2019; Morán et al., 2020). The EC method uses the measurement of vertical wind speed and the covariance with air temperature for the measurement of sensible heat flux (H), and water vapour pressure for the measurement of latent heat flux (LE) (Zapata and Martinez-Cob, 2001; Drexler et al., 2004; Castellví and Snyder, 2009b; Mengistu and Savage, 2010).

This is possible, due to mixing of H and LE occurring within the turbulence in the atmospheric boundary layer, as the scalar fluxes are transported vertically between the atmosphere and the canopy (Drexler et al., 2004). The EC approach does however come with several limitations, such as strict fetch requirements, need for a homogeneous canopy and relatively flat terrain (Castellví et al., 2002; Snyder et al., 2008; Haymann et al., 2019), as well as energy balance closure discrepancies (Linguist et al., 2015). The EC methodology and sensors are also complex and expensive (Snyder et al., 2008; Castellví and Snyder, 2009a; Poblete-Echeverría et al., 2014; Morán et al., 2020). The complexity of the method, combined with the expense, has limited the uptake of the method in resource constrained countries and situations (Rosa et al., 2013; Hu et al., 2018; Suvočarev et al., 2019). These factors have driven evapotranspiration research towards alternatives to EC, with fewer limitations and a simpler methodology, over the recent decades.

An example of an alternative is that of the surface renewal (SR) method (Snyder et al., 2008). The SR method uses high-frequency air temperature measurements and the structure function theory (van Atta, 1977) to estimate H . The ability of SR to estimate H , and to estimate it well is a standout of the method, as H is considered the most intricate component of the energy balance (Snyder et al., 2008; Morán et al., 2020). Further, the SR method also consists of a simpler methodology to achieve ET estimations with less strict fetch and siting requirements (Snyder et al., 2015), and utilises fewer sensors than the EC method (Castellví et al., 2006; Drexler et al., 2004; Snyder et al., 2008; Kelley and Higgins, 2018). Using the surface energy balance, LE can be estimated as a residual once net radiation (R_n) and soil heat flux (G) are accounted for (Snyder et al., 1996; Spano et al., 2000). As a result, accurate measurement of R_n is critical for accurate ET estimations using SR (Hu et al., 2018). The SR method has been shown to be a viable method over both homogeneous and heterogeneous canopies (Mengistu and Savage, 2010; Suvočarev et al., 2014). SR is potentially a more viable option for the long-term monitoring of ET within developing countries where long term datasets are scarce (Kelley and Higgins, 2018).

The SR method uses high-frequency air temperature measurements to estimate H , as an exchange of fluxes occurs when a parcel of air makes contact with the canopy top (Mengistu and Savage, 2010). These exchanges are identified in the high-frequency air temperature measurements as ramp events (Mengistu and Savage, 2010). The original SR approach (SR1) method follows this approach for the estimation of H which is considered uncorrected, due to the understanding that it does not account for the uneven heating of the air parcel (Castellví et

al., 2002; Castellví et al., 2016). An α value is then calculated through calibration, which is carried out by concurrent measurements taken by SR1 and an independent measure of H at the same site. The α is determined as the slope of the regression, between the uncorrected H of SR1 and the independent measure of H , which is often EC (Poblete-Echeverría et al., 2014; Shapland et al., 2014). The α value is applied to the uncorrected H (H_{UCSR1}) to calculate the corrected H (H_{SR1}) estimated by SR1. The calibration of the SR1 method is only required once or twice per season for a canopy that does not significantly change in height or density and can be applied to sites with similar vegetation structure and measurement height (Snyder et al., 2008).

Currently, a considerable limitation of SR1, is the requirement for a calibration period with an independent measure of H (Drexler et al., 2004; Castellví and Snyder, 2009b; Mengistu and Savage, 2010; Poblete-Echeverría et al., 2014). However, alternative SR approaches have been developed that alleviate the requirement for calibration. The alternative SR approach, the SR dissipation (SRDT) method, (Castellví and Snyder, 2009b), follows the same theory as SR1, but uses the standard deviation of air temperature (σ_T) (Mengistu and Savage, 2010) and the determination of zero plane displacement (d) (Castellví and Snyder, 2009b) to determine an α value with no additional sensors to the SR1 method.

Comparisons between EC and SR have been documented for natural vegetation types, such as grasslands (Snyder et al., 1996; Spano et al., 1997; Castellví and Snyder, 2009b; Castellví and Snyder, 2010; Savage, 2014) and wetlands (Zapata and Martinez-Cobb; 2001; Drexler et al., 2004; Clulow et al., 2012). Over grassland, the SR1 method has been shown to compare favourably with EC estimations of H (Snyder et al., 1996; Spano et al., 1997), as has the SRDT method, which provided a good estimation in unstable conditions and thus bodes well for the estimation of ET (Castellví and Snyder, 2009b).

Globally, observation of seasonal ET over grassland (Burba and Verma, 2005; Li et al., 2005; Mielnick et al., 2005; Zhang et al., 2007; Wieser et al., 2008; Krishnan et al., 2012; da Silva et al., 2017; Han et al., 2018; Rubert et al., 2018; Yue et al., 2019) has been widely documented in literature, as well as in degraded grasslands, due to land abandonment (Rosset et al., 2001), or overgrazing and intensive farming, which leads to increased bare soil coverage (Liu et al., 2008; Huizhi and Jianwu, 2012; Coners et al., 2016; Feng and Liu, 2016; Reichert et al., 2017). Interestingly, Li et al. (2012) found ET over a degraded grassland during the growing season to be sensitive to R_n , and compared to a non-degraded area, showed higher ET during the non-growing season and lower ET during the growing season, due to a reduced vegetation cover. Rosset et al. (2001) found that the overall difference in ET of a managed and abandoned

grassland was small, but larger differences were found during early and late stages of canopy development, as compared to the small differences when both canopies were more active. Liu et al. (2008) found degraded grasslands to have an *ET* near to total precipitation for the observation period, while Reichert et al. (2017) found *ET* to be around 30 % of precipitation, indicating that this is potentially related to a difference in climate variables at the site in consideration. The dominant invader of the Drakensberg montane grasslands, bracken, has received attention in literature, where it too, is a common invader in cultivated landscapes in Mexico (Schnieder, 2004; Douterlungne et al., 2010; Berget et al., 2015) and found closely linked to areas of human disturbance in New Zealand (McGlone et al., 2005). The focus of such literature is on the removal and reduction in the spread of bracken, but literature on understanding the hydrological implications of bracken invasion is lacking. The only known study by Springer et al. (2006) investigated the *ET* of a bracken fern and graminoid understory in a semi-arid climate, using temporal change in volumetric water content to draw conclusions regarding *ET*.

Given this background, the objective of the paper was to determine the seasonal pattern of *ET* over a bracken canopy in a degraded montane grassland, including the influence of seasonal variations in rainfall on the *ET*. The focus is on the seasonal *ET* of the bracken canopy, which is the land cover often associated with degradation within the montane grasslands of the uKhahlamba Drakensberg mountain range. To achieve this, SR (with a focus on which SR method, SR1 or SRDT) was evaluated as a viable alternative to EC for the long-term estimation of *ET* over the bracken canopy. There is a dearth of information on seasonal bracken *ET* which is addressed through this research, and besides Clulow et al. (2012), the use of SR within South Africa, and internationally, for long-term *ET* estimates of natural vegetation is rare.

3.2 Materials and methods

3.2.1 Research site

The Cathedral Peak research catchments (28°58'32.14" S; 29°14'8.72" E; Figure 3.1), located within the Drakensberg mountain range, have a long history of hydrological monitoring going back to 1948 (Nanni, 1956). The research catchments consist of ten hydrologically separate catchments, which were used historically to investigate the impacts of different land management treatments on streamflow (Nanni, 1956). This current study was undertaken in Catchment III (CIII) of these ten research catchments. The indigenous fire-adapted *Themeda triandra* grassland catchment was planted to *Pinus patula* in 1959 (Toucher et al., 2016).

Cathedral Peak CIII is located in a high summer rainfall area, within the Drakensberg escarpment, which has been identified as a strategic water resource area (Le Maitre et al., 2018). The region experiences wet hot summers and cool dry winters (Toucher et al., 2016). CIII's mean annual precipitation (MAP) is 1 564 mm (Toucher et al., 2016). Summer rainfall (which occurs mainly between October and March) is driven by orographic mechanisms and is dominated by thunderstorms (Nanni, 1956; Bosch, 1979). The hydrological year in the region begins in October and ends in September. Since the current period of observation (2014 – present) began in CIII, the mean annual precipitation (MAP) has been 1 216 mm. The 2018/2019 hydrological year was drier than average with 182 mm less rainfall than the 2014 – 2020 average, while the 2019/2020 hydrological year received 68 mm more rainfall than average. CIII has a north west aspect, ranges in altitude from 1 845 to 2 317 m.a.s.l., and is the second largest of the research catchments, with a catchment area of 1.4 km² (Toucher et al., 2016).

Following a fire in the catchment in 1981, which burnt out the *P. patula*, rehabilitation of the original grassland was attempted by planting the catchment to *Eragrostis curvula* and an infrequent burning regime informed by experts was implemented (Toucher et al., 2016). The rehabilitation was unsuccessful, and the catchment has transitioned towards a degraded state with severe erosion on the upper steep slopes. The degraded state of the catchment has led to the invasion by bracken, which now dominates the catchment. During the observation period, an arson fire occurred on the 19th July 2019, which burnt out the entire catchment. The soil was left exposed, resulting in further erosion and complete, repeated sedimentation of the weir at the outlet of the catchment.

Although the bracken re-established itself in the two months that followed, there was no litter layer below the bracken canopy and erosion continued. Prior to the arson fire, the catchment had not been burnt for five years. The pre-fire vegetation was denser and had a litter layer, contrasting with the post-fire canopy. The bracken changed seasonally, with a dense green canopy in summer, and senescence's in winter resulting in a sparse canopy cover (Figure 3.2). The canopy height did not exceed 0.6 m during the observation period.

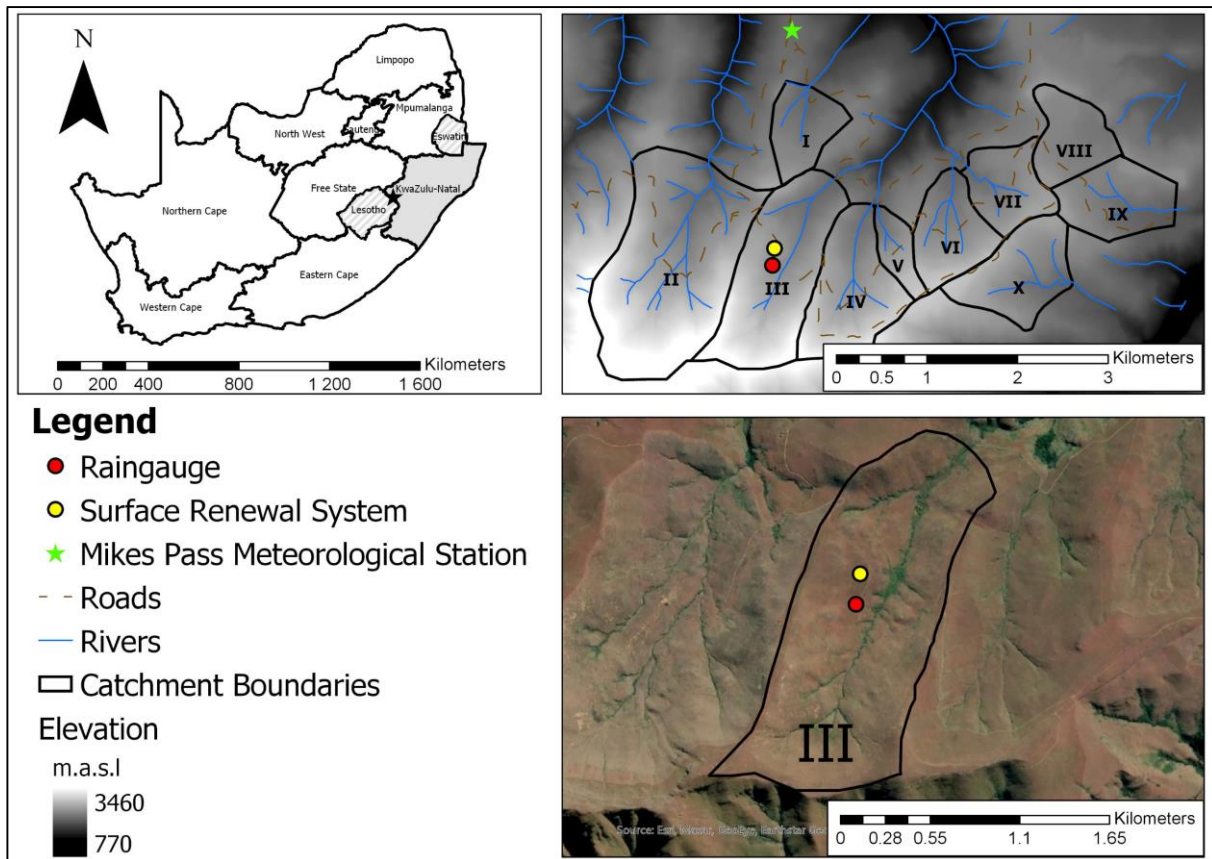


Figure 3.1: The location of the Cathedral Peak research catchment III, the focus site for this research. The locations of the rain gauge, surface renewal system and the Mikes Pass meteorological station are visible within the Cathedral Peak research catchments, South Africa.

3.2.2 Observation equipment

For the long-term estimation of ET (23 months), the SR system was used. The SR system was installed onto a tripod within a level area of CIII (Figure 3.1) on the 18th November 2018. The SR system consisted of two fine-wire thermocouples placed at 1.0 m (primary) and 1.5 m (secondary) above the ground, which were used for high-frequency (10-Hz) air temperature measurements. A four-component net radiometer (CNR4, Kipp & Zonen, Delft, The Netherlands) was positioned 2.5 m above the ground and extended 1.5 m out from the tripod on a cross-arm, and measured net radiation (R_n) and albedo. Two self-calibrating soil heat flux plates (HFP01SC-L, Hukseflux, Delft, The Netherlands) were installed 0.08 m below the soil surface and 1 m apart. Alongside these plates, four soil temperature averaging probes were installed, two placed 0.06 m and the other two placed 0.02 m below the soil surface and above

each soil heat flux plate. Between the soil heat flux plates, a soil water reflectometer was installed at 0.025 m below the soil surface (CS616, Campbell Scientific Inc, Logan, United States of America). These components were used to estimate soil heat flux (G). The sensors mentioned above were coupled to a Campbell datalogger (CR1000). The system was severely damaged in the arson fire on the 19th July 2019. Procurement of replacement equipment took four-months due to budget restrictions and insurance processes, however observations re-commencing on the 31st October 2019.

To demonstrate the adequacy of the SR approach, a summer and winter campaign where an EC system was used alongside the SR system, were conducted. The EC system used included a 3-D sonic anemometer (CSAT3A, Campbell) combined with an open-path gas analyser for H₂O and CO₂ fluxes (EC150, Campbell), which were positioned 2.5 m above the ground and attached to the tripod next to the SR system. These two sensors were connected to an electronics panel (EC100, Campbell). The electronics panel was then coupled to a Campbell datalogger (CR3000). The EasyFlux-DL program was used for EC data collection and processing of the H component measured during the summer and winter campaigns.

Rainfall was measured by a long-term tipping-bucket raingauge (TE525, Texas Electronics, Texas, United States of America, 0.254 mm tip) installed with the rim 1.2 m above the ground and located in close proximity to the tripod (160 m).

3.2.3 Estimation of energy fluxes

Following the estimation of H (H_{SRDT}) by the SRDT method (detailed in the introduction), LE can be calculated as the residual (Castellví, 2004; Hu et al., 2018) of the surface energy balance:

$$R_n - G = H + LE \quad (3.1)$$

where R_n is net radiation, the soil heat flux (G), is calculated by accounting for that measured at a determined depth (z), and then determining the soil heat storage (S) above that depth, by measuring the change in soil temperature (ΔT_s) over time (t), and the calculated heat capacity of moist soil (C_s) following the sampling of the bulk density of the soil at the site (Campbell Scientific, 2018),



Figure 3.2: The bracken canopy change at the monitoring site in CIII with SR and EC systems visible, the day before the summer campaign (11/12/2019; top left), autumn (23/03/2020; top right), day before winter campaign (17/07/2020; bottom left), and spring (05/10/2020; bottom right). All photos are post-fire.

$$S = \frac{\Delta T_s C_s z}{t} \quad (3.2)$$

Following the calculation of LE , ET can be estimated by accounting for the latent heat of vaporisation of water (Hu et al., 2018).

3.2.4 Calculation of ET_o and k_c

The crop coefficient (k_c) is a method used to understand the productivity of the vegetation, which is estimated by comparing the estimate of the grass reference evapotranspiration (ET_o) with the estimated ET (ET_{SRDT}) from the SRDT method.

$$k_c = \frac{ET_{SRDT}}{ET_o} \quad (3.3)$$

The k_c values estimated in Equation 3.3 within this study are non-standard, as they are considered for varied environmental conditions, and not standard conditions as outlined in FAO-56 (Allen et al., 1998). The FAO Penman-Monteith method makes use of weather station data to provide an estimate of the ET_o , and is a representation of the evaporative demand of the atmosphere at a given time (Allen et al., 1998). The FAO Penman-Monteith method uses daily inputs for solar radiation, air temperature and humidity, wind speed, elevation, latitude, and atmospheric pressure data (Allen et al., 1998). The reference surface on which ET_o is based, is a grass reference crop which is an “extensive surface of green, well-watered grass of uniform height, actively growing and completely shading the ground” (Allen et al., 1998). The FAO Penman-Monteith equation can be derived as:

$$ET_o = \frac{0.408\Delta(R_n - G) + \gamma \frac{900}{T+273} u_2 (e_s - e_a)}{\Delta + \gamma(1+0.34u_2)} \quad (3.4)$$

where, ET_o is the reference evapotranspiration (mm day^{-1}), Δ is the slope of the saturated water vapour pressure vs temperature curve ($\text{kPa } ^\circ\text{C}^{-1}$), R_n is net radiation at the crop surface ($\text{MJ m}^{-2} \text{ day}^{-1}$), G is the soil heat flux density ($\text{MJ m}^{-2} \text{ day}^{-1}$), γ is the psychrometric constant ($\text{kPa } ^\circ\text{C}^{-1}$), T is the mean daily air temperature at 2 m ($^\circ\text{C}$), u_2 is the wind speed at 2 m (m s^{-1}), e_s is the saturation water vapour pressure (kPa), e_a is the actual water vapour pressure (kPa), $e_s - e_a$ is the water vapour pressure deficit (kPa), and (Allen et al., 1998).

3.2.5 Data analysis

A summer and winter campaign with EC and SR systems used concurrently was conducted to calibrate and determine α values required to calibrate the SR1 method and evaluate the performance of the SR methods ability to estimate H , and subsequently ET , compared to the EC method. Only unstable atmospheric conditions were considered, as these correspond to the times when most ET occurs. The summer campaign was conducted over eight days from 12/12/2019 to 19/12/2019 and the winter campaign conducted over nine days from 28/07/2020 to 05/08/2020.

The estimation of H (H_{SRI}) by the SR1 method was achieved by processing the 10-Hz high frequency air temperature measurements from the fine-wire thermocouples and collected by the CR1000 datalogger from the primary fine-wire. The secondary fine wire was used as a back-up should the primary fine-wire break. During both the summer and winter campaigns, no fine-wire breakages were experienced. Following download, the calculated 30-minute second- (S_r^2), third- (S_r^3), and fifth-order (S_r^5) air-temperature structure functions were inserted into a formulated SR Excel spreadsheet for the SR1 (Savage, 2017) and SRDT (Savage, 2014) methods. Estimations of H_{UCSRI} were conducted for both time lags of 0.4 and 0.8 s. Time lags of 0.4 and 0.8 s correspond to a sample lag between data points of 4 and 8. The condition of van Atta (1977) is that the lag is much smaller than the ramp period plus the quiescent period. Thus, the lags of 0.4 and 0.8 have been proven to work the best with 10-Hz measurements. For the SR1 method, an α value was calculated for both 0.4- and 0.8-s lags, and applied to the 30-min H_{UCSRI} for both lags to provide 30-min H_{SRI} . The H estimations for each lag were then averaged to provide a final 30-min H_{SRI} and H_{SRDT} , as this method of averaging the different lags produced the lowest standard error, when compared to H_{EC} .

For the estimation of H (H_{EC}) by the EC method, data were processed by the CR3000 datalogger using the EasyFlux-DL program from Campbell Scientific, which is designed for open-path EC systems. The EasyFlux-DL program provided corrected 30-min H_{EC} values, as well as data quality grades and the number of samples taken for each 30-min period. A data quality grade is a rating from 0 to 9 calculated based on a series of criteria developed by Foken et al. (2012). These values are assigned following analysis of measurement characteristics, with an example being wind flow distortion. This is when measurements recorded under a wind direction where the sensor is downwind of the mast or apparatus, negatively impacting the precision of the measurement, will be allocated a poorer quality rating. Using these variables, 30-min periods where a data quality grade of 9 or above was assigned (Foken et al., 2012) and a sample size of 30 % or less, were removed from the comparison. The remaining 30-min H_{EC} values were used in the comparison with H_{SRI} and H_{SRDT} .

Following the comparison of H for all methods, LE (LE_{SRDT}) using the SRDT method, was estimated as a residual of the shortened energy balance equation, from which ET (ET_{SRDT}) was then estimated for the SRDT method only. Stability conditions were considered separately, with unstable conditions defined as periods when R_n was positive ($R_n > 0 \text{ W m}^{-2}$) and the occurrence of a positive SR ramp amplitude given by a negative third-order air temperature structure function under both lags ($S_r^3 < 0$) as stated in Savage (2014). For the SRDT method, canopy

height measurements were taken during each campaign for the calculation of zero plane displacement height (d), which is equal to 2/3 of canopy height. The canopy height for the summer campaign was 0.55 m and 0.40 m for the winter campaign.

Following the analysis of the summer and winter campaigns, for the measurement of the seasonal ET_{SRDT} , the SRDT method was used for the full observation period, which began on the 13th November 2018 and concluded on the 31st October 2020. For the seasonal analysis, summer (December, January, February), autumn (March, April, May), winter (June, July, August) and spring (September, October, November) were considered.

3.2.6 Patching missing data

Due to the occurrence of the fire on the 19th July 2019, and the malfunctioning of equipment during May and June 2020, patching of the data during these periods was conducted to provide an indication of ET_{SRDT} and energy balance partitioning. The patched data for the period following the fire does not provide an indication of ET_{SRDT} immediately following a fire, but ET_{SRDT} expected had the fire not occurred. Following the fire, no data at the site was recorded until the 31st October 2019, while during the period of equipment malfunction, R_n and G were still observed. Daily ET_{SRDT} for both periods were patched using meteorological data available from the nearby (~2 km) Mike's Pass meteorological station. Using the available meteorological data, daily ET_o was calculated using the FAO Penman Monteith method (equation 3.4), and multiplied by the k_c values (equation 3.3) calculated during a representative month (either previous or following year value for that month). The energy balance partitioning was patched for the fire period, by finding the relationship between the solar radiation observed at the Mike's Pass meteorological station and for CIII the R_n observed by the SR system. The relationship was then applied to the solar radiation data to determine the R_n for CIII during the periods when it was not observed. The G component was considered a representative percentage of daily R_n as was found for a representative month. For both periods, the LE component was determined from the patched daily ET_{SRDT} , and the H_{SRDT} component was calculated as the residual of the shortened energy balance (equation 1) having determined the remaining three components.

3.3 Results

3.3.1 Determination of α for calibration of the SR1 method

The initial step required before the methods could be compared, was the calibration of SR1, using EC. An α was calculated from the slope of the linear regression between the H_{UCSR1} (x) and H_{EC} (y) for stable and unstable conditions. Only the unstable α was reported, as ET occurs predominantly when conditions are unstable, and the performance of the method for unstable conditions is of interest. An α was calculated for unstable conditions (Table 3.1) for both the 0.4- and 0.8-s lags and for summer and winter respectively.

Table 3.1: The α determined for summer (12/12/2019 – 17/12/2019) and winter (27/07/2020 – 03/08/2020) and for 0.4- and 0.8-s lags and the average of the two lags for unstable conditions.

Lag (s)	Unstable α	
	Summer	Winter
0.4	0.60	0.59
0.8	0.73	0.74
Average	0.66	0.66

3.3.2 Comparison between EC, SR1 and SRDT methods

Following the calibration of the SR1 method and calculating H_{SR1} , a comparison between the H_{EC} , H_{SR1} , and H_{SRDT} was conducted using linear regressions (Figure 3.3). For both the summer (slope = 0.86; intercept = 20.13 W m⁻²; R² = 0.75; RMSE = 39.56 W m⁻²) and winter campaigns (slope = 0.83; intercept = 40.31 W m⁻²; R² = 0.81; RMSE = 41.84 W m⁻²), H_{SR1} was lower compared to H_{EC} . The estimation of H_{SRDT} showed a good relationship with H_{EC} in the summer campaign (slope = 1.03; intercept = 15.02 W m⁻²; R² = 0.79; RMSE = 38.77 W m⁻²) and a slight underestimation in the winter campaign (slope = 0.91; intercept = 37.08 W m⁻²; R² = 0.84; RMSE = 41.80 W m⁻²). H_{SRDT} showed a closer relationship to H_{EC} for both campaigns, with H_{SR1} and H_{SRDT} being closer to H_{EC} during summer than in winter.

Based on these comparisons, of the two SR methods, the SRDT method showed the closest relationship to the EC method for the estimation of H . Due to this finding, the assumption was made that the SRDT method will accurately estimate long-term H which can be used for the estimation of the long-term ET . The SRDT method was therefore the method chosen for the seasonal analysis of ET over the bracken canopy.

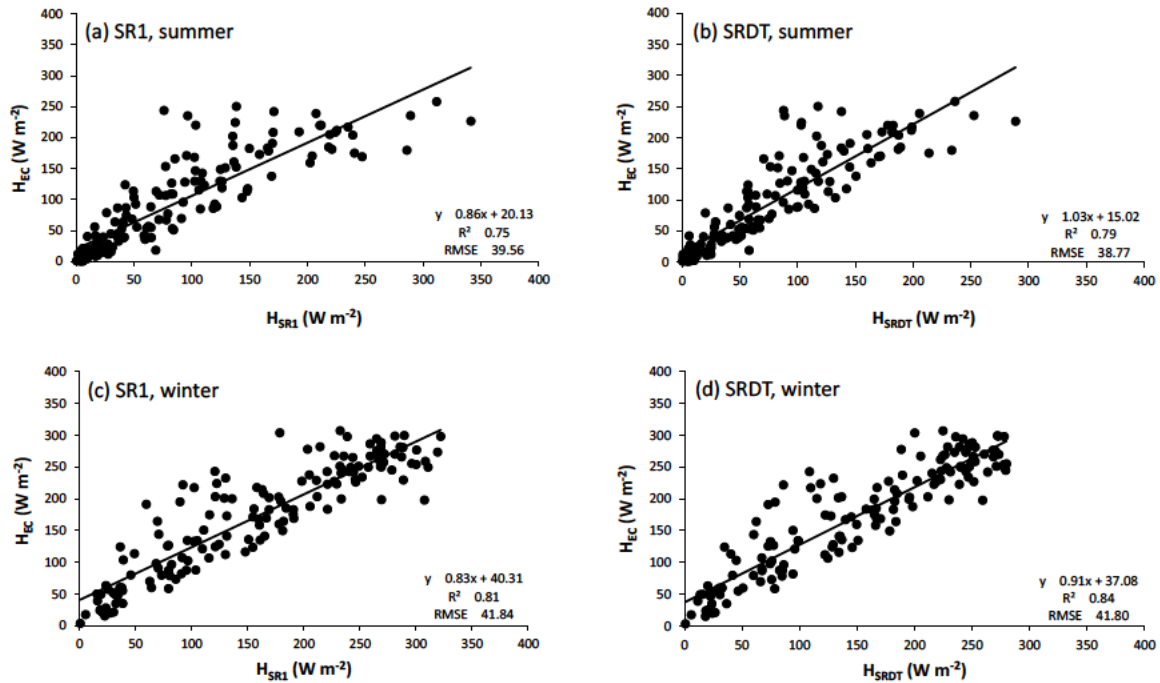


Figure 3.3: The comparison between half-hourly H_{SR1} and H_{SRDT} , with half-hourly H_{EC} for the summer (a, b) and winter campaigns (c, d).

3.3.3 Assessment of seasonality of ET based on H_{SRDT}

The shift in the relationship of the energy balance components between seasons is an important part of understanding the changes in ET between seasons. As expected, R_n was high during summer (Figure 3.4) with late spring (November 2019) experiencing the highest average daily R_n per month during the observation period. A decline in R_n occurred from summer through

autumn and into winter where the lowest daily average R_n per month was experienced. When average daily R_n was high, LE_{SRDT} was the dominant component accounting for, on average, 77 % of R_n in summer. As average daily R_n decreased and conditions became drier through autumn into winter, the LE_{SRDT} component decreased and the H_{SRDT} component increased, while the G component remained low year-round in relation to the average daily R_n , but could be seen as slightly higher in summer, autumn and winter (7 %), and lower in spring (5 %). During winter, H_{SRDT} and LE_{SRDT} were similar, accounting for an average 41 % and 51 % of R_n , respectively. Following the first rainfalls in early spring, LE_{SRDT} increased again as H_{SRDT} decreased. It is clear (Figure 3.4) that during summer, the majority of R_n-G was partitioned into LE_{SRDT} , while in winter, R_n-G was evenly partitioned between H_{SRDT} and LE_{SRDT} .

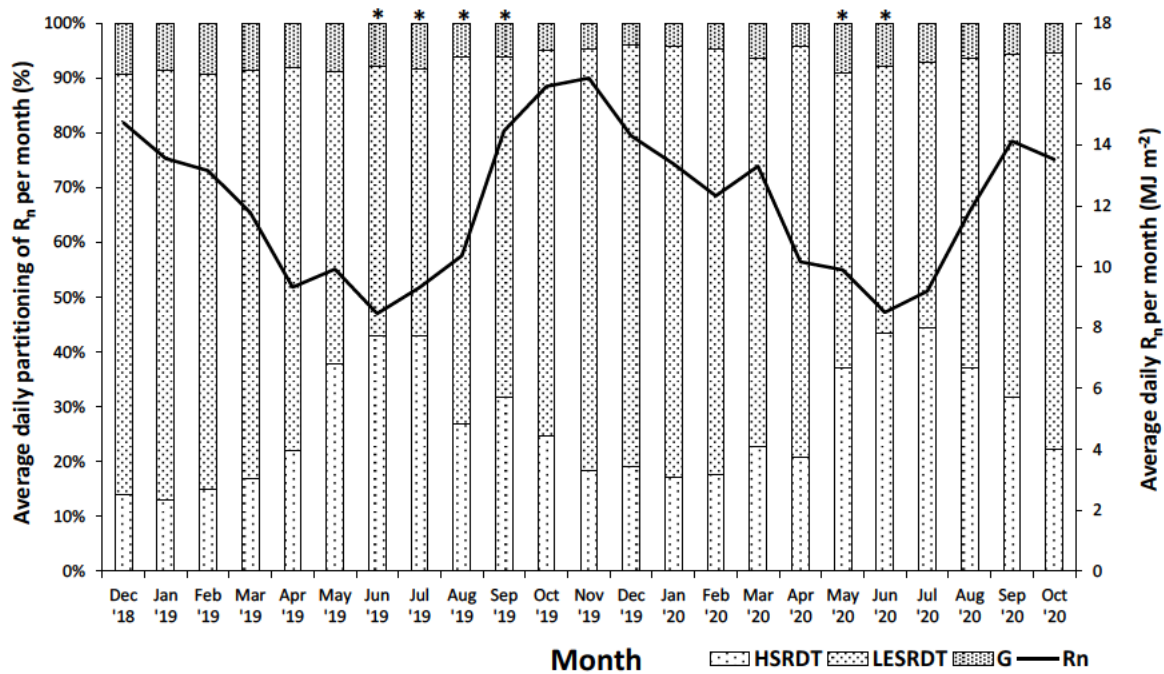


Figure 3.4: The average daily energy balance per month using SRDT, as a percentage of R_n (when $R_n > 0$). The average daily R_n for each month is indicated by the solid line. (The * indicates months where patched data were used due to equipment loss and malfunction).

Over an observation period of 23 months, of which ET_{SRDT} was estimated for 17 months and patched for 6 months, a strong seasonal pattern in ET (Figure 3.5) as indicated by the shifts in energy balance over the same period was evident. The fire created a break in the observed ET_{SRDT} data record due to the loss of the SR equipment. The raingauge was able to be replaced instantaneously after the fire. As the SR system was initially installed in the middle of

November 2018, and the replacement of the SR system following the fire was completed at the beginning of November 2019, two distinct periods in the data set occurred. The start of these two periods were drawn forward to the 1st December. The first period starting on the 1st December 2018 to the 18th July 2018 (7.6 months) and is referred to as the pre-fire period. The second period starting on the 1st December 2019 and ending on the 18th July 2020 (7.6 months), is referred to as the post-fire period. The pre-fire period fell within the drier 2018/2019 hydrological year, with 763 mm of rainfall occurring in the pre-fire period. While the post-fire period experienced 1 115 mm of rainfall, with 42 % of that falling during February 2020 (Figure 3.5). A further standout difference in rainfall between the two periods was that the pre-fire autumn period (Mar – May), received 62 mm more rainfall than the post-fire autumn period, despite the post-fire period being overall much wetter.

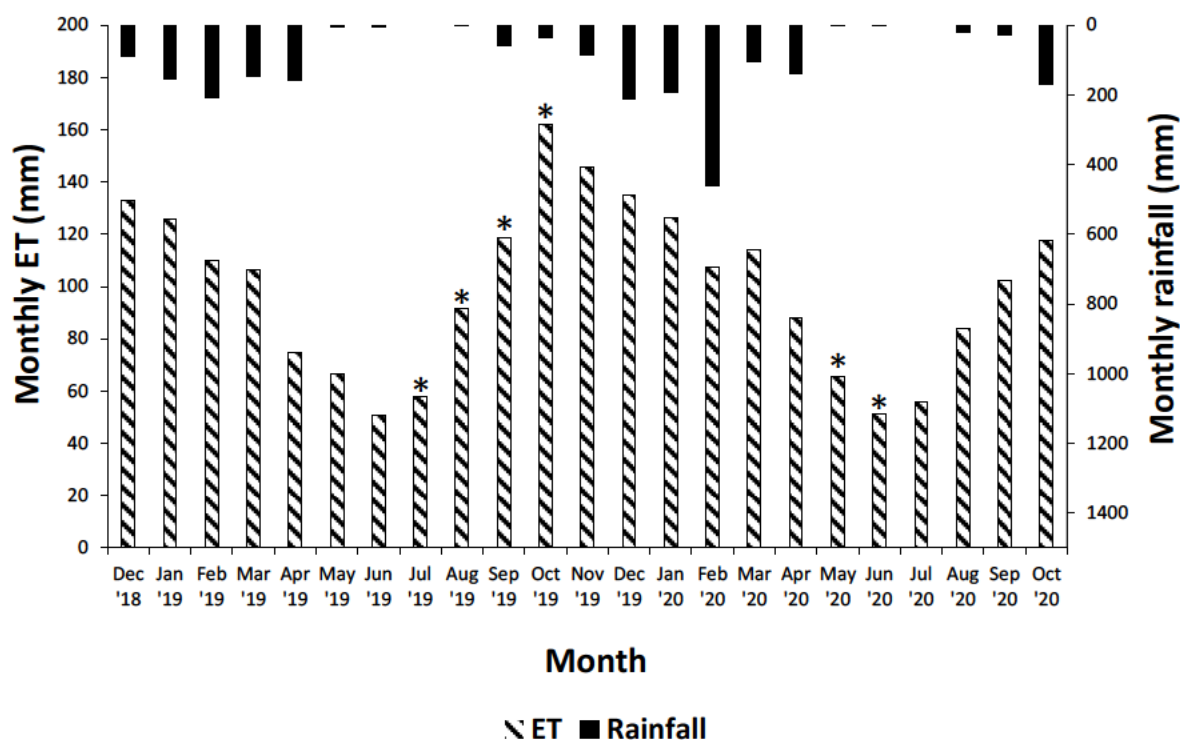


Figure 3.5: The monthly total ET_{SRDT} over the bracken canopy on the bottom axis, with monthly total rainfall on the top axis. (The * indicates the period where patched data are used due to the fire damage and equipment malfunction).

The highest monthly observed total ET_{SRDT} of 146 mm occurred in November 2019 (Figure 3.5). The summer months of December, January and February, showed similar monthly total ET_{SRDT} across both periods despite a difference in rainfall of 416 mm between the two summers

of observation. The seasonal trends highlighted at the monthly scale, are clearly evident when using a 30-day moving average (Figure 3.6). Across the observation period there is a strong seasonal trend in daily ET_{SRDT} , as well as higher inter-daily variability in summer and autumn, compared to spring and winter. The 30-day moving average ET_{SRDT} peaks in late spring/early summer, and although variable day to day, a gradual decline occurs through summer (Figure 3.6). Despite continued rainfall through autumn, daily ET_{SRDT} continues to decline, possibly in response to the decline in R_n .

The k_c was calculated at a daily scale and averaged to provide a monthly k_c (Figure 3.6). A k_c provides an indication of the ET activity of the canopy as well as potential insight into water stress and climate limitations. The highest k_c was found during summer with a maximum at approximately 0.75, when it can be presumed that the activity of the canopy is highest and water and R_n are readily available, as the observed ET was closest to the potential ET . Spring also experienced a comparatively high k_c , with a steep increase following winter, again indicating the two seasons when the canopy is the most active. Despite a higher average daily ET_{SRDT} measured during spring than in summer, the k_c indicates that the canopy is still not meeting the potential ET , as it comes close to doing in summer, possibly suggesting R_n and water availability as limiting factors in spring. This is observed in the patched October values with the highest monthly ET_{SRDT} following a wetter September, increasing water availability in October, leading to a higher ET_o . Autumn sees a steep decline in k_c where observed ET_{SRDT} is much lower than the potential ET , possibly due to the end of the rainfall season and declining R_n . As expected, k_c in winter has the lowest values, when resources are the least available to the canopy.

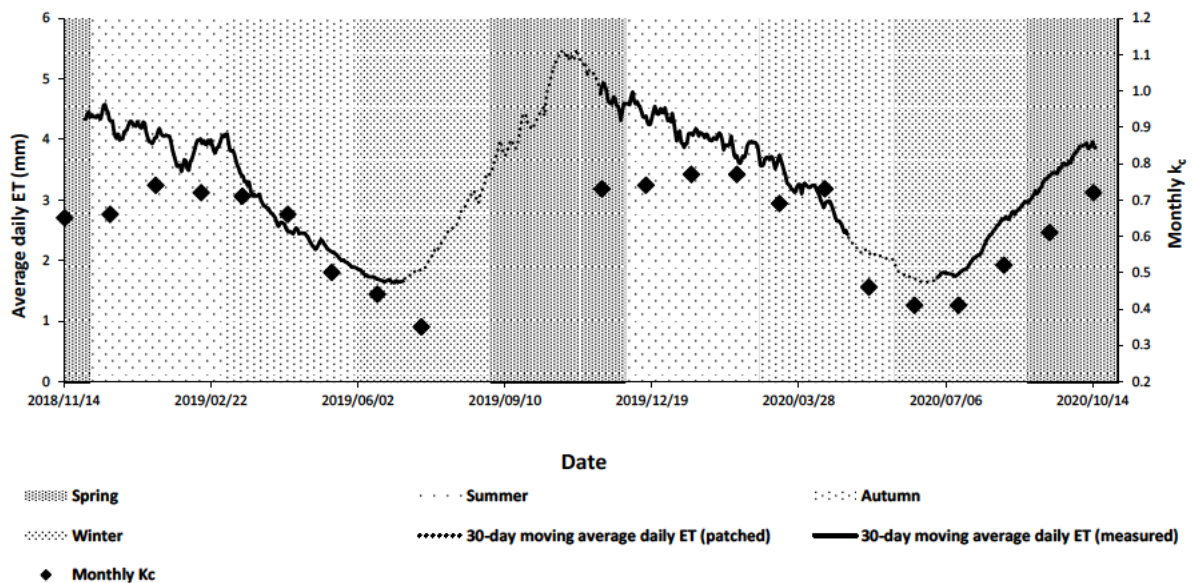


Figure 3.6: The 30-day moving average of daily ET_{SRDT} and the monthly k_c . The seasons are indicated by the background shading. The period where patched data were used is shown as a dotted trendline.

The average daily ET per month, reveals further details of seasonality. From daily ET_{SRDT} , averages were calculated as representatives of each month. The highest average daily ET_{SRDT} (4.86 mm) occurred in November 2019. The second highest was December 2019 (4.35 mm). The lowest average daily ET_{SRDT} was found for June 2019 (1.70 mm) and June 2020 (1.17 mm). For days when rainfall occurred, daily ET_{SRDT} was expected to be reduced due to stomatal closure and reduced R_n . To investigate this, average daily ET_{SRDT} was calculated only including dry days, which were days where no rainfall event occurred (daily rainfall < 2 mm). The highest average dry daily ET (ET_{dd}) occurred in December 2019 (6.13 mm). In general, the ET_{dd} in summer months, exceeded spring, autumn and winter months, unlike the aforementioned average daily ET . The periods, which saw the greatest change in average daily ET_{SRDT} when considering only dry days vs all days, were the months during the transition from summer to autumn, February and March. A maximum daily ET_{SRDT} of 8.09 mm was observed in December 2019, and a minimum of 0.40 mm in June 2020.

A 30-day moving average of daily ET_{SRDT} for the pre- and post-fire periods were compared alongside the cumulative daily rainfall (Figure 3.7). The monthly total ET_{SRDT} of December 2018 and December 2019, had a difference of only 1.64 mm. During early summer (January and February) the ET_{SRDT} response of the pre- and post-fire canopies were similar, with a difference either way due to periods of rainfall which resulted in lower ET_{SRDT} . As shown in Figure 3.7, the accumulated R_n follows a similar pattern to that of accumulated ET_{SRDT} . For the middle of April, and the middle of autumn, a divergence in both accumulated ET_{SRDT} and accumulated R_n occurred. During the autumn period, in March, the post-fire canopy ET_{SRDT} was 7.4 mm more than the pre-fire canopy, which increased to 13.3 mm more in April. The other months never showed a difference greater than 3 mm. Rainfall in both periods ceased around the end of April. Over the comparison period, a difference of 22.2 mm in ET was found, with the post-fire canopy ET_{SRDT} being higher. The pre-fire period received 763 mm of rainfall, while the post-fire period had received 1 115 mm of rainfall. The post-fire canopy also experienced 36.71 MJ m⁻² more R_n over the month than the pre-fire canopy. Thus, over the comparison period, the post-fire canopy experienced more R_n and rainfall, and a higher ET_{SRDT} . Of the rainfall, ET accounted for 91 % during the pre-fire period, and 65 % during the post-fire period.

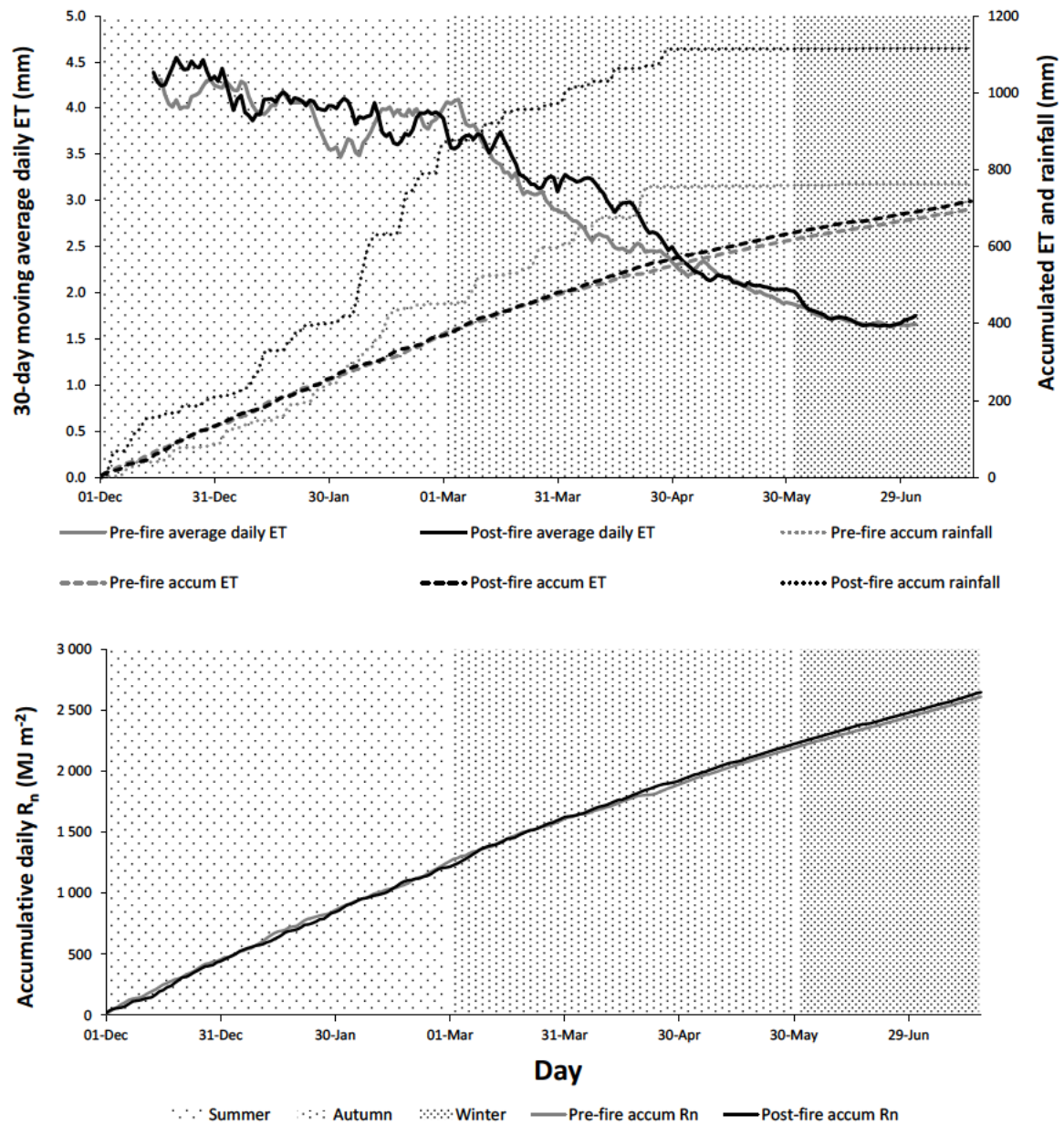


Figure 3.7: A comparison of the daily ET_{SRDT} in consecutive years from 1st December to 18th July for the pre-fire period and the post-fire period over the bracken canopy. The 30-day moving average daily ET_{SRDT} is indicated by the solid line, accumulated daily ET_{SRDT} dashed line (---), accumulated daily rainfall indicated by the dotted lines (•••) (above), and the accumulated R_n (below) for each respective period.

3.4 Discussion

To be able to analyse and understand the seasonal *ET* of a bracken canopy, a suitable long-term method for the observation of *ET* needed to be identified that falls within the requirements of a remote fire-adapted high-altitude grassland monitoring network. The SR method provides a simpler alternative to the EC method for the long-term estimations of *ET*, but has limited validation over natural vegetation types and within mountainous terrain. From the summer and winter campaigns, the performance of the SR1 and the independent SRDT methods for the estimation of *H* was good, as shown by the close relationships found with the benchmark EC method. The relationship between the SR methods and the EC method was closer in summer than winter, with the SRDT closest to the EC method in summer (slope = 1.03; intercept = 15.02 W m⁻²; R² = 0.79; RMSE = 38.77 W m⁻²). Prefaced on the good relationship found between the SRDT method and the EC method for the estimation of *H*, using the remaining energy balance components, *ET* estimations were assumed to follow the same relationship between the methods. The SRDT method was therefore applied for the estimation of *ET* over the bracken canopy within the Cathedral Peak research catchments and will continue to be utilised into the future for long-term observation of *ET* at the site conducted by the South African Environmental Observation Network (SAEON).

The *ET*_{SRDT} showed the invader bracken to have a strongly seasonal *ET*. The bracken canopy structure was highly variable between seasons (Figure 3.2), from a dense summer canopy, which begins to brown in autumn following senescence and completely dies off in winter. The response in spring is slow, with initial spots of greening in October, following the start of the rainfall season. The seasonal cycle of the bracken canopy was found to be similar to that of the montane grasslands of the region (Everson 2001). During summer, water and energy are considered readily available. During summer, *R_n-G* was partitioned mainly into *LE* (Figure 3.4), as expected, due to the wetter soil conditions following summer rainfall. During winter, when conditions were drier, the dominance of *LE* was reduced, and *H* and *LE* were similar. As *H* and *LE* are equally proportioned, this could be an indication that despite drier conditions and a lack of rainfall in winter, there is still no severe water stress as *LE* accounts for up to 50 % of the available energy flux. Across all seasons, *LE* accounted for 74 % of *R_n-G*, which is considerable compared to a grassland. For example, over a mixed grassland community in a humid region following 18 months of observation, Savage et al. (2004) found *LE* to account for just under 50 % of *R_n-G* over a grassland. The final energy balance component *G*, was found to be small under the bracken canopy across all seasons. This could be representative of the dense canopy cover characteristic of the bracken canopy especially in summer, as well as indicating a higher

soil water retention. The G component was found to be similar in summer, autumn, and winter, and slightly reduced in spring. The small differences in soil heat flux between the seasons, could be indicative, in part, of a high soil water holding capacity, explaining the lack of severe water stress during the drier months. The dense nature of the bracken canopy differentiates this form of degradation from other types of degradation. Degradation within a grassland is often considered to be a loss of grassland canopy and results in an increase in bare soil. In terms of this study, degradation is considered to be the loss of natural grassland canopy by the invasion of bracken canopy. The change in canopy structure and characteristics, results in a change in ET . The findings from this study, suggest a similar seasonal ET cycle between the grassland and bracken canopies, but a higher year-round ET from the bracken canopy.

Over the Cathedral Peak CIII bracken canopy, the highest ET occurred during the hot and wet periods of summer and spring. The highest average daily ET_{SRDT} (4.9 mm) and highest monthly total ET_{SRDT} (145 mm) occurred towards the end of spring (Nov '19). The highest daily ET_{SRDT} (8.1 mm) occurred in December 2019 with daily ET during the hot and wet summer periods regularly exceeding 5 mm. The only other known comparable study on the ET of a bracken canopy was conducted by Springer et al. (2006) in the semi-arid Hart Prairie, United States of America. Springer et al. (2006) used volumetric water content to estimate ET of a bracken fern and graminoid understory. Springer et al. (2006) observed only the growing season, and periods when monsoon rainfall did not occur, due to limitations of the method when precipitation occurred. The canopy studied by Springer et al. (2006) consisted of two dominating vegetation types, bracken and Kentucky bluegrass (*Poa pratensis*), which needs to be considered when drawing comparisons between the findings of Springer et al. (2006) and the complete bracken dominated canopy of this study. The study by Springer et al. (2006) also took place over three dry years, with annual rainfalls all under the site MAP. During the drier growing period, the average daily ET was 4.5 mm in the slightly dry year, 3.7 mm in the moderately dry year, and 1.9 mm in the extremely dry year (Springer et al., 2006). This is comparable to the spring period before the summer rainfall in Cathedral Peak, where the daily ET_{SRDT} was > 4 mm (Figure 3.6). In Cathedral Peak towards the start of summer rainfall, daily average ET_{SRDT} peaked, but did not reach the post-monsoon growing period level average daily ET of 7.0 mm in the extremely dry year, 7.1 mm in the moderately dry year and 7.9 mm in the slightly dry year found by Springer et al. (2006). This, however, could be comparable to the daily high of 8.1 mm measured at Cathedral Peak during December 2019, which was following a wet period, with a rainfall of 156 mm in two-weeks. Springer et al. (2006), found the bracken canopy to be sensitive to drought, with evaporation being the larger component of ET than

transpiration. The study site of Springer et al. (2006) is much drier, being semi-arid, and suggests that at the lower end of water availability, bracken is sensitive to water stress, which may not be the case in Cathedral Peak, due to its location in a high rainfall area.

Within the Northern Drakensberg grasslands, in a neighbouring research catchment, Everson (2001) observed the natural grassland seasonal *ET*. Everson (2001) found the grassland *ET* to be high during the wet and hot summer and spring seasons and negligible during the dry cold winter seasons, a similar seasonal trend to that of the bracken canopy shown in this study. However, the bracken summer maximum daily ET_{SRDT} exceeded the maximum daily *ET* (7 mm) measured for the grassland by Everson (2001). The range of daily *ET* observed for the bracken and grassland were found to be similar during the wet season, with a bracken average daily ET_{SRDT} of 4 mm. During the winter dry period, Everson (2001) found the grassland daily *ET* to never exceed 1 mm, while the bracken average daily ET_{SRDT} was 2 mm with a maximum daily ET_{SRDT} of over 3 mm. The average of the monthly totals for ET_{SRDT} in June '19, '20, and July '20 was 53 mm, during which the average monthly rainfall was 1.5 mm for those three months. Based on the comparison with the winter dry season findings of Everson (2001), it could be expected that a transition from grassland to degraded state invaded by bracken would have the greatest impact on the water balance of a catchment during the winter dry season. It was suggested that the bracken canopy is not soil-moisture limited, based on the observation of equal cumulated ET_{SRDT} at the end of summer for the pre- and post-fire periods, despite a difference of 416 mm in rainfall. This is further justified by the finding of Everson (2001), that at an annual scale, changes in *ET* of the neighbouring grassland were not substantial, despite a rainfall variability of ~300 mm over a four-year period, indicating no soil moisture stress was occurring within the grassland.

Suggesting no soil moisture stress occurs within both the bracken and grassland canopy is one perspective. The two observation periods split by the fire, provided a valuable comparison, where despite a large difference in rainfall between the two periods, the ET_{SRDT} was similar at the end of summer. Following summer, autumn was the season during which the largest difference in ET_{SRDT} (20 mm) was measured between the two periods. The post-fire period was the wetter year, with 42 % of the rainfall during February. The autumn of the pre-fire (drier) period experienced 61 mm more rainfall than the post-fire period. Despite this, the post-fire period showed a higher total *ET* for autumn, 20 mm more than the pre-fire period. A potential explanation for this is that the above-average February rainfall resulted in a higher soil water

content during the following autumn, which outweighed the 61 mm deficit in rainfall. Thus, autumn ET could be considered sensitive to the timing and amount of summer rainfall.

The role of R_n also needs to be considered. The pre-fire summer period received 29.23 MJ m⁻² more R_n than the post-fire summer, whereas the pre-fire autumn received 71.90 MJ m⁻² less than the post-fire autumn. Despite the difference in available energy flux during summer, the post-fire and pre-fire summer ET_{SRDT} totals were equal, whereas the larger difference in available energy flux resulted in a lower pre-fire ET_{SRDT} regardless of the wetter pre-fire autumn. The higher rainfall occurrence, is likely associated with a reduced R_n due to more cloud cover. Similarly, Everson (2001), concluded for the neighbouring grassland catchment that the higher ET in the drier years was attributable to the higher solar radiation due to reduced cloud cover over the year. The importance of this observation, is that a later (autumn) rainfall had a larger impact on the available energy flux than an earlier (summer) rainfall, due to the lower solar radiation levels during autumn than summer. Therefore, a later rainfall, reduces R_n and summer soil water content, compared to an earlier and larger summer rainfall.

For the first time, an understanding of the seasonal changes of bracken ET , allows for inferences on the influence of this form of degradation on the water balance of these high altitude, fire-adapted montane grasslands catchments and a base of information from which further studies can be undertaken. It was found that the seasonal cycle of the bracken ET was similar to that of the fire-adapted grassland, however, the ET was much greater, especially in winter, implying an influence on the water balance, particularly during winter. During the dry period, a larger proportion of the available water will be used by bracken for ET , possibly leading to a reduction in streamflow, which should be investigated further. A loss of grassland within these montane areas could therefore have considerable effects on winter low flows and water resources during the dry season. With the high summer rainfalls, the hot, wet season is likely less affected. However, the timing of the wet season rainfall influences the autumn ET of the bracken canopy, with higher rainfall during summer resulting in higher autumn ET , while higher autumn rainfall results in a lower autumn ET . Therefore, a wet summer followed by a drier autumn could result in a higher autumn ET , which may translate through to the water balance, further influencing the dry season flows. The influence of the changes in ET found in this study, need to be further examined, including how they will affect the water balance and water supply, and to what extent degradation followed by invasion by bracken, of the high-altitude, fire-adapted montane grasslands, will have an effect on water supply from this region.

3.5 Conclusions

Following 23 months of observation, it was found that the invader bracken canopy follows a similar seasonal trend compared to that of the natural grassland vegetation cover of the region. The highest *ET* occurred during late spring and early summer when both R_n and soil water availability are at their highest. Autumn was identified as the period most sensitive to rainfall amount and timing, as late annual rainfall during autumn decreases *ET*, while higher summer rainfall with lower autumn rainfall promotes *ET*. Winter is the period when the largest difference between a natural grassland and invaded bracken would influence the water balance, as the bracken canopy winter *ET* is still substantial compared to a dormant grassland, while summer differences are not as large. No soil water stress was considered present, with the rate of *ET* being sensitive to available energy flux and seasonal solar radiation variability. A longer period of observation is therefore recommended to further understand the sensitivities of *ET* to changes in rainfall amount and timing, as well as to provide a better representation of spring. Annual rainfall within this region is highly variable and is an important consideration to keep in mind when assessing the seasonal *ET*. In terms of observation, the surface renewal dissipation theory method was shown to be a suitable alternative to the more expensive EC system for long-term observations of *ET*, which will aid in improving this understanding and provide a valuable dataset on land cover change with the important uKhahlamba-Drakensberg mountain range. The benefit of using the SRDT method for long-term measurement was realised when a fire damaged all the equipment. A full EC system would have been a much greater loss than the SRDT system which was able to be replaced within a few months. The understanding gained on the *ET* of a bracken canopy should be taken forward and used to further the understanding of the implications of an invasion by bracken on the water balance of the high-altitude, fire-adapted grassland catchments, and what it means for water supply generated from the region.

3.6 Acknowledgements

The authors would like to acknowledge the financial and logistical assistance provided by the National Research Foundation's South African Environmental Observation Network (SAEON) business unit. Opinions expressed and conclusions arrived at are those of the author(s) and are not necessarily to be attributed to the NRF or SAEON.

3.7 References

Allen, R., Pereira, L., Raes, D., Smith, M., 1998. Guidelines for Computing Crop Water requirements-FAO Irrigation and Drainage Paper 56; FAO-Food and Agriculture Organization of the United Nations, Rome.

- Asmal, O.E., 1995. Land degradation in the Cathedral Peak area of the Natal Drakensberg: 1945 to 1992. MSc thesis. University of Cape Town, Department of Environmental and Geographical Science, Rondebosch, South Africa.
- Bangamwabo, V.M., 2009. Spatial and temporal extent of land degradation in a communal landscape of KwaZulu-Natal, South Africa. MSc thesis. University of KwaZulu-Natal, Pietermaritzburg, South Africa.
- Berget, C., Duran, E., Bray, D.B., 2015. Participatory Restoration of Degraded Agricultural Areas Invaded by Bracken Fern (*Pteridium aquilinum*) and Conservation in the Chinantla Region, Oaxaca, Mexico. *Human Ecology*, 43, 547-558.
- Bosch, J., 1979. Treatment Effects on Annual and Dry Period Streamflow at Cathedral Peak. *South African Forestry Journal*, 108, 29-38.
- Brown, L.R., Bezuidenhout, H., 2020. Grassland Vegetation of Southern Africa. *Encyclopaedia of the World's Biomes*, 3, 814-826.
- Burba, G.G., Verma, S.B., 2005. Seasonal and interannual variability in evapotranspiration of native tallgrass prairie and cultivated wheat ecosystems. *Agricultural and Forest Meteorology*, 135: 190-201.
- Campbell Scientific, 2018., Model HFP01SC Self-Calibrating Soil Heat Flux Plate Revision: 10/16. Available at: <https://s.campbellsci.com/documents/us/manuals/hfp01sc.pdf> [Accessed 10 October 2018].
- Castellví, F., Perez, P.J., Ibañez, M., 2002. A method based on high frequency temperature measurements to estimate sensible heat flux avoiding the height dependence. *Water Resources Research*, 38(6), WR000486-20.
- Castellví, F., 2004. Combining surface renewal analysis and similarity theory: A new approach for estimating sensible heat flux. *Water Resources Research*, 40(5), W05201
- Castellví, F., Martinez-Cob, A., Perez-Coveta, O., 2006. Estimating sensible and latent heat fluxes over rice using surface renewal. *Agricultural and forest meteorology*, 139, 164-169.
- Castellví, F., Snyder, R.L., 2009a. On the performance of surface renewal analysis to estimate sensible heatflux over two growing rice fields under the influence of regional advection. *Journal of Hydrology*, 375, 546-553.
- Castellví, F., Snyder, R.L., 2009b. Combining the dissipation method and surface renewal analysis to estimate scalar fluxes from the time traces over rangeland grass near Ione (California). *Hydrological Processes*, 23, 842-857.
- Castellví, F., Snyder, R.L., 2010. A comparison between latent heat fluxes over grass using a weighing lysimeter and surface renewal analysis. *Journal of Hydrology*, 381, 213-220.
- Castellví, F., 2011. Is It Worthy to Apply Different Methods to Determine Latent Heat Fluxes? – A Study Case Over a Peach Orchard. *Evapotranspiration-From Measurements to Agricultural and Environmental Applications*, 43-58.

- Castellví, F., Cammalleri, C., Ciraolo, G., Maltese, A., Rossi, F., 2016. Daytime sensible heat flux estimation over heterogeneous surfaces using multitemporal land-surface temperature observations. *Water Resources Research*, 52, 3457-3476.
- Clulow, A.D., Everson, C.S., Mengistu, M.G., Jarman, C., Jewitt, G.P.W., Price, J.S., Grundling, P.L., 2012. Measurement and modelling of evaporation from a coastal wetland in Maputaland, South Africa. *Hydrology and Earth System Sciences Discussions*, 9(2), 1741-1782.
- Coners, H., Babel, W., Willinghöfer, S., Biermann, T., Köhler, L., Seeber, E., Foken, T., Ma, Y., Yang, Y., Miehe, G., Leuschner, C., 2016. Evapotranspiration and water balance of high-elevation grassland on the Tibetan Plateau. *Journal of Hydrology*, 533, 557-566.
- Cui, W., Chui, T.F.M., 2019. Temporal and spatial variations of energy balance closure across FLUXNET research sites. *Agricultural and Forest Meteorology*, 271, 12-21.
- da Silva, P.F., de Sousa Lima, J.R., Antonino, A.C.D., Souza, R., de Souza, E.S., Silva, J.R.I., Alves, E.M., 2017. Seasonal patterns of carbon dioxide, water and energy fluxes over the Caatinga and grassland in the semi-arid region of Brazil. *Journal of Arid Environments*, 147, 71-82.
- Douterlungne, D., Levy-Tacher, S.I., Golicher, D.J., Dañobeytia, F.R., 2010. Applying Indigenous Knowledge to the Restoration of Degraded Tropical Rain Forest Clearings Dominated by Bracken Fern. *Restoration Ecology*, 18(3), 322-329.
- Drexler, J.Z., Snyder, R.L., Spano, D., Paw U, K.T., 2004. A review of models and micrometeorological methods used to estimate wetland evapotranspiration. *Hydrological Processes*, 18, 2071-2101.
- Everson, C.S., 2001. The water balance of a first order catchment in the montane grasslands of South Africa. *Journal of Hydrology*, 241, 110-123.
- Everson, C.S., Dye, P.J., Gush, M.B., Everson, T.M., 2011. Water use of grasslands, agroforestry systems and indigenous forests. *Water SA*, 37(5), 781-788.
- Feng, J., Liu, H., 2016. Response of evapotranspiration and CO₂ fluxes to discrete precipitation pulses over degraded grassland and cultivated corn surfaces in a semiarid area of Northeastern China. *Journal of Arid Environments*, 127, 137-147.
- Foken, T., Leuning, R., Oncley, S.R., Mauder, M., Aubinet, M., 2012. Corrections and data quality control. In *Eddy covariance*, 85-131. Springer, Dordrecht.
- Grab, S.W., Knight, J., 2018. Southern African montane environments. *Southern African Landscape and Environmental Change*. Routledge, United Kingdom.
- Grellier, S., Florsch, N., Janeau, J., Podwojewski, P., Camerlynck, C., Barot, S., Ward, D., Lorentz, S., 2013. Soil clay influences Acacia encroachment in South African grassland. *Ecohydrology*, 7(6), 1474-1484.
- Han, D., Wang, D., Liu, T., Xue, B., Kuczera, G., Xu, X., 2018. Hydroclimatic response of evapotranspiration partitioning to prolonged droughts in semiarid grassland. *Journal of Hydrology*, 563, 766-777.

- Haymann, N., Lukyanov, V., Tanny, J., 2019. Effects of variable fetch and footprint on surface renewal measurements of sensible and latent heat fluxes in cotton. *Agricultural and Forest Meteorology*, 268, 63-73.
- Hoffman, M.T., Todd, S., 2000. A National Review of Land Degradation in South Africa: The Influence of Biophysical and Socio-economic Factors. *Journal of Southern African Studies*, 26(4), 743-758.
- Hu, Y., Buttar, N.A., Tanny, J., Snyder, R.L., Savage, M.J., Lakhari, I.A., 2018. Surface Renewal Application for Estimating Evapotranspiration: A Review. *Advances in Meteorology*, 2018, 1-11.
- Huizhi, L., Jianwu, F., 2012. Seasonal and Interannual Variations of Evapotranspiration and Energy Exchange over Different Land Surfaces in a Semiarid Area of China. *Journal of applied meteorology and climatology*, 51, 1875-1888.
- Kelley, J., Higgins, C., 2018. Computational efficiency for the surface renewal method. *Atmospheric Measurement Techniques*, 11, 2151-2158.
- Krishnan, P., Meyers, T.P., Scott, R.L., Kennedy, L., Heuer, M., 2012. Energy exchange and evapotranspiration over two temperate semi-arid grasslands in Northern America. *Agricultural and Forest Meteorology*, 153, 31-44.
- Le Maitre, D.C., Walsdorff, A., Cape, L., Seyler, H., Audouin, M., Smith-Adao, L., Nel, J.A., Holland, M., Witthüser, K., 2018. Strategic Water Source Areas: Management Framework and Implementation Guidelines for Planners and Managers. WRC Report No. TT 754/2/18, Water Research Commission, Pretoria, South Africa.
- Li, S.G., Lai, C.T., Lee, G., Shimoda, S., Yokoyama, T., Higuchi, A., Oikawa, T., 2005. Evapotranspiration from a wet temperate grassland and its sensitivity to microenvironmental variables. *Hydrological Processes*, 19, 517-532.
- Li, G., Zhang, F., Jing, Y., Liu, Y., Sun, G., 2017. Response of evapotranspiration to changes in land use and land cover and climate in China during 2001-2013. *Science of the Total Environment*, 596-597, 256-265.
- Linquist, B., Snyder, R., Anderson, F., Espino, L., Inglese, G., Marras, S., Moratiel, R., Mutters, R., Nicolosi, P., Rejmanek, H., Russo, A., Shapland, T., Song, Z., Swelam, A., Tindula, G., Hill, J., 2015. Water balances and evapotranspiration in water- and dry-seeded rice systems. *Irrigation science*, 33, 375-385.
- Liu, H., Gang, T.U., Congbin, F.U., Liqing, S.H.I., 2008. Three-year Variations of Water, Energy, and CO₂ Fluxes of Cropland and Degraded Grassland Surfaces in a Semi-arid Area of Northeastern China. *Advances in Atmospheric Sciences*, 25(6), 1009-1020.
- Mbangiwa, N.C., Savage, M.J., Mabhaudhi, T., 2019. Modelling and measurement of water productivity and total evaporation in a dryland soybean crop. *Agricultural and Forest Meteorology*, 266-267, 65-72.
- McGlone, M.S., Wilmshurst, J.M., Leach, H.M., 2005. An ecological and historical review of bracken (*Pteridium esculentum*) in New Zealand, and its cultural significance. *New Zealand Journal of Ecology*, 29(2), 165-184.

- Mengistu, M.G., Savage, M.J., 2010. Surface renewal method for estimating sensible heat flux. *Water SA*, 36(1), 9-18.
- Mielnick, P., Dugas, W.A., Mitchell, K., Havstad, K., 2005. Long-term measurements of CO₂ flux and evapotranspiration in a Chihuahuan desert grassland. *Journal of Arid Environments*, 60, 423-436.
- Morán, A., Ferreyra, R., Sellés, G., Salgado, E., Cáceres-Mella, A., Poblete-Echeverría, C., 2020. Calibration of the Surface Renewal Method (SR) under Different Meteorological Conditions in an Avocado Orchard. *Agronomy*, 10, 730.
- Nanni, U.W., 1956. Forest Hydrological Research at the Cathedral Peak Research Station. *Journal of the South African Forestry Association*, 27(1), 2-35.
- Poblete-Echeverría, C., Sepúlveda-Reyes, D., Ortega-Farías, S., 2014. Effect of height and time lag on the estimation of sensible heat flux over drip-irrigated vineyard using the surface renewal (SR) method across distinct phenological stages. *Agricultural Water Management*, 141, 74-83.
- Pozníková, G., Fischer, M., van Kesteren, B., Orság, M., Hlavinka, P., Žalud, Z., Trnka, M., 2018. Quantifying turbulent energy fluxes and evapotranspiration in agricultural field conditions: A comparison of micrometeorological methods. *Agricultural Water Management*, 209, 249-263.
- Reichert, J.M., Rodrigues, M.F., Peláez, J.J.Z., Lanza, R., Minella, J.P.G., Arnold, J.G., Cavalcante, R.B.L., 2017. Water balance in paired watersheds with eucalyptus and degraded grassland in Pampa biome. *Agricultural and Forest Meteorology*, 237-238, 282-295.
- Rosa, R., Dicken, U., Tanny, J., 2013. Estimating evapotranspiration from processing tomato using the surface renewal technique. *Biosystems Engineering*, 114, 406-413.
- Rosset, M., Montani, M., Tanner, M., Fuhrer, J., 2001. Effects of abandonment on the energy balance and evapotranspiration of wet subalpine grasslands. *Agriculture, Ecosystems and Environment*, 86, 277-286.
- Rubert, G.C., Roberti, D.R., Pereira, L.S., Quadros, F.L.F., Velho, H.F.D.C., Moraes, L.L.D., 2018. Evapotranspiration of the Brazilian Pampa Biome: Seasonality and Influential Factors. *Water*, 10, 1864.
- Savage, M.J., Everson, C.S., Odhiambo, G.O., Mengistu, M.G., Jarman, C., 2004. Theory and practice of evapotranspiration measurement, with special focus on surface layer scintillometry as an operational tool for the estimation of spatially-averaged evaporation. WRC Report No. 1335/1/04. Water Research Commission, Pretoria, South Africa.
- Savage, M.J., 2014. *Web-based teaching, learning and research using real-time data from field-based agrometeorological measurement systems*. Dissertation (MSc Agric). University of KwaZulu-Natal, South Africa.
- Savage, M.J., 2017. Estimation of grass reference evaporation and sensible heat flux using surface renewal and Monin-Obukhov similarity theory: A simple implementation of an iterative method. *Journal of Hydrology*, 547, 742-754.

- Schnieder, L.C., 2004. Bracken fern invasion in southern Yucatán: A case for land-change science. *The Geographical Review*, 94(2), 229-241.
- Shapland, T.M., Snyder, R.L., Paw U, K.T., McElrone, A.J., 2014. Thermocouple frequency response compensation leads to convergence of the surface renewal alpha calibration. *Agricultural and Forest Meteorology*, 189-190, 36-47.
- Snyder, R.L., Spano, D., Paw U, K.T., 1996. Surface renewal analysis for sensible and latent heat flux density. *Boundary-Layer Meteorology*, 77, 249-266.
- Snyder, R.L., Spano, D., Duce, P., Paw U, K.T., Rivera, M., 2008. Surface Renewal Estimation of Pasture Evapotranspiration. *Journal of Irrigation and Drainage Engineering*, 134(6), 716-721.
- Snyder, R.L., Pedras, C., Montazar, A., Henry, J.M., Ackley, D., 2015. Advances in ET-based landscape irrigation management. *Agricultural Water Management*, 147, 187-197.
- Spano, D., Snyder, R.L., Duce, P., Paw U, K.T., 1997. Surface renewal analysis for sensible heat flux density using structure functions. *Agricultural and Forest Meteorology*, 86, 259-271.
- Spano, D., Snyder, R.L., Duce, P., Paw U, K.T., 2000. Estimating sensible and latent heat flux densities from grapevine canopies using surface renewal. *Agricultural and Forest Meteorology*, 104, 171-183.
- Springer, A.E., Amentt, M.A., Kolb, T.E., Mullen, R.M., 2006. Evapotranspiration of two vegetation communities in a high-elevation riparian meadow at Hart Prairie, Arizona. *Water Resources Research*, 42, W03412.
- Suvočarev, K., Shapland, T.M., Snyder, R.L., Martínez-Cob, A., 2014. Surface renewal performance to independently estimate sensible and latent heat fluxes in heterogeneous crop surfaces. *Journal of Hydrology*, 509, 83-93.
- Suvočarev, K., Castellví, F., Reba, M.L., Runkle, B.R.K., 2019. Surface renewal measurements of H , λE and CO_2 fluxes over two different agricultural systems. *Agricultural and Forest Meteorology*, 279, 107763.
- Toucher, M.L., Clulow, A., Van Rensburg, S., Morris, F., Gray, B., Majozi, S., Everson, C.E., Jewitt, G.P.W., Taylor, M.A., Mfeka, S., Lawrence, K., 2016. *Establishment of a more robust observation network to improve understanding of global change in the sensitive and critical water supply area of the Drakensberg*. 2236/1/16. Water Research Commission, Pretoria, South Africa.
- van Atta, C.W., 1977. Effect of coherent structures on structure functions of temperature in the atmospheric boundary layer. *Archives of Mechanics*, 29(1), 161-171.
- Wieser, G., Hammerle, A., Wohlfahrt, H., 2008. The Water Balance of Grassland Ecosystems in the Austrian Alps. *Artic, Antarctic, and Alpine Research*, 40(2), 439-445.
- Williams, C.A., Reichstein, M., Buchmann, N., Baldocchi, D., Beer, C., Schwalm, C., Wohlfahrt, G., Hasler, N., Bernhofer, C., Foken, T., Papale, D., Schymanski, S., Schaefer, K., 2012. Climate and vegetation controls on the surface water balance: Synthesis of

evapotranspiration measured across a global network of flux towers. *Water Resources Research*, 48, W06523.

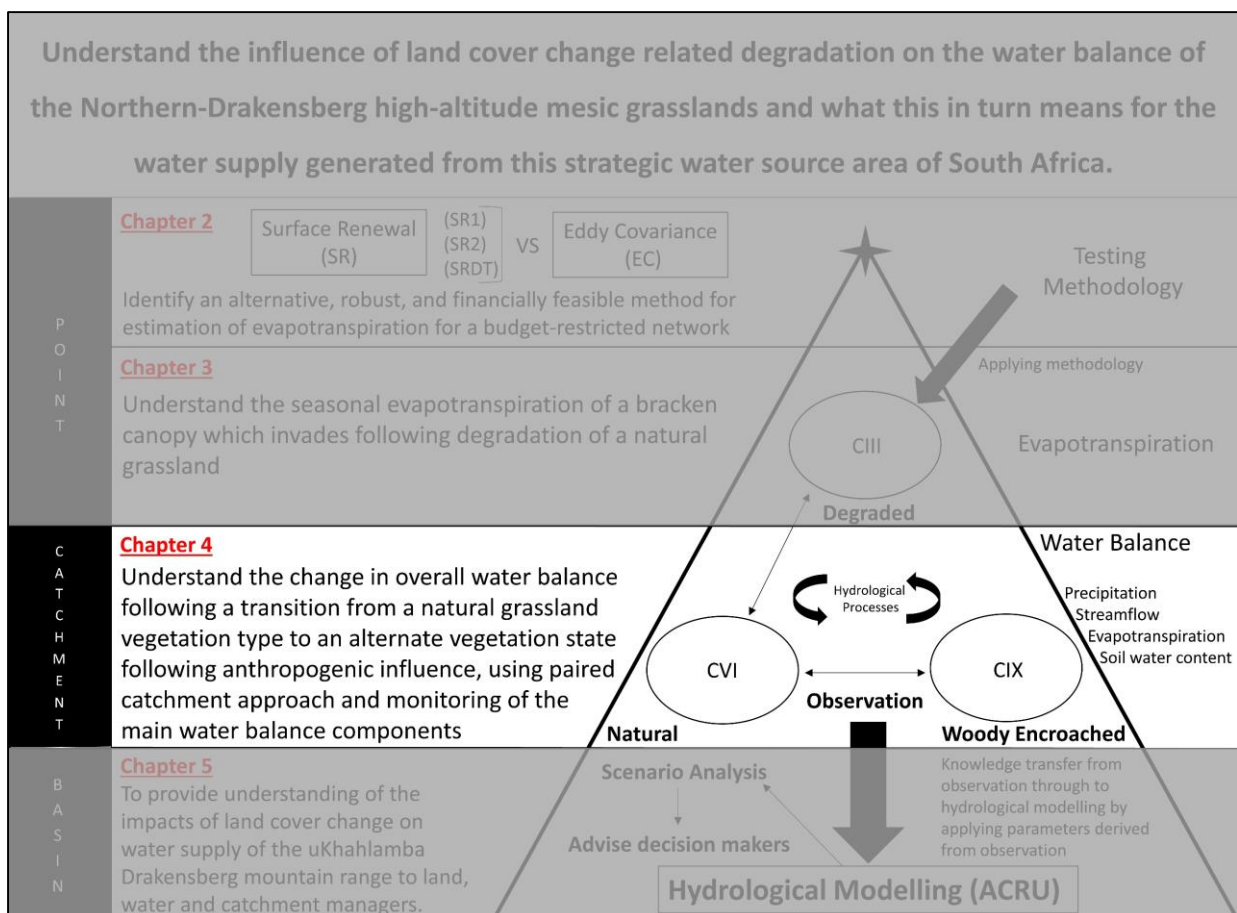
Yue, P., Zhang, Q., Zhang, L., Li, H., Yang, Y., Zeng, J., Wang, S., 2019. Long-term variations in energy partitioning and evapotranspiration in a semiarid grassland in the Loess Plateau of China. *Agricultural and Forest Meteorology*, 278, 107671

Zapata, N., Martínez-Cob, A., 2001. Estimation of sensible and latent heat flux from natural sparse vegetation surfaces using surface renewal. *Journal of Hydrology*, 254, 215-228.

Zhang, Y., Kadota, T., Ohata, T., Oyunbaatar, D., 2007. Environmental controls on evapotranspiration from sparse grassland in Mongolia. *Hydrological Processes*, 21, 2016-2027.

Lead in to Chapter 4

A robust methodology for the estimation of evapotranspiration (ET) was validated in Chapter 2 and applied in Chapter 3 to understand the seasonality of ET over the bracken canopy. Chapter 4 expands from a point to a catchment scale, where the specific objective was to consider the impacts of woody encroachment on the water balance of a montane grassland catchment. A paired catchment comparison method between a neighbouring natural grassland catchment (CVI) and a woody encroached catchment (CIX) under the same climate was used. The long-term streamflow and precipitation record was utilised to identify a decline in catchment response over time as the woody encroachment increased. The seasonal ET pattern of the woody vegetation was also observed. An overall reduction in streamflow under woody encroachment compared to natural grassland was concluded.



4. IMPACT OF LAND COVER CHANGE ON THE WATER BALANCE OF A FIRST-ORDER AFROMONTANE GRASSLAND CATCHMENT IN A STRATEGIC WATER SOURCE AREA

Abstract

The montane grasslands of the uKhahlamba-Drakensberg mountain range, South Africa, are important for the maintenance of water quantity and quality generated within this strategic water source area. However, these montane grasslands are vulnerable to woody plant encroachment. Locally, changes in fire management and land division, are influencing and promoting the establishment of woody communities within grasslands. Within South Africa, studies on the hydrological impacts of woody encroachment are lacking, especially with regard to *Leucosidea sericea*. Using observations within a woody encroached grassland catchment and neighbouring natural grassland catchment, this research aims to understand the hydrological implications of woody encroachment on the water balance of a first-order montane grassland catchment. Over time, as woody encroachment increased, catchment runoff response was reduced as indicated by a change in runoff response from the historical (0.40) to current period (0.26). Evapotranspiration was found to be the largest difference between the two land covers, especially in early spring, late autumn and during winter. Evapotranspiration in the woody encroached grassland exceeded annual precipitation during both hydrological years studied and exceeded the natural grassland evapotranspiration by more than 300 mm annually. From the overall water balance, it was shown that a shift from the natural grassland to woody encroached grassland resulted in a reduction in streamflow in the long term, and therefore water supply from the first-order montane grassland catchment. Thus, land management which uses fire to prevent woody encroachment is advised.

Keywords: *Evapotranspiration, Leucosidea sericea, precipitation, streamflow, woody encroachment.*

4.1 Introduction

Anthropogenic activities are a driver of environmental change around the world (Arnell, 2002; Wagener et al., 2010). Climate change is a well-known form of environmental change (Montanari et al., 2013) that will have an impact on the hydrological cycle and water supply

Submitted as: Gray, B.A., Toucher, M.L., Clulow, A.D., Savage, M.J., 2021. Impact of land cover change on the water balance of a first-order Afromontane grassland catchment in a strategic water source area. *Journal of Hydrology*.

from catchments, through changes in precipitation and air temperature (Green et al., 2011; Zhang et al., 2017). Another form of environmental change, land cover change, impacts how precipitation is partitioned and moves through the catchment (Kurc and Small, 2004; Kurc and Small, 2007; Qiao et al., 2015; Sajikumar and Reyma, 2015; Yin et al., 2017) and thereby the water supply out of a catchment (Archer, 2010; Wang et al., 2018). Landcover change is occurring at an increasing rate due to anthropogenic activities, and differs from region to region (Ozturk et al., 2013; Yin et al., 2017). Therefore, it could be considered that climate change is a more global scale phenomenon, to a large extent beyond the scope of local management, whereas land use management can be influenced by, and is a management tool available to, local catchment managers.

Montane grassland regions are renowned natural resource centres, hosting phenomenal biological diversity (Carbutt, 2019), and are characterised by areas in which climatic conditions change rapidly over short distances along altitudinal gradients. The ecosystem services provided by these grasslands make them of significant local and regional importance. However, the synergistic influence of land cover changes, propensity to biological invasions and sensitivity of high-altitude areas to warming, make the montane grassland ecosystems some of the most vulnerable under global change (Benston and Stoffel, 2014). One such area is that of the uKhahlamba-Drakensberg mountain range, South Africa, which is a strategic water-source area. A main land cover change concern, within the montane grasslands of the uKhahlamba-Drakensberg mountain range, is that of woody plant encroachment (WPE) (Bond and Parr, 2010). A shift to a woody encroached state will alter the ecosystem services provided by the montane grasslands (Everson et al., 2009; Little et al., 2013), which is of particular importance to the supply of water.

The montane grasslands of the uKhahlamba-Drakensberg mountain range are part of the temperate grassland biome, which accounts for 28 % of land cover in southern Africa and is shared with other grassland systems around the world i.e., “the steppe of Russia, Mongolia and China, the north American prairies, the South American pampas, temperate grasslands of Australian Alps, and the tussock grasslands of New Zealand” (Brown and Bezuidenhout, 2020). The southern African grasslands consist of C4 grasses which appeared following the concentration decrease in atmospheric CO₂ over 30 million years ago (Bond et al., 2005; Bond and Parr, 2010). Although the climate of the region suggests forest would be the natural land cover, fire has played an important part in the maintenance of these ancient grasslands as an alternative ecosystem state, due to being fire-adapted (Bond and Parr, 2010; Gordijn et al.,

2018). The role of fire in the grasslands predates anthropogenic influence, and occurs from natural ignition sources such as lightning, mainly during the transition from dry to wet season (Bond et al., 2005; Bond and Parr, 2010; Brown and Bezuidenhout, 2020). The uKhahlamba-Drakensberg grasslands are invaluable for their role in maintaining water quality and quantity (Brown and Bezuidenhout, 2020), and fire as a management tool has been used over the past century to maintain grassland land cover condition (Gordijn et al., 2018).

A shift in the grassland biome to WPE is not only a threat to the uKhahlamba-Drakensberg mountain grasslands, but to grasslands across the world (Wilcox, 2007; van Auken, 2009; Eldridge et al., 2011; Scott et al., 2014; Zou et al., 2015; Axelsson and Hanan, 2018; Wang et al., 2018; Wilcox et al., 2018; O'Connor et al., 2020). WPE is defined as “an increase in density, cover, and biomass of shrubs and trees into areas where they were not present previously” (Archer et al., 2017; Acharya et al., 2018). WPE in a grassland system is considered a form of degradation (Huxman et al., 2005; Peng et al., 2013; Schreiner-McGraw et al., 2020). Globally, grasslands represent some of the most transformed biomes (Hoekstra et al., 2005), and in South Africa only 2 % of grasslands are protected while 65 % are in various stages of degradation (Carbutt and Martindale, 2014). Drivers of WPE stem from anthropogenic environmental change and can be seen to be driven by processes at different scales (O'Connor et al., 2020), which vary between climate zones, making definite attribution difficult (Archer et al., 2017). Globally, increasing CO₂ concentration levels are driving the WPE of grasslands (Archer, 2010; Kulmatiski and Beard, 2013; Miller et al., 2017; O'Connor et al., 2020). Regionally, changes in climate, such as precipitation and air temperature, and their timing, are also improving the suitability of conditions for woody plants to survive (Archer, 2010; Kulmatiski and Beard, 2013; Scott et al., 2014; O'Connor et al., 2020). Locally, land use and management practices, such as changes in fauna and flora, as well as fire management and land division, are influencing and promoting the establishment of woody communities within grasslands (Bond, 2008; Archer, 2010; Miller et al., 2017; Wilcox et al., 2018; O'Connor et al., 2020). A change in climate itself cannot be a sole driver, but required in combination with a secondary change, at a much more local level, to trigger and sustain WPE (Archer et al., 2017). WPE can occur where the grassland is replaced by woody vegetation and results in the loss of ground cover and exposure of bare soil, which is known as xerification (Schreiner-McGraw et al., 2020). This tends to occur in drier regions, while in wetter regions, woody vegetation can replace the grassland without resulting in an increase in bare soil exposure, and this is known as thickening (Schreiner-McGraw et al., 2020), which is the dominant process in the Drakensberg grasslands. WPE can also pass a point, where returning to grassland natural state

is impossible, and a new steady state is achieved (Miller et al., 2017). This has significant consequences for the natural systems (Miller et al., 2017).

An important question surrounding WPE in any landscape, is whether it decreases streamflow and ground water recharge (Archer et al., 2017). Precipitation partitioning is altered through changes in several hydrological processes such as evapotranspiration (*ET*), interception, infiltration, percolation, subsurface flow and ground water recharge, due to physical and phenological differences between the natural and successional vegetation states (Le Maitre et al., 1999; Liu et al., 2016; Acharya et al., 2018; Gwate et al., 2018). This in turn will impact on the catchment water balance and alter streamflow leaving the catchment (Acharya et al., 2017; Gwate et al., 2018).

Evapotranspiration has been found to increase with a transition from grassland to woody vegetation (Scott et al., 2014; Acharya et al., 2017; Scheiner-McGraw et al., 2020). WPE also alters the surface albedo and wind profile, available energy flux, and soil temperature, thereby influencing the relationship between sensible (*H*) and latent heat (*LE*) flux, which directly influences evapotranspiration (Archer, 2010; Zou et al., 2014; Acharya et al., 2017). Further, the rougher canopy surface is seen to increase *ET* (Archer et al., 2017). In addition, woody vegetation tends to be evergreen, and therefore potentially changes the winter *ET* and water use within the catchment compared to grasslands, which are often deciduous and therefore dormant in winter (Zou et al., 2014; Acharya et al., 2017; Archer et al., 2017; Acharya et al., 2018). Interception also plays an active role in the evaporation component of evapotranspiration, and with the associated increase in canopy roughness following woody encroachment, increased canopy interception and evaporation is expected (Honda and Durigan, 2016; Acharya et al., 2017). In a *Juniperus ashei* canopy, which is a common woody vegetation encroaching in the north American tallgrass prairie, Dugas et al. (1998) found an increase in annual *ET* of 35-85 mm compared to the natural grassland.

With the increase in above ground cover, soil surface temperature is reduced, and WPE reduces the available energy flux for upper soil water evaporation, thus reducing this component of soil water loss (Le Maitre et al., 1999; O'Donnell and Caylor, 2012; Daryanto et al., 2013; Peng et al., 2013; Zou et al., 2014; Acharya et al., 2018). WPE further influences soil water through its effects on infiltration (Archer et al., 2017, Qiao et al., 2017). The resultant increase in litter cover has a two-fold effect on infiltration. Firstly, raindrop impact is reduced along with the volume of precipitation available for infiltration (Le Maitre et al., 1999; Zou et al., 2014). Secondly, an increase in organic matter content within the soil increases soil porosity and

consequently the potential rate of infiltration within the soil increases (Le Maitre et al., 1999; Daryanto et al., 2013; Zou et al., 2014). The influence of WPE on infiltration is suggested to be site- and context-specific (Eldridge et al., 2011), and in comparison, to grasslands, shifts runoff generation mechanisms from saturation excess overland flow to infiltration excess overland flow (Qiao et al., 2017). Within the soil, root structures of woody vegetation differ significantly from that of grasslands (Scott et al., 2014; Acharya et al., 2017; Archer et al., 2017). Woody vegetation can reach deeper water reserves (Scott et al., 2014; Archer et al., 2017; Acharya et al., 2018) as grassland vegetation has a shorter root structure, which has been shown to utilise water at soil depths between 0.2 – 0.3 m (Archer et al., 2017). Acharya et al. (2017) showed that soil water at a depth of 0.8 m was found to be lower under WPE by *Juniperus virginiana* in the tall grass prairie. Due to phenological differences, the dry season is the period where the difference between soil water under grassland and under WPE is most evident (Zou et al., 2014; Acharya et al., 2017). Zou et al. (2014) found that WPE by Juniper species into grassland in the Southern Great Plains increased infiltration. However, soil water was lower under WPE, and streamflow was only 2 % of precipitation, compared to 10 % under grassland vegetation.

As the role of fire is vastly different between a near-natural grassland and a woody encroached grassland, its implications for the hydrology under each land cover differs. Fire is often used as a management tool in a grassland, with reduced fuel loads and specific seasonal timing (Fultz et al., 2016; Stavi, 2019). Fire within a woody encroached grassland is often infrequent and in the form of wildfires, which burn hotter and with a higher intensity than when not encroached (Doerr et al., 2000; Neary, 2006). Added to this, fire is often absent from woody encroached grasslands for long periods, leading to a build-up of litter and above ground biomass, further fuelling the fire (Bond et al., 2008; Stavi, 2019). Therefore, a hot wildfire in a woody encroached grassland can lead to hydrophobicity in the soil, and lead to further degradation and reduced infiltration (Doerr et al., 2000; Neary, 2006; Brown and Bezuidenhout, 2020). The same can occur with a prescribed burn if not managed correctly (Neary, 2006; Brown and Bezuidenhout, 2020).

From an ecological perspective, WPE into grasslands and the impact on ecosystem services has been investigated extensively both internationally (e.g. Archer et al., 2001; Mills et al., 2006; van Auken, 2009; Archer, 2010; Eldridge et al., 2011; Puttock et al., 2014; Archer et al., 2017; Miller et al., 2017; Axeleson and Hanan, 2018; Wilcox et al., 2018; O'Connor et al., 2020), and within South Africa (e.g. Bond and Parr, 2010; De Villiers and O'Connor, 2011; O'Connor et al., 2014; Stevens et al., 2016; Gordijn et al., 2018). Water provision is an

ecosystem service identified as changing within a landscape due to WPE into a grassland system, and changes in *ET* (Dugas et al., 1998; Kurc and Small, 2004; Huxman et al., 2005; Kurc and Small, 2007; Nie et al., 2012; Wine and Hendrickx, 2013; Honda and Durigan, 2016; Liu et al., 2016; Gwate et al., 2018; Wang et al., 2018) and infiltration (Daryanto et al., 2013; Eldridge et al., 2014; Zou et al., 2014; Qiao et al., 2017) have received attention globally, with growing interest on the impacts on groundwater recharge (Scott et al., 2014; Acharya et al., 2018; Schreiner-McGraw et al., 2020). A large portion of these observational and modelling studies on the hydrological implications of WPE in grasslands have been conducted in semi-arid and arid lands. Therefore, the justification for the present study is that within South Africa, studies on the hydrological impacts of woody encroachment are lacking, especially around *Leucosidea sercia*, which is a common invader found within the high altitude (> 1000 m) grasslands of southern Africa (Mafole et al., 2017).

Observation is an important first step, which can inform modelling, enabling the scaling up of findings to a more relevant level at which watershed management decisions are made (Qiao et al., 2015). Catchment level observations are rare and thus it is imperative to understand how a transition to woody vegetation affects the water generation from the strategic water source area of the uKhahlamba Drakensberg mountain range. This can generate much needed knowledge on the ecohydrological implications of woody encroachment in a sub-humid fire-adapted high altitude grassland system.

The aim of this research is, therefore, to understand the hydrological implications of woody encroachment on the water balance of a first-order montane grassland catchment within a strategic water source area of South Africa. We used observations to describe changes over time, in the streamflow, catchment runoff response, evapotranspiration, and soil water content, between a woody encroached grassland and a neighbouring natural grassland catchment with the same climate. The findings were then used to draw conclusions on the implications of these changes for the generation of water supply from these first-order montane grassland catchments.

4.2 Material and Methods

4.2.1 Research site

The Cathedral Peak research catchments (28°58'32" S; 29°14'08" E) are located in the UNESCO World Heritage uKhahlamba Drakensberg park. The research catchments,

established in 1948, have been used to determine the influence of various management treatments on the vegetation and water yield of the catchments (Everson et al., 1998; Toucher et al., 2016). The paired nature of the Cathedral Peak research catchments, make them an ideal location for research into the impacts of land cover change on the water balance of a catchment. All the catchments are underlain by basaltic lavas, which are overlain by Clarens Sandstone (Nanni, 1956). It is assumed that each individual catchment is water tight (Bosch, 1979) which is aided by the weirs installed on the bed rock. Thus, it is assumed that the bed rock is impermeable. The catchments fall into the temperate C4 grassland biome. This research focuses on catchment VI and IX (Figure 4.1).

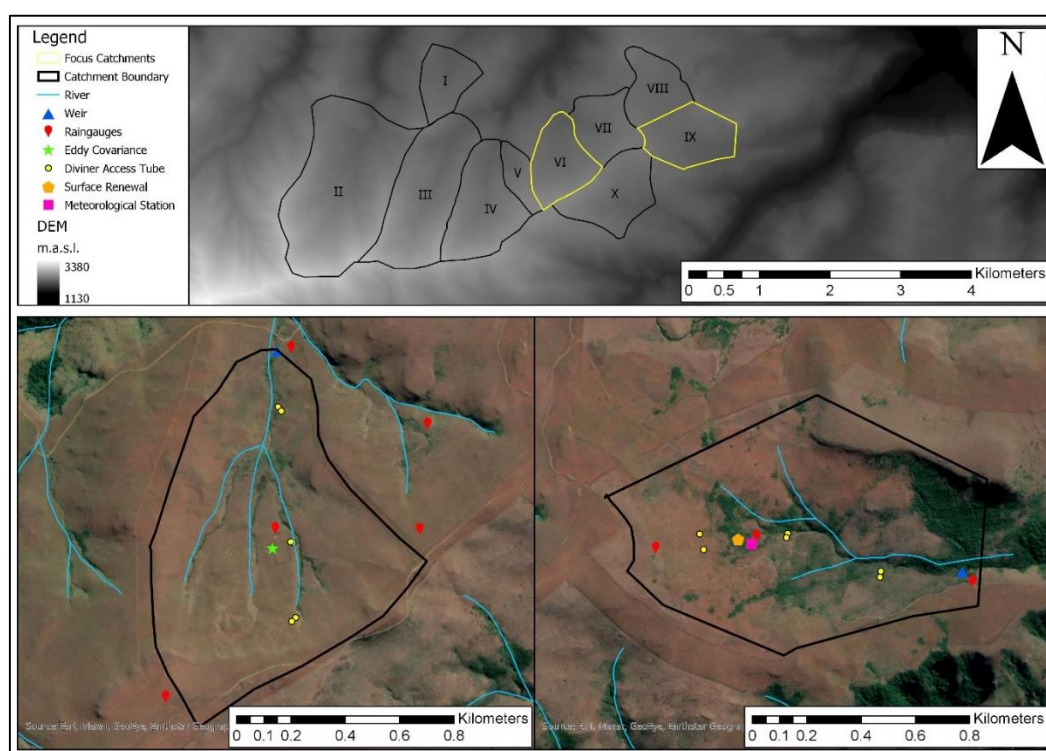


Figure 4.1: The location of the natural grassland and woody encroached grassland catchments within the Cathedral Peak research catchments with the observation equipment locations detailed. The images of CVI and CIX were captured on 28 May 2020 (Source: Esri).

Monitoring at the Cathedral Peak research catchments began in the late 1940s but was stopped in 1995 due to a lack of funds (Toucher et al., 2016). Currently, the land management practices for the research catchments are maintained by Ezemvelo KZN Wildlife with the hydroclimatological monitoring reinstated gradually from 2013 by the South African

Environmental Observation Network (SAEON). The Cathedral Peak research catchments are in the summer rainfall region of South Africa, and experience hot, humid summers and cold, dry winters (Toucher et al., 2016). The mean annual precipitation (MAP) for the Cathedral Peak research catchments is 1 400 mm (Bosch, 1979). The majority of precipitation occurs between October and March (Schulze, 1974; Toucher et al., 2016) mainly as thunderstorms (Schulze, 1974). The highest air temperatures are experienced during the month of November (Everson et al., 1998). High winds are experienced during the dry season, starting around the end of April and continuing until September (Everson et al., 1998).

4.2.2 Catchment VI: Near-natural grassland

Catchment VI is considered the benchmark catchment, as there have been no land cover changes within this catchment in recent history. The catchment is currently in a near-natural state with a dominant cover of *Themeda triandra* and management through a biannual spring burn has continued, as per the accepted management method for the uKhahlamba Drakensberg grasslands (Toucher et al., 2016). The catchment has an area of 0.667 km² with a northwest aspect (Toucher et al., 2016). The catchment ranges in altitude from around 2 073 m.a.s.l. in the upper reaches, to 1 845 m.a.s.l. at the outlet (Toucher et al., 2016). The MAP of the catchment is 1 340 mm.

4.2.3 Catchment IX: Woody encroached grassland

The uKhahlamba Drakensberg mountain range grasslands are considered fire driven (Bond and Parr, 2010; Gordijn et al., 2018). The removal of fire from this landscape, due to human activities through land management and reduced connectivity within the landscape, was believed to promote woody encroachment, which was considered the natural successional endpoint for the grasslands of the uKhahlamba Drakensberg mountain range (De Villiers and O'Connor, 2011). To address the question, catchment IX has been protected from fire since 1952 (De Villiers and O'Connor, 2011; Toucher et al., 2016), and natural grasslands were replaced initially by *Pteridium aquilinum* (bracken), which was then replaced by pioneer woody species, of which *Leucosidia serica* and *Erica evansii* are dominant (De Villiers and O'Connor, 2011). Despite being fire protected, runaway fires have occurred and passed through the catchment on 14 previous occasions (Killick, 1963; Granger, 1976; Adcock, 1990; Rowe-Rowe, 1995; De Villiers, 2012; Toucher et al., 2016). The fires did however not always burn out the whole catchment, as with the 2015 and 2019 fires, with the dense woody encroached areas untouched (Figure 4.2). The catchment area is 0.645 km² with a northeast aspect (Toucher et al., 2016). The catchment ranges in altitude from 1 982 m.a.s.l. at the peak to 1 822 m.a.s.l.

at the outlet (Toucher et al., 2016). The MAP of the catchment is 1 257 mm (Toucher et al., 2016).



Figure 4.2: The extent of the 2019 fire across the lower part of catchment IX. The woody encroached areas remained untouched, while the grassland areas were burnt. (Photo taken from the top of surface renewal tower on 4 July 2019).

4.2.4 Soils

The soils within the Cathedral Peak research catchments extend to a depth of 1.5 m (Scott et al., 2000) and are on average 0.80 m deep across the catchments (Schulze, 1974). Based on the binomial system for South Africa (MacVicar et al., 1977), the soil types are dependent on location within the catchments, with the saturated areas characterised by Katspruit and Champagne soil types, the drier areas consisting of Lateritic Red and Yellow earths soils (Granger, 1976; Toucher et al., 2016). The soil horizons are not easily distinguishable, but the A-horizon typically ranges from 0.16 to 0.20 m and consists of a dark brown loam with considerable roots (Schulze, 1974; Scott et al., 2000). Within catchment VI, the upper region along the ridge line consists of Nomanci and Magwa soil types, while the majority of catchment VI is the Inanda soil type (Botha, 2016). Within catchment IX, the upper reaches are dominated by Kranskop soil type and also feature other humic soil types such as Nomanci (Harrison, 2020). Within the saturated zones, the dominant soil types are Champagne, but also feature Highmoor, Dartmoor and Inanda soil types (Harrison, 2020). The catchments are lined by basaltic lavas, which are topped by Clarens Sandstone (Nanni, 1956). It is also assumed that each individual catchment is water tight (Bosch, 1979) which is aided by the weirs installed on the bedrock.

4.2.5 Equipment and processing

To determine the water balance of the respective catchments, the key water balance component of precipitation (P), evapotranspiration (ET), streamflow (Q), and change in soil water (ΔS), were observed. The equipment utilised for the observation of each component of the water balance is detailed below.

4.2.5.1 Precipitation (P)

Precipitation was measured at three locations within each catchment, at the top, middle and bottom. For the historical period (1961 – 1986), 5” Snowdon raingauges which were positioned parallel to the slope and within Nipher shields were measured monthly and located at the top of the catchments (Toucher et al., 2016). At the middle and bottom of the catchments, 5” Casella Snowdon recording raingauges were used and were measured weekly (Toucher et al., 2016). The monthly raingauges provided the longest records, while the recording raingauges were used for later periods (1972 onwards) and averaged with the monthly raingauges to calculate an annual catchment precipitation.

For the current period of precipitation (2016-present), Texas tipping-bucket raingauges (TE525, Texas Electronics, Texas, United States of America) were used to measure the precipitation and provided event-based measurements with a resolution of 0.254 mm per tip. Raingauges from the top, middle and bottom of the catchments (Figure 4.1) were averaged to provide an overall representative precipitation volume for catchment VI and catchment IX. All precipitation data were processed and corrected based on metadata gathered during routine field trips and surrounding raingauge measurement comparisons. Precipitation data were also available at the Mikes Pass meteorological station located at the entrance to the Cathedral Peak research catchments (Figure 4.1).

4.2.5.2 Evapotranspiration (ET)

Observation of ET within the woody encroached grassland catchment (Catchment IX) was conducted using the Surface Renewal Dissipation Theory (SRDT) approach, as proved best practice by Gray et al. (2021a). The SR system was installed in catchment IX on the 20th November 2018. The components and layout of the systems are described in Gray et al. (2021a). Eddy covariance (EC) was used to measure ET over the near-natural grassland in Catchment VI and was installed on the 12th December 2014. Up until the installation of the SR system, the EC system was the single long-term method for ET measurement in the Cathedral Peak research catchments. The EC system consists of an integrated 3-D sonic anemometer and open-path gas

analyser for H₂O and CO₂ fluxes (IRGASON, Campbell Inc, Logan, United States of America) connected to an electronics panel (EC100, Campbell) and run off a Campbell datalogger (CR6) programmed with the EasyFlux-DL program that applied the necessary EC corrections. The energy balance sensors consisted of a net radiometer (NR-LITE2, Kipp & Zonen, Delft, The Netherlands), soil heat flux sensors (HFP01-L, Hukseflux, Delft, The Netherlands), averaging soil thermocouple probes (TCAV-L, Campbell), water conductivity sensor (CS616, Campbell) and a relative humidity and air temperature sensor (CS215, Campbell).

4.2.5.3 Streamflow (Q)

Streamflow was gauged by concrete weirs which were constructed at the outlet of catchments VI and IX in 1954 (Toucher et al., 2016). The concrete weirs consist of 18-inch 90° V-notches (Toucher et al., 2016) which are backed by a stilling pond and weir hut. A long period of historical streamflow data was available (1961 to 1986). During the current observation period (2016 – present), streamflow is observed using stainless steel SDI-12 Pressure Transducers (CS451, Campbell) which are connected to a Campbell datalogger (CR200) (Toucher et al., 2020). The streamflow is observed at event scale, triggered by a change in stage height. The volume of streamflow is calculated by conversion from stage height to discharge using a calculated calibration curve unique to each weir.

4.2.5.4 Soil water (ΔS)

The soil water observation method consisted of monthly point measurements at 0.1 m increments to a depth of 1.1 m at six locations across both catchments. This approach made use of a portable soil water probe (Diviner 2000, Sentek, Adelaide, Australia) and access tubes (1.10 m long) installed at three positions within the catchment (upper, middle, bottom) with two access tubes per position (Figure 4.1). The volumetric water content measured by the Diviner soil water probe at each depth, was converted to a single average daily volumetric soil water content, through weighted averaging, which provided a single profile soil water content value for each tube. These were then averaged across the six tubes to provide a catchment representative profile soil water content value as a percentage per m of soil per month. Monthly measurements were made from March 2019 until October 2020, except for April 2020 due to the COVID-19 national lockdown.

4.3 Theory/Calculation

4.3.1 Water balance method

The hydrological year at the Cathedral Peak research catchments was taken to start on 1 October and conclude on 30 September. The months were aggregated into seasons relative to the site, of summer (December, January, February), autumn (March, April, May), winter (June, July, August) and spring (September, October, November).

To identify and understand the effects of a change in land cover between the baseline near-natural and the woody encroached grassland, the water balance method was used. The water balance of a catchment is based on continuity, and the understanding that when accounting for the inputs into the catchment, they will be equal to the outputs from the catchment, and any differences that do occur are accounted for by a change in soil water storage (Sokolov and Chapman, 1974). Hydrologically, the input into a catchment is that of P , which is independent of catchment condition (Everson, 2001). The accuracy with which P is measured, determines the accuracy of the water balance calculation (Sokolov and Chapman, 1974). The P input is then transformed within the catchment and culminates in the output components of ET and Q , which are dependent on P and influenced by catchment conditions such as land cover and soil characteristics (Everson, 2001). As mentioned, ΔS is considered to account for the difference between P and the main output variables Q and ET (Sokolov and Chapman, 1974). The ΔS is often negated when the annual water balance is calculated but important to consider when the water balance is calculated at finer temporal scales (Sokolov and Chapman, 1974). The water balance is difficult to close, due to the individual errors associated with each independent method used to measure the water balance components (Sokolov and Chapman, 1974). With a simplified and lumped approach to the water balance, and using the continuity equation, the water balance of a catchment can be considered as:

$$P - ET - \Delta S = Q \quad (4.1)$$

Additionally, a response ratio was calculated, which is the ratio of streamflow to precipitation, and provides an indication of how much of the precipitation over the year is partitioned into runoff from of the catchment. A comparison between the differences between and changes over time in the output variables of the baseline near-natural grassland catchment (VI) and the transformed woody encroached grassland catchment (IX) was assessed. Due to the physical closeness of the catchments, a similar size and the same climate, differences between the

partitioning of P into ET and Q and timing of responses, should provide insight into the impacts of a change in land cover from grassland to a woody encroached state and on the hydrological processes. For the annual water balance, changes in groundwater were not considered as it is assumed that catchments VI and IX are sealed units, with no contributions from outside influencing the groundwater. Therefore, any additional or lost water within the annual water balance is considered to be added or removed from the groundwater store.

4.3.2 Data quality control and patching

During the recent period of observation, equipment malfunction and the COVID-19 national lockdown prevented routine maintenance field trips, resulting in periods of data loss from the EC and SR systems. To reduce the impacts of gaps in data on the understanding of the change in water balance, patching of these periods (10 % of total data) was conducted to maintain the continuous record. For short periods of the observation record and particularly July 2019, the soil heat flux and sensible heat flux data were unavailable from the EC system due to malfunction. During April and May of 2020 (COVID-19 national lockdown), a memory card malfunction of the SR system resulted in the loss of sensible heat flux data. To determine ET during periods of data loss, for the EC system, the nearby (~ 2 km) Mikes Pass Weather Station daily climate data were used, while for the SR system, the catchment IX automatic weather station daily climate data were used. Using the FAO-56 Penman Monteith method for the estimation of potential ET (ET_o), crop coefficient (k_c) values were determined during representative periods when data were available (method detailed in Gray et al., 2021b). These representative k_c values were then applied to ET_o calculated for periods when data were not available, allowing for the estimation of ET for those days. Based on best practices (Allen et al., 2011), k_c values were capped at the upper (1.2) and lower (0.2) limits. This method was also used for the patching of ET data for catchment IX from 1 October 2018 to the 20 November 2018 as the observation equipment was only installed on the 20 November 2018. This was only conducted for the water balance analysis to provide insight into the ET over the complete 2018/2019 hydrological year. For the estimation of soil heat flux (G), the percentage of net irradiance (R_n) determined for the winter season when data were available, was applied for the natural grassland (14.6 %) and woody vegetation (1 %) respectively.

4.4 Results

4.4.1 Long-term change in precipitation, streamflow, catchment response and vegetation

Using the long-term precipitation and streamflow record available for catchment VI and IX, with the current observation record, analysis of changes in precipitation, streamflow and catchment runoff response were conducted (Figure 4.3). The historical observation period (1961 – 1986) showed a higher average annual precipitation consisting of several wet and dry cycles, compared to the current observation period (2016 – 2019) which occurred during a dry cycle. For the historical period, catchment VI experienced higher average annual precipitation (1 403 mm) compared to catchment IX (1 314 mm). During the current observation period, the precipitation experienced between the two catchments was more similar, with the average annual precipitation within catchment IX (1028 mm) like that of catchment VI (1 025 mm). As with the precipitation, the streamflow observed during the historical period of observation was higher than that for the current period. Catchment VI showed a higher average annual streamflow (697 mm) compared to catchment IX (541 mm). The same pattern occurred for the current period of observation with catchment VI (632 mm) showing a higher average annual streamflow compared to catchment IX (275 mm). The difference in average annual streamflow was 156 mm for the historical period, while for the current period, the difference between the catchments was 357 mm (Figure 4.3). This pattern is further revealed in the catchment runoff responses. During the historical period, the average catchment runoff response was higher for catchment VI (0.48) compared to catchment IX (0.40). During the current period of observation, the average runoff response of catchment VI (0.58) was still higher than the average runoff response of catchment IX (0.26). The runoff response for catchment IX has decreased over time, compared to catchment VI, which appears to have remained stationary (Figure 4.3). As indicated, catchment VI has received the same management strategy of a biannual spring burn since 1961 (Figure 4.3), which has maintained the natural grassland state. By contrast, catchment IX has experienced several runaway fire events. Despite the repeated fire occurrences in the 2000s, vegetation surveys (Granger, 1976; De Villiers, 2012) show that fire has not removed or heavily depleted the woody encroachment cover which has increased over time. The occurrences of prescribed burns, runaway fires, and surveys of woody encroachment coverage percentage are detailed in Figure 4.3 based on literature (Killick, 1963; Granger, 1976; Adcock, 1990; Rowe-Rowe, 1995; De Villiers, 2012; Toucher et al., 2016).

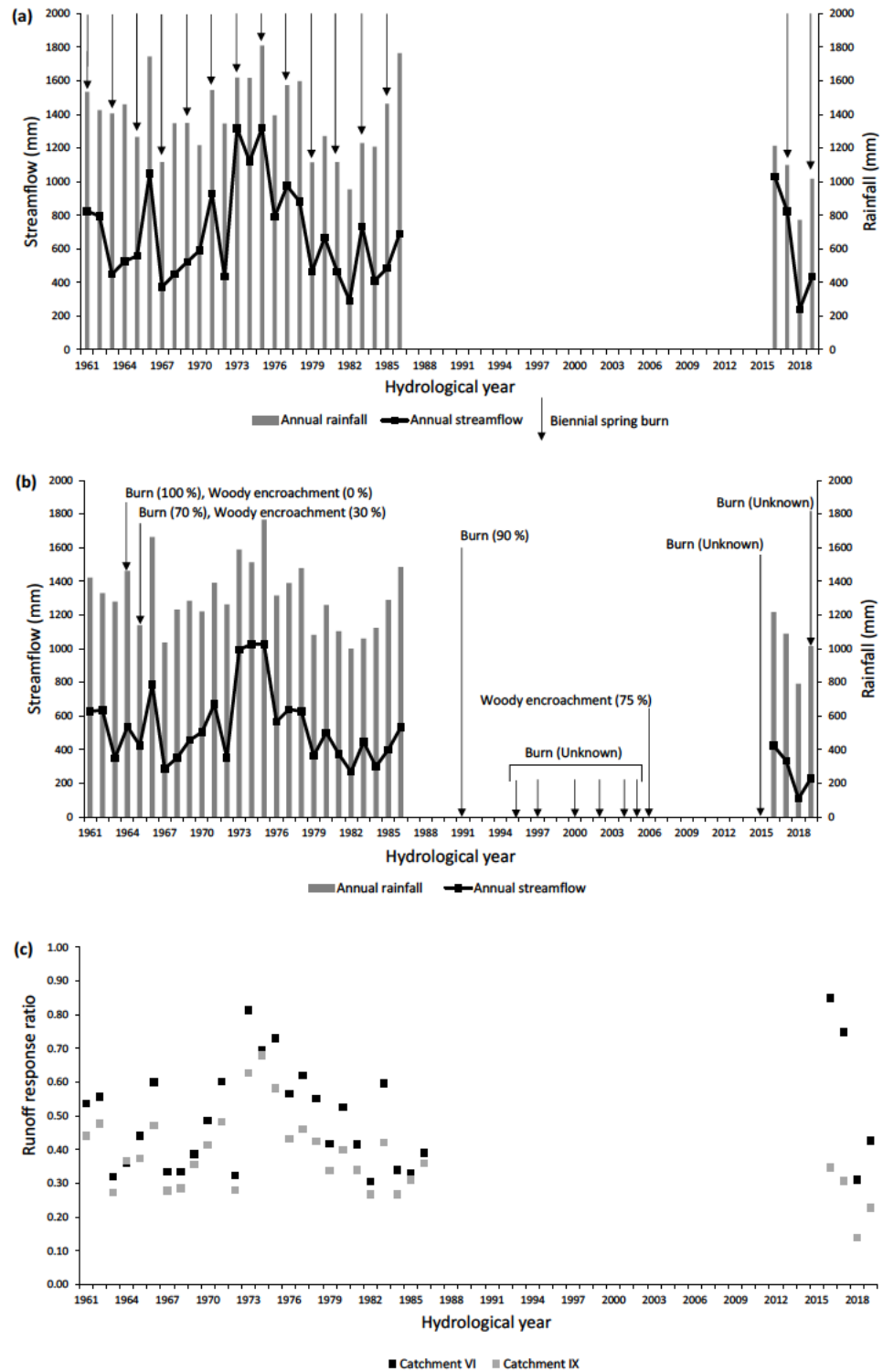


Figure 4.3: A representation of the annual precipitation and streamflow of the (a) natural (CVI) and (b) woody encroached (CIX) grassland catchments for the historical (1961 – 1986) and current (2016 – 2019) observation periods, as well as a comparison of the runoff responses of the respective catchments over time (c).

4.4.2 Recent energy balance

Changes in land cover have a large impact on the partitioning of energy balance components, which is then linked to the water balance by altering ET , identified as a change in the latent energy flux (LE) energy balance component. Using net irradiance (R_n), the percentage composition of each energy balance component was determined as a monthly average for each vegetation cover (Figure 4.4). Over the whole observation period, the average daily R_n was greater within the woody encroached vegetation (12.0 MJ m^{-2}) compared to the grassland (3.9 MJ m^{-2}). As a percentage of R_n , within the woody encroached vegetation, LE is greater than H year-round, with LE being dominant in summer (75 %), with an almost equal partition in winter between LE (55 %) and H (44 %). The soil heat flux (G) component partition does not change much seasonally under the woody vegetation staying consistent at 1 % of R_n throughout the year. The energy balance under the natural grassland vegetation is more variable. The LE was found to dominate in summer to a similar proportion found under the woody vegetation (75 %). During autumn, the partition between H (45 %) and LE (46 %) was even, while H is higher than LE through winter (60 %) and spring (53 %). Compared to the woody vegetation, the G component was highly seasonal, peaking in winter (15 %), but lower in summer (6 %) while remaining around 8 % during the transitional seasons of spring and autumn. Overall, across the year, LE remains the largest component across both the woody vegetation (67 %), and natural grassland (47 %). The H component is greater within the natural grassland (44 %) compared to the woody vegetation (32 %), as is the G component within the natural grassland (9 %) compared to the woody vegetation (1 %).

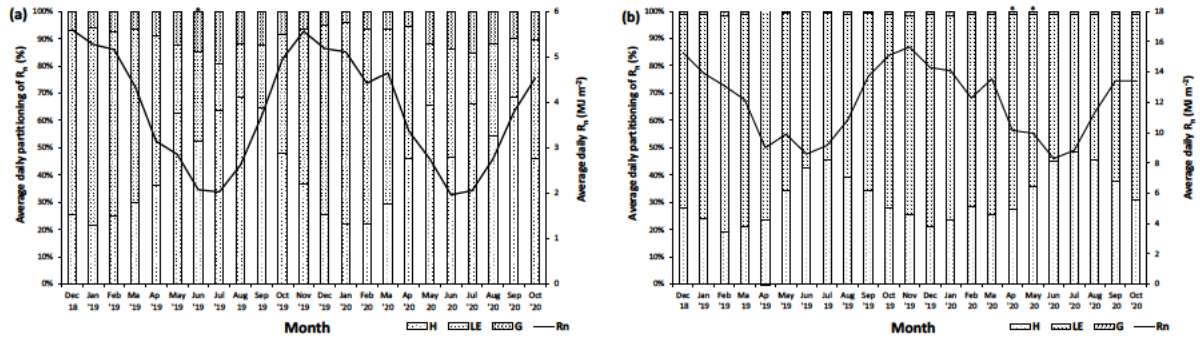


Figure 4.4: The partitioning of R_n between the remaining three energy balance components (G , H and LE) for the respective land covers of the (a) natural grassland in Catchment VI, and (b) woody encroachment in catchment IX. (The * denotes months where patching was used).

4.4.3 Evapotranspiration

As the SR system was installed on the 20th November, the accumulated ET comparison in Figure 4.5 was started on the 1st December each year to allow for comparison. Over both hydrological years, the ET for the woody encroached vegetation cover was higher than the natural grassland (Figure 4.5). From December 2018 to September 2019, the total ET over the woody encroached grassland was 379 mm higher than for the natural grassland. During the wetter hydrological year (2019/2020), the total ET over the woody encroached grassland was 373 mm greater between December and September, and 472 mm when considering October to September. The largest difference between the ET of the two land covers is evident, during late autumn and early spring, while during summer, the 30-day moving averages indicates that the difference is reduced, to near similar results (Figure 4.5). During the drier year (2018/2019), the accumulated ET and the 30-day moving average shows that the woody encroached grassland has a higher ET . The higher precipitation during the wetter hydrological year (2019/2020) had an influence on the average daily ET of the natural grassland, which increased in summer and autumn, compared to the drier hydrological year (2018/2019). Both vegetation cover types showed a higher average daily ET during the drier hydrological year. During summer, the average daily ET was higher in the woody encroached grassland (4.1 mm; Appendix 4A) compared to the natural grassland (3.6 mm; Appendix 4A). The difference increased in winter, where again, the woody encroached grassland had an increased average daily ET (2.1 mm; Appendix 4A) compared to the natural grassland (0.9 mm; Appendix 4A). The maximum daily ET was similar between the woody encroached grassland (7.4 mm; 15 December 2019;

Appendix 4A) and the natural grassland (7.2 mm; 12 January 2019; Appendix 4A). During the wetter hydrological year (2019/2020), daily *ET* exceeded 6 mm (Appendix 4A) for more days in the woody encroached grassland (21 days) than the natural grassland (9 days). The same occurred during the drier hydrological year (2018/2019), where the daily *ET* exceeded 6 mm (Appendix 4A) for more days in the woody encroached grassland (12 days) than the natural grassland (7 days).

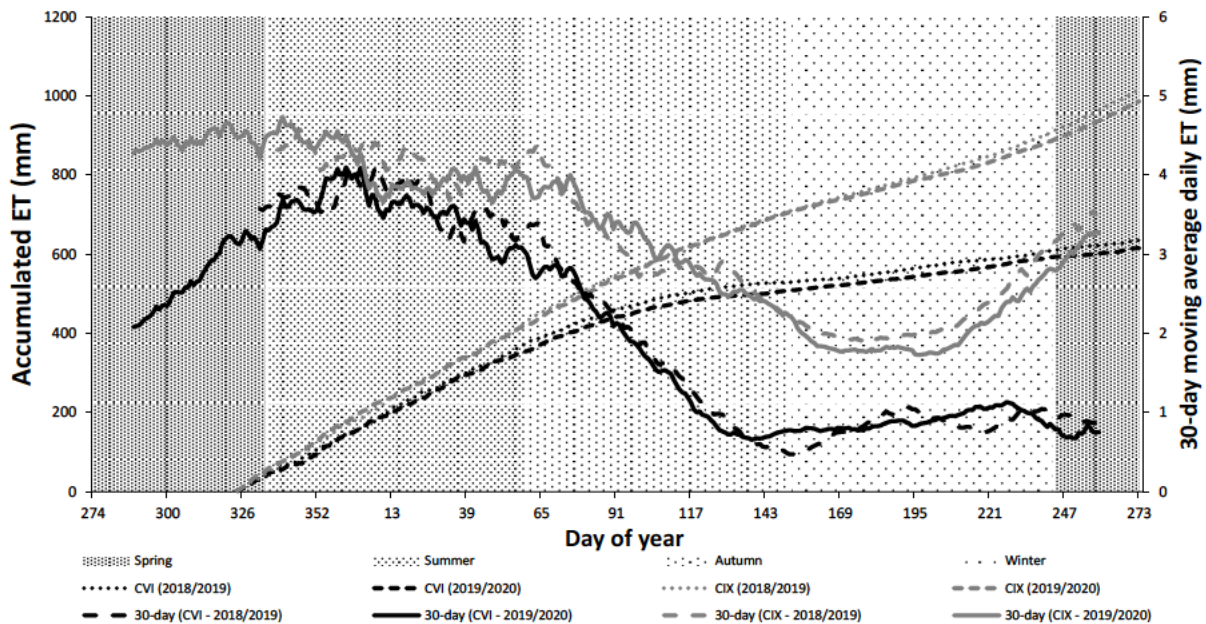


Figure 4.5: A comparison between the accumulated *ET* and 30-day moving average daily *ET* of the natural (black) and woody encroached (grey) grassland, over two hydrological years (2018/2019; 2019/2020).

4.4.4 Soil water content

The Diviner soil water probe provided an average monthly soil profile volumetric soil water content measurement at six locations across each catchment to a depth of 1.10 m (Figure 4.1). The monthly average profile volumetric soil water content was generally slightly higher within the woody encroached catchment than the natural grassland catchment over the entire measurement period. The profile volumetric soil water content peaked in summer across both catchments due to the increased precipitation and decreased in winter during the dry season. The highest and lowest average volumetric soil water contents observed across the six-point measurements are indicated by the upper and lower boundaries (Figure 4.6). The variation in volumetric soil water content across the woody encroached catchment was less than that of the near-natural grassland catchment. This could represent a more uniform soil water content across

the woody encroached catchment, than the natural grassland catchment. Both catchments followed a similar trend, responding to precipitation. The average profile volumetric soil water content in the woody encroached catchment reached a high of 37 % (Feb '20) during the wettest month of observation, and a low of 28 % (Oct '19) during the middle of spring, at the start of the rainfall season. The highest point profile volumetric soil water content within the woody encroached catchment was 39 % (Feb '20) again in the wettest month of observation, and the lowest was 24 % (Oct '19) corresponding to the lowest average soil water content. Within the natural grassland, the highest average profile volumetric soil water content was 35 % (Apr '19) which was 2 % less than the woody encroached catchment; observed at the end of the rainfall season. The lowest average profile volumetric soil water content observed was 26 % (Oct '19) and as with the woody encroached catchment, occurred in the middle of spring at the start of the rainfall season. The highest point profile volumetric soil water content within the natural grassland catchment was 42 % (Feb '20) which occurred in the wettest month of observation and was 3 % higher than the highest volumetric soil water content observed in the woody encroached catchment. The lowest point profile volumetric soil water content was 19 % (Oct '19) at the start of the rainfall season and was 5 % less than observed in the woody encroached catchment. The difference between the two catchments was generally higher under dry conditions.

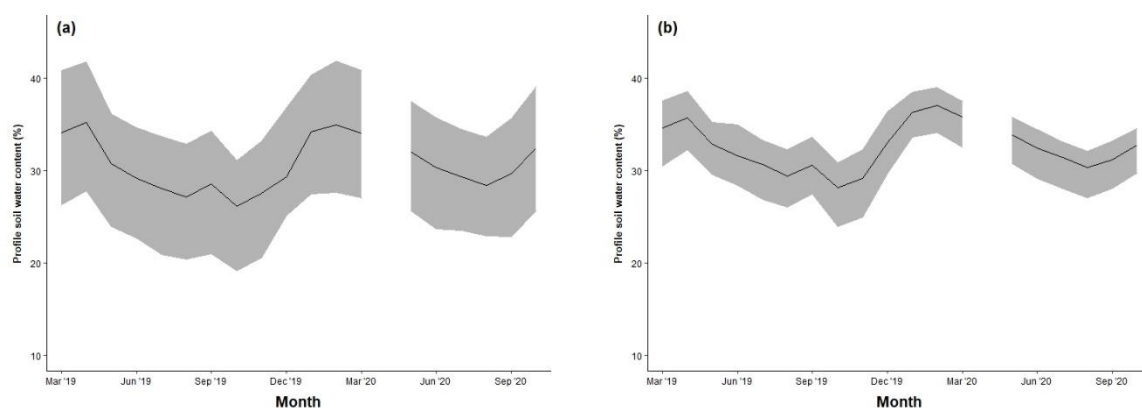


Figure 4.6: The average, upper and lower volumetric soil water content within 1 m of the soil profile across both catchment (a) VI and (b) IX based on the point measurement across the six Diviner tubes per catchment from March 2019 to October 2020.

A key difference between the two forms of land cover was the above-ground cover, and the rooting depths of the respective vegetation. To understand how these differences influence soil

water, selected depths (as recommended by existing literature) of 0.1 m (upper soil surface), 0.3 m (grass active rooting depth), 0.6 m (*Leucosidea* active rooting depth) and 0.9 m (zone without active roots) were compared. At these depths, measurements across the six representative tubes per catchment were averaged and compared over the observation (Figure 4.7). Within the upper soil surface, the average soil water was visibly higher during winter within the woody encroached catchment, but during summer, the soil water under both landcovers types was similar. Further evidence for the difference below the two canopies, was the soil temperature below the woody encroached canopy, which was found to be $\sim 2^{\circ}\text{C}$ lower year-round, than that of the soil below the natural grassland canopy. Within the grass rooting zone, the soil water content was consistently higher under the woody encroached catchment throughout the year, suggesting that the grassland is accessing soil water at this depth to a greater extent than the woody vegetation. At the *Leucosidea* active rooting depth, the difference in soil water content between the two catchments was less than at the grass rooting active depth, with near similar soil water content at the start and end of observation. At the deepest depth, the soil water content between the two catchments was similar. There was very little difference throughout the measurement period at the zone without active roots (0.9 m), indicating that the soil water content at a depth of 0.9 m is independent of land cover.

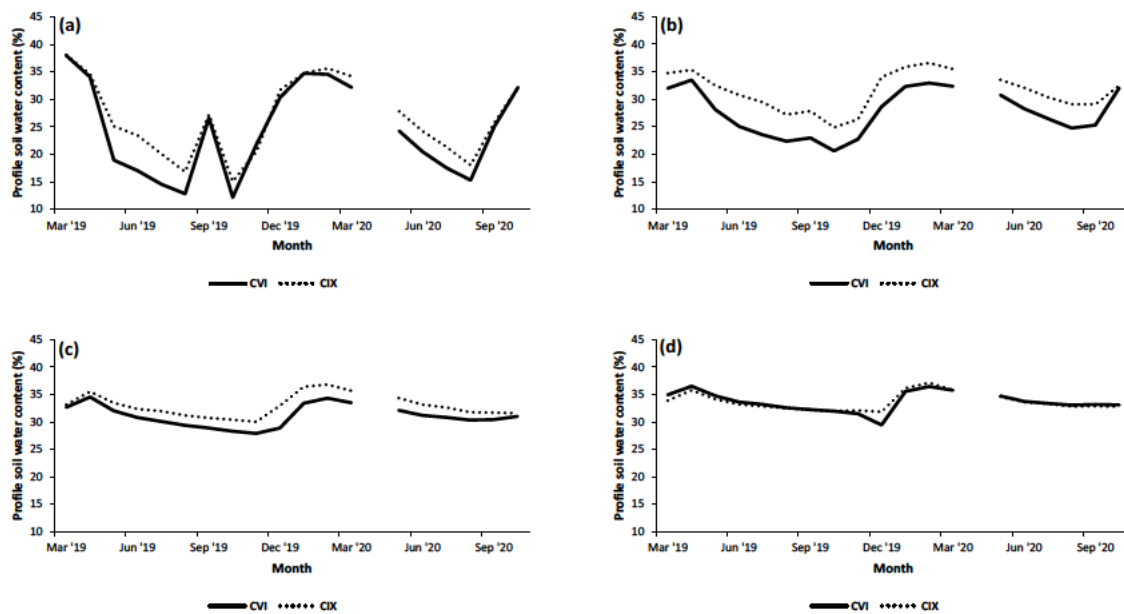


Figure 4.7: The average volumetric soil water content within the first metre of soil at a depth of (a) 0.1 m, (b) 0.3 m, (c) 0.6 m, and (d) 0.9 m across both catchment VI and IX.

4.4.5 Water balance

Comparing the recent monthly water balance when all variables (Equation 1) were measured (2018 – 2020) of the near-natural and the woody encroached catchments provides an indication of how the land cover change alters the partitioning of precipitation into both streamflow and *ET*. Patched *ET* data for October and half of November 2018 were used for catchment IX to allow for two complete hydrological years. From the water balance of the respective catchments (Table 4.1), it is evident that within both catchments, *ET* exceeded streamflow, and was the largest proportion of precipitation. Of precipitation, a higher percentage leaves catchment VI as streamflow, than leaves catchment IX. This is evident from the higher response ratio in catchment VI, as shown in Figure 4.3. The *ET* for the woody encroached vegetation cover was much higher than the near-natural grassland (Figure 4.5), resulting in there being less water available for streamflow. In both the dry and average hydrological years, *ET* exceeded precipitation for the woody encroached catchment. Within the near-natural grassland catchment, *ET* largely exceeded precipitation, despite being similar during the drier hydrological year. Despite a slightly higher precipitation, and a higher soil water content, the woody encroached catchment has a lower streamflow than the near-natural grassland catchment.

Table 4.1: The water balance of catchment VI (near-natural grassland) and catchment IX (woody encroached grassland) over the two respective hydrological years.

Hydrological year	Catchment	Precipitation (mm)	ET (mm)	Streamflow (mm)
2018/2019	VI	772	782	240
	IX	791	1242	110
2019/2020	VI	1017	732	435
	IX	1014	1204	230

4.5 Discussion

Although there have been infrequent wildfires, the protection of catchment IX since 1952 from fire (De Villiers and O'Connor, 2011) has led to woody encroachment of the natural grasslands of this uKhahlamba Drakensberg mountain catchment. Following the 26-year period from 1965 to 1991 when no fires occurred, the woody vegetation established, to a point that subsequent fires never burnt out the entire catchment, and the dense patches of woody vegetation remained intact (Figure 4.2). The litter layer is dense, and the roots are well established. Catchment IX,

therefore, illustrates the long-term effects of land cover transition to woody encroachment in the form of *Leucosidea* invasion, and is not a depiction of a recent land cover change.

Comparing the historical long-term precipitation and streamflow data with the current period of observation (2018 – 2020), the effects of woody encroachment on streamflow is evident. The precipitation received for the two catchments during both the historical and current periods was similar. Despite this, the streamflow and the catchment response ratio were reduced over time under the woody encroachment, compared to the natural grassland. As the woody encroachment became more established over time, the difference between the catchment runoff response of the natural and woody encroached grassland catchments has increased under the same climatic conditions. This was further confirmed through the analysis of the water balance during two current hydrological years, a drier and an average rainfall year. Despite only a 16-mm difference in precipitation between the two catchments over the two years, of which the woody encroached catchment received more, a difference of 335 mm in streamflow was observed, with the natural grassland catchment converting a higher proportion of precipitation into streamflow. This was also shown by the response ratio in the long-term analysis. This difference between the two catchments has evidentially increased with time, as the woody encroachment cover became more established. This is supported by the reduction in catchment response ratio of catchment IX, compared to the stationarity of the catchment VI response ratio following the long-term fire management.

A standout difference between the natural grassland and woody land cover was the difference in *ET*. The *ET* under woody land cover was greater than that under natural grassland land cover by 460 mm and 472 mm for the near-average (2019/2020) and drier (2018/2019) hydrological years respectively. These differences between the two land cover types are large, but small between the hydrological years. For both land cover types, *ET* was greater in the drier hydrological year, which could be attributed to less cloud cover and greater available energy flux. The woody land cover *ET* was also found to exceed the annual precipitation in both hydrological years, which is an indication for the observed reduction in streamflow. By comparison, during the drier year, *ET* of the natural grassland land cover was similar to the total precipitation, and well below during the near-average year. This suggests that recharge is possible during average rainfall years, which maintains the water availability during dry years. It is critical to consider the water storage of these mountainous catchments, which are able to maintain flows during below average and dry years.

The soil water content was found to be greater within the woody encroached catchment compared to the natural grassland catchment. At the grassland rooting depth (0.3 m), the soil water content was less than that for the woody encroached catchment due to the grassland accessing this region of the soil profile, in contrast to the woody vegetation, which accesses water at a deeper zone. This is indicated by the reduced deficit between the soil water contents at the *Leucosidea* rooting depth (0.6 m). Although the Walter hypothesis (Ward et al., 2013) was never proposed for moist Afromontane areas, it does describe and provide justification for the events observed within this study. Beyond the rooting zones (0.9 m), the two soil water contents were similar. This highlights the influence of different land cover types, on soil water at different depths of the soil profile. Increased soil water content found under the woody encroachment could be due to a greater clay content, as the response to changes in precipitation were similar between the catchments. The ground water contribution is also unknown. The increased soil water content under woody encroachment is an anomaly which needs further research.

It is commonly understood that a change in land cover results in a change in the energy balance due to changes in surface albedo, wind profile, soil temperature and available energy flux (Archer, 2010; Zou et al., 2014; Acharya et al., 2017), all of which directly influence ET . The first evident change in energy balance between the woody vegetation and the natural grassland is that of the available energy flux ($R_n - G$). Within the woody vegetation canopy, the available energy flux was nearly three times greater than that within the natural grassland (data not shown). This was a potential result of a reduction in surface reflectance and albedo associated with woody vegetation. A second noticeable change is that of the G component of the energy balance. Under natural grassland, G varies seasonally and reaches as high as 15 % of R_n in winter, potentially due to increased soil exposure following winter senescence of the grassland and drying of the soil. Under the woody vegetation canopy, G remains around 1 % of R_n year-round, and is a small component of the energy balance. This could be due to the increased soil shading from the canopy and dense litter. The most significant change is the partitioning of H and LE from available energy flux. As expected from the different vegetation phenology, the relationship between H and LE varies throughout the year. Within the woody vegetation canopy, LE is greater than H year-round, with the greatest difference occurring in summer resulting in an increased ET . During winter the relationship between H and LE is more equal, but with LE still greater. Under the natural grassland, the relationship between H and LE fluctuated through the year, as an indication and possible result of, the grass senescence in winter. As with the woody vegetation, LE dominated the energy balance in summer

corresponding to the higher ET in summer. Following summer and during the autumn transition into winter, LE begins to dominate and remains small even into spring. Towards the end of spring as the vegetation returns from senescence, LE increases its portion of R_n . The difference in energy balance characteristics between the land covers, are likely a direct result of the differences between the phenology and physical characteristics of the two vegetation types. Such changes in partitioning of the energy balance, plays a role in explaining and understanding the ET differences between the two land covers.

There are no known studies globally that specifically focus on *Leucosidea*, although there is information on a woody vegetation known as such as *Juniperus*, which is a common invasive species in North America found in areas with a lower precipitation (MAP ~ 800 mm). Zou et al. (2014) found *Juniperus ashei* encroachment into a grassland to reduce soil water, which was more evident in winter due to continuous transpiration as compared to the dormant grassland. This resulted in a significantly reduced spring streamflow. It was also found that the *Leucosidea* encroached catchment ET was greater than the grassland catchment, being most noticeable in winter due to the grassland senescence, but also the streamflow from the *Leucosidea* encroached catchment was less than the grassland catchment. However, the increase in soil water content under the *Leucosidea* contrasted with the decreased soil water content found under the *Juniperus ashei* (Zou et al., 2014) and *Juniperus virginiana* encroached sites (Acharya et al., 2017). This further highlights the anomaly and requirement for further research.

Everson (2001) assessed the water balance of the natural grassland of catchment VI from 1980 to 1992. During a year (1984) which experienced comparable precipitation of 1 025 mm to the 2019/2020 hydrological year where 1 017 mm fell, the ET (614 mm) and streamflow (411 mm) were comparable to the 2019/2020 ET (732 mm) and streamflow (435 mm). During the drier years (1982, 1992) of Everson's (2001) observation, where annual precipitation was below 1 000 mm, ET ranged from 614 – 655 mm, which was similar to the drier hydrological year (2018/2019) of this study. Daily ET from Everson (2001) also matched those of this study ranging from 3 to 7 mm day⁻¹ during summer, and less than 1 mm day⁻¹ during winter. These similarities indicate a stationarity in the natural grassland catchment behaviour, also found within the long-term runoff response ratios, and provide justification for this representation of the natural grassland within this study.

Overall, the study showed that the change from the natural grassland cover to woody vegetation resulted in a reduction in streamflow from the catchment. Therefore, a reduction in the supply of water from the catchment to downstream areas can be expected, especially in the

long-term following the change from grassland to woody vegetation. The importance of management practices such as prescribed burning, are clearly critical for the maintenance of the natural grasslands, and therefore for maintaining the water supply and ecosystem services provided by this region.

4.6 Conclusions

Using the long-term historical precipitation and streamflow data and following 23 months of concurrent water balance component observation, between a neighbouring natural grassland catchment, and a well-established woody encroached catchment, it is evident that the change in land cover from the natural state has had an impact on the water and energy balances of the encroached catchment. The water balance impact is in the form of a reduction in streamflow and catchment response, which could be attributed to a change in the energy balance and resultant increase in annual *ET*. Winter was identified as the period when the change in *ET* between the two vegetation types is most noticeable, due to the difference in phenology between the seasonal natural grassland and evergreen *Leucosidea*. In contrast to findings in other woody encroachment research, there was a slight increase in soil water content under the well-established *Leucosidea* canopy, compared to the natural grassland. By considering soil water depletion, it was found that the woody vegetation used the deeper (0.6 m) soil water, compared to the natural grassland which utilised the upper (0.3 m) soil water. This research study provides a clear indication that the woody encroachment of the natural grasslands within the uKhahlamba Drakensberg mountain range will have a negative impact on the water balance and water supply from these catchments. This provides a good basis for understanding from which land and catchment managers can be informed, especially of the negative effects of encroachment of the Drakensberg mountain ranges on the water supply from this strategic water source area. This also stresses the importance of fire as a management tool to maintain the natural grassland land cover to preserve the key ecosystem service of water supply from the region. This headwater catchment scale observation study provides a valuable dataset and initial understanding from which upscaling is possible using hydrological modelling to improve future management decision making. This study provides an important first step to understanding the importance of land use management to ensure the optimal and sustainable management of South Africa's water resources.

4.7 Acknowledgements

The authors would like to acknowledge the support provided by the National Research Foundation's (NRF) South African Environmental Observation Network (SAEON) business

unit. Opinions expressed and conclusions arrived at are those of the author(s) and are not necessarily to those of the NRF or SAEON.

4.8 Funding

This research did not receive any specific grant from funding agencies in the public, commercial, or not-for-profit sectors.

4.9 References

- Acharya, B.S., Hao, Y., Ochsner, T.E., Zou, C.B., 2017. Woody plant encroachment alters soil hydrological properties and reduces downward flux of water in tallgrass prairie. *Plant Soil*. 414, 379-391.
- Acharya, B.S., Kharel, G., Zou, C.B., Wilcox, B.P., Halihan, T., 2018. Woody plant encroachment impacts on groundwater recharge: A review. *Water*. 10, 1466.
- Adcock, K., 1990. Vegetation changes since the withdrawal of fire from Catchment IX, Cathedral Peak, Natal Drakensberg. Thesis (MSc). University of the Witwatersrand, South Africa.
- Allen, R., Pereira, L., Raes, D., Smith, M., 1998. Guidelines for Computing Crop Water requirements-FAO Irrigation and Drainage Paper 56: FAO-Food and Agriculture Organization of the United Nations, Rome.
- Archer, S.R., 2010. Rangeland conservation and shrub encroachment: New perspectives on an old problem. *Wild Rangelands: Conserving Wildlife While Maintaining Livestock in Semi-Arid Ecosystems*. 53-97.
- Archer, S., Boutton, T.W., Hibbard, K.A., 2001. Trees in grasslands: Biogeochemical consequences of woody plant expansion. *Global Biogeochemical Cycles in the Climate System*. 115-137.
- Archer, S.R., Andersen, E.M., Predick, K.I., Schwinning, S., Steidl, R.J., Woods, S.R., 2017. Woody Plant Encroachment: Causes and Consequences. In: Briske, D.D. (Eds), *Rangeland Systems: Processes, Management and Challenges*. Springer., Gewerbestrasse, Switzerland, pp. 25-84.
- Arnell, N., 2002. *Hydrology and Global Environmental Change*. Pearson Education Limited, UK.
- Axelsson, C.R., Hanan, N.P., 2018. Rates of woody encroachment in African savannas reflect water constraints and fire disturbance. *Journal of Biogeography*. 45, 1209-1218.
- Beniston, M., Stoffel, M., 2014. Assessing the impacts of climatic change on mountain water resources. *Science of the Total Environment*. 493, 1129-1137.
- Bond, W.J., 2008. What limits trees in C₄ grasslands and savannas? *Annual review of ecology, evolution and systematics*. 39, 641-659.

- Bond, W.J., Parr, C.L., 2010. Beyond the forest edge: Ecology, diversity and conservation of the grassy biomes. *Biological Conservation*. 143, 2395-2404.
- Bond, W.J., Woodward, F.I., Midgley, G.F., 2005. The global distribution of ecosystems in a world without fire. *New Phytologist*. 165, 525-538.
- Bosch, J., 1979. Treatment effects on annual and dry period streamflow at Cathedral Peak. *South African Forestry Journal*, 108, 29-38.
- Botha, C., 2016. Personal communication of soil survey data, Natural Resources KwaZulu-Natal Department of Agriculture and Rural Development, Hilton, South Africa, [29/05/2020].
- Brown, L.R., Bezuidenhout, H., 2020. Grassland vegetation of southern Africa. *Encyclopedia of the World's Biomes*. 3, 814-825.
- Carbutt, C., 2019. Nature of Alpine Ecosystems in Tropical Mountains of Africa. *Encyclopedia of the World's Biomes*. 1, 292-299.
- Carbutt, C., Martindale, G., 2014. Temperate indigenous grassland gains in South Africa: Lessons being learned in a developing country. *Parks*. 20(1), 105-125.
- Daryanto, S., Eldridge, D.J., Wang, L., 2013. Spatial patterns of infiltration vary with disturbance in a shrub-encroached woodland. *Geomorphology*, 194, 57-64.
- De Villiers, A.D., 2012. Fire-mediated succession and reversion of woody vegetation in the KwaZulu-Natal Drakensberg, South Africa. Thesis (MSc). University of the Witwatersrand, South Africa.
- De Villiers, A.D., O'Connor, T., 2011. Effect of a single fire on woody vegetation in Catchment IX, Cathedral Peak, KwaZulu-Natal Drakensberg, following extended partial exclusion of fire. *African Journal of Range and Forage Science*, 28(3), 111-120.
- Doerr, S.H., Shakesby, R.A., Walsh, R.P.D., 2000. Soil water repellency: its causes, characteristics and hydro-geomorphological significance. *Earth-Science Reviews*. 51, 33-65.
- Dugas, W.A., Hicks, R.A., Wright, P., 1998. Effect of removal of *Juniperus ashei* on evapotranspiration and runoff in the Seco Creek watershed. *Water Resources Research*. 34(6), 1499-1506.
- Eldridge, D.J., Bowker, M.A., Maestre, F.T., Roger, E., Reynolds, J.F., Whitford, W.G., 2011. Impacts of shrub encroachment on ecosystem structure and functioning: towards a global synthesis. *Ecology Letters*. 14, 709-722.
- Eldridge, D.J., Wang, L., Ruiz-Colmenero, M., 2014. Shrub encroachment alters the spatial patterns of infiltration. *Ecohydrology*. 8(1), 83-93.
- Everson, C.S., 2001. The water balance of a first order catchment in the montane grasslands of South Africa. *Journal of Hydrology*, 241, 110-123.
- Everson, C.S., Molefe, G.L., Everson, T.M., 1998. Monitoring and Modelling Components of the Water Balance in a Grassland Catchment in the Summer Rainfall Area of South Africa. WRC ReportNo. 493/1/98. Water Research Commission, Pretoria.

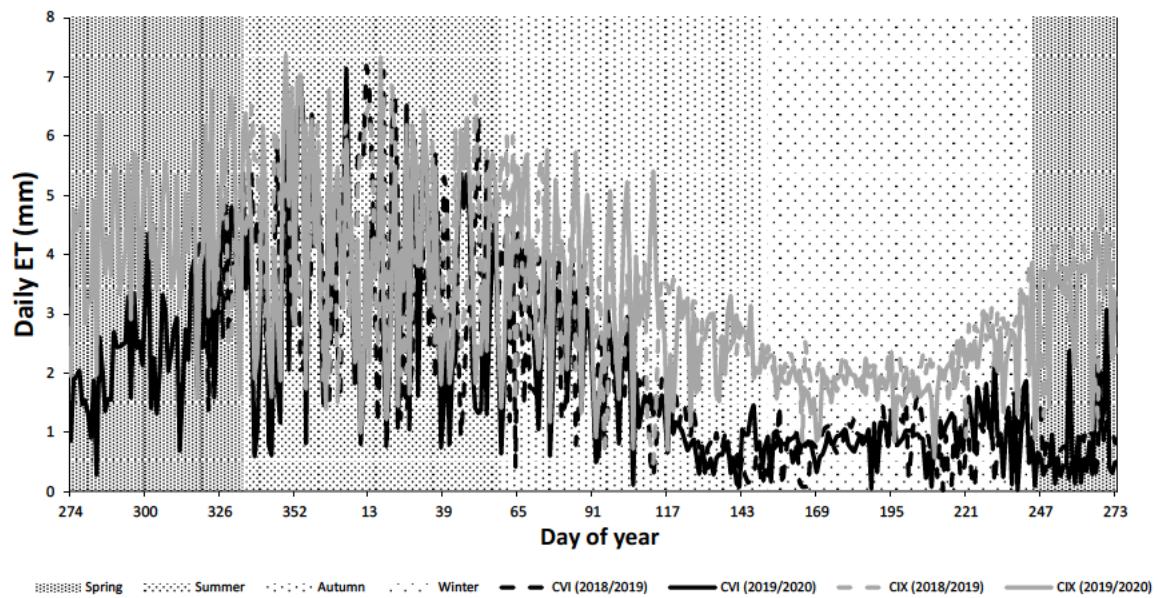
- Everson, T.M., Yeaton, R.I., Everson, C.S., 2009. Seed dynamics of *Themeda triandra* in the montane grasslands of South Africa. *African Journal of Range & Forage Science*. 26(1), 19-26.
- Fultz, L.M., Moore-Kucera, J., Date, J., Davinic, M., Perry, G., Wester, D., Schwilk, D.W., Rideout-Hanzak, S., 2016. Forest wildfire and grassland prescribed fire effects on soil biogeochemical processes and microbial communities: Two case studies in the semi-arid Southwest. *Applied Soil Ecology*. 99, 118-128.
- Gordijn, P.J., Everson, T.M., O'Connor, T.G., 2018. Resistance of Drakensberg grasslands to compositional change depends on the influence of fire-return interval and grassland structure on richness and spatial turnover. *Perspectives in Plant Ecology, Evolution and Systematics*. 34, 26-36.
- Granger, J.E., 1976. The vegetation changes, some related factors and changes in the water balance following 20 years of fire exclusion in the Catchment IX; Cathedral Peak Forestry Research Station. Thesis (PhD). University of Natal, South Africa.
- Gray, B.A., Toucher, M.L., Savage, M.J., Clulow, A.D., 2021a. The potential of surface renewal for determining sensible heat flux for indigenous vegetation for a first-order montane catchment. *Hydrological Sciences Journal*. 1-13.
- Gray, B.A., Toucher, M.L., Savage, M.J., Clulow, A.D., 2021b. Seasonal evapotranspiration over an invader vegetation (*Pteridium aquilinum*) in a degraded montane grassland using surface renewal. Submitted to *Journal of Hydrology: Regional Studies*.
- Green, TR, Taniguchi, M, Kooi, H, Gurdak, JJ, Allen, DM, Hiscock, KM, Treidel, H., Aureli, A. 2011. Beneath the surface of global change: Impacts of climate change on groundwater. *Journal of Hydrology*. 405, 532-560.
- Gwate, O., Mantel, S.K., Gibson, L.A., Munch, Z., Palmer, A.R., 2018. Exploring dynamic of evapotranspiration in selected land cover classes in a sub-humid grassland: A case study in quaternary catchment S50E, South Africa. *Journal of Arid Environments*. 157, 66-76.
- Harrison, R., 2020. Personal communication of soil survey data, South African Environmental Observation Network: Grassland-Forest-Wetland Node, Pietermaritzburg, South Africa, [29/01/2021].
- Hoekstra, J.M., Boucher, T.M., Ricketts, T.H., Roberts, C., 2005. Confronting a biome crisis: global disparities of habitat loss and protection. *Ecology Letters*. 8, 23-29.
- Honda, E.A., Durigan, G., 2016. Woody encroachment and its consequences on hydrological processes in the savannah. *Philosophical Transactions Royal Society B*. 371, 20150313.
- Huxman, T.E., Wilcox, B.P., Breshears, D.D., Scott, R.L., Snyder, K.A., Small, E.E., Hultine, K., Pockman, W.T., Jackson, R.B., 2005. Ecohydrological implications of woody plant encroachment. *Ecology*. 86(2), 308-319.
- Killick, D.J., 1963. An account of the plant ecology of the Cathedral Peak area of the Natal Drakensberg. *Botanical Survey of South Africa Memoir No. 345*. Botanical Research Institute. Department of Agricultural Technical Services. Government Printer, Pretoria.

- Kulmatiski, A., Beard, K.H., 2013. Woody plant encroachment facilitated by increased precipitation intensity. *Nature Climate Change*. 3, 833-837.
- Kurc, S.A., Small, E.E., 2004. Dynamics of evapotranspiration in semiarid grassland and shrubland ecosystems during the summer monsoon season, central New Mexico. *Water Resources Research*. 40, W09305.
- Kurc, S.A., Small, E.E., 2007. Soil moisture variations and ecosystem-scale fluxes of water and carbon in semiarid grassland and shrubland. *Water Resources Research*. 43, W06416.
- Le Maitre, D.C., Scott, D.F., Colvin, C., 1999. A review of information on interactions between vegetation and groundwater. *Water SA*. 25(2), 137-152.
- Little, I.T., Hockey, P.A.R., Jansen, R., 2013. A burning issue: Fire overrides grazing as a disturbance driver for South African grassland bird and arthropod assemblage structure and diversity. *Biological Conservation*. 158, 258-270.
- Liu, Y., Xiao, J., Ju, W., Xu, K., Zhou, Y., Zhao, Y., 2016. Recent trends in vegetation greenness in China significantly altered annual evapotranspiration and water yield. *Environmental Research Letters*. 11, 094010.
- MacVicar, C.N., De Villiers, J.M., Loxton, R.F., Verster, E., Lambrechts, J.J.N., Merryweather, F.R., Le Roux, J., Van Rooyen, T.H., Harmse, H.J. von M., 1977. Soil classification – A binomial system for South Africa. Department of Agricultural Technical Services, Pretoria, South Africa.
- Mafole, T.C., Aremu, A.o., Mthethwa, T., Moyo, M., 2017. An overview on *Leucosidea sericea* Eckl. & Zeyh.: A multi-purpose tree with potential as a phytomedicine. *Journal of Ethnopharmacology*. 203, 288-303.
- Miller, J.E.D., Damschen, E.I., Ratajczak, Z., Ozdogan, M., 2017. Holding the line: three decades of prescribed fires halt but do not reverse woody encroachment in grasslands. *Landscape Ecology*. 32, 2297-2310.
- Mills, A.J., Rogers, K.H., Stalmans, M., Witkowski, E.T.F., 2006. A framework for exploring the determinants of savanna and grassland distribution. *BioScience*. 56(7), 579-589.
- Montanari, A., Young, G., Savenije, H.H.G., Hughes, D., Wagener, T., Ren, L.L., Koutsoyiannis, D., Cudennec, C., Toth, E., Grimaldi, S., Blöschl, G., Sivapalan, M., Beven, K., Gupta, H., Hipsey, M., Schaeffli, B., Arheimer, B., Boegh, E., Schymanski, S.J., Di Baldassarre, G., Yu, B., Hubert, P., Huang, Y., Schumann, A., Post, D.A., Srinivasan, V., Harman, C., Thompson, S., Rogger, M., Viglione, A., McMillan, H., Characklis, G., Pang, Z., Belyaev, V., 2013. “Panta Rhei-Everything Flows”: Change in hydrology and society-The IAHS Scientific Decade 2013-2022. *Hydrological Sciences Journal*. 58(6), 1256-1275.
- Nanni, U.W., 1956. Forest hydrological research at the Cathedral Peak research station. *Journal of the South African Forestry Association*, 27(1), 2-35.
- Neary, D.G., 2006. Impacts of Wildfire Severity on Hydraulic Conductivity in Forest, Woodland, and Grassland Soils. *Hydraulic Conductivity – Issues, Determination, and Application*. InTech Publishers, Rijeka, Croatia.

- Nie, W., Yuan, Y., Kepner, W., Erickson, C., Jackson, M., 2012. Hydrological impacts of mesquite encroachment in the upper San Pedro watershed. *Journal of Arid Environments*. 82, 147-155.
- O'Connor, R.C., Taylor, J.H., Nippert, J.B., 2020. Browsing and fire decreases dominance of a resprouting shrub in woody encroached grassland. *Ecology*. 101(2), e02935.
- O'Connor, T.G., Puttick, J.R., Hoffman, M.T., 2014. Bush encroachment in southern Africa: changes and causes. *African Journal of Range & Forage Science*. 31(2), 67-88.
- O'Donnell, F.C., Caylor, K.K., 2012. A model-based evaluation of woody plant encroachment effects on coupled carbon and water cycles. *Journal of Geophysical Research*. 117, G02012.
- Ozturk, M., Copt, NK, Saysel, AK. 2013. Modeling the impact of land use change on hydrology of a rural watershed. *Journal of Hydrology*. 497, 97-109.
- Peng, H., Li, X., Li, G., Zhang, Z., Zhang, S., Li, L., Zhao, G., Jiang, Z., Ma, Y., 2013. Shrub encroachment with increasing anthropogenic disturbance in semiarid Inner Mongolian grasslands of China. *Catena*. 109, 39-48.
- Puttock, A., Dungait, J.A.J., Macleod, C.J.A., Bol, R., Brazier, R.E., 2014. Woody plant encroachment into grasslands leads to accelerated erosion of previously stable organic carbon from dryland soils. *Journal of Geophysical Research: Biogeosciences*. 119, 2345-2357.
- Qiao, L., Zou, C.B., Stebler, E., Will, R.E., 2017. Woody plant encroachment reduces annual runoff and shifts runoff mechanisms in the tallgrass prairie, USA. *Water Resource Research*. 53, 4838-4849.
- Qiao, L., Zou, C.B., Will, R.E., Stebler, E., 2015. Calibration of SWAT model for woody plant encroachment using paired experimental watershed data. *Journal of Hydrology*. 523, 231-239.
- Rowe-Rowe, D.T., 1995. Small-mammal recolonisation of a fire-exclusion catchment after unscheduled burning. *South African Journal of Wildlife Research*. 25, 133-137.
- Sajikumar, N., Reyma, R.S., 2015. Impact of land cover and land use change on runoff characteristics. *Journal of Environmental Management*. 161, 460-468.
- Schreiner-McGraw, A.P., Vivoni, E.R., Ajami, H., Sala, O.E., Throop, H.L., Peters, D.P.C., 2020. Woody Plant Encroachment has a Larger Impact than Climate Change on Dryland Water Budgets. *Scientific Reports*. 10, 8112.
- Schulze, R.E., 1974. Catchment evapotranspiration in the Natal Drakensberg. Thesis (PhD). University of Natal, South Africa.
- Scott, DF, Prinsloo, FW, Moses, G, Mehlomakulu, M., Simmers, ADA. 2000. A Re-Analysis of the South African Catchment Afforestation Experimental Data. 810/1/00. Water Research Commission, Pretoria, South Africa.
- Scott, R.L., Huxman, T.E., Barron-Gafford, G.A., Darrel Jenerette, D., Young, J.M., Hamerlynck, E.P., 2014. When vegetation change alters ecosystem water availability. *Global Change Biology*. 20, 2198-2210.

- Sokolov, A.A., Chapman, T.G., 1974. Methods for water balance computations, an international guide for research and practice. UNESCO press. Paris, France.
- Stavi, I., 2019. Wildfires in grasslands and shrublands: A review of impacts on vegetation, soil, hydrology, and geomorphology. *Water*. 11, 1042.
- Stevens, N., Erasmus, B.F.N., Archibald, S., Bond, W.J., 2016. Woody encroachment over 70 years in South African savannahs: overgrazing, global change or extinction aftershock? *Philosophical Transactions Royal Society B*. 371, 20150437.
- Toucher, M.L., Clulow, A., Van Rensburg, S., Morris, F., Gray, B., Majozi, S., Everson, C.E., Jewitt, G.P.W., Taylor, M.A., Mfeka, S., Lawrence, K., 2016. Establishment of a more robust observation network to improve understanding of global change in the sensitive and critical water supply area of the Drakensberg. 2236/1/16. Water Research Commission, Pretoria, South Africa.
- van Auken, O.W., 2009. Causes and consequences of woody plant encroachment into western North American grasslands. *Journal of Environmental Management*. 90, 2931-2942.
- Wagener, T, Sivapalan, M, Troch, PA, McGlynn, BL, Harman, CJ, Gupta, HV, Kumar, P, Rao, PSC, Basu, NB., Wilson, JS. 2010. The future of hydrology: An evolving science for a changing world. *Water Resources Research*. 46, W05301.
- Wang, J., Xiao, X., Zhang, Y., Qin, Y., Doughty, R.B., Wu, X., Bajgain, R., Du, L., 2018. Enhanced gross primary production and evapotranspiration in juniper-encroached grasslands. *Global Change Biology*. 24, 5655-5667.
- Ward, D., Wiegand, K., Getzin, S., 2013. Walter's two-layer hypothesis revisited: back to the roots! *Oecologia*. 172, 617 – 630.
- Wilcox, B.P., 2007. Does rangeland degradation have implications for global streamflow? *Hydrological Processes*. 21(21), 2961-2964.
- Wilcox, B.P., Birt, A., Archer, S.R., Fuhlendorf, S.D., Kreuter, U.P., Sorice, M.G., van Leeuwen, J.D., Zou, C.B., 2018. Viewing woody-plant encroachment through a social-ecological lens. *BioScience*. 68(9), 691-705.
- Wine, M.L., Hendrickx, J.M.H., 2013. Biohydrologic effects of eastern redcedar encroachment into grassland, Oklahoma, USA. *Biologia*. 68(6), 1132-1135.
- Yin, J., He, F., Xiong, Y.J., Qiu, G.Y., 2017. Effects of land use/land cover and climate changes on surface runoff in a semi-humid and semi-arid transition zone in northwest China. *Hydrology and Earth System Sciences*. 21, 183-196.
- Zhang, L., Karthikeyan, R., Bai, Z., Srinivasan, R., 2017. Analysis of streamflow responses to climate variability and land use change in the Loess Plateau region of China. *Catena*. 154, 1-11.
- Zou, C.B., Caterina, G.L., Will, R.E., Stebler, E., Turton, D., 2015. Canopy Interception for a Tallgrass Prairie under Juniper Encroachment. *PLoS One*. 10(11), e0141422.

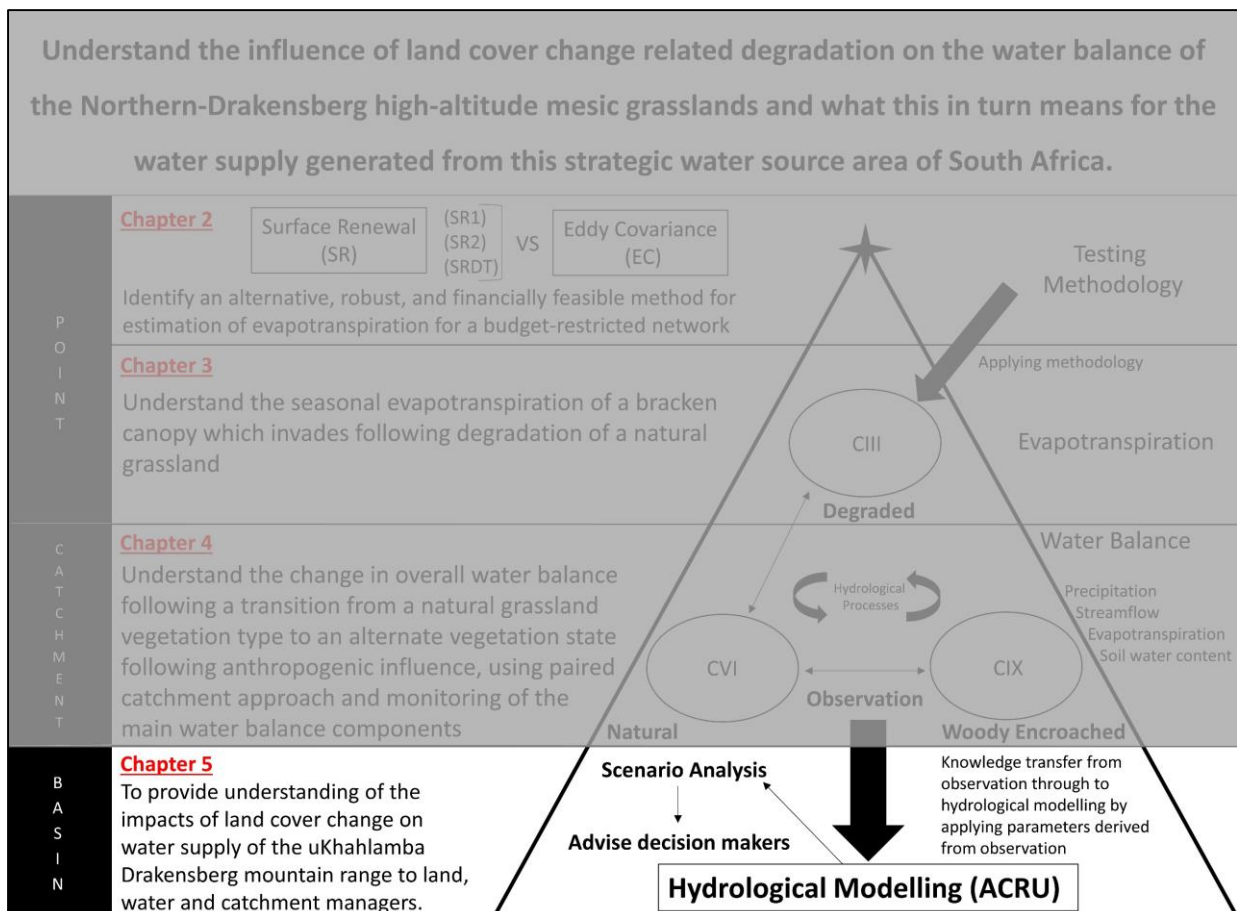
4.10 Appendix



Appendix 4A: A comparison between the daily evapotranspiration (ET) of the natural (black) and woody encroached (grey) grassland, over two hydrological years (2018/2019; 2019/2020).

Lead in to Chapter 5

Having started at methodology, progressing to a point measurement, and scaling up to a catchment, the final research component of this thesis aims to expand this understanding to the basin scale using hydrological modelling in combination with scenario analysis to provide recommendations to water, land and catchment managers. The specific objective of Chapter 5 was to take what was learnt through observation at the various scales on the *Leucosidea sericea* (woody) and *Pteridium aquilinum* (bracken) vegetations and derive land cover parameters to be used within the Agricultural Catchments Research Unit (ACRU) agrohydrological model. Following which, a land cover change scenario analysis was conducted to provide a better understanding of the potential impacts of these two forms of land cover change on the water supply generated within the upper-uThukela catchment if left unmanaged.



5. THE HYDROLOGICAL IMPACTS OF LAND DEGRADATION WITHIN A STRATEGIC WATER SOURCE AREA OF SOUTH AFRICA

Abstract

The upper-uThukela catchment forms part of the headwater catchments for the Northern Drakensberg strategic water source area (SWSA). The natural land cover of the upper-uThukela is natural mesic-grasslands. These mesic-grasslands are under threat from two forms of land-degradation, the invasion of bracken fern, and the encroachment of woody vegetation. The aim of this study was to understand the impacts of degradation related land cover change on the hydrology of the upper-uThukela catchment using hydrological modelling in combination with scenario analysis. The Agricultural Catchments Research Unit (ACRU) agrohydrological model was selected as it has been previously successfully used within the region and is sensitive to land cover change. As no meaningful hydrological model parameters exist for either land cover change vegetation types, recent observation-based studies were used as a basis from which to derive the parameters. The ability of the ACRU model to simulate the current land cover conditions of the upper-uThukela was successfully confirmed prior to which scenario analysis compared the current land cover streamflow with streamflow simulated under incremental levels (25, 50, 75, 100 %) of invasion and encroachment. The analysis showed that both forms of land degradation result in a reduction in mean annual streamflow. Woody encroachment resulted in the largest reduction in streamflow, particularly in the dry winter low flows months. The water balance of the headwater catchments, which fall within the protected area of the SWSA, were found to be the most sensitive to land cover change. Should the landscape not remain as a fire-adapted grassland and become degraded, the downstream consequence for water supply will be significant.

Keywords: *land cover change, hydrological modelling, scenario analysis, headwater catchments, bracken, woody plant encroachment*

5.1 Introduction

Land cover change alters the partitioning of precipitation into the hydrological components within the catchment (Cao et al., 2009; Warburton et al., 2012; Yin et al., 2017), and thereby the long-term flow dynamics, impacting mean annual discharge from a catchment (Zhang et

al., 2017; Saddique et al., 2020). Thus, management of land cover is tied to the provision of water resources (Alvarenga et al., 2016). A region which requires an understanding of how land cover change could impact upon hydrology of the area if left unmanaged, is the Northern Drakensberg strategic water source area (SWSA) which headwaters lie within the Drakensberg mountain range, South Africa. The upper-uThukela catchment falls within the Northern Drakensberg SWSA. The Northern Drakensberg SWSA, within which the upper-uThukela catchment falls, is natural mesic grassland biome. This biome is under threat from two forms of land degradation, namely, the invasion of bracken fern, and the encroachment of woody vegetation. Even though a portion of the SWSA headwaters falls within the protected areas of the Maloti-Drakensberg Transfrontier Park, the high-altitude fire-adapted grasslands are susceptible to invasion by woody vegetation and bracken fern despite conservation efforts (Grab and Knight, 2018). Outside the protected areas, subsistence and commercial agriculture dominate and have led to extensive degradation (Blignaut et al., 2010). The contrasting forms of land cover change are challenges to the management and provision of this area as a water source area. Observations in small, headwater catchments of the upper uThukela have shown that both forms of land cover change alter the water balance (Gray et al., 2021a, b, c). However, to date, no studies have assessed the potential impacts of these land cover changes at a scale relevant to water management. Nor have any considered how water supply could be impacted under widespread land cover change and whether there are tipping points in the system where the extent the land cover change becomes problematic.

Hydrological models have been widely used in the research community for the assessment of the impacts of land cover change on streamflow (e.g. Cao et al., 2009; Birkel et al., 2012; Salemi et al., 2013; Ahn and Merwade, 2017; Gashaw et al., 2018), as well as within the management community for planning and decision making (Devi et al., 2015). The ability to provide insight into the mechanisms occurring under change, to provide results immediately (Li et al., 2007), and to simulate hydrological processes in ungauged areas (Boongaling et al., 2018), contribute to the usefulness of hydrological models. Within South Africa, hydrological modelling change studies have focussed on streamflow impacts due to alien plant invasion, overgrazing, commercial forestry, agriculture (irrigation) and urban areas (Gush et al., 2002; Jewitt et al., 2004; Warburton et al., 2012; Rebelo et al., 2015; Gyamfi et al., 2016).

A widely used hydrological model in South Africa and internationally for land cover change assessments is the Agricultural Catchments Research Unit (ACRU) agrohydrological model (Kienzle and Schmidt, 2008; Schmidt et al., 2009; Kienzle, 2010; Forbes et al., 2011; Mugabe

et al., 2011; Kienzle et al., 2012; Aduah et al., 2017), which was developed from data from the Cathedral Peak research catchments and designed to be sensitive to changes in land use/cover and management strategies (Aduah et al., 2017). Of relevance, the ACRU hydrological model was used to determine the influence of degradation by overgrazing and overly frequent burning on the streamflow of the upper uThukela as input required for an economic scenario analysis (Blignaut et al., 2010). The findings showed that land cover degradation within this area has significant financial costs, but also ecosystem service losses (Blignaut et al., 2010). Beyond this, to the authors knowledge no studies have considered the influence of woody encroachment or bracken invasion within the upper uThukela catchment, nor any other site within the Northern-Drakensberg, despite the threat posed. As the influence has not been considered, no meaningful hydrological model parameters are available for either vegetation types and, as noted by Kirchner (2006) and Karlsson et al. (2016), a source of uncertainty when modelling land cover change impacts is the parameterisation of the hydrological model. Qiao et al. (2015), for example, highlighted the importance of parameterisation when investigating the impact of juniper encroachment. Previous studies which consider Juniper substituted Pine parameters for the modelling of Juniper, which creates other issues due to the different phenology between Juniper and Pine, and thus large uncertainty in model results (Qiao et al., 2015). Qiao et al. (2015) determined parameters for juniper using observational data and expressed the need for improved representation of the woody encroachment process in hydrological modelling as it provides unique change characteristics for the hydrological and soil properties of a catchment compared to the more researched land cover changes, such as agriculture and forestry.

Further to this, environmental change is creating a dynamic where the uncertainty in model prediction into the future is increasing, as systems move to new states in which previous expectations of behaviour are no longer valid (Wagener et al., 2010; Ehret et al., 2014). Models do not generate knowledge, but expand on and create understanding from knowledge and facts gained through observation (Schulze, 1995), thus, to improve models representation of change we need to look to field based data (Burt and McDonnell, 2015). Field observations and experimental catchments provide a good understanding of the complex relationship between land cover changes and hydrological processes (Ahn and Merwade, 2017), and can improve model parameterisation and representation of environmental changes (Qiao et al., 2015), particularly land cover change.

According to available literature, the ACRU agrohydrological model (or any other) has not been used to simulate the effects of woody encroachment or bracken invasion within the upper-

Thukela catchment, nor any other site. A possibility could be parameter uncertainty as until recently no observed evapotranspiration values existed for the two vegetation types from which parameters could be derived. The recent observational studies conducted within Cathedral Peak research catchments (Gray et al., 2021a, b, c) which are nested within the upper-Thukela catchment, provided a base on which to select and develop parameters, offering a suitable representation of the vegetation behaviour within the hydrological model. The understanding from the observation at the small-scale showed that the change in land cover from the baseline grassland had a significant impact on the water balance of a small catchment (Gray et al., 2021c). But changes in land cover at a small scale can have a significant effect, but be diluted within a bigger watershed (Dey and Misha, 2017). It is therefore important to scale up the findings within the smaller catchments and understand the impact, at the larger scale on the water resources from this important region. This approach does come with an associated level of uncertainty (Bloschl and Sivapalan, 1995).

The aim of this study was therefore to understand the impacts of degradation related land cover change on the hydrology of the upper-Thukela catchment. Furthermore, an objective was to confirm the ACRU agrohydrological models ability to adequately simulate the streamflow for the catchment using observed data to drive the vegetation and hydrological parameter selection prior to undertaking degraded land cover scenario analyses to determine the effects on the supply of water from this strategic water source area.

5.2. Materials and Methods

5.2.1 ACRU hydrological model

The ACRU agrohydrological model (Schulze, 1995; Figure 5.1) is a physical conceptual model which was developed in the 1970s by the Agricultural Catchments Research Unit (ACRU) in the former School of Bioresources Engineering and Environmental Hydrology at the University of KwaZulu-Natal, South Africa (Schulze, 1995; Warburton et al., 2010). The ACRU model uses a daily time step and requires daily rainfall and air temperature values as a minimum climate data input to drive the hydrological processes (Schulze, 1995). As the model has been developed around a multi-layer soil water budgeting structure, and close to a total evaporation model, the model is sensitive to climate and land cover, as well as the changes thereof (Smithers and Schulze, 2004) and their impact on hydrology (Aduah et al., 2017). The ACRU model is not a parameter fitted model, rather consists of variables which are based on the physical catchment characteristics (Schulze, 1995; Warburton et al., 2010; Aduah et al., 2017). The

model can be used in lumped mode for small, uniform catchments or in distributed mode for larger catchment with varying soils and land cover characteristics (Aduah et al., 2017). In distributed mode, hydrological response units (HRU) and sub-catchments are created to represent individual land uses/covers (Schulze, 1995) allowing for the spatial variability of rainfall, land cover and soil characteristics to be accounted for (Schulze, 1995).

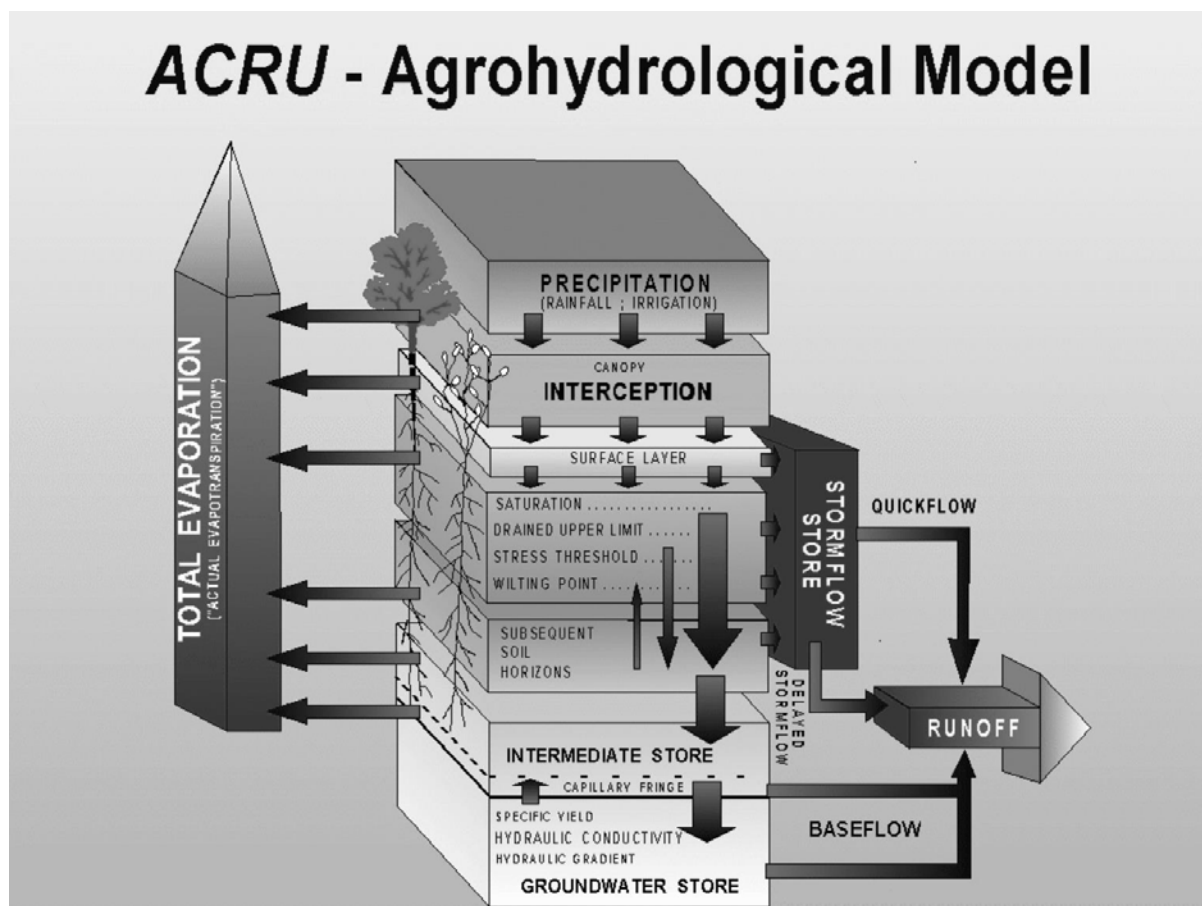


Figure 5.1: Flow diagram of the representation of the water budget in the ACRU model (Schulze, 1995).

The way ACRU represents vegetation, and through manipulation of parameters by the user, land cover change, is important for this study. The ACRU model represents land cover through three processes, canopy interception, total evaporation and soil water extraction via plant roots (Warburton et al., 2010). Of these three processes, evapotranspiration is expected to be the largest point of change within this study. Total evaporation is considered in the ACRU model as both soil water evaporation and transpiration from vegetation, which is determined by rooting patterns (Schulze, 1995). The ACRU model allows for these two components to be lumped or considered separately (Warburton et al., 2010). The vegetation parameters required as monthly

inputs to the model are the percentage of active roots in the A-horizon of the soil, crop coefficients (k_c), leaf area index and canopy interception losses (Schulze, 1995), and they determine the behaviour of the soil water component. The model considers two upper soil horizons where abstraction takes place simultaneously, as determined by root distribution (Warburton et al., 2010).

5.2.2 Catchment description

Within South Africa, the hierarchy for the division of catchments for planning and water management, spans from primary as the largest catchment delineation to quaternary as the smallest, as endorsed by the Department of Water and Sanitation (DWS). The catchment considered for this study (Figure 5.2) covered two quaternary catchments (V11G and V11H) located in the upper reaches of the Tugela (primary V) river catchment in KwaZulu-Natal, South Africa. The catchment, referred to as the upper-uThukela catchment (466 km²) in this study, falls within the Northern Drakensberg strategic water source area (Le Maitre et al., 2018) and summer rainfall region of South Africa. The headwaters of the catchment are on the Lesotho escarpment at a high altitude (3 378 m.a.s.l) with steep topography. The catchment drains into Driel Dam at a lower altitude (1 134 m.a.s.l) with flatter terrain. Driel dam, in combination with the larger Woodstock dam, flows into Spioenkop dam. These three dams form the lower part of the Drakensberg pumped water scheme, which is responsible for the transfer of water to Gauteng province, the economic hub of South Africa, as well as providing an important source of peak electricity through hydroelectric power (Eskom, 2021).

The upper-uThukela catchment has a strong precipitation and temperature gradient linked to the changing topography (Figure 5.2), with a mean annual precipitation (MAP) of 1 205 mm and mean annual temperature of 14 °C near the escarpment, to 746 mm and 17 °C at the catchment outlet. The upper areas of the catchment fall within the Maloti-Drakensberg park, a protected, world heritage site under the management of Ezemvelo KZN Wildlife. Outside the protected areas, the main land use within the catchment is rural homesteads interspersed with subsistence agriculture. Towards the catchment outlet, near the town of Bergville, the occurrence of commercial agriculture increases (Figure 5.3). There is a heavy dependence on the natural resource base by those living in the catchment, as well as a national dependence through the hydroelectricity and pump storage scheme. Years of over-grazing and inappropriate land management practices have heavily degraded parts of the catchment outside of the protected areas (Yalew et al., 2018).

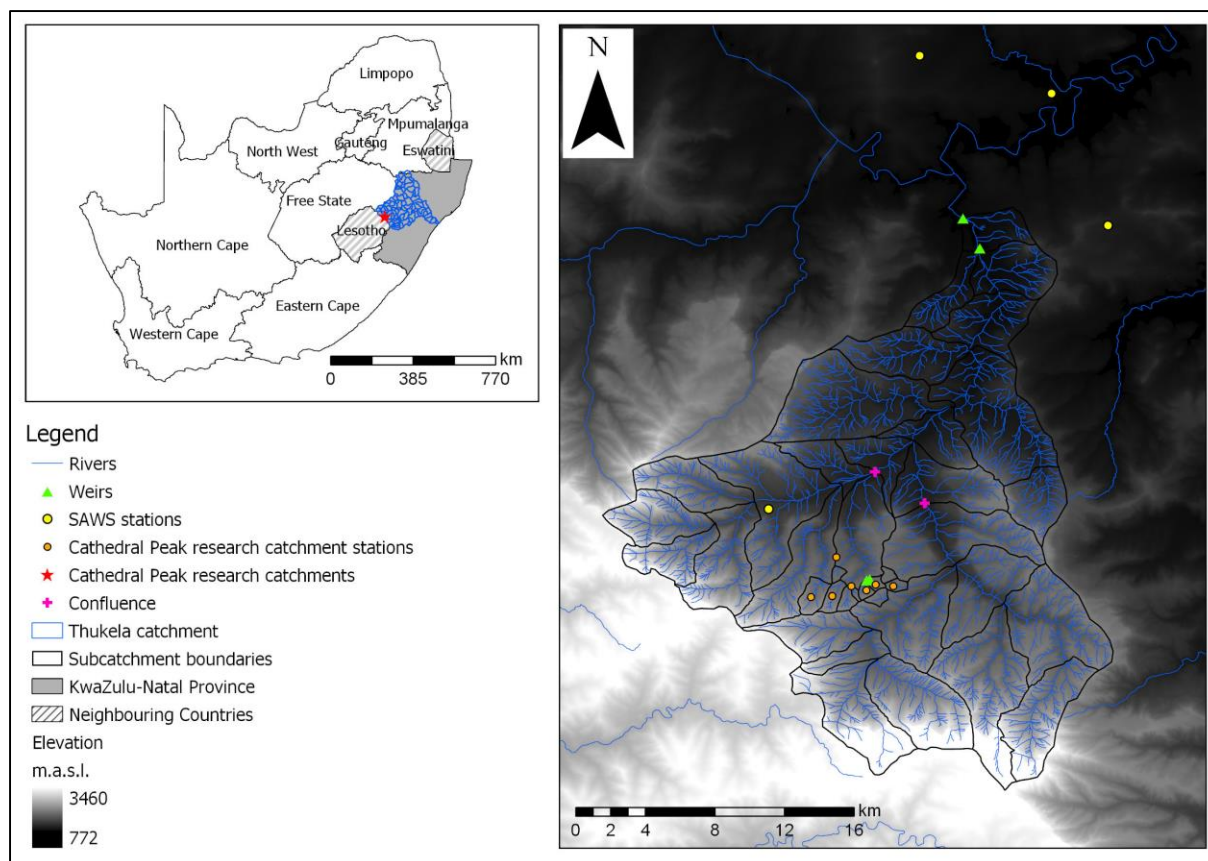


Figure 5.2: The location and layout of the upper-uThukela catchment area with climate stations and streamflow gauging weirs indicated, as well as an illustration of the 39 subcatchments delineated.

The complex socio-ecological challenges with respect to land use practices (eg; value of cattle considered greater than land condition), ecosystem resilience (reduced through pressure from over grazing and climate change), downstream influences and the role of the area in land use-based climate mitigation that are present in this catchment are reflective of many areas in the summer rainfall region of South Africa. A unique aspect of the catchment as compared to others, is that the long-term, intensively monitored Cathedral Peak research catchments fall within the upper areas. The data from the research catchments facilitates hydrological model parameterisation and confirmation of model results. Recent studies on the impacts of bracken invasion and woody encroachment on the water balance of the headwater catchments (Gray et al., 2021c) undertaken in the Cathedral Peak research catchments can be used to derive bracken and woody vegetation parameters for the model, to investigate land cover change impacts which previously have not been determined.

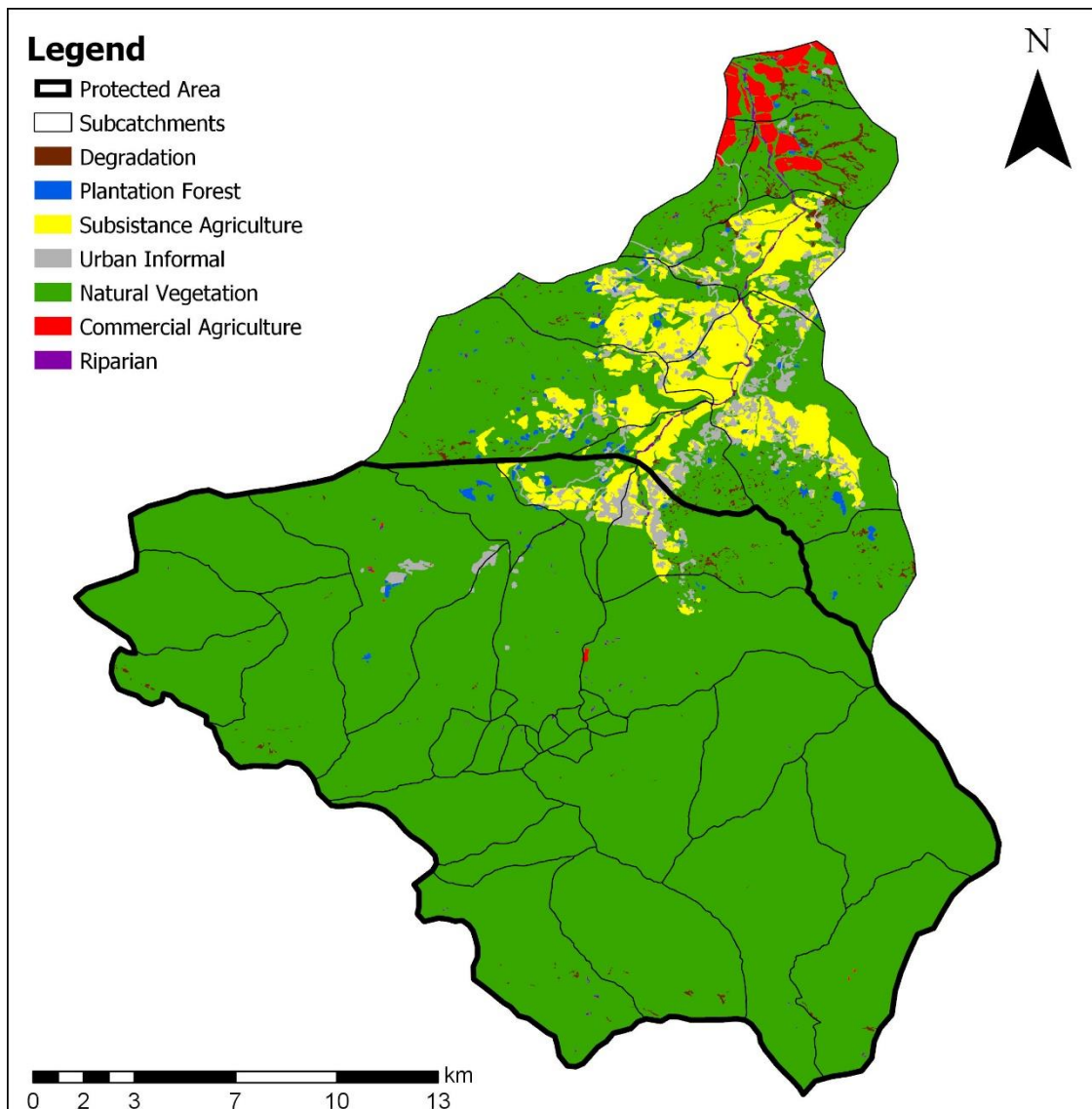


Figure 5.3: The layout of the respective land covers which were used to form the HRU's within the subcatchments.

To account for the land cover present in each catchment, the catchments were further subdivided into land cover HRUs. The land cover classes were derived using the 2017 Ezemvelo KZN Wildlife (EKZNW) land cover classification dataset and grouped into 7 hydrologically similar and relevant land covers as shown in Figure 5.3. The degradation HRU consisted of the following land cover classifications: bare sand, degraded bushland, degraded forest, erosion, degraded grasslands and mines and quarries. The area of each HRU was calculated using Geographic Information System (GIS) analysis. The monthly vegetation model parameters for the degraded, plantation forest, subsistence agriculture, urban informal,

commercial agriculture and riparian area land cover classes were obtained from Schulze (2004). The natural vegetation HRU parameters were obtained from Toucher et al. (2019).

5.2.3 Model configuration and input data sources

5.2.3.1 Delineation and streamflow routing

The quaternary catchments V11G and V11H were further delineated into 39 smaller subcatchments (< 30 km² suitable for ACRU) based on the land cover, altitude and topography using a 5 m Digital Elevation Model (DEM) (sourced from the Maloti-Drakensberg Transfrontier Aerial Mapping Project Data, 2016) as well as monitoring points. These 39 subcatchments (Figure 5.2) were then further divided into hydrological response units (HRU) based on land cover and land use (Figure 5.3). In total, 102 HRUs were determined. The HRUs within each subcatchment were routed to flow into each other as depicted in Figure 5.4, with the routing being representative of the cascading river flow through the catchment.

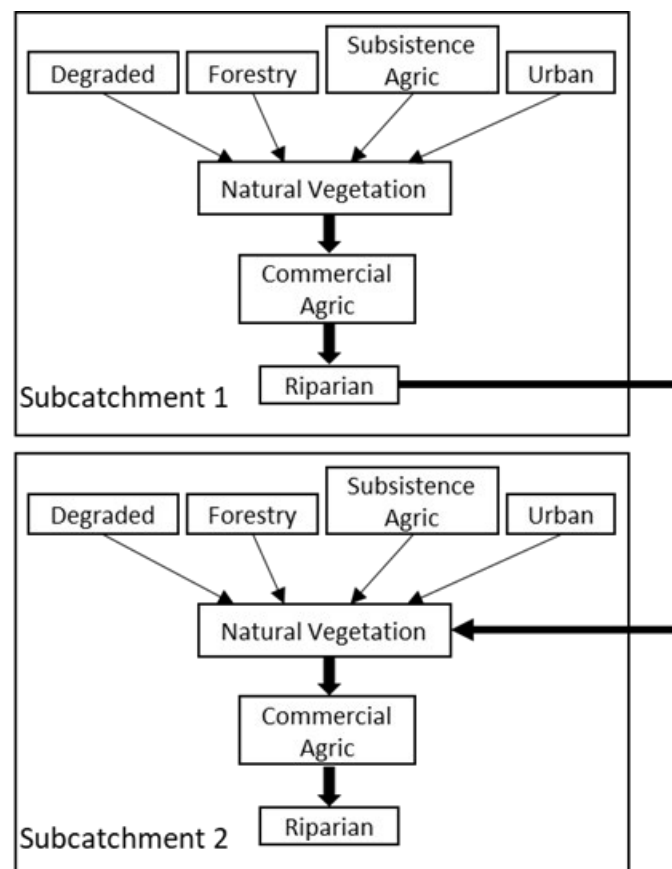


Figure 5.4: The cascading routing structure of Hydrologic Response Units (HRU) for each subcatchment in the ACRU agrohydrological model.

5.2.3.2 Dams and Irrigation

Within the catchment, based on the 2017 EKZ_{NW} land cover classification and verified from satellite imagery, 15 dams were identified. The surface area of these dams was determined from the 2017 EKZ_{NW} land cover map and used to calculate the capacity of the dams using the algorithm developed by Tarboton and Schulze (1992). As suggested by Schulze (1995), seepage from the dam was assumed to be equal to 1/1500 of the dam's capacity and, as no environmental flow estimates were available, environmental flows were assumed to be equal to seepage.

Commercial irrigated areas were also identified from the 2017 EKZ_{NW} land cover map. As the form of irrigation is mainly centre pivots, the irrigation schedule was set to 20 mm applied in a fixed 7-day cycle, with the cycle interrupted only after 20 mm of rain on a given day. Spray evaporation and wind drift losses were input at 12 % and conveyance losses at 10 % following typical values summarised by Smithers and Schulze (2004).

5.2.3.3 Climate Data

The ACRU hydrological model requires daily rainfall, air temperature and daily reference evaporation (which can be substituted for by daily maximum and minimum temperature) (Warburton et al., 2010). Daily rainfall, maximum and minimum air temperature data were sourced from South African Environmental Observation Network (SAEON) for the Cathedral Peak research catchments and the South African Weather Service (SAWS) (Figure 5.2; and detailed in Appendix 5A). Daily rainfall from the Lynch (2004) rainfall database was used to patch missing records where necessary. For stations where air temperature data were unavailable, daily maximum and minimum air temperatures were calculated following the methodology outlined by Schulze and Maharaj (2004), and applying a monthly lapse rate correction factor to the Mikes Pass Meteorological station air temperatures. For each subcatchment, a representative rainfall station was identified and assigned based on proximity, altitude, MAP, data availability and reliability. To improve the spatial rainfall representation of the point raingauge, a monthly rainfall correction factor derived from surfaces of gridded monthly rainfall was applied as per the recommendation in Schulze (1995). As daily A-pan evaporation values were not available, the Hargreaves and Samani (1985) daily A-pan equivalent reference evaporation equation, which is an option in the ACRU model and only requires daily maximum and minimum air temperatures as inputs, was used to estimate daily values.

5.2.3.4 Soils data

The ACRU model operates with surface layer characteristics and a topsoil and subsoil layer. Subsurface processes in the form of capillary movement and saturated drainage are also accounted for in the model (Schulze, 1995). Thus, information is required on the depths and soil water contents at the soil's permanent wilting point, field capacity and saturation for both the topsoil and subsoil. Furthermore, the model requires information on the fraction of 'saturated' soil water (above field capacity) to be redistributed daily from the topsoil to the subsoil, and from the subsoil into the intermediate/groundwater store (Schulze, 1995). Values for these variables for each subcatchment were obtained from the electronic data accompanying the "South African Atlas of Climatology and Agrohydrology" (Schulze et al., 2008). Adjustments to the soil horizon depths obtained from the Atlas for the higher altitude, steeper subcatchment based on the physical understanding gained from the Cathedral Peak research catchments were made.

5.2.3.5 Streamflow parameters

In the ACRU model, streamflow response variables are used to govern the portion of generated stormflow exiting a catchment on a particular day, and the portion of baseflow originating from the groundwater store, which contributes to streamflow. The groundwater store contribution to baseflow was set as 0.9 % of the available groundwater as this is representative of the contribution found within southern African catchments (Schulze et al., 2004; Warburton et al., 2010). The portion of stormflow to leave the catchment on the same day as the rainfall event, was set between 28 - 32 % dependent on the catchment topography with the stormflow response assumed to occur at the depth of A-horizon (Schulze, 1995). The coefficient of initial abstraction is a variable in ACRU which is used to estimate the rainfall abstracted by soil surface interception, detention surface storage and initial infiltration before stormflow commences (Schulze, 1995). This value varies from month-to-month and differs according to land use, soil surface conditions and typical seasonal rainfall intensity characteristics (Schulze, 2004) and ranged from 0.15 to 0.30. Due to the cascading nature of the routing structure in the ACRU model, streamflow is a representation of the runoff generated within a specific catchment, combined with the runoff from all upstream catchments (Aduah et al., 2017).

5.2.4 Confirmation of ACRU model results

A confirmation of the model outputs was conducted, as opposed to a calibration and verification. A confirmation demonstrates the model's ability to represent conditions within the upper-uThukela catchment following configuration which utilised available land use/cover and

soil datasets, as well as applying observation and experience derived parameters. Confirmation studies were undertaken at two scales, a small headwater subcatchment (Cathedral Peak research catchment CPVI, weir V1H022) and then at the catchment outlet (weir V1H004). The period for which the observed and simulated flows were compared was 1972 to 1985 for CPVI, and 1962 to 1975 for the outlet.

For this study, objectives for an adequate simulation were set at: (i) the percentage difference between the mean observed and mean simulated streamflow should not be greater than 15 %, (ii) the Nash-Sutcliffe model efficiency (NSE) should be greater than 0.50, and the coefficient of determination (R^2) should be greater than 0.60 (Awotwi et al., 2015, Aduah et al., 2017).

5.2.5 Land cover scenarios

The two main land cover change scenarios considered were those of bracken invasion and woody encroachment. The influence of bracken invasion and woody encroachment at a catchment scale is unknown, thus this research explored the potential impacts through hydrological modelling. A worst-case scenario of both land cover changes was considered being 100 % change of natural areas. In addition, thresholds or tipping points where the impacts occurred from 75, 50, and 25 % change of natural vegetation areas were considered. The scenarios were compared to the simulated streamflow under current land cover. A further aspect considered was the location of the change of land cover and the impact. Scenarios comparing the 100 % land cover change within the headwaters only, the lower catchments only, and outside the protected areas only were also considered.

5.2.5.1 Parameterisation of land cover scenarios

When undertaking the scenarios, all parameters were held constant following the confirmation studies except for those representing the vegetation changes. The vegetation parameters changed to represent the land cover scenarios were the crop coefficient (k_c), the portion of active roots within the A-horizon (referred to as ROOTA) and percentage of surface cover (referred to as PCSUCO). The monthly parameters used are shown in Table 5.1. Monthly parameters for the bracken invasion and woody encroachment scenarios (Table 5.1) were derived from observational studies conducted within the Cathedral Peak research catchments (Gray et al., 2021b, c). The k_c parameters were calculated directly from observed monthly ET estimates. The ROOTA parameters were assessed based on the monthly activity indicated by the k_c values, the MAP and the soil horizon depth. The PCSUCO parameter was calculated as a factor of

monthly k_c using a sigmoidal relationship between PCSUCO and k_c as conducted by Schulze (2004).

Table 5.1: The monthly parameters used for the ACRU model in simulation of 100 % bracken invasion and Woody encroachment.

Parameter	Bracken invasion			Woody encroachment		
	k_c	ROOTA	PSCUCO	k_c	ROOTA	PSCUCO
JAN	0.75	0.83	81.4	0.74	0.78	80.3
FEB	0.75	0.83	81.8	0.81	0.78	92.4
MAR	0.70	0.83	73.3	0.78	0.78	87.4
APR	0.70	0.83	72.7	0.75	0.78	83.0
MAY	0.50	0.83	38.5	0.54	0.78	44.2
JUN	0.44	0.95	27.0	0.46	0.78	31.5
JUL	0.38	1.00	18.0	0.41	0.78	20.9
AUG	0.52	0.95	41.1	0.50	0.78	37.1
SEP	0.61	0.90	57.9	0.59	0.78	54.4
OCT	0.72	0.83	77.3	0.67	0.78	68.0
NOV	0.69	0.83	71.9	0.77	0.78	85.1
DEC	0.70	0.83	73.3	0.72	0.78	76.6

5.2.5.2 Analysis of ACRU model simulated streamflows under the scenarios using IHA software and parameters

The Indicators of Hydrologic Alteration (IHA) is a software tool used to understand anthropogenic hydrologic alteration using streamflow data (Richter et al., 1996; The Nature Conservancy, 2009). The IHA approach has been used in several studies to identify the impacts of anthropogenic activity on streamflow using observation (Mathews and Richter, 2007; Leach et al., 2015) and modelled (Gao et al., 2009; Kim et al., 2011; Kusangaya et al., 2018; Lopez-Ballesteros et al., 2020) datasets. For this study the group 1 and group 2 IHA parameters were considered. These parameters are based on characterising the hydrological characteristics of magnitude of monthly water conditions (Group 1), and magnitude and duration of annual extreme water conditions (Group 2) (Richter et al., 1996; The Nature Conservancy, 2009). A comparison of two periods was conducted. The baseline model simulation of streamflow under the current catchment conditions was used as the pre-impact period. The scenario simulation of streamflow under 100 % land cover change by bracken invasion, and then alternatively by woody encroachment, were used respectively as the post-impact periods. This was conducted for the full time series from 1962 to 2019. The IHA software was then used to identify the significance of the difference in the pre- and post-impact periods. Three sites were used to assess the significance, the first two at significant confluences in the upper catchment (Figure

5.2) representing the catchment headwater areas and the last the catchment outlet. For the parameters, significant counts (SC) were considered, which provide an indication of whether there is a significant difference between the baseline streamflow and the land cover change streamflow. The SC can be treated in a similar manner to a p -value (The Nature Conservancy, 2009) and therefore any SC lower than 0.1 was considered to indicate a significant difference.

5.3. Results

5.3.1 Confirmation studies

To have confidence in the ACRU model's ability to simulate the streamflow responses from the upper-uThukela, comparisons between simulated and observed streamflow were made at two scales. The model was run for the full period 1960 – 2019, however the period used for the confirmation study was determined by the availability of gauged data at the two scales. At the small scale, a confirmation was conducted for one of the Cathedral Peak research catchments (CPVI), a natural grassland catchment, for the period 1 October 1972 to 30 September 1985. At the large scale, comparison between observed and simulated streamflow was made at the catchment outlet for the period 1 October 1962 to 30 September 1975.

The statistics of performance of the ACRU model at both scales showed a satisfactory simulation of the observed data as shown by the mean (CPVI = 15 %; Outlet = 8.1 %), the NSE (CPVI = 0.52; Outlet = 0.82) and the R^2 (CPVI = 0.64; Outlet = 0.83) values (Table 5.2). At both scales the simulation was considered adequate as the statistics fell within the objectives outlined above.

Table 5.2: Statistics of performance from the ACRU model between observed and simulated streamflows for subcatchment CPIV and the upper-uThukela catchment (outlet)

Statistics	CPVI (1972 – 1985)	Catchment outlet (1962 – 1975)
Total Observed flows (mm)	9643.61	5876.15
Total simulated flows (mm)	8136.66	6353.06
Average error in flows (mm/month)	-9.66	3.06
Mean observed flows (mm/month)	61.82	37.67
Mean simulated flows (mm/month)	52.16	40.73
% Difference between means	15.63	-8.12
Std. deviation of observed flows (mm)	59.32	46.80
Std. deviation of simulated flows (mm)	65.06	45.43
% Difference between standard deviations	-9.66	2.94
Coefficient of determination (R^2)	0.64	0.83
Nash Sutcliffe efficiency (NSE)	0.52	0.82

With confidence in the ability of the ACRU model to simulate the upper-uThukela catchment under current land cover established, the focus shifted to determining the impacts of land cover scenarios of woody encroachment and bracken invasion on the streamflow responses of the catchment.

5.3.2 Bracken invasion scenario results

The streamflow simulated under current landcover, was initially compared to the streamflow simulated under bracken invasion scenarios of 25 %, 50 % and 100 % of the natural vegetation HRUs. The catchment outlet was the focus for the initial analysis, as changes at the catchment outlet provide an indication of the integrated impacts of land cover change on the water supply generated from this catchment area. The mean annual streamflow was found to reduce as the percentage of invasion increased. At the catchment outlet, this reduction was from a mean annual accumulated streamflow of 419 mm under current land cover, to 402 mm under 100 % bracken invasion equating to a 4 % reduction in mean annual streamflow. Relative changes in mean annual streamflow, the mean streamflow of the driest three months (June, July, August) and mean streamflow of the three wettest months (December, January, February) accumulated through the catchment were considered (Figure 5.5). A further consideration within the catchment, is the distinctive feature related to the contrast between the protected and non-protected area. This is also a distinctive separation between the high-lying catchments and the low-lying catchments. The largest changes in mean annual streamflow could be seen in the

headwater catchments, which accounted for reductions in mean annual accumulated streamflow in excess of 5 %. In the dry period, the number of subcatchments showing reductions in mean streamflow exceeding 5 % increases and includes lower land subcatchments beyond the protected area including the outlet subcatchment. The largest reduction was determined as 9 % for a headwater subcatchment. For the wet period, only headwater subcatchments show reductions in mean streamflow in excess of 5 %, with the largest reduction determined as 7.3 %.

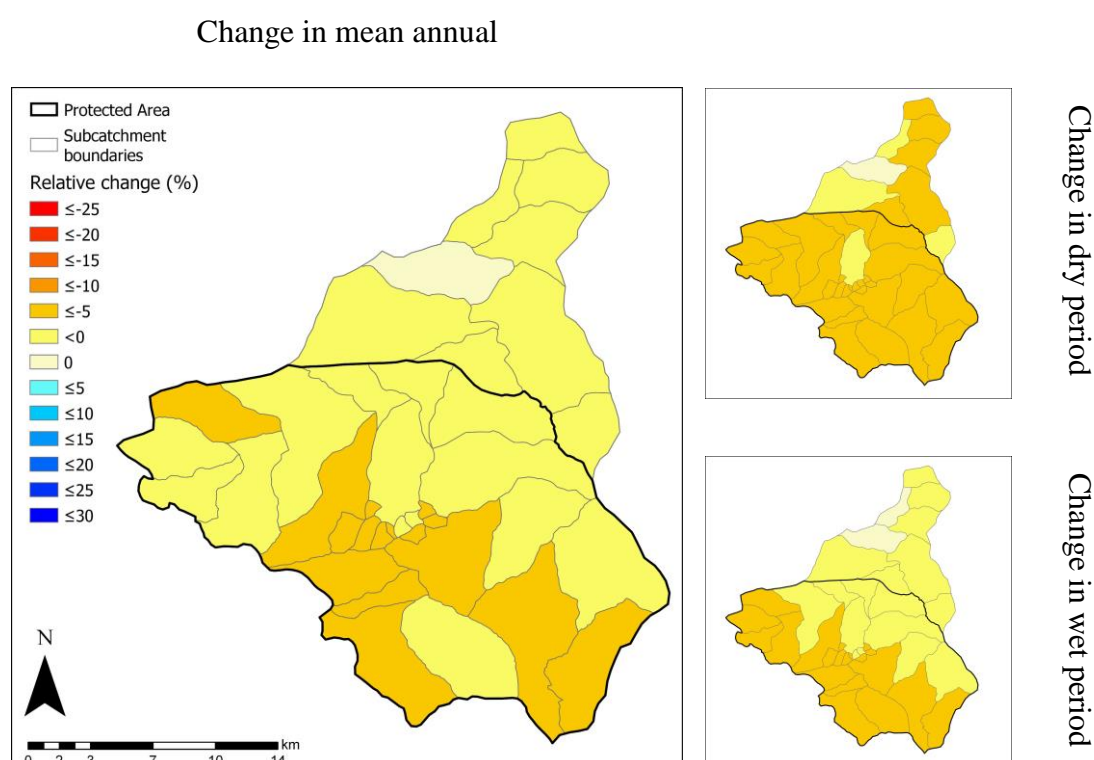


Figure 5.5: The relative change per subcatchment for the mean annual, mean of the three driest months (June, July, August) and mean of the three wettest months (December, January, February) streamflows following 100 % bracken invasion.

Thereafter, analysis on the impacts on average annual, winter (June, July, August), and summer (December, January, February) flows under current land cover and 100 % invasion of natural HRU for the extremes of 1 in 10 dry year, and 1 in 10 wet year were considered (Figure 5.6). A clear pattern across all conditions is that changes are larger and more noticeable and larger within the headwater subcatchments and protected area. This pattern is especially evident during the 1:10 year dry period and the winter months, where the majority of headwater subcatchments experience reductions exceeding 5 %. Toward the outlet of the catchment,

reductions in streamflow were not as large. Changes at the catchment outlet only exceeded a 5 % reduction in streamflow during winter of the 1 in 10 dry year, where a reduction in streamflow of 16 % resulted. The largest reduction in streamflow occurred during the winter period of the 1 in 10 dry year, where a 24 % reduction occurred in a small headwater subcatchment. For the 1 in 10 wet year, streamflow reductions of greater than 10 % only occur within the high headwater subcatchments at the annual scale, with this extending to the majority of headwater subcatchments for the winter months. During the summer months, only eight subcatchments which are all in the headwaters, exceed 5 % reductions in streamflow.

Having identified that reductions in streamflow occur following bracken invasion and result in a varied impact on different seasonal flow periods, the IHA software was used to analyse the significance of the reduction in streamflow identified between the 100 % bracken invasion and current landcover scenario. Under bracken invasion, no significant differences between the baseline and the 100 % bracken invasion were found in the IHA Group 2 hydrological parameters (Table 5.3).

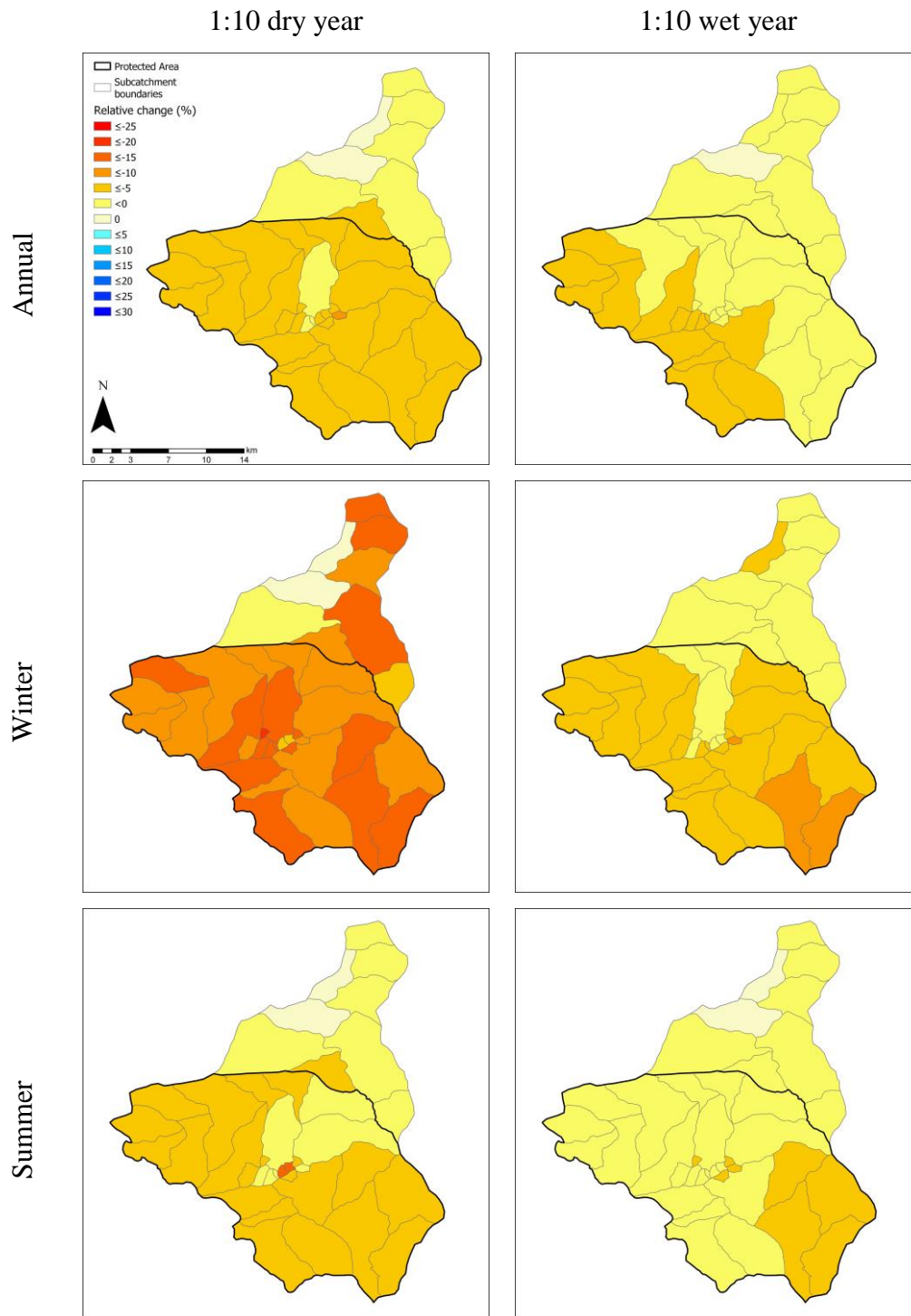


Figure 5.6: The relative change in streamflow following 100 % bracken invasion of each subcatchment for the 1:10 dry and 1:10 year wet periods, annual, winter months (June, July, August), and summer months (December, January, February).

Table 5.3: The significant counts (SC) determined for Group 2 parameters using the Indicator of Hydrologic Alteration (IHA) software for comparison of the simulated baseline streamflow and 100 % bracken invasion land cover change streamflow at three separate locations within the focus catchment.

	Confluence 1 SC	Confluence 2 SC	Outlet SC
1-day minimum	0.32	0.34	0.35
3-day minimum	0.38	0.34	0.59
7-day minimum	0.34	0.33	0.39
30-day minimum	0.23	0.59	0.32
90-day minimum	0.58	0.41	0.57
1-day maximum	0.89	0.92	0.89
3-day maximum	0.88	0.91	0.84
7-day maximum	0.93	0.84	0.88
30-day maximum	0.85	0.82	0.90
90-day maximum	0.67	0.78	0.82
Base flow index	0.50	0.47	0.46

5.3.3 Woody encroachment scenario results

As with the bracken invasion, streamflow simulated under current landcover was initially compared to the streamflow simulated under woody encroachment scenarios with 25 %, 50 % and 100 % natural vegetation HRUs. Again, the catchment outlet was the focus of this initial analysis. Similar to the bracken scenarios, the most noticeable reductions in streamflow occurred at the 100 % encroachment level. Under current conditions, the mean annual streamflow was 419 mm, which reduced to 398 mm under 100 % woody encroachment. This equated to a 5 % reduction in mean annual streamflow.

The most noticeable changes were within the protected headwater subcatchments, where reductions in mean annual, winter and summer streamflow more than 5 % occurred (Figure 5.7). The largest reductions in accumulated mean streamflow were evident for the winter dry period, where eight headwater subcatchments showed reductions in streamflow in excess of 10 % with largest reduction being 13 %. For the winter dry period, reductions in streamflow were evident throughout the catchment, including the catchment outlet, unlike for mean annual and summer flows.

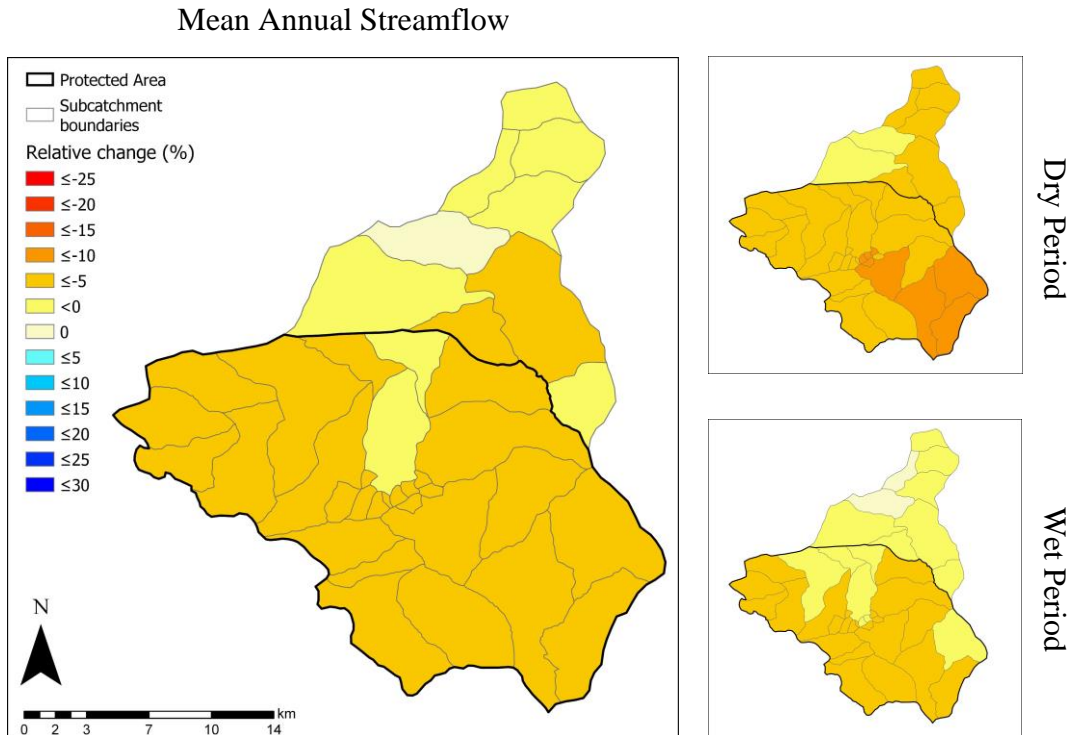


Figure 5.7: The relative change per subcatchment for the mean annual, mean of the three driest months (June, July, August) and mean of the three wettest months (December, January, February) streamflows following 100 % woody encroachment.

Again, the impact of changes within the protected headwater catchment was noticeable compared to the smaller changes in the lowland catchments (Figure 5.8). That the largest reductions in accumulated streamflow occurred for the 1 in 10 dry year, particularly in the winter period where the majority of the subcatchments showed reductions in streamflow in excess of 10 % with the greatest reduction being 28 %. Notable was the 23 % reduction in the winter 1:10 dry year flows at the catchment outlet.

For the 1 in 10 wet year, only a few of the extreme headwater subcatchments had reductions in excess of 5 % in annual summer accumulated streamflow (Figure 5.8). Greater reductions in the 1:10 wet year flows during winter months were evident, with reductions in excess of 10 % occurring in five headwater catchments as well as the reductions occurring in lowland catchments unlike at the annual time scale and summer flow period.

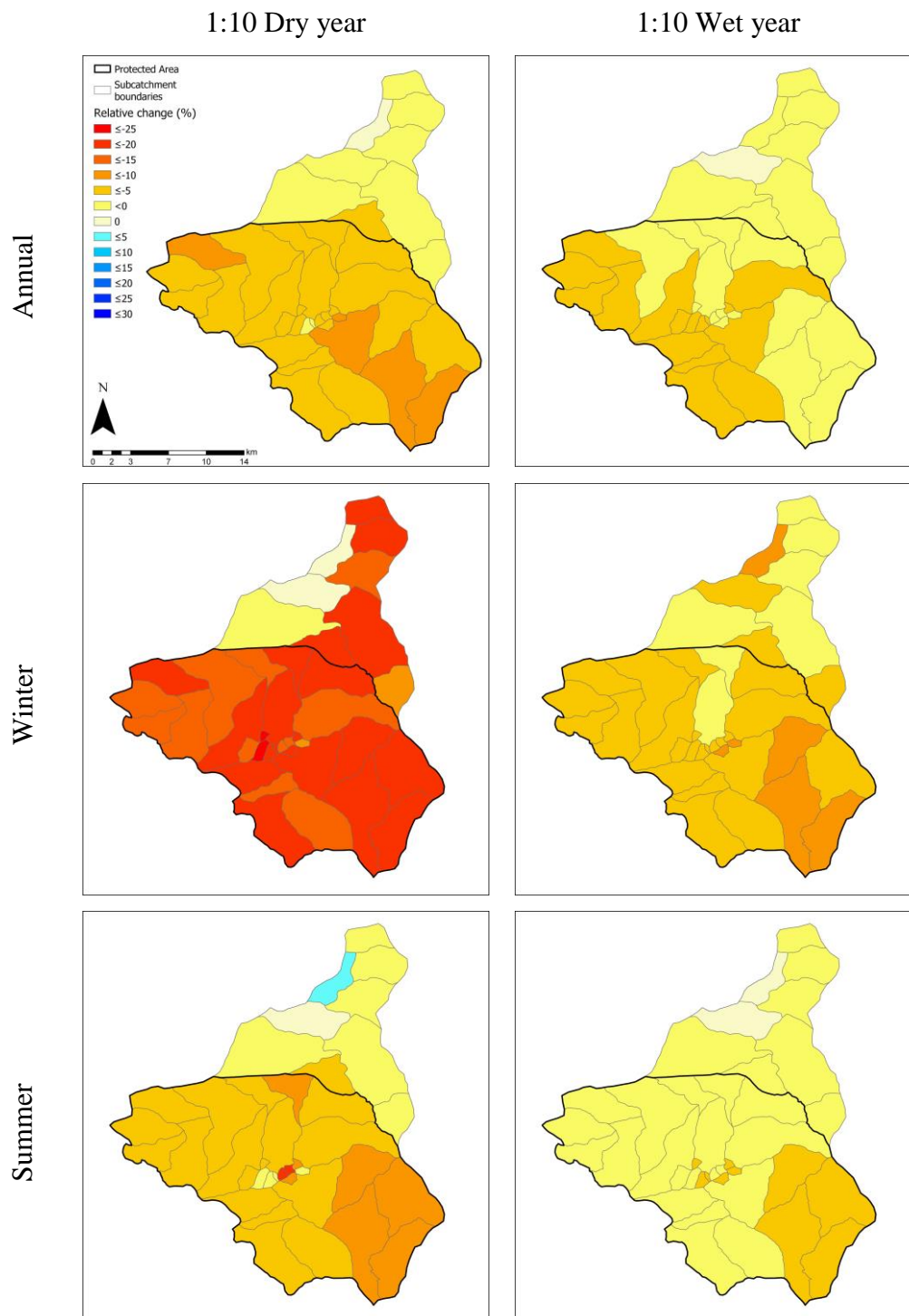


Figure 5.8: The relative change in streamflow following 100 % woody encroachment of each subcatchment for the 1:10 dry and 1:10 year wet periods, annual, winter months (June, July, August), and summer months (December, January, February).

Unlike under bracken, significant changes in the low flow Group 2 IHA hydrological parameters were found under woody encroachment relative to current land cover (Table 5.4). At Confluence 1, a significant difference was identified for both 1-day minimum flows as well as 3-day minimum flows. At Confluence 2, a significant difference in the 7-day minimum flows was identified. At the catchment outlet, a significant difference in the 30-day minimum flows was identified. No significant impact was found for the high flow group 2 parameters.

Table 5.4: The significant counts (SC) determined for the Group 2 hydrological parameters using the Indicator of Hydrologic Alteration (IHA) software for comparison of the simulated baseline streamflow and 100 % woody encroachment land cover change streamflow at three separate locations within the focus catchment.

	Confluence 1	Confluence 2	Outlet
	SC	SC	SC
1-day minimum	0.03	0.27	0.28
3-day minimum	0.06	0.22	0.50
7-day minimum	0.11	0.10	0.16
30-day minimum	0.15	0.20	0.09
90-day minimum	0.34	0.31	0.47
1-day maximum	0.98	0.94	0.91
3-day maximum	0.81	0.91	0.85
7-day maximum	0.91	0.87	0.88
30-day maximum	0.96	0.74	0.91
90-day maximum	0.86	0.74	0.78
Base flow index	0.65	0.21	0.26

5.4. Discussion

The ACRU hydrological model was found to have the ability to simulate the current land cover within the upper-uThukela catchment to a satisfactory level, as it fell within the objectives set for a satisfactory simulation (Awotwi et al., 2015). This gave confidence in using the model and the configuration for the catchment to undertake scenarios of land cover change.

Bracken invasion and woody encroachment were found to reduce the streamflow generated by the upper-Thukela catchment, with woody encroachment having a larger impact. The changes in streamflow were most noticeable in the protected headwater catchments, as well as during the winter dry period low flows and 1:10 year low flows. The greater reduction in streamflow under woody encroachment than under bracken invasion, are attributed to the higher evapotranspiration (ET) of woody encroachment which is maintained year-round relative to the bracken and grassland which senesce during the winter months (Gray et al., 2021b).

Furthermore, the woody encroachment has a greater surface cover and deeper roots than the bracken and grassland. The vegetation parameters used in the ACRU model for the bracken and woody vegetation were derived from in-situ ET measurements, thus are reflective of the higher ET patterns observed for woody vegetation.

Headwater catchments, such as the upper-uThukela, are invaluable for generating streamflow, thus any change in their land cover that impacts on their streamflow affects downstream users and ecosystems. Even within the upper-uThukela, the headwater catchments due to their protected status were shown to be more sensitive to change. Streamflow leaving the catchment area is of great importance as this water flows into the Drakensberg pumped water scheme storage for electricity production as well as transferring water to Gauteng province. Beyond this, the catchment contributes to the water required for irrigation and the urban supply to towns in the greater Thukela catchment. Changes in the catchments' water production capacity could have far reaching implications, impacting a large downstream area in terms of water supply and national electricity supply. In particular, the headwater catchments of the Thukela catchment are crucial to sustain river flows to downstream areas during the dry, winter months as the Drakensberg mountains store significant water. Thus, the demonstrated changes woody encroachment and, to lesser extent, bracken invasion would have on dry, winter low flow periods is of particular concern.

Under woody encroachment, within the western headwater catchments, significant impacts on low flows were found for the 1-day and 3-day minimum flows, and for the eastern headwater a significant change in 7-day minimum flows. Whereas at the catchment's outlet a significant change in the 30-day minimum flows was found indicating the extent of buffering of change moving down through the catchment. The significant changes in low flows could be attributed to the difference in the ET between the natural grassland vegetation and the woody vegetation being greatest during the dry months, when the natural grassland of the region is dormant (Gray et al., 2021b). During this period, ET is still observed over the bracken vegetation, although at a reduced rate, while the woody vegetation showed a continued ET rate greater than bracken and the natural grassland, due to the evergreen nature of the woody vegetation (Gray et al., 2021c). As these aspects were represented within the parameterisation of the model, it would be an outcome from the simulation. Due to this difference, the change in land cover driven either by bracken invasion or woody encroachment was expected to impact the low flows and has been well represented within the scenario simulations.

However, despite the crop coefficients used being determined from observed ET estimates, the monthly ET simulated by the ACRU model was an under representation of monthly ET measured over the bracken and woody vegetation types by Gray et al. (2021b, c). Following the use of the k_c values for bracken and woody vegetation, it was found that the mean annual ET output from the ACRU model was below that observed by Gray et al. (2021b, c). How the conceptualisation of soil water availability or plant stress are likely to have contributed to this as they limit the vegetation's ability to transpire within the model could contribute to this underestimation. The objective of this study was to simulate the respective land cover changes using parameters derived from observations, and improvement of the model's mechanisms for simulating the change was beyond the scope.

In the South African context, the results from this study indicated the importance of protecting headwater catchments and added further weight to the importance of ensuring the protection of strategic water source areas have been identified as important areas which require protection (Le Maitre et al., 2018). Currently, approximately 11 % of strategic water source areas fall within a protected area, of which the majority are within the protected mountain areas of the Western Cape, and the Kwazulu-Natal and Mpumalanga Drakensberg (Le Maitre et al., 2018). This is driven partly by the Mountain Catchment Areas Act, which supports the conservation and management of mountainous water catchments (Le Maitre et al., 2018). The protected areas were shown to be sensitive to changes in land cover. Whereas, due to the extent of land cover change which has already occurred outside of the protected (as illustrated in Figure 5.3), through human activities such as overgrazing and subsistence and commercial agriculture (Blignaut et al., 2010; Grab and Knight, 2018), streamflow responses were not as sensitive to further change through the degradation scenarios simulated. From this scenario analysis, it has been shown the key importance to preventing land cover change. Allowing the protected areas to change partially, has as much impact as allowing entire areas of the downstream catchment to change. By maintaining the headwater catchments, despite increasing land cover change within the lower reaches, which can only be expected to increase over time, the impact on streamflow may be minimal.

This provides further justification for the protection of headwater catchments within this SWSA. Fortunately, the Maloti-Drakensberg mountain range is a World Heritage site with around 25 000 km² of the area is under protection by Ezemvelo KZN Wildlife. In the light of these findings, there is a good argument for considering the additional 25 000 km² of mountain

range that remains unprotected but part of the headwater catchments (Blignaut et al., 2010; Grab and Knight, 2018).

5.5 Conclusions

Using the ACRU agrohydrological model the current land cover conditions within the upper-uThukela catchment were simulated satisfactorily. The site observation data was critical from which to derive parameters for the woody encroachment and bracken invasion land covers. This in turn allowed for simulations of land cover change scenarios for both forms of land cover degradation to be conducted for the upper-uThukela catchment. The physically based ACRU agrohydrological model and its sensitivity to land cover change was invaluable in running the scenario analysis and determining the hydrological impacts of both forms of land cover degradation. The hydrological impact of woody encroachment and bracken invasion were not static. They were found to vary spatially across the catchment (headwater to outlet) and temporally with the headwater areas and dry low flow periods being the most sensitive to these two forms of land cover degradation. The findings from this larger scale modelling of the upper-Thukela confirm and agree with the findings of from the smaller catchment level observation.

This study provides a clear indication of the importance in maintaining the natural grassland condition within the upper-uThukela catchment, as well as the vital role protection of the grasslands has played already. Management to maintain optimal grassland health such as fire is critical to preserve the important water resources and ecosystem services provided by the Northern-Drakensberg SWSA. Continued protection of these areas is recommended with continued efforts to control and reduce degradation occurring within the protected areas.

5.6 References

- ADUAH MS, JEWITT GPW, and WARBURTON TOUCHER ML (2017) Assessing suitability of the ACRU hydrological model in a rainforest catchment in Ghana, West Africa. *Water Science* **31** 198-214. <http://dx.doi.org/10.1016/j.wsg.2017.06.001>.
- AHN KH and MERWADE V (2017) The effect of land cover change on duration and severity of high and low flows. *Hydrological processes* **31** 133-149. <http://dx.doi.org/10.1002/hyp.10981>.
- ALVARENGA LA, DE MELLO CR, COLOMBO A, CUARTAS LA and BOWLING LC (2016) Assessment of land cover change on the hydrology of a Brazilian head-water watershed using the Distributed Hydrology-Soil-Vegetation Model. *Catena* **143** 7-17. <http://dx.doi.org/10.1016/j.catena.2016.04.001>.

- AWOTWI A, YEBOAH F and KUMI M (2015) Assessing the impact of land cover change on water balance components of White Volta Basin in West Africa. *Water and Environment Journal* **29** 259-267. <http://dx.doi.org/10.1111/wej.12100>.
- BIRKEL C, SOULSBY C and TETZLAFF D (2012) Modelling the impacts of land-cover change on streamflow dynamics of a tropical rainforest headwater catchment. *Hydrological Sciences Journal* **57**(8) 1543-1561. <http://dx.doi.org/10.1080/02626667.2012.728707>.
- BLIGNAUT J, MANDER M, SCHULZE R, HORAN M, DICKENS C, PRINGLE C, MAVUNDLA K, MAHLANGU I, WILSON A, MCKENZIE M and MCKEAN S (2010) Restoring and managing natural capital towards fostering economic development: Evidence from the Drakensberg, South Africa. *Ecological Economics* **69** 1313-1323. <https://dx.doi.org/10.1016/j.ecolecon.2010.01.007>.
- BLOSCHL G and SIVAPALAN M (1995) Scale Issues in Hydrological Modelling: A review. *Hydrological Processes* **9** 251-290. <https://doi.org/0885-6087/95/030251-40>.
- BOONGALING CGK, FAUSTINO-ESLAVA DV and LANSIGAN FP (2018) Modeling land use change impacts on hydrology and the use of landscape metrics as tools for watershed management: The case of an ungauged catchment in the Philippines. *Land Use Policy* **72** 116-128. <https://doi.org/10.1016/j.landusepol.2017.12.042>.
- BURT TP and MCDONNELL JJ (2015) Whither field hydrology? The need for discovery science and outrageous hydrological hypotheses. *Water Resources Research* **51** 5919-5928. <https://doi.org/10.1002/2014WR016839>.
- CAO W, BOWDEN WB, DAVIE T and FENEMOR A (2009) Modelling impacts of land cover change on critical water resources in the Motueka River Catchment, New Zealand. *Water Resources Management* **23** 137-151. <https://doi.org/10.1007/s11269-008-9268-2>.
- DEVI GK, GANASRI BP and DWARAKISH GS (2015) A review on hydrological models. *Aquatic Procedia* **4** 1001-1007. <https://doi.org/10.1016/j.aqpro.2015.02.126>.
- DEY P and MISHRA A (2017) Separating the impacts of climate change and human activities on streamflow: A review of methodologies and critical assumptions. *Journal of Hydrology* **548** 278-290. <https://doi.org/10.1016/j.jhydrol.2017.03.014>.
- EHRET U, GUPTA HV, SIVAPALAN M, WEIJS SV, SCHYMANSKI SJ, BLOSCHL G, GELFAN AN, HARMAN C, KLEIDON A, BOGAARD TA, WANG D, WAGENER T, SCHERER U, ZEHE E, BIERKENS MFP, DI BALDASSARRE G, PARAJKA J, VAN BEEK LPH, VAN GRIENSVEN A, WESTHOFF MC and WINSEMIUS HC (2014) Advancing catchment hydrology to deal with predictions under change. *Hydrology and Earth System Sciences* **18** 649-671. <https://doi.org/10.5194/hess-18-649-2014>.
- ESKOM (2021) Eskom: Drakensberg Pumped Storage Scheme. URL: https://www.eskom.co.za/Whatweredoing/ElectricityGeneration/PowerStations/Pages/Drakensberg_Pumped_Storage_Scheme.aspx (Assessed 27 July 2021).
- FORBES KA, KIENZLE SW, COBURN CA, BYRNE JM and RASMUSSEN J (2011) Simulating the hydrological response to predicted climate change on a watershed in southern Alberta, Canada. *Climate Change* **105** 555-576. <https://doi.org/10.1007/s10584-010-9890-x>.

- GAO Y, VOGEL RM, KROLL CN, LEROY PUFF N and OLDEN JD (2009) Development of representative indicators of hydrologic alteration. *Journal of Hydrology* **374** 163-147. <https://doi.org/10.1016/j.jhydrol.2009.06.009>.
- GASHAW T, TULU T, ARGAW M and WORQLUL AW (2018) Modeling the hydrological impacts of land use/land cover changes in the Andassa watershed, Blue Nile Basin, Ethiopia. *Science of the Total Environment* **619-620** 1394-1408. <https://doi.org/10.1016/j.scitotenv.2017.11.191>.
- GRAB SW and KNIGHT J (2018) Southern African montane environments. In: Southern African Landscapes and Environmental Change. Routledge, United Kingdom.
- GRAY BA, TOUCHER ML, SAVAGE MJ and CLULOW AD (2021a). The potential of surface renewal for determining sensible heat flux for indigenous vegetation for a first-order montane catchment. *Hydrological Sciences Journal* **66(6)** 1015-1027. <https://doi.org/10.1080/02626667.2021.1910268>.
- GRAY BA, TOUCHER ML, SAVAGE MJ and CLULOW AD (2021b) Seasonal evapotranspiration over an invader vegetation (*Pteridium aquilinum*) in a degraded montane grassland using surface renewal. *Submitted to Journal of Hydrology: Regional Studies*.
- GRAY BA, TOUCHER ML, CLULOW AD and SAVAGE MJ (2021c) Impact of land cover change on the water balance of a first-order Afromontane grassland catchment in a strategic water source area. *Submitted to Journal of Hydrology*.
- GUSH MB, SCOTT DF, JEWITT GPW, SCHULZE RE, LUMSDEN TG, HALLOWES LA and GORGENS AHM (2002) Estimation of streamflow reductions resulting from commercial afforestation in South Africa, Water Research Commission, South Africa, Report TT173/02.
- GYAMFI C, NDAMBUKI JM and Salim RW (2016) Hydrological responses to land use/cover changes in the Olifants basin, South Africa. *Water* **8** 1-16. <https://doi.org/10.3390/w8120588>.
- HARGREAVES GH and SAMANI ZA (1985) Reference crop evapotranspiration from temperature. *Applied Engineering in Agriculture* **1(2)** 96-99. <https://doi.org/10.13031/2013.26773>.
- JEWITT GPW, GARRAT JA, CALDER IR and FULLER L (2004) Water resources planning and modelling tools for the assessment of land use change in the Luvuvhu Catchment, South Africa. *Physics and Chemistry of the Earth, Parts A/B/C* **29(15-18)** 1233-1241. <https://doi.org/10.1016/j.pce.2004.09.020>.
- KARLSSON IB, SONNENBORG TO, REFSGAARD JC, TROLLE D, BORGESSEN CD, OLESEN JE, JEPPESEN E and JENSEN KH (2016) Combined effects of climate models, hydrological model structures and land use scenarios on hydrological impacts of climate change. *Journal of Hydrology* **535** 301-317. <https://doi.org/10.1016/j.jhydrol.2016.01.069>.
- KIENZLE SW and SCHMIDT J (2008) Hydrological impacts of irrigated agriculture in the Manuherikia catchment, Otago, New Zealand. *Journal of Hydrology (NZ)* **47(2)** 67-84.

- KIENZLE SW (2010) Effects of area under-estimations of sloped mountain terrain on simulated hydrological behaviour: a case study using the ACRU model. *Hydrological Processes*. <https://doi.org/10.1002/hyp.7886>.
- KIENZLE SW, NEMETH MW, BYRNE JM and MACDONALD RJ (2012) Simulating the hydrological impacts of climate change in the upper North Saskatchewan River basin, Alberta, Canada. *Journal of Hydrology* **412-413** 76-89. <https://doi.org/10.1016/j.hydrol.2011.01.058>.
- KIM BS, KIM BK and KWON HH (2011) Assessment of the impact of climate change on the flow regime of the Han River basin using indicators of hydrologic alteration. *Hydrological Processes* **25** 691-704. <https://doi.org/10.1002/hyp.7856>.
- KIRCHNER JW (2006) Getting the right answers for the right reasons: Linking measurements, analyses, and models to advance the science of hydrology. *Water Resources Research* **42** W03S04. <https://doi.org/10.1029/2005WR004362>.
- KUSANGAYA S, Warburton Toucher ML and Van Garderen EA (2018) Evaluation of uncertainty in capturing the spatial variability and magnitudes of extreme hydrological events for the uMngeni catchment, South Africa. *Journal of Hydrology* **557** 931-946. <https://doi.org/10.1016/j.jhydrol.2018.01.017>.
- LEACH JM, Kornelsen KC, Samuel J and Coulibaly P (2015) Hydrometric network design using streamflow signatures and indicators of hydrologic alteration. *Journal of Hydrology* **529(3)** 1350-1359. <https://doi.org/10.1016/j.hydrol.2015.08.048>.
- Le Maitre DC, Walsdorff A, Cape L, Seyler H, Audouin M, Smith-Adao L, Nel JA, Holland M, Witthuser K, (2018) Strategic Water Source Areas: Management Framework and Implementation Guidelines for Planners and Managers. Water Research Commission, Pretoria, South Africa, Report TT 754/2/18.
- LI KY, COE MT, RAMANKUTTY N and DE JONG R (2007) Modeling the hydrological impact of land-use change in West Africa. *Journal of Hydrology* **337** 258-268. <https://doi.org/10.1016/j.hydrol.2007.01.038>.
- LOPEZ-BALLESTEROS A, SENET-APARICIO J, MARTINEZ C and PEREZ-SANCHEZ J. 2020. Assessment of future hydrologic alteration due to climate change in the Arachthos River basin (NW Greece). *Science of The Total Environment* **733** 139299. <https://doi.org/10.1016/j.scitotenv.2020.139299>.
- LYNCH DS (2004) The development of a Raster Database of Annual, Monthly and Daily Rainfall for Southern Africa, Water Research Commission, Pretoria, South Africa, Report 1156/1/04.
- MATHEWS R and RICHTER BD (2007) Application of the Indicators of Hydrologic Alteration Software in environmental flow setting. *Journal of the American Water Resources Association* **43(6)** 1400-1413. <https://doi.org/10.1111/j.1752-1688.2007.00099.x>
- MUGABE FT, CHITATA T, KASHAIGILI J and CHAGONDA I (2011) Modelling the effect of rainfall variability, land use change and increased reservoir abstraction on surface water resources in semi-arid southern Zimbabwe. *Physics and Chemistry of the Earth* **36** 1025-1032. <https://doi.org/10.1016/j.pce.2011.07.058>.

- QIAO L, ZOU CB, WILL RE and STEBLER E (2015) Calibration of SWAT model for woody plant encroachment using paired experimental watershed data. *Journal of Hydrology* **523** 231-239. <https://doi.org/10.1016/j.jhydrol.2015.01.056>.
- REBELO AJ, LE MAITRE DC, ESLER KJ and COWLING RM (2015) Hydrological responses of a valley-bottom wetland to land-use/land-cover change in a South African catchment: making a case for wetland restoration. *Restoration Ecology* **23(6)** 829-841. <https://doi.org/10.1111/REC.12251>.
- RICHTER BD, BAUMGARTNER JV, POWELL J and BRAUN DP (1996) A Method for Assessing Hydrologic Alteration within Ecosystems. *Conservation Biology* **10(4)** 1163-1174.
- SADDIQUE N, MAHMOOD T and BERNHOFER C (2020) Quantifying the impacts of land use/land cover change on the water balance in the afforested River Basin, Pakistan. *Environmental Earth Sciences* **79** 448. <https://doi.org/10.1007/s12665-020-09206-w>.
- SALEMI LF, GROppo JD, TREVISAN R, DE MORAES JM, DE BARROS FERRAZ SF, VILLANI JP, DUARTE-NETO PJ and MARTINELLI LA (2013) Land-use change in the Atlantic rainforest region: Consequences for the hydrology of small catchments. *Journal of Hydrology* **499** 100-109. <https://dx.doi.org/10.1016/j.jhydrol.2013.06.049>.
- SCHMIDT J, KIENZLE SW and SRINIVASAN MS (2009) Estimating increased evapotranspiration losses caused by irrigated agriculture as part of the water balance of the Orari catchment, Canterbury, New Zealand. *Journal of Hydrology (NZ)* **48(2)** 73-94.
- SCHULZE RE (1995) Hydrology and Agrohydrology: A Text to Accompany the ACRU 3.00 Agrohydrological Modelling System. Water Research Commission, Pretoria, South Africa.
- SCHULZE RE, LORENTZ S, KIENZLE S and PERKS L (2004) Case Study 3: modelling the impacts of land use and climate change on hydrological responses in the mixed underdeveloped/developed Mgeni catchment, South Africa. In: Kabat P, Claussen M, Dirmeyer PA, Gosh JHC, De Guenni LB, Meybeck M, Pielke RA, Vorosmarty CJ, Hutjes, RWA, Lutkemeier S (ed) *Vegetation, Water, Humans and the Climate: A New Perspective on an Interactive System*. Springer, Germany.
- SCHULZE RE (2004) Determination of baseline land cover variables for applications in addressing land use impacts on hydrological responses in South Africa. In: Schulze RE and Pike A (ed), *Development and Evaluation of an Installed Hydrological Modelling System*. Water Research Commission, Pretoria, South Africa, Report 1155/1/04.
- SCHULZE RE and MAHARAJ M (2004) Development of a Database of Gridded Daily Temperatures for Southern Africa. Water Research Commission, Pretoria, South Africa, Report 1156/2/04.
- SCHULZE RE, MAHARAJ M, WARBURTON ML, GERS CJ, HORAN MJC, KUNZ RP and CLARK DJ (2008) Electronic data accompanying the South African Atlas of Climatology and Agrohydrology, Water Research Commission, Pretoria, South Africa, Report 1489/1/08.
- SMITHERS JC and SCHULZE RE (2004) ACRU Agrohydrological Modelling System: User Manual Version 4.00. School of Bioresources Engineering and Environmental Hydrology. University of KwaZulu-Natal, South Africa.

- TARBOTON KC and SCHULZE RE (1992) Distributed Hydrological Modelling System for the Mngeni Catchment. Water Research Commission, Pretoria, South Africa, Report 234/1/92.
- THE NATURE CONSERVANCY (2009) Indicators of Hydrologic Alteration Version 7.1 User's Manual.
- TOUCHER ML, RAMJEAWON M, MCNAMARA MA, ROUGET M, BULCOCK H, KUNZ RP, MOONSAMY J, MENGISTU M, NAIDOO T and VATHER T (2019) Resetting the baseline land cover against which stream flow reduction activities and the hydrological impacts of land use change are assessed. Water Research Commission, Pretoria, South Africa, Draft Report K5/2437.
- WAGENER T, SIVAPALAN M, TROCH PA, MCGLYNN BL, HARMAN CJ, GUPTA HV, KUMAR P, SURESH P, RAO C, BASU NB and WILSON JS (2010) The future of hydrology: An evolving science for a changing world. *Water Resources Research* **46** W05301. <https://dx.doi.org/10.1029/2009WR008906>.
- WARBURTON ML, SCHULZE RE and JEWITT GPW (2010) Confirmation of ACRU model results for applications in land use and climate change studies. *Hydrology and Earth System Sciences* **14** 2399-2414. <https://dx.doi.org/10.5194/hess-14-2399-2010>.
- WARBURTON ML, SCHULZE RE and JEWITT GPW (2012) Hydrological impacts of land use change in three diverse South African catchments. *Journal of Hydrology* **414-415** 118-135. <https://dx.doi.org/10.1016/j.jhydrol.2011.10.028>.
- YALEW SG, PILZ T, SCHWEITZER C, LIERSCH S, VAN DER KWAST J, VAN GRIENSVEN A, MUL ML, DICKENS C and VAN DER ZAAG P (2018) Coupling land-use change and hydrologic models for quantification of catchment ecosystem services. *Environmental Modelling and Software* **109** 315-328. <https://dx.doi.org/10.1016/j.envsoft.2018.08.029>.
- YIN J, HE F, XIONG YJ and QIU GY (2017) Effects of land use/land cover and climate changes on surface runoff in a semi-humid and semi-arid transition zone in northwest China. *Hydrology and Earth System Sciences* **21** 183-196. <https://dx.doi.org/10.5194/hess-21-183-2017>.
- ZHANG L, KARTHIKEYAN R, BAI Z and SRINIVASAN R (2017) Analysis of streamflow responses to climate variability and land use change in the Loess Plateau region of China. *Catena* **154** 1-11. <https://dx.doi.org/10.1016/j.catena.2017.02.012>.

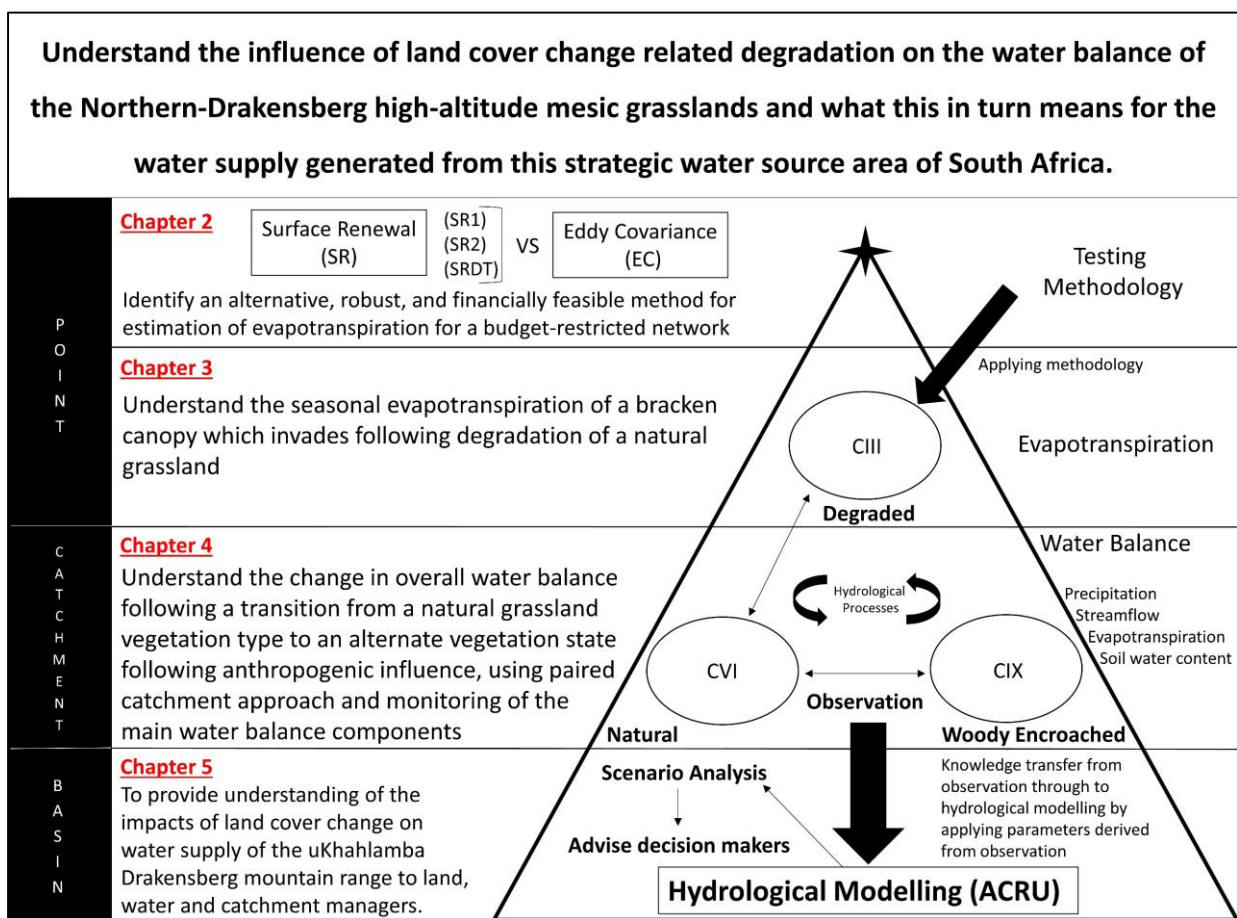
5.7 Appendix

Appendix 5A: A summary of the details of the weather stations and rain gauges utilised for the generating of the climate files for the ACRU hydrological model.

Station	Climate variable <small>R = Rainfall T = Temperature</small>	Start of record	End of record	Latitude	Longitude
Mikes Pass Meteorological Station	R + T	01/01/1950	31/12/2020	-28.975590	29.235750
2B	R	01/01/1950	31/12/2020	-28.996770	29.222590
3B	R	01/08/1950	31/12/2020	-28.996140	29.233740
4C	R	01/01/1972	31/12/2020	-28.990970	29.243880
6B	R	01/11/1972	31/12/2020	-28.993108	29.251738
7B	R	26/02/2018	31/12/2020	-28.990010	29.256773
9C	R	01/06/1954	31/12/2020	-28.992130	29.273380
Cathedral Peak Hotel	R + T	01/01/1950	31/12/2020	-28.950000	29.200000
Beaulieu	T	01/01/1968	31/01/1989	-28.800000	29.380000
Eastlynn	T	01/10/1970	28/02/1989	-28.710000	29.280000
Bergville MAG	R	01/01/1950	29/02/2020	-28.730000	29.350000

Lead in to Chapter 6

The overall objective of this thesis was to understand the influence of land cover change related degradation on the water balance of the Northern high-altitude mesic grasslands and what this in turn means for the water supply generated from the strategic water source area of South Africa. Having presented the point-catchment-basin scale investigation and the upscaling using hydrological modelling in Chapter 5, the key conclusions, management and future research recommendations are drawn out in Chapter 6.



6. SYNTHESIS: KEY CONCLUSIONS AND RECOMMENDATIONS

The Northern Drakensberg SWSA falls in the grassland biome, where it is understood that the grassland is maintained by fire (Bond et al., 2005; Bond and Parr, 2010; Brown and Bezuidenhout, 2020). Based on the climate of the region, it could be suggested that these mountainous areas should be naturally forested. However recurrent fire has been responsible for the ancient grasslands alternate fire-adapted state (Bond and Parr, 2010; Gordijn et al., 2018). Increasingly, tree planting is being promoted (internationally) as a restoration and mitigation measure. Given that the climax vegetation is forests and the carbon emissions from grassland burning, global initiatives often highlight the grasslands as degraded forest areas. Well-intentioned initiatives and policies often lack the inclusion of African data and insights. Thus, there is a need to advance the scientific understanding of the value of these grasslands in terms of biodiversity, water provision and carbon sequestration, as well as the potential risks to ecosystem provision from these areas. The overall aim of this thesis was to understand the influence of land cover change related degradation on the water balance of the Northern-Drakensberg high-altitude mesic grasslands and what this in turn means for the water supply generated from this strategic water source area (SWSA) of South Africa.

To achieve the aim a progression from observation of a hydrological process at a point, to understanding changes in hydrological processes and water balance at a headwater catchment scale through to hydrological model parameterisation and scenario analysis at a larger catchment scale was undertaken. The point-based sites and headwater catchments considered fell within the Cathedral Peak research catchments. These in turn fall within the upper-uThukela, the catchment for which the modelling was undertaken, and in turn the upper-uThukela forms part of the Northern Drakensberg SWSA (Le Maitre et al., 2018). The two forms of land cover change related degradation considered were woody encroachment and following disturbance, the invasion of bracken fern.

The key conclusions from this research are drawn out below and, in light of these, land cover management recommendations made.

6.1 Key conclusions from the study

The first key conclusion is *that the surface renewal methodology is a viable alternative for obtaining estimates of evapotranspiration over indigenous vegetation types*. Through the study the surface renewal (SR) method was tested as an alternative to the well-accepted but

costly and stringent eddy covariance (EC) method. Three SR methods were considered, the original SR method (SR1) (Paw U et al., 1995; Snyder et al., 1996) which requires calibration using the EC method, and two independent methods of EC that required further testing over different vegetation types and under a variety of climate conditions, the SR dissipation theory (SRDT) (Castellví and Snyder, 2009) and SR2 (Castellví et al., 2002; Castellvi, 2004) methods. In comparison to the prominent EC method, all three of the SR methodologies provided satisfactory estimates of the sensible heat flux (H). Along with the SR1 method, the independent SRDT method provided the best relationship of H with H derived from EC. The SRDT method also proved reliable in terms of data output as well as providing measurements again shortly after rainfall events, which is typically problematic with EC (Liu et al., 2013; Hu et al., 2018). Before this research, the SR method had never been tested over both *Leucosidea sericea* (woody) or *Pteridium aquilinum* (bracken) canopies, nor within a mountainous headwater catchment according to available literature. Through this research, α was derived for both summer and winter conditions, for the SR1 method over both indigenous vegetation types. Beyond the reliability and adequacy of the method, the SRDT method was also the most financially feasible of the three SR methodologies and highly suitable for use within a budget restricted monitoring network. Given the risk from fire and theft in remote mountainous areas to equipment, as well as the limited financial resources available in developing countries for monitoring networks, the financial feasibility was crucial. The lower sensor cost and lower power needs of the SR systems make them 75 % cheaper to install and maintain than EC systems.

Having established the reliability of the SR method, the energy balance and seasonal ET for the natural grassland, woody encroachment and bracken vegetation's was determined. A key finding was ***that the energy balance and ET of woody vegetation in comparison to the natural grassland was significantly altered***. The albedo was reduced under woody encroachment as the vegetation was greener and denser, which in turn increased the available energy. The woody vegetation transpires more than the natural grassland vegetation, with the largest difference occurring during the dry, winter period, due to the evergreen nature of the woody vegetation, compared to the deciduous natural grassland. As indicated through observation, for a drier than average year, the ET of the woody vegetation exceeds the precipitation.

The bracken vegetation was found to have a similar seasonal pattern of ET to that of the grassland vegetation, however with higher ET rates during the wet summer and spring periods and dry winter periods. The winter ET of the bracken vegetation was lower than the woody

vegetation. The bracken vegetation was also found to be sensitive to the timing of summer rainfall. During years with less rainfall, ET was found to increase in all canopies due to the higher R_n experienced because of the reduced cloud cover. This illustrated that, in this high rainfall area, soil water was not a limiting factor, and therefore ET was driven, more by available energy than by rainfall, and soil water availability. The higher rates of ET during lower rainfall years, as well as the winter deficit between the natural vegetation and bracken and woody vegetation, provides an added area of concern. Especially when these two forms of degradation are likely to become of greater concern in the Northern-Drakensberg under the predicted future climate conditions. For this region, it is expected that due to climate change the mean annual rainfall is predicted to decrease. This could be expected to result in a reduction in precipitation, increased ET, leading to larger reductions in streamflow.

Changes in ET ultimately alter the streamflow response of the catchment. An analysis of the water balance of the woody encroached catchment IX indicated a reduction in streamflow over time. Drawing comparisons between observations made in a natural grassland catchment and the woody encroached catchment with the same climate, it was evident that the grassland catchment converts a higher volume of precipitation into streamflow. The woody encroached catchment, which is representative of the long-term (>70 years) conditions of woody encroachment, generated 50 % less streamflow than the grassland catchment over a two-year period, largely attributable to the difference in ET found between the two vegetation types. The reduction in the catchments ability to convert precipitation into streamflow is a direct indication of the catchment's ability to generate and supply water for downstream regions. Woody encroachment has been shown within Cathedral Peak research catchment IX to be the result of the removal of fire within these natural grasslands (De Villiers and O'Connor, 2011). Thus, these findings demonstrate *the importance of fire as not only a management tool for the maintenance of the natural grasslands, but to ensure the sustainability of the vital water resources and ensuring water security*. Fire is responsible for the maintenance of the natural mesic grasslands, which in turn are responsible for key ecosystem services within these sensitive mountainous headwater catchments, such as maintaining the water resources generated within this SWSA.

The 50 % reduction in streamflow found under woody encroachment through the water balance analysis are as mentioned, a representation of the impacts of long-term woody encroachment (>70 years). Through the analysis of the long-term streamflow records (dating back to 1962) it was identified that the catchment response ratio (rate at which precipitation is

converted to streamflow) has declined within the woody encroached Cathedral Peak research catchment IX over the past 70 years following fire protection. During the first 20 years, the response of catchment IX was similar to the natural grassland catchment VI, but within the last 10 years, the difference has increased largely. A key conclusion drawn from this was ***that there is an evident lag between the onset of degradation in the form of woody encroachment and the resultant impacts on streamflow being evident***. It is expected that in the future, as the level of woody encroachment increases, the response ratio of the catchment is expected to continue to decline. Along with the catchment response decline, the realisation that with a higher ET than precipitation, the water available for ET is evidently coming from long-term multi annual groundwater stores. This begs the question, along with a declining surface water response, how will long-term woody encroachment impact the availability of these groundwater stores, and at what point, if any, will they eventually dry up? The mountainous catchments groundwater stores are critical for the maintenance of flows during the dry period, and would be a far-reaching loss, if depleted over time.

It is well understood that the Northern Drakensberg headwater catchments are part of a vital SWSA (Le Maitre et al., 2018). It is also well understood that headwater mountainous catchments are some of the most sensitive to anthropogenic change (Benston, 2003; Huber et al., 2005; Benston and Stoffel, 2014; Moran-Tejeda et al., 2014; Haro-Monteagudo et al., 2020). In line with this, and a key conclusion drawn from this research, is ***the disproportionately large impact degradation related land cover change within these headwater catchments has on the downstream water balance relative to low land catchments***. Chapter 5, through upscaling of the observation using the ACRU agrohydrological model to the larger upper-uThukela, highlighted the importance of the protected areas, and how any land cover change within this area had negative impacts on streamflow, which translated downstream. It illustrated the importance of these headwater catchments protected and remaining protected. The high level of degradation found outside of the protected areas (Grab and Knight, 2018; Yalaw et al., 2019) within the Drakensberg mountain range will require substantial effort and cost to rehabilitate. It is therefore important to protect and preserve the headwaters in their current state, and to manage the already degraded areas in such a way to prevent continued degradation from occurring. This is required to ensure the longevity of the water resources and ecosystem services provided by this nationally important SWSA.

6.2 Revisiting the aims and objectives

The overall aim of this thesis was to understand the influence of land cover change related degradation on the water balance of the Northern-Drakensberg high-altitude mesic grasslands and what this in turn means for the water supply generated from this strategic water source area of South Africa.

To achieve the overall aim, the following objectives were pursued:

- a) Identify an alternative method, for the estimation of evapotranspiration, which is robust enough for use within a remote mountainous area and financially feasible for a budget restricted monitoring network. (Chapter 2)
- b) Understand the seasonal evapotranspiration of the bracken canopy which invades following the degradation of a natural grassland. (Chapter 3)
- c) Understand the seasonal evapotranspiration of the woody encroached canopy which invades following removal of fire for a natural grassland. (Chapter 4)
- d) Understand the change in overall water balance following a transition from a natural grassland vegetation type to an alternative vegetation state following anthropogenic influence, using the paired catchment approach and monitoring of the water balance components. (Chapter 4)
- e) To use hydrological modelling with parameters determined from observation, in combination with scenario analysis, to understand the potential changes in the water supply from the upper-uThukela catchment following different levels of land cover change. (Chapter 5)

6.3 Contributions to new knowledge

The contributions of this research to new knowledge is listed below:

- Demonstrated the feasibility of SR for use over two different indigenous vegetation types within a mountainous headwater catchment, as well as the financial feasibility of the method compared to common EC method. (Objective a)

- Further, of the three different SR methodologies that were applied, the EC-independent, SR dissipation theory (SRDT) methodology was found to be the best alternative for estimation of sensible heat flux over *Leucosidea sericea* (woody) and *Pteridium aquilinum* (bracken) both indigenous vegetation types, as well as being the most financially feasible of the three methodologies. (Objective a)
- Generated summer and winter alpha calibration values for the *Leucosidea sericea* (woody) and *Pteridium aquilinum* (bracken) for use with the SR1 methodology under a summer rainfall climate. (Objective a)
- Quantified the seasonal trend of ET for *Leucosidea sericea* (woody) and *Pteridium aquilinum* (bracken) within the Drakensberg mountain range (Objectives b and c).
- Modelled monthly k_c values *Leucosidea sericea* (woody) and *Pteridium aquilinum* (bracken), as well as monthly land cover parameters for use within the ACRU and other similar hydrological models. (Objectives b, c, and e)
- Determined the impact of a land cover change transition from natural grassland to woody encroachment on the water balance of a headwater mountainous catchment within a SWSA of South Africa. (Objective d)
- Confirmation of the ability of the ACRU hydrological model for use in land cover change scenario analysis within the upper-uThukela catchment. (Objective e)
- Illustrated the impacts of a shift in land cover to both *Leucosidea sericea* (woody) and *Pteridium aquilinum* (bracken) on the streamflow generated within the upper-uThukela catchment, and the potential impact this could have within the greater SWSA area of the larger Drakensberg mountain range. (Objective e).
- Showed the importance of land management with regards to maintaining the natural grassland state (using fire as a management tool) within the protected headwater catchments of the upper-uThukela for water supply to the downstream region. (Objective e).

6.4 Management and future research recommendations

6.4.1 Importance of observation and monitoring to optimise management

Environmental change has increased the requirement and importance of observation and monitoring networks. The location of these networks is key to understanding the critical processes impacted upon through change. Within the environmental change context, the value of long-term data sets has rapidly increased. Understanding is gained through data, which is generated through observation. This understanding is needed to drive and direct management strategies, to ensure informed decisions are made.

Sensitive mountainous headwater catchments within the SWSA are key areas to conduct monitoring as they provide valuable insight into the impacts of environmental change in a sensitive and important area. This emphasises the importance of continuing and maintaining such networks as the Cathedral Peak research catchments. Without monitoring and observation within the Northern Drakensberg SWSA, management is unlikely to be optimal. Observation and monitoring should form a key part of management. A key challenge to such networks, especially within developing countries is the cost. Therefore, a potential future area of research is in methodologies such as SR, which reduce the cost and broaden the availability of monitoring to a larger audience. Focus is recommended for SR.

The application of SR beyond the agricultural setting and within hydrological monitoring networks needs further investigation. This research has shown the applicability of the SR independent methods over *Leucosidea sericea* (woody) and *Pteridium aquilinum* (bracken) indigenous vegetation types in South Africa. It has provided the Cathedral Peak research catchment with a viable long-term method for the monitoring of ET over both indigenous vegetation types. What is required now, is to test the SRDT method over several other indigenous vegetation found within South Africa and across different climate regions, to increase the knowledge and database of climatic and vegetation conditions under which these methods can be applied.

Following this research, the SR systems installed within the Cathedral Peak research catchments have remained and will be continued to be used by the South African Environmental Observation Network (SAEON) for the long-term monitoring of ET over bracken and woody vegetation. The continued use illustrates the potential of this method, and an example of the successful implementation, following testing of the method, where it will be of benefit to the

long-term understanding of a critical environmental change process in an important water resource area.

6.4.2 Nexus approach for process understanding and management

Within the Northern Drakensberg mountain range, the impact of land cover change on water resources is only a single aspect of a more complex nexus between water-biodiversity-carbon-fire. Currently within the Northern Drakensberg mountain range, the interconnection within this nexus is poorly understood. This research provided an initial insight from a water perspective, however, in order to manage the SWSA optimally and to ensure system resilience, a full understanding of the nexus is needed.

This need for understanding should drive the direction of research within the Northern Drakensberg SWSA to better understand the impacts of woody encroachment and bracken invasion from a biodiversity perspective as well the carbon aspect. As recommended within this research from a water perspective, fire is vital for maintaining the natural grassland, and ensuring the water resources and associated ecosystem services. However, little is known what implications this could have from a carbon perspective, where fire is considered as a global source, while woody vegetation is considered a carbon sink. Research on the carbon implications of natural grasslands and their management with fire, compared woody encroachment and bracken invasion is required. Understanding the balance between global carbon and local water needs is crucial as it is already a global debate. Added to this, the impact of woody encroachment and bracken invasion on biodiversity currently lacks understanding. These combined with the current understanding from a water perspective as the research develops, should be used to inform and guide an integrated management approach to the sensitive Northern Drakensberg SWSA.

6.4.3 Consideration of uncertainty

When considering the findings of an upscaled hydrological modelling study such as this, to inform management decisions, the level of uncertainty within the findings need to be considered. Several uncertainties could be considered within this study, however, the main area of uncertainty surrounds the ET water balance component. A further consideration is the uniqueness of place (Beven, 2000) of this study in general. It is assumed that the findings within the Northern Drakensberg will be applicable across the whole Drakensberg mountain range, but needs to be understood that this may vary from north to south as climate and land use varies.

This is a key consideration when interpreting or applying these findings within other regions of the Drakensberg mountain range for management decision making.

The uncertainty requiring consideration regarding the ET water balance component stems firstly from using a new method (SR) for the estimation, along with deriving the hydrological parameters for modelling the respective vegetation types from a two-year observation period as a representation for all periods. Further consideration also needs to consider that the observation took place within the higher altitude areas of the little berg, and were applied as a representation for the lowland areas within the model. These uncertainties are generated as a result of the limitations of the study, such as time and budget.

The SR method was tested for the first time within the Drakensberg mountain range. Further, there is little to no literature on the use of the method over indigenous vegetation such as woody or bracken canopies. This method was also calibrated against an EC system which is known and was shown to partially close the energy balance. The relationship between the EC and SR was also conducted over select periods and therefore partially biased towards the conditions during these periods. This is however the accepted approach.

The k_c values derived for the woody vegetation as well as for the bracken vegetation and applied within the degraded and encroached scenarios were developed using the SR method with the before mentioned uncertainty as well as being specific to the two years of observation from which they were derived. Across the catchment, the altitude varies between the upper little berg and the lowland area. All observations in terms of ET and water balance were conducted at the higher altitudes. When applying the findings from this area within the model, it is assumed the similar ET behaviour occurs within the lowland. This does introduce a level of uncertainty into the overall findings. It should be noted however, that this was not a poor approach, but a good alternative to having to adapt k_c values of another vegetation type presumed to behave in a similar manner. Adapting well known vegetation parameters is a common approach used within hydrological modelling and introduces significantly larger uncertainty. To address this, a consideration moving forward would be to continually update these k_c values over time following a larger period of observation, as well as observation within the lowland regions. Observation within the lowland region does however come with several other challenges making this approach uncertain.

6.4.4 Climate change lens

An aspect not considered within this study, but a significant part of global change is that of climate change. The impact climate change is likely to have on the water resources within the Northern Drakensberg SWSA needs consideration and is likely to affect the ongoing woody encroachment and bracken invasion. An example, already identified within this research was the finding that ET increased during lower rainfall years, due to increased available energy flux, which under land cover change, further reduces streamflow and exacerbates the impact on low flows. Along with this, it was shown that the volume and timing of rainfall, particularly during summer and autumn, influences the rate of ET. It is well known that climate change is going to influence and alter both the spatial and temporal distribution of rainfall globally. It is predicted for the eastern region of South Africa, that rainfall will decline, thus potentially increasing ET rates, which could result in further streamflow reductions under both forms of degradation with this future climate outlook. The system is more complex than this, as soil water conditions could also play a role, but this illustrates why understanding the system as a whole is critical to preservation and management of the ecosystem.

6.5 References

- Beniston, M., 2003. Climate change in mountain regions: a review of possible impacts. *Climate Change*. 59, 5-31.
- Beniston, M., Stoffel, M., 2014. Assessing the impacts of climatic change on mountain water resources. *Science of the Total Environment*. 493, 1129-1137.
- Beven, K.J. 2000. Uniqueness of place and process representations in hydrological modelling. *Hydrology and Earth System Sciences*. 4(2), 203-213.
- Bond, W.J., Woodward, F.I., Midgley, G.F., 2005. The global distribution of ecosystems in a world without fire. *New Phytologist*. 165, 525-538.
- Bond, W.J., Parr, C.L., 2010. Beyond the forest edge: Ecology, diversity and conservation of the grassy biomes. *Biological Conservation*. 143, 2395 – 2404.
- Brown, L.R., Bezuidenhout, H., 2020. Grassland Vegetation of Southern Africa. *Encyclopedia of the World's Biomes*. 3, 814-826.
- Castellví, F., Perez, P.J., Ibañez, M., 2002. A method based on high frequency temperature measurements to estimate sensible heat flux avoiding the height dependence. *Water Resources Research*. 38(6), WR000486-20.
- Castellví, F., 2004. Combining surface renewal analysis and similarity theory: A new approach for estimating sensible heat flux. *Water Resources Research*. 40(5), W05201
- Castellví, F., Snyder, R.L., 2009. Combining the dissipation method and surface renewal analysis to estimate scalar fluxes from the time traces over rangeland grass near Ione (California). *Hydrological Processes*. 23, 842-857.

- De Villiers, A.D., O'Connor, T., 2011. Effect of a single fire on woody vegetation in Catchment IX, Cathedral Peak, KwaZulu-Natal Drakensberg, following extended partial exclusion of fire. *African Journal of Range and Forage Science*. 28(3), 111-120.
- Gordijn, P.J., Everson, T.M., O'Connor, T.G., 2018. Resistance of Drakensberg grasslands to compositional change depends on the influence of fire-return interval and grassland structure on richness and spatial turnover. *Perspectives in Plant Ecology, Evolution and Systematics*. 34, 26 - 36.
- Grab, S.W., Knight, J., 2018. Southern African montane environments. *Southern African Landscapes and Environmental Change*. Routledge, United Kingdom.
- Haro-Monteagudo, D., Palazon, L., Begueria, S., 2020. Long-term sustainability of large water resource systems under climate change: A cascade modeling approach. *Journal of Hydrology*. 582, 124546.
- Hu, Y., Buttar, N.A., Tanny, J., Snyder, R.L., Savage, M.J., Lakhari, I.A., 2018. Surface renewal application for estimating evapotranspiration: A review. *Advances in Meteorology*. 2018, 1-11.
- Huber, U.M., Bugmann, K.M., Reasoner, M.A., 2005. *Global change and mountain regions: an overview of current knowledge*, Springer, Dordrecht, Netherlands.
- Le Maitre, D.C., Walsdorff, A., Cape, L., Seyler, H., Audouin, M., Smith-Adao, L., Nel, J.A., Holland, M., Witthüser, K., 2018. Strategic water source areas: management framework and implementation guidelines for planners and managers. WRC Report No. TT 754/2/18, Water Research Commission, Pretoria, South Africa.
- Liu, S.M., Xu, Z.W., Zhu, Z.L., Jia, Z.Z., Zhu, M.J., 2013. Measurements of evapotranspiration from eddy-covariance systems and large aperture scintillometers in the Hai River Basin, China. *Journal of Hydrology*. 487, 24-38.
- Moran-Tejeda, E., Zabalza, J., Rahman, K., Gago-Silva, A., Lopez-Moreno, J.I., Vicente-Serrano, S., Lehmann, A., Tague, C.L., Beniston, M., 2014. Hydrological impacts of climate and land-use changes in a mountain watershed: uncertainty estimation based on model comparison. *Ecohydrology*. 8(8), 1396-1416.
- Paw U, K.T., Qiu, J., Su, H.B., Watanabe, T., Brunet, Y., 1995. Surface renewal analysis: a new method to obtain scalar fluxes. *Agricultural and Forest Meteorology*. 74, 119-137.
- Snyder, R.L., Spano, D., Paw U, K.T., 1996. Surface renewal analysis for sensible and latent heat flux density. *Boundary-Layer Meteorology*. 77, 249-266.
- Yalew, S.G., Pilz, T., Schweitzer, C., Lierschl, S., van der Kwast, J., van Griensven, A., Mul M.L., Dickens, C., van der Zaag, P., 2018. Coupling land-use change and hydrologic models for quantification of catchment ecosystem services. *Environmental Modelling and Software*. 109, 315-328.